

ER Mapper Applications

24 July 2000

ER Mapper

Helping people manage the earth

Asia/Pacific :

Earth Resource Mapping
Level 2
87 Colin Street
West Perth
Western Australia 6005
Telephone: +618 9388-2900
Facsimile: +618 9388-2901

Europe, Africa and Middle East:

Earth Resource Mapping
Blenheim House
Crabtree Office Village
Eversley Way, Egham
Surrey, TW20 8RY, UK
Telephone: +44 1784 430-691
Facsimile: +44 1784 430-692

Americas:

Earth Resource Mapping
4370 La Jolla Village Drive
Suite 900
San Diego, CA
92122-1253, USA
Telephone: +1 858 558-4709
Facsimile: +1 858 558-2657

ER Mapper and ER Storage software and documentation is proprietary to Earth Resource Mapping Pty Ltd.

Copyright © 1988, 1989, 1990, 1991, 1993, 1994, 1995, 1996, 1997, 1998, 1999, 2000 Earth Resource Mapping Ltd

All rights reserved. No part of this work covered by copyright hereon may be reproduced in any form or by any means - graphic, electronic, or mechanical - including photocopying, recording, taping, or storage in an information retrieval system, without the prior written permission of the copyright owner.

While every precaution has been taken in the preparation of this manual, we assume no responsibility for errors or omissions. Neither is any liability assumed for damages resulting from the use of the information contained herein.

PostScript is a registered trademark of Adobe Systems, Inc.

Unix is a registered trademark and OPEN LOOK is a trademark of AT & T.

Windows 95, Windows 98, Windows NT and Windows 2000 are trademarks of Microsoft Corp.

ARC/INFO and ArcView are trademarks of Environmental Systems Research Institute, Inc.

Autodesk World, AutoCAD and AutoCAD MAP are trademarks of Autodesk, Inc.

MapInfo is a trademark of Mapinfo Corporation.

All other brand and product names are trademarks or registered trademarks of their respective owners.

Revision History

Revision	Date	Comments
β	19 Feb 1990	Australian Beta Version
$\beta 2$	6 Apr 1990	U.S. Beta Version
1.0	1 May 1990	Release 1.0
1.1	9 Jul 1990	Update 1.1
1.2	21 Sep 1990	Update 1.2
2.0	10 Jan 1991	Release 2.0
3.0	22 Nov 1991	Release 3.0
3.1	20 May 1992	Update 3.1
3.2	26 Aug 1992	Update 3.2
4.0	15 Jan 1993	Release 4.0
4.1	25 Oct 1993	Update 4.1
4.1a	4 Feb 1994	Update 4.1a
4.2	18 Oct 1994	Update 4.2
5.0	30 Jun 1995	Release 5.0
6.0	30 Sep 1998	Release 6.0
6.1	30 Oct 1999	Release 6.1
6.2	24 July 2000	Release 6.2

Summary Contents

Preface xvii

Part One - ER Mapper Applications 19

- 1 Data Fusion and Mosaicing 21
- 2 Digital Elevation Models 39
- 3 Map Production 61
- 4 Change Detection 67
- 5 Crop Type Classification and Area Inventory 79
- 6 Vegetation in Remote Sensing FAQs 95
- 7 Geophysical Data Imaging and Presentation 121
- 8 Image Processing in Mineral Exploration 155
- 9 Semi-Automatic Interpretation of Aeromagnetic Datasets 159
- 10 Custom-built Dynamic Links 167
- 11 Fast Fourier Transforms 189
- 12 Principal Component Analysis 205

Part Two - Case Studies 209

- 13 Aerial Photography and Data Integration 211
- 14 Monitoring Crop Production and Assessing Irrigation Requirements

Summary Contents

217

- 15 Coastal Habitat Mapping 221
- 16 Monitoring Environmental Change in Lake Turkana 227
- 17 Monitoring the Gulf of Gdansk 233
- 18 Boreal Forest Monitoring 237
- 19 SAR imagery in mineral and oil exploration 243
- 20 Mapping Shelf Circulation 251

Part Three - Oil and Gas 261

- 21 Oil and gas 263
- 22 Importing seismic data 267
- 23 Importing geological and cultural vector data 279
- 24 Updating geological and cultural vector data 285
- 25 Generating hardcopy prints 289
- 26 Data viewing tips 295

Part Four - Supplied Processing 301

- 27 Supplied Algorithms 303
- 28 Supplied Filters 363
- Index 383



Table of Contents

Revision History iii

Preface xvii

Acknowledgements xviii

Part One - ER Mapper Applications

- 1 Data Fusion and Mosaicing 21
 - Author 21
 - Abstract 21
 - Introducing data fusion and mosaicing 21
 - Common ways of fusing data 25
 - Pseudocolor colordrape data fusion 27
 - RGBI (RGB->HSI->RGB) data fusion 28
 - Brovey transform RGBI data fusion 29
 - Data fusion using attribute highlighting 31
 - Data fusion using region highlighting 33
 - Fusion of vector and raster data 35

- Useful formulas for data fusion and mosaicing 36
- 2 Digital Elevation Models 39**
 - Author 39
 - Abstract 39
 - Introduction 39
 - Sources and quality of DEM data 40
 - Typical DEM applications 42
 - Displaying DEMs 43
 - Integrating DEM and other data 50
 - Processing DEMs 51
 - What-if processing 56
 - Classification using DEM data 59
 - Correcting SAR data with DEMs 59
- 3 Map Production 61**
 - Producing quality combined image/vector maps 61
 - Sub-sectioning data for GIS/CAD systems with limited imagery capabilities 63
 - Directly sharing image files between different systems 65
- 4 Change Detection 67**
 - Author 67
 - Introduction 67
 - Data sources 68
 - Registering data to ground control points 69
 - Rectifying raster data to vector data 70
 - Rectifying raster data to raster data 71
 - Eliminating seasonal and atmospheric effects 73
 - Creating a change image 74
 - References 77
- 5 Crop Type Classification and Area Inventory 79**
 - Authors 79
 - Introduction 79
 - Project 80

- Multispectral classification 81
- Getting to know your image 82
- Image display 82
- Image enhancement 82
- Classification schema 83
- Sequence of operations 83
- Multispectral sensing of crops 84
- Ground truth 88
- Classification methodology 90
- Displaying classification results 92
- A note about unsupervised classification 92
- Classification accuracy assessment 93
- Summarizing the position of remote sensing in crop analysis 93
- References 94

6 Vegetation in Remote Sensing FAQs 95

- Author 95
- Acknowledgements 95
- Revision history 96
- Conventions 96
- List of questions 97
- General 99
- Vegetation index 102
- Basic indices 103
- Indices to minimize soil noise 106
- Indices to minimize atmospheric noise 109
- Other indices 111
- Problems 113
- Future directions 115
- Final question 116
- References 117

7 Geophysical Data Imaging and Presentation 121

- Author 121
- Introduction 121

- Geophysical methods 122
- Other datasets to aid geophysical interpretation 123
- Gridding and imaging 124
- General approach to geophysical imaging 127
- Filters 132
- Interpretation using annotation 137
- Imaging magnetics 137
- Airborne radiometrics imaging 139
- Seismic reflection data imaging 144
- Gravity imaging 147
- Airborne electromagnetics imaging 150
- Topography 151
- References and further reading 152
- 8 Image Processing in Mineral Exploration 155**
 - Author 155
 - Introduction 155
 - Displaying geochemical data 156
 - Combined geochemical data 156
 - Geochemical fused with Landsat 157
 - Conclusion 157
- 9 Semi-Automatic Interpretation of Aeromagnetic Datasets 159**
 - Authors 159
 - Introduction 159
 - The semi-automatic interpretation algorithm 160
 - Abbreviated time and motion study of the interpretation process 160
 - Traditional interfacing of algorithm output with data and interpreter 161
 - Interfacing with ER Mapper 162
 - Summary 164
 - Acknowledgments 165
 - References 165

10 Custom-built Dynamic Links 167

Authors 167

Abstract 167

Introduction 167

Advantages of digital data integration 168

Data Integration at CNGC 168

What is SQL? 170

Data storage considerations 170

Dynamic link construction 171

Dynamic operation within ER Mapper 172

Example: Talbot Island 173

Future implications 179

Conclusion 180

References 180

Appendix A 181

Appendix B 187

11 Fast Fourier Transforms 189

Author 189

Introduction 189

The Fourier transform of an image 190

Notch filtering 190

Low-pass and High-pass Fourier filtering 193

Fourier processing of potential-field data 194

Aeromagnetic data from Cape York Peninsula, Queensland 196

Appendix 200

References 202

12 Principal Component Analysis 205

Author 205

Using Principal Component Analysis 205

References 207

Part Two - Case Studies

13 Aerial Photography and Data Integration 211

Authors 211

Context: Data Gathering 212

Example: Transport Corridor Development 213

Conclusion 216

14 Monitoring Crop Production and Assessing Irrigation Requirements 217

Authors 217

Introduction 218

Context: Agricultural development 218

Example: Irrigation development 219

Conclusion 220

15 Coastal Habitat Mapping 221

Author 221

Abstract 221

Introduction 222

Available imagery 222

Geographe Bay 223

The Abrolhos and Montebello islands 224

Conclusion 225

16 Monitoring Environmental Change in Lake Turkana 227

Authors 227

Introduction 228

Water resources, agricultural development and environmental change
228

Example: Erosion, Siltation and Lake Capacity 229

Conclusion 230

17 Monitoring the Gulf of Gdansk 233

Authors 233

Background 233

Image processing 234
Comments 235
The future 236

18 Boreal Forest Monitoring 237

Author 237
Abstract 237
Locations 237
Introduction 238
Lightning project 238
Boreal forest project 239
Customizing forestry applications 239
Fusing, mosaicing, and virtual datasets 241
Implications 242
Conclusion 242

19 SAR imagery in mineral and oil exploration 243

Authors 243
Abstract 243
Introduction 243
Characteristics of ERS-1 SAR imagery 244
Panama case study 245
Irian Jaya case study 247
Concluding points 248

20 Mapping Shelf Circulation 251

Author 251
Synopsis 251
Introduction 252
Data 252
Algorithms 253
Data processing 254
References 259

Part Three - Oil and Gas

21 Oil and gas 263

Schlumberger Geoquest and Landmark imports 264

22 Importing seismic data 267

Seismic raster grid formats supported 267

SEG-Y 269

Zycor ASCII grid 270

GeoQuest (IESX) ASCII grid dump 271

Charisma 2D XYZ ASCII grid 272

Charisma 3D Inline Xline XYZ ASCII grid 273

GeoQuest (IESX) MapView ASCII Grid 276

Generic issues related to importing raster grid data 277

23 Importing geological and cultural vector data 279

OpenWorks 3.1 Wells—Import 280

SeisWorks Fault Polygons 281

SeisWorks Manual Contours 282

24 Updating geological and cultural vector data 285

Moving updated vector data back to other products 286

25 Generating hardcopy prints 289

Generating maps as a TIFF file 289

How to create a map 290

Using the Page Setup Wizard 294

26 Data viewing tips 295

The Intensity layer 295

Colordrapping 297

Training 299

Part Four - Supplied Processing

27 Supplied Algorithms 303

Applications 304

Airphoto 304
Fire_Risk 304
Land_Information 305
Mineral_Exploration 305
Mt_St_Helens 306
Oil_and_Gas_Exploration 307
Telecommunications 307
World_Topography 307
Data_Types 307
Airphoto 307
Arc_info 308
AutoCAD_DXF 309
Digital_Elevation 309
Ers1 313
Landsat_MSS 313
Landsat_TM 315
Magnetics_And_Radiometrics 323
RadarSat 327
Seismic 327
SPOT_Panchromatic 330
SPOT_xs 331
Functions_And_Features 332
3D 332
3D_multi_surface 336
Airphoto_Tutorial 336
Class_Interactive_Compute 336
Classification 338
Classification_Display 339
Contours 339
Data_Fusion 340
Data_Mosaic 344
Dynamic_Links 345
Fft 345
Geocoding 346

Contents

Gridding	347
HSI_Transforms	347
Language_Specific_Links	347
Map_Objects	348
Map_Production	349
Radar	350
Regions	350
Spatial_Filters	351
Vectors_and_Imagery	355
Virtual Datasets	355
Miscellaneous/Templates	356
Common	356
Dataset_Output	357
FFT	358
Virtual_Datasets	360
Miscellaneous/Test_Patterns	361
Shared_Data	362

28 Supplied Filters 363

DEM filters	363
Edge filters	364
Gaussian filters	364
Geophysics filters	365
High pass averaging filters	367
Low pass averaging filters	368
Ranking filters	370
SAR filters	371
Seismic	373
Standard Filters	374
Sunangle Filters	378
Usercode	380

Index 383



Preface

The purpose of this manual is to show you examples of ER Mapper at work. It attempts to go deeper than the other manuals in the set, discussing the application of general concepts to particular circumstances. The topics have been grouped roughly into parts for convenience but the chapters are by no means exclusive. The aim has been to go for breadth of coverage rather than duplication. By the nature of the product and disciplines in which it is used, some techniques will apply to many applications. You may want to approach the manual by reading the chapters most relevant to your application and then skimming the headings in the other chapters to see if they discuss other techniques you are interested in. You may also want to use the index to find references to particular applications or techniques.

This manual assumes that you already know your way around ER Mapper - for example how to change histograms or add filters. If not, you will have to look these techniques up in the User Guide or tutorial manual. For example, the User Guide will describe how to add a filter while this manual will suggest which filter to use in a particular instance.

If you haven't used ER Mapper before you may still want to browse through this manual to get an idea of the diverse ways in which the product can be used.

Note: Reference is made in certain chapters to files in the "examples" directory. This directory is located in the ER Mapper installation directory (on PC's usually "C:\Program Files\ER Mapper\ER Mapper 6.2"). Note that the examples files may not be installed. This will depend on the configuration option you specified when first running the setup program.

Acknowledgements

This manual is the result of many hours of work by many people and encapsulates even more hours and years of experience. Thank you to all who have willingly shared this experience to swap ideas and help others on their way. This manual would not have been possible without you. All material in this manual has been used by permission and provided in good faith. All techniques are suggestions only and may not work in your circumstances.

Part One -
ER Mapper
Applications

Data Fusion and Mosaicing

Author

Stuart Nixon is the Founder and Managing Director of Earth Resource Mapping.

Abstract

ER Mapper is unique in that its algorithm concept includes several innovative features such as automatic data fusion and mosaicing. Data fusion (also known as data merging) is the combination of different types of data over the same area. Mosaicing is the tiling of images showing different areas to generate a composite view of a larger area.

Introducing data fusion and mosaicing

An integral part of image processing is the fusion and mosaicing of different types of data.

Fusion

Data fusion is the combination of different types of data over the same area in some way. Common uses include:

- Sharpening Landsat TM imagery with SPOT Panchromatic imagery.
- Fusion of airborne magnetics data with radiometrics data.
- Generating a map that shows the existing known road network as a GIS vector map over an image which highlights road changes between years, and all of that over a backdrop satellite map.
- Producing several options for powerline placements, by showing land use within 200 meters of the alternative routes and using a mosaiced set of airphotos as a backdrop.
- Showing land use changes computed from classified satellite images. Also, measuring all changes in land use related to vegetation only, by removing or highlighting natural forests.
- Showing existing oil wells over 3-D seismic data by highlighting areas worthy of further exploration.
- Showing geochemical assay information over mineralogy, classified from a radiometrics survey, and draped over a magnetics survey. This highlights subsurface structure and correlates it with known geochemical assays.

Mosaicing

Mosaicing is the tiling of more than one image to generate a composite view of larger areas. The typical example is the generation of a high resolution regional view based on the tiling of 40 or 50 air photos. Another example is the mosaicing of several cloudy satellite images to produce a cloud-free image. This is similar to data fusion.

ER Mapper Fusion and Mosaicing

Unlike older image processing systems which have a number of programs that do specific functions, ER Mapper is built on a unique algorithm concept which encompasses several innovative ideas. These are fundamental to the way that ER Mapper works. Thus, ER Mapper has:

- Algorithms, for generating an image from one or more source raster and vector datasets.
- Automatic data fusion, allowing a particular combination of two or more datasets over the same area.
- Automatic mosaicing, allowing the mosaicing of two or more datasets which cover an area.
- Arbitrary raster dataset resolutions and formats, as raster datasets can be fused regardless of their resolution or formats. For example, an 8-bit integer based Landsat TM image with a ground resolution of 28.5 meters can be combined with a floating-point based elevation image with a ground resolution of 100 meters.
- Interactive integration of datasets, as it is not necessary to write intermediate datasets prior to integrating different data.
- Interactive formula and kernel (filter) processing, for complete integration of raster and vector data, with the ability to specify the priority of different layers of data.

ER Mapper possesses a combination of different processing functions giving it considerable power. These functions can be combined in an almost limitless number of ways.

Before different datasets can be fused or mosaiced together, they must be in the same map projection (although they may have different spectral resolutions, data format and cell size, and cover different areas).

What you need to know

This chapter assumes that you are familiar with the algorithm concept and how to carry out a number of common ER Mapper functions such as how to:

- Load, save, and modify algorithms;
- Add layers to an algorithm, including data fusing (different layer types) and data mosaicing (the same layer types);
- Modify a formula within a layer;
- Change transform limits to rescale data, particularly after a formula has changed the dynamic range of the data;
- Use the INREGION function within a formula;
- Generate vector polygons from raster images;
- Create and use virtual datasets.

These issues are covered in detail in the Tutorial and User Guide.

Using data fusion to provide an integrated view into several datasets

There are often cases where it is desirable to see two or more types of data at the same time. Most procedures involve one of the following techniques, which are explained in more detail in the next sections.

Color and intensity

We perceive object color differently compared to actual object shape. This means that we can use structure to represent one type of data, and color for another type of data - over the same area - simultaneously. For example, we can show fire risk in color over a monochromatic airphoto in an intensity layer. This makes it easy to see roads that lead to an area of high fire risk.

Attribute highlighting

If the features you are interested in cover only small portions of the entire map area, you can generate a base map, and show the areas of interest highlighted in color. For example, a greyscale satellite image could be used as a basemap, and over it areas that have increased in vegetation over the past 5 years could be shown in green, and areas that have decreased in vegetation in red. Areas of no change would show through as the backdrop satellite image. This technique requires deciding, on a pixel by pixel basis, the state of a given part of the map.

Region highlighting

This is similar to the previous example, except in this case the areas of interest are known in advance in the form of polygon regions. This could be obtained from a GIS system or from earlier classification of a satellite image. An example of this type of data fusion would be to show classified forest stands, only for the regions (polygons) of interest, rather than for the entire area. Again, a backdrop image could be added, to show in the areas that are not the regions of interest. The region highlighting technique is suited to both raster and vector data. A vector example would be to only show vectors within a given county.

Vectors over raster data

Selective use of vectors in front of raster data allows fusion of information gathered from raster and vector data. An example would be to view access roads into a forest stand by overlaying it on a classified image of the forest stand.

By combining these different techniques on a single map or image, it is possible to show quite complex information simply. It is best to start with one technique, then add additional techniques to the map as required. Only two or three different types of information should be shown on a single map. If more information is required it is better to create two or three maps of the same area.

ER Mapper's algorithm concept works well here because it is possible to generate many different views from the same data, without requiring intermediate datasets to be computed or stored. Furthermore, as the algorithm is run on demand to compute the final image, the final image need not be stored on disk. Only the algorithm (which requires small disk space) need be stored, and the resultant image called up when required.

Data fusion using color and intensity

Images made by data fusion using color and intensity are easy to generate, and very easy to explain and interpret. Some common types of images visualised in this way could be:

- Fire danger maps for an area, color coded red as high risk, and scaled down to green as low risk, over an air photo over the same area. It is easy to correlate the risk of a fire (red being high risk) against the actual terrain, or against access into areas of high fire risk.

- Forest management maps showing different types or growths of forest as a color coded image over a satellite image, to plan the placement of access roads and fire breaks.
- Mineral exploration maps showing radiometrics in red, green and blue (potassium, thorium and uranium respectively) over a magnetics image processed to show structure. The resultant image makes it easy to correlate radiometrics to show mineralogy over the sub-surface magnetics structure.

These types of maps are created by using color to represent one type of data, and intensity to show another type of data.

The human eye is sensitive to small changes in structure (for example, a road running through an image), and to overall patterns in color. This means that high variability information (that is, high frequency information) should be shown as intensity, whereas overall trends or patterns should be shown in color. When looking at data, it generally becomes obvious as to which way one should represent the data.

Consider the case of a map that combines precipitation, measured every 1 kilometer, with a map of vegetation, derived from a 30-meter pixel satellite image. In this instance, the precipitation (which changes slowly over distance) would be shown in color, whereas the vegetation would be shown as intensity.

Common ways of fusing data

There are a number of common combinations of data. They include:

Landsat TM (30 meter resolution) and SPOT Panchromatic data (10 meter resolution)

Landsat TM data has 7 wavelengths of data, whereas the SPOT Panchromatic data has only one wavelength of data, but at a higher resolution. An effective technique is to combine these two sources of data, resulting in a higher resolution image (using the 10 meter SPOT data) with the spectral information from the Landsat TM (using some combination of the 7 bands). In this case, color is used to show the Landsat TM image (often as a red-green-blue image) and intensity is used to show the SPOT Pan image.

Landsat TM and airborne magnetics surveys

This allows surface geology—mapped from the Landsat TM imagery—to be correlated with sub-surface magnetics. Common techniques are to show the Landsat TM in color, and the structure from the magnetics image as intensity.

Typically, the Landsat TM would be shown as red-green-blue (bands 7, 4, 1, are good to highlight geology), and the magnetics image is “sun-shaded” to highlight structure, which is used for intensity in the image.

Radiometrics (potassium, thorium and uranium) and airborne magnetic surveys

Once again, radiometrics is shown in color, and magnetics in intensity.

Classified images that can be shown over air photos or high resolution satellite images

This combination gives a feeling for locality and structure to the classified imagery.

Combining some information (vegetation, water shed factors, fire hazards, etc.) with elevation

The information (for example, fire danger level) is generally shown in color, against the elevation data which is shown by intensity.

Using both absolute values and structure from a single source of data

A single source of data is usually processed to show the absolute high/low values as a color graduation. This is integrated with the same data processed to show structure.

This technique, known as *pseudocolor colordrape*, is a powerful method for on-screen interpretation and annotation of data.

Common types of data displayed this way include:

Elevation: where color represents the height, and intensity represents the structure (slopes and values).

Magnetics images: where color represents the height, and intensity represents the structure from the magnetics.

3-D seismic two-way-time horizons: where color represents the time response on the two-way-time, and intensity is used to highlight structure.

Bathymetry data: where color shows depth, and intensity shows structure.

In order to fuse these or other types of data, one of several different data fusion techniques may be used. It should be noted that this list is not exhaustive. You may find other techniques of interest, and choose to use them. Because data fusion is implemented using algorithms, it is not necessary to have specialised programs to carry out data fusion. New techniques can be implemented by the user using the ER Mapper Graphic User Interface, within the standard structure.

The rest of this section explains some of the common techniques in more detail.

Pseudocolor colordrape data fusion

Pseudocolor colordrape data fusion is the simplest of all. It is often used to show two variables: one in color, and one in intensity. The information shown in color would be shown in a Pseudocolor layer, and the information to be shown in intensity would be shown in an Intensity layer.

To create a pseudocolor colordrape image, the normal technique is clarify the data to display the data as separate layers, and then combine the layers.

This technique is called pseudocolor because the colors are all generated from a single layer of data, resulting in a range of colors. The exact colors used depend on the lookup table selected for the algorithm. Common lookup tables range from red as high values down to blue as low values.

An example of color drape is to drape a magnetics image, as color, over a satellite image, as intensity. Another (more common) example is to use the same band of data for both color and intensity, with the intensity being a processed version of the data to highlight structure.

It is quicker to use an existing colordrape algorithm and simply change the datasets being used. However, below is the technique to create a *pseudocolor* image from scratch:

To create a colordrape algorithm from scratch

- 1 Create a Pseudocolor layer.

Specify the dataset, and the band in the dataset to be shown as color. Transform the data so that the color range is acceptable.

- 2 Turn the Pseudocolor layer off.

This way, you can work on the Intensity layer without being distracted by the color information.

- 3 Add an Intensity layer, and specify the dataset to use.

If the dataset is different to the one used in the Pseudocolor layer, remember to click on the ‘OK - this layer only’ button rather than the OK button, as the latter would also change the dataset being used in the Pseudocolor layer.

- 4 Transform the data so that the intensity is acceptable.

You might need to apply a logarithmic or piecewise transform (a linear transform with multiple segments) to get the image to look acceptable.

- 5 Turn the Pseudocolor layer back on.

- 6 Save the algorithm so that the resulting image can be recalled at any time.

RGBI (RGB->HSI->RGB) data fusion

The RGBI technique takes a Red-Green-Blue image (for example, a Landsat TM image), and sharpens it by replacing intensity with data from another source (for example, SPOT Panchromatic).

ER Mapper has an inbuilt transformation for the common RGB to HSI, replacing Intensity, then back to RGB formula. Other variations (such as HSV transforms or the Brovey transform) can also be implemented by using virtual datasets and formula processing. For the simple RGBI case, a color image is defined in a Red-Green-Blue space. This means that three layers are defined in the algorithm—a Red, a Green and a Blue layer. These are loaded with the data appropriate for these colors. For example, bands 5, 4 and 1 from Landsat TM highlight vegetation and cultural information, whereas bands 3, 2 and 1 show a natural image.

A fourth layer, the Intensity layer, is also defined. When ER Mapper sees an algorithm which has an Intensity layer and Red, Green and Blue layers, it knows to automatically do the RGB to HSI to RGB transform.

It is important to appreciate that this transform is done on a pixel by pixel basis, and only transforms non-NULL data for a given pixel, changing it in the Intensity layer. This is a useful feature, as quite often two images (for example, a Landsat TM and a SPOT Panchromatic image) will not overlap exactly. There will be some places with both the Landsat TM and the SPOT Pan, some places with only Landsat TM, and some places with only the SPOT Pan. ER Mapper tries to provide the best result for each pixel.

Where both datasets exist for a pixel, the full transform is done. Where only the intensity data exists for a pixel, that pixel is shown in greyscale. Where only the color information exists, the raw color information is shown without the RGB->HSI->RGB transform being carried out which generally results in less detailed imagery at those pixels.

An RGBI algorithm can be built up from scratch—often you will have an RGB algorithm that you wish to sharpen by simply adding an Intensity layer.

When starting from scratch, it is faster to load and modify an existing algorithm—a similar one you have previously defined, or one of the Templates algorithms.

To create a RGBI display using the Templates/RGBI algorithm:

- 1 Load the examples/Miscellaneous/Templates/Common/RGBI algorithm into a window.
- 2 In the Algorithm dialog box, select the Red layer.
- 3 Select the dataset (for example, Landsat TM) to be used for the Red, Green and Blue layers and click on 'OK - all layers'.

This will change the Red, Green and Blue layers to use your new dataset.

- 4 Set the band to display in the Red, Green and Blue layers (click on each layer, then change the band).

Note: As the Intensity layer was defined to use a different dataset to the Red, Green and Blue layers, it will not have the new dataset. Also, if your new dataset has a different map projection from the template dataset, you may find that the Intensity layer has been turned off as it has an incompatible map projection.

- 5 Click on the Intensity layer, and load (this layer only) the new dataset (for example, SPOT Panchromatic).
- 6 For a multi-band dataset, select the appropriate band to use.
- 7 If the layer was turned off, turn it back on.
- 8 Set up the transforms.
- 9 Save your new algorithm if you wish to use it in the future to re-create this image.

Brovey transform RGBI data fusion

The Brovey transform is a highly effective transform that generates a better looking image than the normal RGBI image for many types of data, in particular for combining Landsat TM and SPOT Pan imagery. In this case, it generates natural looking water, and a crisp image that may be further sharpened without degradation by applying a sharpening filter to the SPOT Pan layer.

The Brovey transform is a formula based process that works by dividing the band to display in a given color (for example, the Green layer) by the sum of all the color layers (for example, Red, Green and Blue) and then multiplying by the SPOT Panchromatic layer.

Thus, to combine bands 5,4,1 of Landsat TM as Red, Green and Blue layers, with SPOT Panchromatic as intensity, the generic formula is:

$$(\text{Input1} / (\text{Input2} + \text{Input3} + \text{Input4})) * \text{Input5}$$

We use four inputs for the Landsat TM image because it makes the formula setup easier to modify. The above generic formula is mapped to actual bands as follows (B5, B4 and B1 are Landsat TM, Pan is the SPOT Pan):

Red layer:

$$(B5 / (B5 + B4 + B1)) * \text{Pan}$$

Green layer:

$$(B4 / (B5 + B4 + B1)) * \text{Pan}$$

Blue layer:

$$(B1 / (B5 + B4 + B1)) * Pan$$

It can be seen that to be effective, the Brovey transform requires:

- Pixels from the Landsat TM and the SPOT Pan to be processed together.
- Floating point operations.

ER Mapper can carry out the complete Brovey transform in a single step, without requiring intermediate datafiles to be created. Also, the Landsat TM and the SPOT Panchromatic data remains in their original resolution—it is not necessary to regrid the Landsat TM down to 10 meter resolution first.

To use the Brovey Transform you must create a virtual dataset containing both Landsat TM and SPOT Pan data and then apply the processing to it.

To create a virtual dataset with Landsat TM and SPOT Pan data

- 1 Create an 8 band virtual dataset that contains the 7 band Landsat TM image and the 1 band SPOT Panchromatic image.

Although we are only going to use three of the Landsat TM bands, we may as well create a virtual dataset with all seven Landsat TM bands, as it does not add to storage space (a virtual dataset is simply an algorithm that looks like a dataset—it is computed on demand) and allows you to try different RGB band combinations at a later date.

The easiest way to create the virtual dataset is to use an existing template. For Landsat TM and SPOT Panchromatic, there is an existing template that can be used called:

```
examples\Miscellaneous\Templates\Virtual_Datasets\Landsat_TM_and_SPOT_Pan
```

- 2 Load this template algorithm.
- 3 Change the datasets to reflect your own Landsat TM and SPOT Panchromatic datasets.
- 4 Save your new algorithm as a virtual dataset, ideally in the area that you store the true Landsat TM and SPOT Pan images.

Follow the convention of ending virtual dataset names with the letters **_vds**, making it easy to see at a glance that a dataset is really a virtual dataset. The Landsat TM image represents the first 7 bands of the algorithm/virtual dataset, and the 8th and final band (and also layer) is the SPOT Pan layer.

Make sure the SPOT Pan layer is turned on after you finish loading it. Once you create this virtual dataset, it can be used by any algorithm requiring processing of both Landsat TM and SPOT Pan within the same formula.

To use the Brovey Transform algorithm

- 1 Load the examples\Functions_And_Features\Data_Fusion\Brovey_Transform algorithm.

Note that it has three layers: Red, Green and Blue (intensity is computed from within the formula for each layer).

- 2 Select one of the layers and change the dataset to your new virtual dataset.
- 3 Click 'OK - all layers' to load the virtual dataset into all layers.
- 4 Adjust the transforms if required.

You can sharpen the image without undue degradation by applying a sharpening filter to the SPOT Panchromatic. You can apply a sharpening filter to the SPOT Pan input for each of the layers (you need to load the filter three times, once for each layer), or you could modify the original virtual dataset to sharpen the SPOT Pan layer. Alternatively, you can create a new layer in the virtual dataset called '0.65_sharp_Pan' and add a sharpened filter to it.

The Brovey transform works well for a wide range of data, and in general is a better choice than the RGBI transform. However, as it causes visual change to colors (generally for the better), the RGBI transform is better for pure intensity sharpened transforms.

Data fusion using attribute highlighting

The attribute highlighting technique is good for highlighting certain parts of the image, based on a pixel by pixel formula. The general concept is to define a backdrop image (depicting non-valid attributes) and add another layer to emphasize the highlighted parts of the image (depicting valid attributes).

For example, an effective image highlighting water in a region can be created using SPOT Panchromatic for the backdrop, and computing and highlighting water based on the Landsat TM imagery. The SPOT Panchromatic would be used for the backdrop because of its superior resolution (10 meters), whereas the Landsat TM would be used to decide if water exists, as water cannot be reliably detected from the single band 0.65 μ m SPOT Panchromatic imagery.

To create an algorithm for data fusion with attribute highlighting

- Create an algorithm which displays the backdrop image.

This involves creating a Pseudocolor layer loaded with the SPOT Panchromatic image. Use a greyscale lookup table to create a simple greyscale image. A more complex color backdrop image could be created; however, a greyscale backdrop makes it easier to see highlighted areas.

- Highlight required areas.

For each type of highlight to be shown, create a Classification (not Classification Display) layer. A Classification layer is a layer that has a higher priority than normal raster layers (such as Pseudocolor or Red), so it shows on top of any normal raster data.

A Classification layer will only be shown if the pixel value is non-NULL for that pixel. Note that this is non-NULL, not non-zero, which is a different meaning. If, for a given pixel, more than one Classification layer is valid, then the layer with the highest numerical value for that pixel is shown.

So, to show highlights using the Classification layers:

- 1 Add a Classification layer.
- 2 Load the dataset to be used for decision making.

For example, for water detection, you could use Landsat TM.

- 3 Set up the formula for the layer, to return 1 if true for this pixel, or NULL if false for this pixel.

Many common formulas have already been defined and can simply be loaded with the **Load Formula** menu inside the formula dialog box. You can also create any formula that returns a true/false type of answer.

As water is a high absorber of infrared, the infrared channels from Landsat TM have a very low reflectance over water. The exact values depend on the region. Generally, any value below about 20 for band 5 can be considered to be water. Use ER Mapper Traverses and Cell Coordinates to look at pixel values point by point to help decide the exact value for the threshold. A more robust water test is to divide a high reflectance wavelength (blue or red wavelengths) over a low reflectance wavelength.

For the simple water test case, the formula for the Classification layer would be:

```
IF INPUT1 < 20 THEN 1 ELSE NULL
```

Where INPUT1 is mapped to one of the infrared channels, for example Band 5:

```
IF B5:1.65µm < 20 THEN 1 ELSE NULL
```

- 4 Select a color for the highlighted areas.

For example, choose blue for water, by clicking on the color chooser button on the Classification layer.

- 5 Only areas that are water will be shown in the color selected. For other areas, the underlying backdrop image will be visible.

The above is a simple example of how to highlight certain parts of the image based on conditions. Complex maps can also be generated by combining different techniques.

More complex examples of attribute highlighting

Some examples of additional attribute highlighting techniques include:

- Combining different datasets to show time-based changes

By comparing two classified images, changes in certain classes can be picked out and highlighted. To use a formula that accesses data from different datasets, a virtual dataset that combines the different datasets must be defined.

- Assuming two classified datasets for 1990 and 1994

For example, with class number 12 for urban development, the following formula would highlight urban growth between 1990 and 1994:

```
IF CLASS_1990 != 12 and CLASS_1994 = 12 THEN 1 ELSE NULL
```

- Highlighting more than one attribute

For example, one Classification layer could be colored red, to show areas of vegetation decrease, and another area could be colored green, to show vegetation increase.

- Only showing attribute data within a region.

For example:

```
IF inregion('Colorado') and B5:1.65um < 20 then 1 else NULL
```

would highlight water only in the region defined as Colorado.

- Using noise removal or averaging filters to remove small areas, to show a smoother image, or to highlight only larger areas.

It is important to put any filters before rather than after the formula, as the formula inserts NULLs into the data, and the filters would cause the resulting data to shrink by rejecting areas bounded by the NULLs. If the formula is a true/false from complex input data, create a virtual dataset which generates the desired data, and then run that data through a filter before the final 'IF <true> THEN 1 ELSE NULL' formula.

Two good filters are the median filter, to remove small areas, and smoothing filters, to generate more regular looking areas.

Data fusion using region highlighting

Region highlighting entails using the INREGION() function within formulas to decide if the area to display falls within the region(s) of interest. It will only be displayed if it does.

As with attribute highlighting, this technique can be combined with backdrop maps to generate detailed information only within areas of interest.

For example, a greyscale SPOT Panchromatic image could be used as a backdrop behind a classified image of Landsat TM, that is only shown within certain areas of interest (perhaps forest stands).

The region highlighting technique (like attribute highlighting) can be applied to any raster layer type. However, the attribute highlighting technique is most effective for Classification layer types.

In the following examples, the term `INREGION('my region')` will return true/false if inside the region named 'my region', whereas the term `INREGION(REGION1)` means that in the formula the variable `REGION1` must first be mapped to a valid region for the dataset before it is used. By default, when adding a region variable (`REGION1`) to a formula the region 'All' is used, which is unlikely to be the region you want.

It is much better to use `REGION1` (or `REGION2`, `REGION3`, etc.) and map it to a region, rather than specifying an absolute region name, as it makes your formula much more flexible and easy to change.

Common region highlighting techniques for different layers include:

- Region highlighting by a single blocked out color.

Use a Classification layer set to the appropriate color, with the formula:

```
IF inregion(REGION1) THEN 1 ELSE NULL
```

Note: Use '... ELSE NULL' not '... ELSE 0', which would set the entire image to be classified.

- Classification highlighting only within a region of interest.

Use a Classification Display layer (not a Classification layer), and the formula:

```
IF inregion(REGION1) THEN INPUT1 ELSE NULL
```

Note: Use '... THEN INPUT1 ...', as the Classification Display layer type takes the input value, and runs it through the colors defined for the classified file. This can be used to advantage. For example, to display certain classes only within a region, you can use:

```
IF inregion(REGION1) and INPUT1>10 and INPUT1<20 THEN INPUT1  
ELSE NULL
```

This would only show classes if they are within the range 11 to 19, and in the region defined by `REGION1`.

- Color highlighting only for a colordrape image

By leaving intensity still in the image, this leaves an overall feel for the map, but draws attention to the area defined by the colored image. The `INREGION()` would be applied to the Pseudocolor region. The same concept also applies to RGBI images.

- Imagery highlighting only within a certain area

For example, it might be desirable to only show data within a certain map sheet, or within a certain county or state. In this case, for each raster layer, add the `INREGION()` to the formula:

```
IF INREGION(REGION1) THEN INPUT1 ELSE NULL
```

Regions are associated with raster datasets. They also contain other, statistical, information for the polygon region.

It is sometimes desirable to use a vector polygon as a region across different datasets. In this case, use the vector polygons <-> raster dataset regions function in ER Mapper to create regions within raster datasets from vector file polygons and vice versa.

Note: Regions are stored as polygons (not bitmaps) within the raster dataset header. Because raster regions contain additional statistical information, they must be associated with each raster dataset, which is why simple vector polygons from vector files are not used for INREGION() and associated functions within formulas.

Fusion of vector and raster data

ER Mapper can also show vector based data over raster (and classification) layers.

This data can come from many sources. It can be from ER Mapper vector files, or from external GIS or DBMS systems.

Access to vector data is via a technique know as Dynamic Links. Each link may have its own processing techniques. For example, the ARC/PLOT based link (UNIX only) allows entire ARC/PLOT (and AML) based scripts to extract data from a ARC/INFO GIS and display it in an integrated fashion with other ER Mapper information.

Some points to consider when working with vector overlays:

- Vector layers may or may not allow additional selection and processing of the vector data.

This depends on the actual link implementation.

- Data is left in the external system, and the dynamic link is run on demand each time the algorithm is processed and displayed or used to generate hardcopy.

The ER Mapper algorithm always shows the latest information in the external system.

- The Raster to Vector conversion function within ER Mapper can be used to define polygons and vectors based on raster data.
- Each layer may be either a single color, or may generate multiple colors within that layer. This is up to the dynamic link of that layer.

Single color layers are known as MONOCOLOR layers, and multiple color layers are known as TRUCOLOR layers. MONOCOLOR layers may be any color—but only one color per layer.

- You can change priority on vector layers, just as with raster layers.

Moving a layer up or down means it will be drawn over or under another vector layer.

- The Map Composition functions can have dynamic links within map objects.
This means that you can clip a vector layer (for example, a road network) to only display within a polygon region defined by a map object.
- You can add your own dynamic links to your own custom vector layers, for access to proprietary systems.

Useful formulas for data fusion and mosaicing

There are a number of formulas and processing techniques that are useful for data fusion and mosaicing. Many of these techniques can be applied in varied situations, so some ideas are listed here:

Using PC1 to show terrain and terrain changes

For Landsat TM, PC1 (principal component number 1) is often the terrain. This is because the most significant change on a pixel by pixel basis is often the effect of shadow on terrain. This is most apparent in hilly or mountain areas, but less effective in urban regions. Band 6 (the thermal band) should not be included in this calculation.

By showing PC1 as intensity, good structure is visible from most Landsat TM imagery.

By using an algorithm to compute PC1 for two different Landsat TM images, then subtracting one from the other, areas that have had structural change (for example, hill slippages, water erosion, sand dune movement) become visible—without having digital elevation changes for the area.

To generate this sort of image, create a virtual dataset that contains the 14 bands from both Landsat TM images. Then use the 14 band virtual dataset to create a principal component number one for each dataset, which in turn are used in another calculation.

The formula $(I1 - I2) / (I1 + I2)$, where $I1=[\text{scene\#1 PC1}]$ and $I2=[\text{scene\#2 PC1}]$, is an effective method of normalizing the data.

Using INREGION() on a conditional basis

It is often desirable to do processing based on INREGION if the pixels in question are within a region (that is, vector based polygons). For example:

```
IF INREGION('Forest') THEN . . .
```

This will process only data in the region called 'Forest'.

Complete AND and OR logic can be used for regions. For example, the formula:

```
IF INREGION('Forest') and INREGION('West County') THEN ...
```

will only process pixels that are both of the regions 'Forest' and 'West County'. Note that an ER Mapper region is defined as one or more polygons, so the result of the above can be quite complex.

As another example, to process pixels that are inside the region 'Forest' but not in the region 'West County', whose values are less than 100 use:

```
IF I1 > 100 and (INREGION('Forest') and not inregion('West County')) THEN ...
```


Digital Elevation Models

Author

Stuart Nixon is the Founder of Earth Resource Mapping.

Abstract

Digital Elevation Models (DEMs) are a digital representation of elevation, organized as a regular grid of numbers. A great many applications, such as laying pipes or assessing fire risks, have a direct use for DEMs. This study examines how DEMs are created, ways to enhance DEMS and extract information from them, how to combine DEMs with other types of data, and how to do what-if processing with them.

Introduction

Digital Elevation Models are represented as a regular grid of numbers. The spacing between grid elements represents the interval between samples. For example, a 30 meter grid spacing means that there is one elevation sample every 30 meters. The numerical value in each grid element represents the elevation at that point. This is often a floating point number, to ensure that small variations in elevation can be recorded accurately.

This chapter discusses the generation and quality of DEMs, the display and integration of DEMs with other types of data, and how to carry out what-if processing and classification of DEMs and related data.

Sources and quality of DEM data

DEM creation

DEMs may be created from a number of sources, including:

- **Measuring selected elevation points over an area, and then gridding them into a regular grid using a gridding package.** This technique has several disadvantages, including the effort required to collect the individual elevation points, and inaccuracies in the regular grid in areas where limited numbers of points have been gathered. Any area that has had gravity surveys will also have elevation heights collected at each point. Otherwise, the source for individual elevation points are likely to be from analytical plotters.
- **Generating a DEM from a contour line source of elevation, for example, from a map or from an LIS system.** Contour maps are generally created using analytical plotters, and thus have a large range of points gathered. Also, contour maps typically have valley floors and ridge lines defined, ensuring that these crucial aspects of a DEM are well preserved. When generating a DEM from a contour source, care must be taken to ensure that the resultant DEM does not have a “terraced” effect between contour lines.
- **Interferometric SAR processing.** This computationally intensive technique uses phase between Radar signals to derive a complete elevation map. Advantages include good accuracy regardless of climatic conditions. Disadvantages include some range of errors over the resultant DEM, and currently a limited range of SAR systems capable of being used to generate these DEMs.
- **Softcopy Photogrammetric generation of DEMs by comparing stereo airphoto or satellite images using autocorrelation techniques.** This technique allows a quite dense mesh of DEM points to be computed. There can be a wide range of output from different DEM generation systems. Some systems generate a sample of DEM points, which are then gridded up to a higher resolution. Other systems generate a high number of points, but a significant number of points can be inaccurate.

DEM quality

An important consideration is the quality of the DEM being generated. Ideally, you should know the original source of data and the processing technique used to convert the original elevation samples into a regular grid.

Before working with a DEM, your first step is often to carry out *real time shading* on the DEM grid, to observe if any gridding errors exist. You should examine the DEM from different elevation and azimuth perspectives, as many errors only become obvious from certain angles or while interactively carrying out the shading. Errors to look for include:

- **Terraces of regular flat areas** (indicating a poor gridding result from a contoured line source).
- **Large, very regular areas as compared to areas with many small variations.** This might be an indication of a poor source of data, with only a few grid points in the large regular areas.
- **Regular shadow strips in the DEM, in a particular direction, often more visible when the shading elevation is near the horizon.** This is indicative of a gridding system introducing artifacts in a certain direction. This is a very common gridding problem, and shows up on most DEMs generated using gridding techniques. The problem can often be minimized or eliminated with different gridding techniques. Also, *FFT filtering* of the data in the frequency domain can remove gridding artifacts. Another cause of regular variations in DEMs can be systematic errors in autocorrelated DEMs, in particular from satellite images.
- **Areas with sharp variations in height.** This is often an error introduced by automated DEM generation systems which incorrectly assign an elevation height to points, due to shading or other problems in the original stereo pair. If the data can't be reprocessed, selective use of a *median* or other form of ranking filter can remove most of these errors; as with all filtering techniques, care must be taken that valid data is not removed during the filtering process.
- **Incorrect registration.** A surprising number of DEMs are gridded using incorrect map projection/datum details—or the data may have been generated using a map projection/datum different to that of other data you are working with. Unlike airborne photo and satellite data, where mis-registrations are obvious, mis-registrations in DEMs may not be obvious unless looked for. When looking for mis-registration, either examine the elevation value at several known locations (use the **geoposition - zoom center of image** window to center an image window on a specific location), or compare river forks, etc., with the same location in other imagery or vector data over the same area. If the DEM is in a different map projection and/or datum, use the **Image Rectification - Map Projection to Map Projection** function to rectify (warp) the DEM into your desired projection.

Displaying and processing DEMs

Once your DEM has been gridded to your satisfaction, and is in the appropriate map projection and datum, a considerable range of processing and display techniques are available to you to extract the information held with a DEM.

In general, these can be divided into three categories:

- Displaying DEM data in a number of ways.
- Integrating and displaying DEM data with other sources of vector and/or raster based data.

- Processing DEM data using what-if rules.

The following sections examine the above in more detail.

Typical DEM applications

Because the processing and display of DEM data is largely dependant on the resultant application, ER Mapper's ability to quickly and easily process and integrate DEMs makes it quite easy to make effective use of DEM data. For example:

- You need to identify areas of high fire risk, considering the direction of prevailing hot winds, and the dry vegetation content. This can be quickly done by comparing the dry vegetation index from Landsat TM, with the slope (steepness) and aspect (direction) of a DEM. The threshold could be applied to the resultant image, indicating areas of high fire risk.
- A new water pipeline is to be constructed. Key factors are the slope, and the variation in height, between proposed starting and ending points for the pipeline. An image showing regions of low slope, and within the desired height band, can be constructed. This image can then be draped over the original DEM and viewed in 3-D to select optimum pipeline locations.
- You need to identify fire-break roads that must be constructed in a forested area, to reduce fire impact. After doing on-screen annotations identifying the required roads, a stereo pair hardcopy image can be generated which is a merge of DEM data to show height, air photo data, and vector based annotations showing where the required fire-break roads must be built. These stereo pair images can be given to construction teams in the field, who now have accurate maps that show the location of the required fire-break roads in context with air photo images of the area. The stereo pair images appear as true stereo images when viewed through a standard stereo pair viewer.
- A new development which must meet strict visibility impact guidelines is to be carried out. By draping air or satellite images over a DEM, the proposed development can be viewed from any position, in stereo, using the real-time perspective stereo capabilities of ER Mapper.
- You wish to carry out geological interpretations in the field, to identify candidate locations for exploration drill locations, based on a combination of aeromagnetic data, geochemical data, and elevation observations. By generating a false color aeromagnetic image, adding the geochemical data (stored in vector or point form, possibly in an external system) to a DEM, and then printing a hardcopy stereo pair of the image, the geologist can take an image to the field that can be viewed in stereo using conventional stereo viewers. ER Mapper has the ability to generate a stereo pair that has one image orthographically correct and the other image containing the elevation changes. The geologist can carry out interpretations in the field on the orthographically correct image. These interpretations can then be entered into the computer back at the office using a digitizer.

- You need to observe sedimentation and erosion effects from a recent severe flood. ER Mapper can compare before and after DEM images of the affected area, highlighting areas where elevation has decreased, or increased, in different colors. The volumes of erosion can also be computed from this differencing of DEM images.

As can be seen, the applications for DEM data are quite varied, and the actual techniques used to process, integrate, and display the DEM data vary depending on the required results.

Keeping this in mind, the following sections cover in detail the different display, processing and integration that can be carried out on DEM data. Where appropriate, real world examples are given for the use of the different techniques.

As with using any part of ER Mapper, it is important to appreciate that, like a spread-sheet, ER Mapper provides a powerful what-if tool. The effective use of this tool comes from understanding the underlying functionality and how to apply it.

Displaying DEMs

There are a number of basic ways to enhance and display DEM data (in all of the following discussion, any technique used for display can also be output to a hardcopy print). The basic techniques can in turn be combined to come up with superset display techniques, which combine the DEM data with other types of data.

Many of these techniques are useful because of the nature of DEM data: unlike the spectral responses from a satellite image, which might vary wildly from one location to the next, there is often a correlation between one DEM location and the next. In this respect, there is a close affinity between display techniques for DEMs, and for field strength datasets such as gravity datasets or magnetic datasets. Indeed, all of the display techniques discussed here for DEMs are also applicable to field strength datasets.

As with all of ER Mapper display techniques, the display techniques can be applied directly to the original data—or to virtual datasets containing more than one source of data—without having to generate intermediate image files.

Note that vector overlays and dynamic links to external systems such as GIS and DBMS systems operate in all ER Mapper display modes detailed below. Thus, you can, for example, carry out an annotation interpretation while sun-shading a DEM to show structure. Also, the following display techniques don't have to be applied to just the basic DEM data. For example a false color image can be made of the Slope computed from a DEM, rather than from the original DEM.

The basic display techniques and combination techniques are as follows.

Greyscale image

A greyscale DEM is the simplest image that can be displayed—by assigning a grey shade to each elevation value. A greyscale DEM image is also one of the least useful images, as it does not enhance structure, and as it is difficult to see changes in elevation in a grey image (because your eyes are less sensitive to grey scale changes than to color changes). You can generate a greyscale by clicking on the “Common Toolbar: Greyscale” button, or by loading the “examples\Data_Types\Digital_Elevation\Greyscale” algorithm and loading your own dataset. A greyscale image can be generated using a Pseudocolor layer in the algorithm with a greyscale lookup table loaded, or using an Intensity layer in the algorithm which is automatically a greyscale image (if no other raster layers exist in the algorithm).

False color image

A false color image is similar to a greyscale image except that a palette of colors is allocated to the different DEM values. By selecting a color lookup table that highlights differences in values, such as the step lookup table, you can differentiate subtle differences in elevation height. Also, the transform can be changed in realtime to selectively highlight a certain range of DEM values. You use a Pseudocolor raster layer for false color images.

Realtime “Sun” shaded image

The realtime sun-shaded image is a powerful mode used to highlight structure within a DEM. It is called “sun” shading because it simulates how a terrain surface would look if the sun were in different positions (defined as azimuth rotation from North, and elevation above the horizon). ER Mapper will update the sun-shaded image in realtime, as the “sun” is moved via the sun-shading window for the raster layer. A sun shaded layer is normally set up as an Intensity layer, so that it can be combined with a Pseudocolor layer to generate a colordrape image. To produce a sun-shaded layer, turn the sun-shading on for the desired layer. ER Mapper 5.0 can update a real-time sun shaded image on any display type (that is, on both 24 bit and on 8 bit displays).

When the sun is overhead the resultant image shows “dip” for the DEM. In other words, it shows features in the DEM regardless of angle. If the DEM is a high detail DEM, and you are interested in seeing only major structures within the DEM, you can add averaging filters to the layer prior to carrying out the sun-shading.

When displaying a sun shaded image, using a logarithmic transform often generates a more balanced looking image than the default linear transform.

Realtime combined “Sun” and “False Color” Colordrape image

This is a very powerful technique, created by combination a False color Pseudocolor layer (or possibly Red, Green and Blue layers) with a “Sun” shaded layer in Intensity. With this display technique, you can modify the structure highlighting by moving the sun shading position (on the Intensity layer) in real-time, and you can modify the color highlighting (on

the Pseudocolor layer) in real time. You can also modify the transform in the Intensity layer to brighten or darken the overall image; a logarithmic enhancement works well for this.

The advantage of this technique is that you can see both absolute elevation height variations (the color of the image) and the structure in the DEM (the shaded intensity).

Shiny (HSI model) Colordrape image

The “shiny” colordrape is a technique developed by an ER Mapper user to provide a different reflectance model for colordraped images. It is a good example of how quite different display techniques can be achieved, using the standard ER Mapper software and user interface. As with the standard colordrape image, this technique results in a colordrape image showing the DEM height as color, and the structure from the DEM as shaded intensity.

Unlike the standard colordrape model, which uses two layers (Pseudocolor and Intensity) with an internal calculation of reflectance, the shiny colordrape uses three layers in the algorithm: Hue, Saturation and Intensity. The original height values are assigned to the Hue layer, and the shaded intensity to both the Saturation and the Intensity layers. By modifying the transforms for the Intensity and in particular for the Saturation layer, we can achieve a “shiny” look to the colordraped image.

In this processing, we apply transforms after the sun-shading is carried out. To do this, we use an algorithm (or virtual dataset) containing two layers: Height (the original DEM data) and Structure (the sun-shading we wish to use). This algorithm, instead of the original data, is used as input to the HSI mode.

To create a shiny colordrape image

The easiest way to create the required algorithm to input to the shiny colordrape HSI display mode is to:

- 1 Create a normal colordrape algorithm (with two layers: Pseudocolor and Intensity). The intensity layer has sun shading turned on.
- 2 Name the Pseudocolor “Height” to indicate that it is the original data, and name the Intensity layer “Structure” to indicate that it is a shaded version of the original data.
- 3 Save the colordrape algorithm.
- 4 Create an HSI algorithm with three layers.

The easiest way to do this is to load the “examples\Data_Types\Digital_Elevation\Colordrape_shiny_look” algorithm. Load your colordrape algorithm, saved in step (3) above, as the input dataset for the colordrape algorithm. Make sure you are using the “Height” input for Hue and the “Structure” input for both Saturation and Intensity.

You can now call up the transforms for the Hue, Saturation and Intensity layers. Changing the transforms will have the following effect, all in real time (regardless of display type):

- Hue layer: This will change the color of the image.
- Saturation layer. This will change how saturated (or white looking) colors will be. Because this layer uses the “Structure” you will not change the overall saturation but rather the saturation on areas with changing structure. Generally, an image that shows a white looking surface on structure changes will look as though it is shiny.
- Intensity layer. This will change the overall intensity of the image.

Mosaicing DEMs

In ER Mapper, any time there are more than one of a type of raster layer, those layers are automatically mosaiced. For example, if you have more than one Intensity layer, all the intensity layers are automatically mosaiced together. Each of the Intensity layers can display a different dataset, and each dataset can have a different resolution and data format. The act of having more than one raster layer of the same name automatically tells ER Mapper that you want to mosaic the datasets in question—nothing else is required.

Some issues that make mosaicing easy to do:

- You can use the Image Display and Mosaic Wizard on the Common Functions Toolbar to automatically create a mosaic of all files of the same type in a particular directory. The wizard does all the basic setup work for you and the resulting mosaic can then be fine tuned by hand if necessary.
- After mosaicing and balancing the DEMs, it can be convenient to treat all the input DEMs as a single “dataset”. Unlike older image processing systems, which require you to generate an output dataset which is a merge of all the input datasets, you can simply save your mosaiced algorithm, and then use the algorithm as input to other algorithms, thus making the datasets appear to be a single dataset. (You can also use the **Save as Dataset** option on the **File** menu to create a true output dataset, for example to use in an external system as a single gridded file).
- You specify the priority of the DEMs to be mosaiced by the order of the layers. For example, you may have several DEMs to mosaic together of different resolutions—perhaps a coarse DEM covering a large area, and several detailed, higher resolution DEMs over parts of the area. In this case, you would put the higher resolution DEMs at the top.
- DEMs quite often have leveling problems—they are not exactly the same level along the edges, resulting in a quite noticeable lip along each edge. You can remove this lip in several ways:
 - turn on feathering in the algorithm (the feathering menu will automatically be enabled when you have more than one raster layer of the same type in an algorithm). This will feather datasets, left to right, along the overlap line.

- Define polygon regions that you wish to bound a DEM by. For example, you might choose to use a river as the border of a DEM. Use these regions in the layer formula, to selectively mask out portions of a DEM, for example:

```
IF inregion(REGION1) THEN input1 ELSE NULL
```

In the above, you would use the formula window graphical user interface to map REGION1 to the region you wish to use to bound the dataset.

- You can use histogram equalization to equalize the histograms for each of the DEM datasets. However, this should be used with caution, as the resultant values for the DEMs, while looking balanced between images, will no longer reflect the true DEM values (this is always a problem with histogram equalization).
- Apply linear leveling across the image, using statistics for edges, to level the image. In this case, you would apply a linear ramp (or polynomial ramp) to a dataset to match edges exactly with another dataset.

In most cases, mosaicing will be all that is needed. Note that, when shading DEMs you will not see mosaic lines anyway, as a shaded image ignores level differences between images. Thus, for most common DEM mosaicing operations, feathering might not be needed at all.

- If you have DEMs at very different resolutions you might find that coarse DEMs are so coarse they are at a lower resolution than the display (or hardcopy). Selecting **Smoothing** on the algorithm will automatically interpolate images, removing the blocky pixel look to the imagery.

Edge enhancement and other filters

More correctly processing techniques, these are filter operations that process the DEM data in such a way as to highlight only certain features and structures. Filters can be added to any raster layer by selecting the **Filter** button (in the **Algorithm** dialog box) and loading a filter. You can append more than one filter to a layer if you wish. The filters process data in double floating point precision so no DEM accuracy is lost.

Some useful filters for DEM display include:

- **Sun angle filters.** These filters are edge filters, and highlight structures in a specific direction. Unlike the real-time sun-shading mode, you must load (or create) a new filter if you wish to change the angle of the filter. The size of the filter affects the size of the structures being highlighted. Thus, a 3 x 3 filter will highlight considerable detail, including smaller structures, whereas a 9 x 9 filter will only highlight major structures present in the DEM.
- **Averaging filters.** These blur the data, by taking an average of neighboring cells. These are useful for smoothing noisy DEMs prior to sun-shading them. Average filters are also handy for showing high frequency information in the DEM, in other words areas that have considerable variation. By subtracting an averaging filter from the original DEM, the resultant image is a high frequency image showing areas that are rough. To subtract a filter from the original data, create a layer with the following formula:

INPUT1 - INPUT2

On the INPUT2 input stream to the formula, add the average filter.

- **Ranking filters.** So called because they “rank” data in various ways, ranking filters are useful for cleaning up noisy DEMs—especially useful for DEMs that have a lot of noise due to a poor autocorrelator taking some DEM values from tree crown height and some values from the ground. The best filters here are majority filters which replace the DEM value for a cell if it is significantly different from the neighboring cells.

Raster contour line generation

The best way to generate contours with ER Mapper is to use the Contouring Wizard on the Common Functions toolbar.

Another approach is to generate a quick raster contour line from a DEM is outlined below. (Note: the examples\Data_Types\Digital_Elevation\ Contours_from_Raster algorithm is already set up—just load it and change the dataset to your DEM).

To generate a simple raster contour line

- 1 Add a Classification layer to your algorithm, and load the DEM into this new layer. Select a color for the layer. This will be the color of your contour lines.
- 2 For the formula for the Classification layer, define the following formula. For the “base” variable put in the starting level for the contour lines (for example, 1200 meter height) and for “interval” put in the interval between contour lines (for example, 100 meters).

```
(CEIL(((input1 - base)/interval))*interval)
```

- 3 After the formula, add a laplacian filter. This filter will set all values between contours to zero.
- 4 Change the final transform to a notch transform. The transform should stay at zero until the value 0.5 on input, then go straight up to maximum output (e.g. 255) then stay there until the final value of output.

When run, the above layer will “classify” the DEM into contour lines. It is simple to enhance the above formula to only show contours within a certain range of DEM heights, using IF ... THEN ... ELSE ... processing.

Because these contour lines are raster based it is best to use a dynamic link to a contouring system for more advanced contouring.

Realtime 3-D Perspective views

The 3-D perspective viewing capability in ER Mapper can be used to examine DEMs as a 3-D perspective. The 3-D viewer takes a standard algorithm and uses Height layers to produce a perspective view of the algorithm. When working with perspective views, remember that:

- When you save algorithms, ER Mapper will store your view position, background color, and so on, to allow you to easily generate the same perspective view again.
- If you don't have any Height layers in your algorithm the 3-D viewer will search for and use Intensity layers instead. Thus, you can directly load a normal Colordrape (Pseudocolor/ Intensity) algorithm into the 3-D viewer without changing Intensity to Height and it will work.
- Any algorithm (that has one or more Height and/or Intensity layers) can be used to generate 3-D perspectives. Thus, you can drape a satellite image and GIS vectors over a DEM and view the result as a perspective.
- ER Mapper has two different 3-D viewers. One, which runs on all platforms, is a software based viewer. The other, which is not yet available on all platforms, is faster and also allows stereo glasses to be used.
- You can drape vectors over perspective views; however, you need to process the view at a higher resolution in order to make effective use of vector overlays.
- You can run the viewers in fallback modes, which process the image at a lower resolution while moving the image, then redraw at a higher resolution once you stop moving the perspective.
- On workstations capable of real time texture mapping the ER Mapper 3-D viewer can generate the texture for the displayed image at a different (higher) resolution to the triangulated mesh used for height. You may need to try different resolution texture maps and different resolution triangle meshes to obtain the optimum resolution and speed for your workstation.

Realtime 3-D Flythrough views

The flythrough views are available from the Realtime 3-D viewer in ER Mapper. The notes in the 3-D Perspective section above are also applicable to Flythrough views. In flythrough mode you can bring up a bird's eye view which allows you to see the look direction for your current flythrough position.

Stereo Realtime 3-D Perspective or Flythrough views

On some platforms, you can view both perspective and flythrough views in true stereo. To do this you will need stereo glasses for your computer. Some computers, such as Silicon Graphics workstations, come “stereo ready”. You just need to add a stereo transmitter and stereo glasses. Other computers require specialized display boards and/or displays to accept the higher refresh rates used by stereo glasses.

The notes in the 3-D perspective section above are also applicable to stereo mode.

Hardcopy Left/Right Stereo pair images

Any algorithm that can be displayed as a perspective (or flythrough) can also be output as a hardcopy stereo pair. In this case, you select **Stereo...** options in the **Print** window (from the **File** menu).

Some points to consider when generating stereo pairs:

- You can vary the stereo angle (which varies the apparent height) of the stereo pair.
- When generating stereo pairs, if you wish to annotate over the images, generate one of the images as an orthoimage. This image will then have no height distortions (all distortions are in the other image of the pair) allowing you to annotate on the image in the field and then digitize directly from the image.
- Vectors, and any other form of dynamic link such as links to GIS systems and to DBMS systems, can be included over stereo pairs. Because stereo pairs are produced at hardcopy device resolution, the vectors will be of high quality.
- When generating stereo pairs, each image printed is limited to a maximum of the size of one page of output. However, as you can output to graphics formats, you can if desired generate very large stereo pair images by generating to a graphics output format such as TIFF.

Other display techniques combinations are also possible. For example, you can generate a Red, Green, Blue image, each layer consisting of the DEM data shaded from a different direction. While somewhat confusing for interpreting complex areas, such an image allows easy examination of the major strike directions for the entire area in a single image.

Integrating DEM and other data

It is quite often desirable to combine DEMs with other sources of data: for processing (discussed in more detail in the following section); or for integrated display of DEMs and other data.

There are several ways to integrate the display of DEM data and other sources of data. These include:

Colordrape et al

All of the display view modes discussed above can be used for integration. For example, the NDVI (a vegetation index that measures biomass) from Landsat TM could be color coded, with red being high vegetation content, through the spectrum to blue being low vegetation content. This could be draped over the DEM in an Intensity layer (or viewed in 3-D), to see the correlation between vegetation and DEM height.

RGB-Height display views

The RGB-Height combination is often used when you have a color image, for example a satellite image, which is to be shown over a DEM image. The term RGB-Height is not a special display mode: it simply indicates an algorithm that has Red, Green and Blue layers (containing the satellite image), and a Height layer containing the DEM. If you use an Intensity layer instead of a Height layer, and turn on sun-shading for the layer, you get a form of colordrape image: that is, RGB, converted to HSI color space, with intensity replaced by the Height from the DEM, and then converted back to RGB colorspace.

Classification-Height display views

In this combination, imagery that has been classified into land use can be displayed as Classification Display layers, over a DEM in an Intensity or Height layer.

Raster and Vector data integration

Algorithms that process and display DEMs can also show other data. This other data can be data in vector formats (for example GPS coordinate information from a GPS unit, shown as a DXF format file overlay), or data from a GIS (for example displaying a road network from an ARC/INFO coverage over the DEM), or from dynamic links to external products, such as a custom link to an Oracle database showing microcell locations for a cellular network.

All of the normal vector dynamic link capabilities and vector editing can be carried out over processed DEM data.

These links are also visible in 3-D views (perspectives, flythroughs, and hardcopy stereo pairs) that can be generated by ER Mapper.

Processing DEMs

In addition to the display modes described in the previous section, DEMs can be processed using what-if processing. This adds considerable value to the use of DEMs, especially when the DEM data is combined with other types of data.

In general, there are a number of types of processing that you might want to do with DEM data, reflected by the nature of DEM data. This processing includes:

- **Generating slope from a DEM.** Slope is a measure of how steep any given area of a DEM is. Two slope filters are provided: *slope*, which returns a number from 0 to 200 as a percent of slope, where 0% is no slope, 200% is maximum slope, and 100% is a 45 degree slope; and *slope_degrees* which is slope measured as degrees, from 0 degrees (no slope) to 90 degrees.

The slope filters have been implemented as standard filters in ER Mapper. You can create your own variations of the slope filter in the same way—these filters are not hard coded into ER Mapper.

As with all ER Mapper processing of this nature, a feature is that the slope filter can be directly applied to the DEM, and the results used. It is not necessary to create an intermediate “slope” dataset on disk.

Because filters are processed in double floating point precision, the results are accurate to the accuracy of the original data.

- **Generating aspect from a DEM.** Aspect is a measure of the direction a slope is facing, with 0 being North, 90 being East, 180 being South, and so on. Aspect is implemented as a standard filter, which you may inspect and use as a basis for creating your own specialized slope filters.
- **Selecting a range of heights from a DEM.** For example, there might be a range of heights that are allowable for building a road or pipeline (in conjunction with an allowable range of slopes within that height range).
- **Selecting DEM values within certain regions.**
- **Abstracting data.** Using Virtual Datasets or Algorithms to give abstracted views of the original data.
- **What-if processing** on the above can be carried out to perform general queries, such as all areas with a limited range of slope, within a certain height range.
- **Combining DEM data with other sorts of data, for what-if processing.** For example, highlighting all polluted areas (from an assay database) at lower height levels, or highlighting all areas with a certain slope that are very wet—indicating possible mud slide danger areas.
- **Combining DEM data with other sorts of data for classification work.** It has been shown that classification techniques can be dramatically improved if DEMs are used as one of the layers of the input data being classified. For example, certain types of trees only grow above certain heights. In this case, the raw DEM height data would be used. The slope from a DEM can also be used as input to classification techniques, to improve classification in regions where slope makes a difference to the type of vegetation cover.

The following sub-sections discuss each of these types of processing in more detail. In many cases, combinations of the above are used, along with combinations of display methods and integration with other types of data.

Slope from a DEM

Slope from a DEM is computed by comparing the value for a DEM cell with the value of its neighbouring cells. The result is normalized, so that slope is measured regardless of the direction of the slope.

The standard slope filters supplied with ER Mapper work from a 3 x 3 region. This can be expanded by modifying the slope filters, or smoothing or other averaging filters can be inserted into the layer prior to the slope filter to smooth the DEM prior to computing slope. (Large slope variations over small areas can be a problem with DEMs generated by some stereo pair autocorrelation DEM software products.)

The slope filter is added to a layer simply by adding the filter_DEM/slope or filter_DEM/slope_degrees filter to the layer. The slope filter returns a slope number from 0 to 200; the slope_degrees filter returns a number from 0 to 90.

Aspect from a DEM

Aspect from a DEM is computed in much the same way as slope, except that the value returned by the filter is the direction of slope, measured in degrees from 0 to 360.

The aspect filter is added to a layer by adding the filter_DEM/aspect filter to the layer. The filter returns a number from 0 to 360.

Selecting a range of heights from a DEM

Selecting ranges of heights from a DEM is achieved by the use of IF ... THEN ... ELSE ... logic within a layer formula. For example, to only show DEM heights between 1200 and 1500 meters, the following formula would be used (INPUT1 would be mapped to the DEM height band):

```
IF input1>=1200 AND input1 <=1500 THEN input1 ELSE NULL
```

The use of upper and lower case in the above formula is optional; it is only used to clarify the formula.

If the above formula were added to a Pseudocolor layer for a colordrape algorithm (an algorithm with both a Pseudocolor layer and an Intensity layer) the image would be greyscale in areas outside the height range of 1200 to 1500, and colored in areas within that range. This is an effective way to draw attention to areas that meet the height range criteria.

Showing DEM values within Regions

The formula INREGION function can be used to selectively work with a DEM, within one or more polygons in the DEM.

In this case, the formula would contain the INREGION function, for example as in the following generic formula:

```
IF inregion(region1) and not inregion(r2) THEN i1 ELSE NULL
```

The term “r2” has the same meaning as “region2” (it is an abbreviation), and the term “i1” has the same meaning as “input1”.

Once again, in the above example, input1 would be mapped to the height band from the DEM. Using the Formula dialog box, you would map “region1” to the region you wish to include in the output image, and you would map “r2” (that is, “region2”) to the region you do not wish included. Thus, the specific formula once mapped might look like:

```
IF inregion('buffer zone') and not inregion('towns') THEN  
B1:DEM_HEIGHT ELSE NULL
```

The above example would only show the DEM where it falls within a buffer zone, but not if it is within towns (a logical region such as ‘towns’ may consist of more than one polygon).

Abstracted views into DEMs

Given the above types of processing, we might find it convenient to have a “dataset” that contains all of the above, and possibly other, processed views of the original data. Unlike older image processing systems, ER Mapper has a concept known as “Virtual Datasets”. These virtual datasets look like real data, but are actually recomputed, on demand, from the original data, as required. This processing is carried out by an algorithm attached to the Virtual Dataset.

This concept has a number of advantages:

- Less disk space. As the processing we are doing often produces floating point precision results, we need to store the results at high precision. Virtual datasets allow us to work in high precision without wasting large amounts of disk storage.
- High precision. The processing always works from the original data, at the original resolution. You do not need to store reduced precision temporary output datasets.
- High performance. Because less data is being processed (only the original data is read), processing of virtual datasets is very fast. This is also because of the dynamic algorithm compiler built into ER Mapper, which optimizes algorithms when they are run. Also, only bands of the virtual dataset that are required for processing are generated. Thus, if only slope and aspect from a DEM view dataset are required, only these are computed.
- Unlimited processing. Algorithms and virtual datasets are not limited by disk or memory (a virtual dataset does not have to fit into memory—it is pipelined through processing).

- Simpler data views. Instead of complex processing of input data, we can construct a virtual dataset that gives “views” into the original data. For example, we might wish to look at a DEM as height, as slope, as aspect, within a certain height range, or within a set of polygon regions. Each of these views can be defined as a band in a virtual dataset.

Creating a virtual dataset requires nothing more than defining an algorithm with one layer for each band we wish to have in the virtual dataset (actually, you can do more than this, for example mosaicing several layers together into a single virtual dataset layer).

To create a virtual dataset

To create a virtual dataset, you would carry out the following steps:

- 1 Define an algorithm with one layer per view into the original dataset.

For example, we might wish to have a virtual dataset that provides us, from a single DEM, with the following information as bands; we would create a layer for each of these, and apply the appropriate formulae and/or filters (see above) to the layers:

DEM_HEIGHT	(the original DEM height)
SLOPE	(slope, as a percentage)
SLOPE_DEGREES	(slope, as degrees)
ASPECT	(slope aspect)
GOOD_HEIGHTS	(heights between 1200 and 1400 meters)
GOOD_REGIONS	(in 'buffer zone' and not in 'towns')
TM_NDVI	(The Vegetation Index from Landsat TM)

- 2 For each of the above layers make sure the layer has a name. This name will appear in the virtual dataset as the band name. Note that the final layer is not from the DEM—it is being generated from a different dataset, this time from a Landsat TM image. A virtual dataset can have bands from different datasets (this is how you get bands from different datasets into a single formula).
- 3 Make sure that the final transform for each layer is deleted (unless we actually want to scale the data to 0..255, which is not what we want in this case).
- 4 Save the algorithm, perhaps calling it “DEM_view.alg”.

This is so we can call up the algorithm at a later time, perhaps to add more bands to it, or to see what processing is being done within the algorithm.

- 5 Save the algorithm as a virtual dataset, calling it “DEM_view.ers”.

As you can actually use algorithms as input to layers, we could directly use the “DEM_view.alg” as our input dataset. However, in this case we are also saving the algorithm as a virtual dataset because virtual datasets can have statistics computed for them and can have regions added to the virtual dataset—just like a real dataset.

If you have a common view you often use for different DEMs, you can save the algorithm as a template view algorithm. To create a view for a new dataset, you would load the template view algorithm, change the dataset, and save the algorithm as a view for the dataset in question.

What-if processing

This section on what-if makes use of the example DEM virtual dataset view created above. Although not necessary, it makes the following examples easier to follow (by abstracting the DEM height data into specific, processed views).

However, in all cases it is important to note that when these examples refer to slope, aspect and so on—the original data is being used. No intermediate disk files need to be generated.

The key to what-if processing is to be able to:

- Express the problem in terms of what-if processing of your data; and
- Work with algorithm formula, kernels and transforms to achieve the results.

It is most important to appreciate that ER Mapper is not a “black box” of processing techniques. Rather, it is like a spreadsheet, allowing you to generate your own interactive processing. The following give examples of some types of processing to demonstrate how to put together what-if processing for some real world applications. When convenient, the virtual dataset created using the previous section is used as an example.

Highlighting areas of fire risk

Application: in many cases, fire risk is defined by the direction of prevailing hot winds, by the slopes that trend up from that direction, and from the vegetation biomass on those slopes. Slopes facing away from the prevailing wind, that have high vegetation biomass, are at high risk. Also, steeper slopes are at higher risk, as the flame front can travel quickly up the slope.

In this case, we have three factors to take into account: slope (from the DEM), aspect (from the DEM), and vegetation mass (from Landsat TM).

Given the view into the DEM and Landsat TM shown in the previous section, this problem reduces to a simple formula in a layer.

In this formula, we would like to express fire risk as a number from 0 to 1; with 1 being higher fire risk.

Looking at each of the three factors, the formula would be made up of the following components:

Slope

A slope of 90 degrees is maximum danger, and a slope of zero is lowest danger. To reduce this to a portion of the formula, we would do:

$$(\text{SLOPE_DEGREES} / 90)$$

which will result in 1 being high fire risk. We could weight this, against the other factors, by multiplying it by a weighting factor if we choose.

Aspect

Slopes facing south have the highest fire risk, slopes facing North have the lowest. We express this as a number from 1 (high) to 0 (low) fire risk as follows:

$$(1 - (\text{ABS}(180 - \text{ASPECT}) / 180))$$

Vegetation

In this case, the vegetation ratio returns a number from -1 to 1, with 1 being high vegetation biomass, -1 being lowest. We reduce this to a number from 1 (high risk) to 0 (low risk):

$$((\text{TM_NDVI} + 1) / 2)$$

The complete formula

Putting all this together, we get a generic formula, adding these three factors together and dividing by three:

$$((\text{I1} / 90) + (1 - (\text{ABS}(180 - \text{I2}) / 180)) + ((\text{I3} + 1) / 2)) / 3$$

Which, as the specific formula after mapping I1 to SLOPE_DEGREES, I2 to ASPECT and I3 to TM_VEGETATION, looks like:

$$((\text{SLOPE_DEGREES} / 90) + (1 - (\text{ABS}(180 - \text{ASPECT}) / 180)) + ((\text{TM_NDVI} + 1) / 2)) / 3$$

This will result a fire risk layer being output, with 1 as high fire risk, and 0 as low fire risk.

We would use the final transform in the layer to scale this number, to color code the fire risk map, using a Pseudocolor layer.

Also, we could drape the above fire risk layer over the original DEM, as a Height layer, and view the processed result in 3-D.

Showing areas at risk within regions

We could add a region selection to the above formula, to only show fire risk areas if they are within regions. We could add the following to the formula to achieve this:

General:

```
IF INPUT4 THEN <fire risk formula> ELSE 0
```

Specific formula:

```
IF GOOD_REGIONS THEN <fire risk formula> ELSE 0
```

The “GOOD_REGIONS” input is, via the virtual dataset, doing “INREGION()” functions to decide if locations are within acceptable regions of interest. Note we are using ELSE 0 here, not ELSE NULL, so that if we decide to add filters after the formula processing, the regions do not “shrink” because of null cell value processing.

Classification of fire risk

If we choose to, we could change the layer to a Classification layer, and apply a threshold to the final transform (perhaps only selecting regions with a greater than 80% fire risk).

Generating Vector polygons of high fire risk

The above fire risk Classification layer, which is computed from the original data, could be converted into vector polygons for input into a GIS system.

Before doing so, we might choose to run a median filter to remove small regions over the image (this filter would be inserted into the layer after the above formula). A median ranking filter will reject small regions of fire risk, ensuring that we only end up with large fire risk polygons for the GIS.

The raster to vector module in ER Mapper can do this conversion directly from the above algorithm (save the algorithm to disk first, then use it as input to the Raster to Vector converter).

It is important to appreciate that no intermediate image disk files were created in this entire process. The only thing that needs to be stored on disk is the virtual dataset and the algorithms—these files express how to generate the results from the original data, and are quite small files.

Deciding placement of a pipeline

In this example, we are interested in highlighting any area of the DEM that meets the following criteria:

- Slope is less than 15%
- DEM heights are within the range 1200 meters to 1500 meters

In this example, the generic formula would be:

```
IF input1<15 AND input2>=1200 AND input2<=1500 THEN 1 ELSE  
NULL
```

And the specific formula would be mapped to the following inputs:

```
IF SLOPE<15 AND DEM_HEIGHT>=1200 AND DEM_HEIGHT<=1500 THEN 1
ELSE NULL
```

In this case, I chose to use the original DEM_HEIGHT band, rather than the GOOD_HEIGHTS band, just to show the processing. Using the example DEM_view virtual dataset, a simpler formula would be:

```
IF SLOPE<15 AND GOOD_HEIGHTS THEN 1 ELSE NULL
```

which would generate the same results as the previous example.

The layer outputs 1 (valid) or NULL (no data, therefore, invalid). We would use a Classification layer to display the results of this processing. If we drape this layer over a Height layer containing the DEM_HEIGHT, we could view the results in 3-D perspective (or generate a stereo pair output) to help us decide where the best placement for the pipeline would be.

Classification using DEM data

DEM data is effective when used, in conjunction with other data, for classification. To do this create an algorithm that contains:

- the bands from the imagery you wish to classify (for example, bands 1-5, and band 7, from Landsat TM); and
- the DEM height, and possibly the DEM Slope and/or Aspect.

Make sure the algorithm has no final transforms, then save it as an algorithm (for possible use again later), and as a virtual dataset. You need to save it as a virtual dataset, since statistics must be calculated for classification.

Use the created virtual dataset, which now contains “bands” from both the imagery and the DEM, to do your supervised or unsupervised classification as you would normally.

Note: You can also use the virtual dataset as input to the Scattergram Display function of ER Mapper, to aid you in defining training regions, or for checking accuracy of the resultant classified file.

Correcting SAR data with DEMs

DEMs can be used to correct Radar layover effects, by back calculating the actual reflectance points for the radar signal. Refer to the ER Radar manual for further details on processing of Radar data in association with DEM data.

Map Production

This chapter describes the production of high quality real-world maps containing both image and vector data.

Producing quality combined image/vector maps

In addition to image processing functions such as creating aerial photograph mosaics, ER Mapper contains very advanced map production abilities.

ER Mapper is unique in that it is designed to handle image based data as well as vector data when producing maps.



Integrating GIS and CAD data with aerial photos using ER Mapper

Using ER Mapper for map production offers a range of benefits:

- Easy creation of real-world maps, containing aerial photographs as backdrops, GIS and CAD data, and map objects such as scale bars, and so on.
- Integration of all types of data. ER Mapper dynamic links enable easy combination of data from not just one, but *multiple* sources. For example, you can integrate data from ARC/INFO, AutoCAD, MapInfo, Oracle, tabular data, and proprietary systems, into a single map.
- Easy and intuitive to use map production. Rather than complex commands, ER Mapper's map production is built using an intuitive drag and drop design.
- Smart map objects. When a map object, such as a scale bar, is placed onto a map, it automatically uses the scale information appropriate to the current map, and updates automatically if you change it. For example, if you resize a scale bar map object, it automatically recreates itself to take into account the new size.
- User extendible map objects. You can add your own smart map objects to ER Mapper. Also, company logos and other symbols may be easily added.

- No limits to file sizes, for image or vector data. This also applies to printing the map. ER Mapper can print a map of any complexity to any of the printer or graphics formats supported.
- Built in RIP (Raster Image Processing) engine. Whereas other products require you to purchase an addition press printing RIP engine, ER Mapper contains a complete RIP engine built in. This engine handles the merging of image and vector data at print time, ready for output to the hardcopy device. Because the RIP engine is built into ER Mapper, you get consistent output *regardless* of output device (no changes because of different fonts, etc), and you are not limited to printer memory - as the RIP work is all done in ER Mapper, the printer simply has to print, not process, the output.
- Print at any scale. Maps can be printed at any scale, even a scale larger than the printer can handle (ER Mapper will cut the map up into strips that can fit onto the printer, in this case). Also, ER Mapper can rotate a map so it better fits onto your printer page.

The ER Mapper map production system is well suited for use as a production system for GIS and CAD users who wish to integrate aerial photography with vector data, and produce high quality maps.

Sub-sectioning data for GIS/CAD systems with limited imagery capabilities

GIS and CAD systems are designed to handle vector based data, not image based data. There are often limits to the size of files or the format of data that a GIS or CAD system can handle. For example, some products can only use greyscale imagery, and very few systems can handle the large (10,000 x 10,000 pixels or larger) image files that cover an entire project area at high resolution.

ER Mapper makes it easy to side-step these limits, in several ways:

- Sub-sectioning the mosaic into files small enough to be handled by the GIS or CAD system.
- Produce lower resolution overview image files that are small enough to be handled by the GIS or CAD system.
- Direct use of ER Mapper image handlers within some GIS or CAD systems.
- Use ER Mapper's extensive vector capabilities to bring data from the GIS or CAD system into ER Mapper, and integrate it with image data within ER Mapper.

Sub-sectioning data into smaller files

ER Mapper can easily re-process an image file into any size file needed for a GIS or CAD system. Zoom to the sub-section area of interest using the Zoom pointer, or using the Geoposition window to set exact extents. Then use the "Save As" icon on the ER Mapper

toolbar, to output an image at the desired resolution. 

Note: You can automate this procedure, and many others, by using the powerful ER Mapper scripting language. For example, you might want to divide a single large mosaic into a set of sub-section files, each covering a specific area, in a cookie cutting fashion. Use the scripting language to define a procedure to step through a mosaic, creating sub-section files, writing these out to your GIS or CAD image file format. This entire procedure can be linked to an ER Mapper menu or toolbar icon, making the whole procedure a one-click operation.

Producing lower resolution overview image files

Use the same procedure detailed for producing sub-sectioned images, except in the “Save As...” menu, specify the size of the image your GIS or CAD system can handle in number of cells across and down. While saving the new image dataset, ER Mapper automatically sub-samples the image down to the resolution you specify.

For example, suppose your aerial photograph mosaic covers 20km x 30km at 1 meter resolution. This would be a 20,000 x 30,000 cell file. Unlike ER Mapper, few GIS or CAD systems can handle this size of file. If you output the file at 2,000 x 3,000 cells, the file will be much smaller—but the size of each cell will be 10 meters instead of 1 meter. If you wish to view the higher resolution data within a GIS or CAD product with limited image handling capabilities, sub-section the mosaic into multiple smaller files, as described in the previous section.

Directly use the ER Mapper image handlers within your GIS or CAD system

Some GIS and CAD systems can directly use the ER Mapper image handlers within the GIS or CAD environment. For example, the free add-ons for ArcView, AutoCAD Map, Autodesk World, and MapInfo enable users to directly use ER Mapper images and algorithms, without having to import the data. This resolves the image file size limits in these systems.

Contact Earth Resource Mapping for details about how to best integrate your GIS or CAD system with large image files.

Overlay your GIS or CAD data in ER Mapper, over aerial photo mosaics

One of ER Mapper’s strengths is the ability to share vector based data with popular GIS and CAD systems. In many cases (for example ARC/INFO coverage format), ER Mapper can directly access the data in the native GIS format. If you don’t need to edit the data ER Mapper can directly overlay the data in the exchange format such as DXF without

having to import it, making integration a simple one-step process. If you do want to edit the data in ER Mapper, you must import it into ER Mapper format (except for ARC/INFO format, which ER Mapper can directly edit in the native format).

There are several benefits to doing the integrated mapping within ER Mapper, using your GIS or CAD data:

- ER Mapper has no image file limits, and can handle very large vector based files.
- There are no limits to the number of vector or image layers of data in an ER Mapper map.
- ER Mapper supports integration of multiple types of data, from multiple sources. For example, you may have data in AutoCAD CAD format, ARC/INFO GIS formats, and Oracle tables (as well as the aerial photo mosaic created using ER Mapper). ER Mapper can integrate data from all these and other sources into a single map. This way, you can keep the data in its native format best suited to that type of data while using ER Mapper as the integration tool.

Note: New Dynamic Links can be added to access data stored in proprietary systems in your company.

- ER Mapper has very powerful map production capabilities, ideal for giving your GIS or CAD data a real-world feel, by combining aerial photograph imagery with your GIS or CAD based vector data.
- ER Mapper has a complete printing RIP engine built in, that generates very high quality image/vector based maps, with no limit to file size. Unlike most products which rely on the printer to do the RIP work for a map, ER Mapper has its own RIP engine, so you can produce maps of any complexity without problems, to all supported printer or graphics formats.
- The key to these abilities is ER Mapper's extensive range of data translators, and the unique ER Mapper *Dynamic Links* concept, which enables ER Mapper to reach out to external systems and directly share data with them.

Directly sharing image files between different systems

There is a large assortment range of different image data formats. ER Mapper supports most of these either directly through raster translators or indirectly through import programs which can convert other formats into ER Mapper's native format.

This presents a question to users who wish to share the same file between different systems. Ideally, one copy of the imagery should be maintained, as this reduces maintenance and disk space requirements.

There is a common sub-set of image formats, known as the BIL (Binary Interleaved by Line) image file format. Many systems, including ER Mapper, use this as the basis of the storage of image data. Systems still need to know details such as the geocoding of the imagery, number of cells and lines, etc. These are generally stored in a separate header file. You can use ER Mapper to create BIL imagery files to be shared by different systems.

For example, ARC/INFO and ER Mapper both support BIL image files. Each system has its own header file; a “.hdr” file for ARC/INFO, and an “.ers” header file for ER Mapper. Thus, to share the same imagery, there would be three disk files:

<filename>	The actual imagery, in BIL format. This is a large file, containing the imagery.
<filename>.ers	The ER Mapper header file. This is a small header file.
<filename>.hdr	The ARC/INFO (and ArcView) header file. This is a small header file.

Whenever ER Mapper exports or imports a file that is in a format that is compatible with ER Mapper, it simply adds the .ers file (or the appropriate header file for an export), and does not re-create the image file.

Many systems support BIL based imagery. Check your GIS or CAD system to see if it directly supports this style of image file, in which case you can directly share the data with ER Mapper without having to import or export the imagery.

Note: Although ER Mapper handles data in any byte order (data larger than 1-byte format, such as floating point data, must have a byte order defined), many other systems can not. You may have to swap the byte order to conform to a more limited product’s capabilities. The *Customizing ER Mapper* manual gives information on how to share information between different systems.

Some systems embed the header information directly in the BIL file, at the start of the file. For example, the ERDAS 7.5 format does this. ER Mapper can also handle this form of BIL file, and can be instructed to skip the header bytes at the front of the file.

Change Detection

Author

Amy Hall, Main Roads Western Australia, Don Aitken Centre Waterloo Crescent, East Perth, 6004, Western Australia.

Introduction

The issue of data currency is particularly pertinent to organisations that deal in large volumes of land related data. Change detection processing using satellite imagery is an ideal way to determine changes in land cover in order to enable organisations to maintain the integrity of the data that they manage. The periodic availability of remotely sensed data makes it well suited to change detection applications. Multidate imagery can be processed to highlight changes in pixel spectral response between image dates. Such information can be used in the decision making process, or used to monitor changes over time as an aid to updating information databases.

One particular application of change detection techniques is to highlight where new road development has occurred between two dates. Such information is used by Main Roads Western Australia (MRWA) to update their digital centreline network files, to ensure the integrity and currency of the network. This is important as the digital centreline network forms the frame of reference for road and road related data, and hence needs to explicitly represent the current state of the road network.

The advantage of using image processing and change detection methods is that there is no need for reliance on ‘third parties’ for information, and the branch can independently update the digital network.

This chapter documents the change detection process as applied to detecting new road development from the initial stage of ordering the satellite data through to the production of a change image.

Data sources

The raster and vector data used in this project and their sources are described below.

Raster Data

SPOT Panchromatic data was used for this project. The SPOT satellite in panchromatic mode detects information in a single band (0.51-0.59 μm) and has a spatial resolution of 10 x 10 m. A typical full SPOT scene covers a ground area of approximately 60 x 88 km, and costs A\$1800. Partial scenes are also available at a cost of A\$600 for each 10km by 10km area. Repeat coverage for SPOT data is obtained every 26 days (Richards 1986).

Supply of remotely sensed data in Australia is co-ordinated by the Australian Centre for Remote Sensing (ACRES) in Canberra. All data supplied by ACRES has been radiometrically corrected to account for varying detector responses that often cause striping in a digital image. Satellite data from ACRES is classified into levels according to the amount of pre-processing that has been performed on the data.

- Level 4 data is path oriented. This means that the angle between east and the scan lines is 11 degrees. Data has been resampled to the Superficial conic map projection, and original pixel size has been maintained.
- Level 5 data is path oriented, has been resampled to the Australian Map Grid (AMG), and the original pixel size has been maintained.
- Level 6 data is path oriented, generated from ground control points from 1:100 000 series mapping, has been resampled to the AMG, and original pixel size has been maintained.
- Level 8 data is a map sheet product based upon 1:100 000 or 1:50 000 map sheets and data is rotated to align with the grid of the map sheets. Data has been resampled to derive a smaller pixel size.
- Level 9 data is a map sheet product based upon 1 :100 000 or 1:50 000 map sheets, and has been rotated to align with the grid of the map sheets. Data is generated from ground control points from topographic maps. Data has been resampled to derive a smaller pixel size than that of the raw data (source: ACRES).

For the best results from any multirate change detection process, all images should ideally be captured at the same time of the year in order to eliminate any seasonal variations that may cause differing spectral responses on the ground (for example, healthy versus

unhealthy crops). Differences in atmospheric conditions (summer/winter) can effect pixel responses. The aim is to reduce the likelihood of ‘false’ change responses being generated, and to maximise the likelihood of all changes pixels representing ‘true’ changes.

ACRES supplies data in a variety of formats. Before importing the raster data it is necessary to be aware of the format the data is stored on the tape, as this will determine the import module that is used. This information is usually identifiable from the tape itself. It is also necessary to be aware of how to extract the data from the tape. This information can easily be obtained from ACRES.

Additional information that may be required is the number of bands, cells and lines in the dataset, and the name of the sensor. It is not necessary to load the entire scene into the system if the study area only comprises a small area.

In terms of storage space, a typical raw SPOT Panchromatic scene requires between 50-53 megabytes equating to around 10 000 bytes per square kilometre of ground data, and can be used as a guide where partial scene processing is desirable.

Vector Data

A vector dataset is ideal for warping the raster datasets into real world co-ordinate systems. A road network dataset covering the same ground area as the satellite image can be used to select ground control points. ER Mapper supports a large number of external vector formats, which can be converted to ER Mapper datasets or can be accessed via dynamic linking. A list of supported formats can be found in the ER Mapper reference manual.

Registering data to ground control points

Rectifying the satellite data to ground control involves the selection of a number of ground control points (GCPs). These are defined as points that are clearly identifiable on both the satellite image and the control image (that is, vector road centreline network). A first, second or third order best fit polynomial is then used to model the image to the ground control co-ordinates. A rectified dataset will require more storage space than an unwarped dataset. A single SPOT Panchromatic scene will require around 70-73 megabytes. ER Mapper will let you know if you have insufficient space available to store a rectified dataset.

Selecting Control Points

Control points should be widely distributed across the image to provide the most stable solution possible. Common practice is to choose the majority of control points around the edges of the image with several uniformly spaced points in the central portion of the image (Richards, 1986). Each order of rectification requires a minimum number of control points

in order to define the rectification equation. A general rule is to select no less than twice the number of control points required in order to allow the calculation of a root mean square (RMS) error that quantifies the accuracy of control point selection.

For a single SPOT scene, 30 ground control points should be sufficient to accurately rectify the data. A SPOT scene typically contains 6000 x 8800 pixels. This equates to approximately one control point per 16 square kilometres, and can be used as a rough guide to the number of GCPs to select.

Data Enhancement

Some form of contrast enhancement can be used on the raw satellite image to redistribute the pixel values to make use of the full range of intensity values available. This increases the contrast of the image, and makes features stand out more clearly. Best results are obtained by using the greyscale look up table with SPOT Panchromatic images. Turning on 'Smoothing' in the Algorithm dialog box enhances the raster image by removing the 'blocky' effect of individual pixels. Significant saving in processing time can be achieved by saving the above enhancements and features as algorithms particularly where more than one image is to be warped. Remember to add a title to each algorithm that reflects the origin of the data and the processing carried out.

Once three or more control points have been defined, the efficiency of the exercise can be increased by setting up the workspace with one half screen window containing the 'To' dataset (vector) and two half screen windows containing the 'To' and 'From' datasets respectively. An approximate point is then selected in the large vector window and the **Compute FROM** button used to calculate the corresponding pixel co-ordinates in the raster dataset. This point can then be zoomed to more closely to allow refinement of the control point location.

RMS Error

The RMS error listed for each point signifies the number of pixels in error for the current order of rectification. It is advisable to keep the RMS error below one pixel. This signifies an error of $\pm 10\text{m}$ for SPOT Panchromatic imagery.

Rectifying raster data to vector data

Once sufficient control points have been defined, the raster image can be rectified to the vector data. There are no predefined rules as to the best type of resampling or the order of polynomial to use with images to obtain the best results. Results from rectification are dependent on a number of factors, including local reflectance characteristics and the location and number of control points selected.

Resampling

Nearest neighbour resampling assigns the value of the closest input pixel to the output pixel and preserves the spectral values of the original dataset. Spatial shift errors may be introduced and can cause edges to occur in the direction of resampling, resulting in a blocky image. Bilinear resampling uses the four surrounding input pixels to determine the output pixel value and has the effect of smoothing the dataset, as spectral values are modified rather than spatial relationships. The resultant image may contain blurred edges.

Cubic convolution uses the closest 16 input pixel values to determine the output pixel value. Cubic convolution may increase the high frequency component of the data, causing the introduction of noise and can distort the image considerably (Lodwick et al., 1992).

Polynomial Order

Linear order rectification is often used for a quick rectification where precise co-ordinate accuracy is not required, as it is less sensitive to control point variations and processing time is considerably less. A general rule is that it is best to use the lowest order polynomial possible to achieve the best results and to avoid introducing distortion in the output image. The control point error table shows the magnitude of RMS errors in each part of the image. Unevenly distributed RMS errors indicate that there is differential distortion in the image, and suggests that a polynomial order higher than linear is justified. Before making this assumption, it is necessary to re-check these erroneous points to ascertain that it is not human error that has caused this effect.

Results

A SPOT image was subjected to all nine combinations of resampling and polynomial order. In all cases where nearest neighbour resampling has been used, the image appears blocky and linear features appear stepped compared to the original unrectified dataset. Bilinear resampling tends to produce a smoother image with roads and other linear features occurring more as straight lines. Cubic convolution seems to have introduced noise into the data making it slightly blocky but linear features are preserved well. Of the three methods, the integrity of the original dataset seems best preserved on the images resampled using bilinear techniques.

To validate the results achieved from various polynomial orders, the raster dataset can be overlaid with the vector control image and a visual comparison undertaken to determine which image the vector data fits best.

Rectifying raster data to raster data

In order to create a meaningful difference image from change detection, pixel to pixel registration between images is of utmost importance, as even half a pixel in error between images will produce erroneous results. To reduce the likelihood of this occurring, the

remaining raster images should be registered to the first rectified image as it is far easier to select corresponding pixels on two raster images than corresponding locations on vector and raster datasets. Additionally, to ensure some consistency between rectifications, a suggestion is to use the same control point locations that were used for the initial rectification. This may reduce the likelihood of error as the polynomial function used to rectify the data will be similar to the function used to rectify the original image. You can load the GCPs from the first image into the second image in the GCP edit dialog box.

To determine the average error in each pixel, divide the total RMS error by the number of control points. The average error should ideally never be above one pixel. For change detection purposes, less than half a pixel average error is highly desirable.

Comparing Results

To compare the results of two raster rectifications, a good technique is to produce a normalised difference image. This is accomplished by creating a virtual dataset that contains both of the rectified images. A virtual dataset is simply a type of algorithm that treats multiple datasets as a single dataset so that the information can be collectively manipulated. To create a normalised difference image, the virtual dataset of both raster images is subjected to an equation of the form:

$$(\text{input1} - \text{input2}) / (\text{input1} + \text{input2})$$

The resultant image contains response values between -1 and 1. Values of 0 indicate where pixel values have not changed between images and deviations from 0 indicate where pixel values are different to a greater degree. A totally grey image would indicate that pixel values are identical on both images and would suggest perfectly registered datasets.

It should be emphasised that a normalised difference image will highlight differences in absolute pixel values between datasets, as well as misregistered pixels. For this reason a normalised difference image will obviously show change information where ground cover has changed between images, and this should not be confused as indicating misregistered datasets. A normalised difference index is simply a quick and easy way of gauging registration between datasets. It should highlight obvious misregistration problems and indicate if re-registration is necessary.

If a Gaussian Equalise histogram stretch is applied to each dataset before calculation of the normalised difference index this will 'normalise' the pixel values in each dataset and allow a more accurate comparison to be made. If misregistration is apparent, examine the control point location table and check that sufficient control points have been selected in accordance with the guidelines set out previously. Select additional control points if necessary and rewrap the image. This time, when you create the normalised difference image, manipulate the image histogram to highlight those areas where the difference is between -0.01 and 0.01 (indicating very small or no change between pixels). If most of the roads on this image are highlighted this indicates good registration between datasets.

Eliminating seasonal and atmospheric effects

For the most effective comparison, both images should ideally be captured at the same time of the year in order to eliminate any seasonal variations that may cause different spectral responses. Spectral variations may also occur owing to atmospheric factors. If one image was captured on a day when the atmosphere was full of smog or smoke, the pixel values will be affected. There are many ways to reduce the effects of the earth's atmosphere on satellite imagery. The most applicable method will depend on whether the effect is constant over the entire image or random. A comprehensive discussion of techniques is not presented here but can be found in any remote sensing textbook. The following two methods are quick and simple ways of standardising datasets, and can be applied in a variety of situations.

A Gaussian Equalise histogram transformation applied to each dataset may be of use. Another technique used to reduce atmospheric effects on imagery and normalise scenes for comparison is documented by Richards (1986) and Schowengerdt (1983). The technique involves subtracting the pixel value of the darkest pixel over water from all pixel values in the same image. This is perhaps the quickest and easiest technique and assumes that the atmosphere has affected each pixel in the dataset equally. This cannot always be assumed, and care should be taken.

This technique is made easier by opening up two windows, one with each dataset, and geolinking them so that, at all times, they show the same ground area. It is best to select an area of the image where pixel values are relatively uniform such as a waterbody. By using the Cell Values Profile window, you can determine corresponding pixel responses in each dataset, and build up a table that will allow you to work out if one dataset exhibits brighter or darker responses on average. You should sample at least 20 pixels across the entire image in order to establish an appropriate pattern. If, on average, the pixels in image A are brighter or darker than image B by a constant amount, then you can standardise the images by altering the formula of one image to read $\text{Input1} \pm (\text{some constant value})$. You will need to save this as a new dataset in order to carry out any further processing.

It should be noted that a Gaussian Equalise transform has no actual effect on the absolute spectral values of the pixels, and simply changes the way we perceive the image. Conversely, subtracting a constant value from all pixels does affect the spectral values and is perhaps more desirable where further processing or thresholding is to be carried out to avoid the introduction of error based upon perception.

Creating a change image

Once you have two or more datasets registered to your satisfaction, a change image can be produced. There are many ways to produce a change image; each has its own benefits and limitations. The optimum change detection method is defined as the method that combines accuracy with ease of implementation and computational efficiency. The method you choose will be determined by the purpose of the project you are undertaking.

The underlying principle behind change detection is that a change in land cover causes a change in pixel response. Whether pixels become brighter or darker depends on the type of change being detected. For example, clearing land of vegetation will typically cause an increase in pixel brightness (from darker vegetation to lighter soil) whereas planting a crop would typically cause a decrease in pixel brightness (bare soil to vegetation). Once you have determined what to look for you are ready to begin! Numerous change detection techniques will be discussed briefly, followed by a more in-depth discussion of the method deemed to be the most efficient for detecting changes to the road network and how it is applied using ER Mapper.

Red Green Difference Image

The production of a red/green difference image is a widely used technique, and is particularly useful for interactive viewing of change areas. This technique involves displaying simultaneously one dataset in green and one dataset in red. The resultant combined image will contain mainly shades of yellow (indicating the same response between dates), but areas which have changed will appear as green or red. Red areas tend to have more contrast than green areas, therefore it is suggested that the most current image uses the red layer if increases in pixel brightness are of importance and vice versa. A viewing scale of 1:20 000 or larger is ideal for panning across the image to delineate areas of interest. This technique is most effective where the magnitude of the areas to be found is anticipated as being quite large, such as cleared fields or changes in crop growth.

Band Ratios

The technique of ratioing bands involves dividing the spectral response value of a pixel in one image with the spectral value of the corresponding pixel in another image. This is done in order to suppress similarities between bands. The nature of band ratioing is that every pixel that has the same spectral response between input bands will have a value of 1 in the output image; deviations from 1 indicating progressively different initial spectral values. Areas of greatest change are found in the tails of the resultant histogram. Production of a change image will involve thresholding the image histogram to suppress those areas where little or no change has occurred. The thresholding process will be discussed in greater detail in a following section.

Principal Components Analysis

Principal components analysis (PCA) is a technique employed in image processing to reduce the correlation between bands of data and enhance features that are unique to each band. A characteristic of PCA is that information common to all input bands (high correlation between bands) is mapped to the first Principal Component (PC) whilst subsequent PCs account for progressively less of the total scene variance. This principle can be applied to multi temporal datasets. If two images covering the same ground area but taken at different times of the year are subjected to PCA, then the first PC will contain all of the information that has not changed between the two dates whilst the second PC will contain all the change information. The areas of greatest change are found in the tails of the image histogram.

Image Differencing

Image differencing is perhaps the most simple of all change detection methods. It is based upon the principle that by subtracting the pixel responses in one image from the corresponding pixel responses in another image, any negative value in the output image represents an increase or decrease in pixel response depending on the order of subtraction. For example, if the response from the latest image was subtracted from the response from the older image then all negative values in the output image would indicate an increase in pixel brightness.

All increases in scene brightness would cause negative pixel values in the output image but this is not to say that all negative values indicate significantly 'changed' pixels. The histogram of the resultant dataset needs to be manipulated to isolate areas of increase/decrease that are significant.

To create a difference image

The following documents a procedure for creating a meaningful difference image that isolates areas of interest.

- 1 The first step is to create a virtual dataset comprising both warped images (that have been corrected for atmospheric effects if necessary).

Before any further processing is carried out, it is advisable to display both datasets side by side, set Geolink to Window and simply scroll through the image to get a feel for the sorts of things that you may be looking for. If you already know of an area where change has taken place, take a look at how the pixel responses have been affected between dates. This will help you determine what levels of brightness change you are interested in and will later aid the thresholding process.

- 2 Depending upon the change detection application, you may wish to apply a filter to each image before calculating a difference image.

Median filters are ideal for reducing the variation between adjacent pixels, by smoothing each dataset (Ingram et al., 1981) and are most effective where large areas of change are to be detected. For small changes such as changes to the road network, leave the pixels ‘raw’ to avoid introducing any errors or to avoid ‘smoothing’ the dataset too much and losing smaller details. If you decide to apply a filter, make sure you save the filtered image as a new dataset before producing the virtual dataset.

- 3 When producing the virtual dataset, edit the layer description of each dataset layer to reflect the dataset contents.

For example, if the image is rectified, give it a prefix of ‘rectified’ followed by the date of the image. This way, each band can be manipulated separately in the virtual dataset. If you leave the overlay descriptions as ‘pseudocolor’, the two images will be combined into one band in the virtual dataset.

- 4 Create a change image by applying a formula to the virtual dataset of the form:

$\text{Input1} - \text{Input2}$

Save this formula into an algorithm and call it ‘Create a change image’ or similar so that you can use it again to compare other datasets.

- 5 Assign bands (datasets) to the formula inputs.

Which image you make Input1 depends upon whether you are looking for increases or decreases in pixel brightness. For increases in brightness, make the newest image Input1.

- 6 Redisplay the image after applying the formula using the greyscale look up table.
- 7 The next step is to manipulate the image histogram in order to extract those areas of interest.

The selection of threshold boundaries is one of the most critical elements in change detection processing. You want to eliminate all pixels that have no chance of being change pixels, at the same time being careful not to reject any pixels that may be of interest.

Making the newest image Input1 means that all increases in pixel brightness will have a positive response in the output image. It follows that if you are interested in increases in pixel brightness then you can immediately eliminate all negative pixels in the output image. Conversely, if you are interested in decreases in pixel brightness then reject all positive pixel responses.

To modify the histogram, first set the output limits to ‘actual’ using the transform dialog and refresh the display. Thresholding is typically an iterative, interactive process which requires some prior knowledge of the types of changes in order to obtain a meaningful result. Thresholding can be significantly aided by selecting a feature with the highest probability of no change between dates, and manipulating the histogram accordingly. Waterbodies are ideal for this process.

Open up three windows, two containing the original images and one containing the ‘change’ image. Set Geolink to Window on all three images to ensure that they are displaying the same ground area. If you can locate a waterbody, use this as a ‘benchmark’

for thresholding by manipulating the histogram to eliminate any change pixels that are occurring in water. You should make sure that the reflectance of the waterbody in the original image is not affected by sun glare. Alternatively, if you know of some areas where change has occurred, pan to these areas and manipulate the histogram to maintain the relevant pixels and reject the others. Large scale aerial photographs are ideal for locating target change areas. Be careful not to reject too much. If this process is undertaken for a few small test areas, threshold values can be chosen that maximise the likelihood of pixels in the entire image actually representing true change. Once you are satisfied with the threshold level that you have chosen, refresh the display.

8 Further processing can be carried out to eliminate false change responses.

If you have regions defined, you can use them to mask out unwanted change pixels. For example, if you are interested in changes to crop growth and you have a vector dataset comprised of polygons representing forested areas, waterbodies, urban areas (that is, areas that you are not interested in) and so on, then you can convert this vector information to region information. Then you can use the regions in the change image, applying a formula that sets the pixel value to null if it is within one of the defined regions. Alternatively, if you are using a GIS or similar system for further processing you may wish to carry out this stage of processing in that system.

9 You are now ready to save your change image as a new dataset.

Use the transform dialog box to make sure that all of the 'change' pixels are given an output value of 255 and all other pixels an output value of 0, then change the layer type from Pseudocolor to Classification. This will produce an image in which all 'change' pixels have an output value of 1 and all other pixels are 'null'. Save this as a dataset using the Save as Dataset option. The dataset can now be used as an layer. It can be draped over another SPOT scene or it can be exported for further analysis in another system such as a GIS.

References

- Ingram, K., Knapp, E. and Robinson, J.W. (1981), *Change Detection Technique Development for Improved Urbanized Area Delineation*, Technical Memorandum CSC/TM-81/6087, Computer Sciences Corporation, Silver Springs, Maryland, USA.
- Lodwick, G.D. and S.H. Paine (1992), *Remote Sensing and Image Interpretation*, Perth, Curtin University School of Surveying and Land Information, pp 145-146.
- Richards, J.E. (1986), *Remote Sensing Digital Image Processing - An Introduction*, New York, Springer-Verlag.
- Schowengerdt, R.A. (1983), *Techniques of Image Processing and Classification in Remote Sensing*, New York, Academic Press.

Crop Type Classification and Area Inventory

Authors

L.A. Chisholm and R. Rumbachs, Centre for Image Analysis, Charles Sturt University—
Riverina, Locked Bag 678, Wagga Wagga, NSW 2650, Australia.

Introduction

This chapter illustrates the use of ER Mapper for crop type inventory. This involves the use of formulae enabling the user to define complex processing techniques such as classification and a sequence of steps for image processing to achieve this end.

In the field of agriculture, a dominant requirement is for information on crop conditions and areas for efficient management purposes, in particular:

- crop identification
- area measurement
- identification of crop stress.

According to Barrett and Curtis (1992), any inventory designed to determine areas of one particular land characteristic should be compared with the total land area concerned. In the study presented, a land cover classification schema was determined, from which agricultural land was subdivided as required.

Project

The sample project used for illustration is based upon a study area at Charles Sturt University located near Wagga Wagga, NSW. The University Farm comprises 490 ha of University-owned land and 370 ha of leased land of which 150 ha is river flats. The farm system is winter crops, cereals, legumes and oilseed with rain-fed lucerne and subclover pastures for beef and sheep production. The University Farm maintains a valuable role in demonstrating modern farming practices, and providing a valuable resource for academic and research pursuits. There is a need to provide an automated crop inventory, primarily to support farm management practices, and to provide accurate production figures to regional and State agronomy departments.

Image processing was performed using ER Mapper on a Sun Sparc 10 workstation on a local network. Geometrically corrected SPOT imagery obtained in July 1992 was imported into ER Mapper format and subsetted according to the boundaries of the project area. Various image enhancements and classifications were performed to help identify the features of interest in the data. A dye sublimation printer was used to produce final hardcopy of images.



Multispectral classification

Important thematic information can be extracted from remotely-sensed imagery through a process called *multispectral classification*. Classification is a statistical process which groups homogeneous pixels into areas of interest based upon a concept referred to as *spectral pattern recognition*. Several classification algorithms are popular in image processing, the most common being: parallelepiped, minimum distance to means, and maximum likelihood. While each algorithm has its advantages and disadvantages, the maximum likelihood algorithm is most commonly used due to its rigour.

Classification can be categorised into two methods: supervised (human assisted), or unsupervised (clustering) techniques. Each method serves a particular purpose, and the two methods are often used in conjunction. Results from the process are typically in the form of a thematic map from which information can be used to solve a particular problem or to provide important data unobtainable from other sources.

The steps taken using ER Mapper for this study are presented below as a general guide, with more detail outlined later:

- classification schema
- initial image display

- image interpretation
- ground truth
- training site selection
- supervised classification
- accuracy assessment

Getting to know your image

Once the data has been imported into the system, the first step is to determine image quality and obtain information on general image characteristics. It is usually based upon the information gained from this step that further processing is determined: atmospheric corrections to remove distortion from the image; and necessary image enhancements to obtain the best visual display for interpretation and/or analysis. It is often necessary to apply a range of image enhancement procedures to image data to display it more effectively and increase the amount of information which can be visually interpreted from it (Lillesand and Kiefer, 1994). This is particularly true for training site selection, an essential precursor to supervised classification.

Image display

Typically an image analyst initially views the image in the standard three band colour composite (green, red, and infrared brightness values to the blue, green and red colour guns, respectively). While the merit of other three-band colour composites should not be overlooked, it is wise that the composite with which the analyst is most comfortable for interpretation be used prior to the classification procedure to establish the location of ground truth, and to determine training sites as input to the classification process.

Image enhancement

Image enhancement techniques are applied to the data to improve visual interpretation. There are no hard and fast rules for producing the single “best” image for interpretation; the analyst should enhance the image in the manner to which they are comfortable. Typically, initial enhancements serve as input to further image processing steps, with thematic information extracted from the image using either supervised or unsupervised classification techniques (Jensen, 1986).

Classification schema

Particularly with agricultural studies, the analyst must attempt to account for all major land cover areas present in the image. The schema in which the image is to be classified is worth considerable attention before proceeding. For this study, the following schema was arrived at based upon the major crops and cover types present in large quantity in the project area based upon the classification system proposed by Anderson:

Level 1	Level 2
Urban or built-up land	residential
Agricultural land	oats barley subclover wheat lucerne pasture other agricultural land
Forest	eucalypt
Water	dams
Barren	bare soil transitional

(Modified from Anderson, et al., 1970)

These are the classes which are to be extracted as thematic classes from the image and for which area statistics are to be generated.

Sequence of operations

In general, the sequence of operations for crop identification/surveys includes data preprocessing, training set selection and classification by statistical pattern recognition. Data preprocessing includes radiometric correction and registration of each pixel in geometric coincidence. The training sample selection phase aims to determine the separable classes and subclasses in a given data set. Pattern analysis systems have been developed that allow several methods of class selection to be employed. Statistics can be computed and printed out in the form of histograms, correlation matrices, and spectral plots. One of these types of output can then be used to group areas having similar spectral responses. Another method of class separation consists of using clustering techniques to group image points to minimise the overall variance of the resultant sets

Histograms and statistics are often computed and printed for each training site. An adequate statistical sample (>30) for each crop type is necessary. Samples of data from each class identified by the statistical process are then used for training the pattern classifier; for example, the histograms for barley can be used as training sets for the automatic classification of barley.

Following the pattern recognition phase, which produces automatic classification of the land cover, it is necessary to evaluate the classification accuracy quantitatively. A large number of test fields are necessary. These are located in the computer classification and the ground data is compared with the computer result.

There are drawbacks which should be considered. In the case of supervised classification methods, there can be considerable difficulty when spectral signatures show high variability. Further, accuracy assessment demands that reference signatures be collected directly from a training area lying within or nearby the survey area. The unsupervised technique avoids this by not requiring reference signatures in the data processing phase. Unsupervised techniques group the multispectral data into a number of classes based on the same intrinsic similarity within each class. Classes are labelled after data processing by checking a small area belonging to each class.

Where crops have been affected by disease or adverse environmental conditions, dead portions of the crop can be identified readily by using the infrared portion of the spectrum. In this spectral region, healthy plants are typically red whereas diseased, dead or otherwise stressed plants assume different colours. The colours of diseased plants often range from salmon pink to dark brown depending on the severity of the stress. Dead portions image in green or bluish grey.

Crop discrimination using infrared bands has been studied closely and it has been found that the percentage accuracy depends on time of year, location and environment (Barrett and Curtis, 1987) as well as the spatial resolution of the sensor.

A common problem is that occasionally nearly all crops image red. It has been noted that the quality of grass pasture can often be detected by variations in the intensity of the red hue. Multi-temporal analysis can help to distinguish between crops when this situation arises.

Multispectral sensing of crops

Spectral Reflectance Characteristics

Many studies have been performed to determine the different spectral responses of plant types, particularly the characteristics of a number of crops. Crop signatures can be useful throughout the preprocessing and classification processes. It is important to note, however, that the spectral response of a field crop depends partly on the layering within the crop and the percent soil background.

A fundamental problem occurs when crop identification is attempted where field sizes may be less than 1 ha. From space many of the ground resolution elements are individually composed of a mixture of crop categories. Thus many of the pixels generated by sensors are not characteristic of any one crop, but relate to a mixture of several crops.

The radiance of crop canopy is more complex than modelling a complete cover for natural vegetation. As the crop grows different plant characteristics are developed and simultaneously the amount of underlying soil visible to the sensor changes through the growing season. Remote sensing devices primarily detect radiance from the canopy but additional complicating factors must be kept in mind. The reflectance characteristics are dependent on a number of variables which change during the growing season, including:

- optical properties of stems and reproductive structures within the canopy
- leaf area indices
- canopy densities
- leaf orientations and shapes
- foliage height distribution
- transmittance of canopy components
- amounts of soil background viewed and their reflectance contribution

(Barrett and Curtis, 1992).

Radiometric data were acquired from field trial sites located at the Wagga Wagga campus of Charles Sturt University for the period February 1991 through December 1992. The field trials were undertaken to catalogue the changes in plant reflectance throughout the growing season, to assess crop vigour by ground radiometric measurements and remotely-sensed imagery. It was found that the spectral response of the crop canopy significantly changed due to:

- sky conditions and time of day
- plant development
- plant nutrition
- plant stress
- plant species.

Examples of the signatures obtained for certain crops using a hand-held spectrometer are given in Figures 1 through 4.

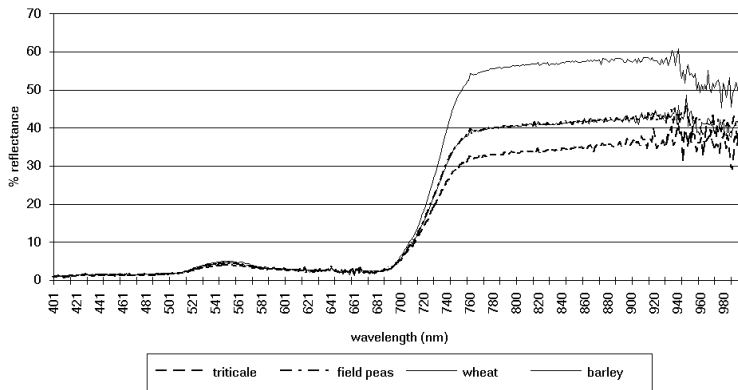


Figure 1. Spectral response of crop species, 6 September 1991

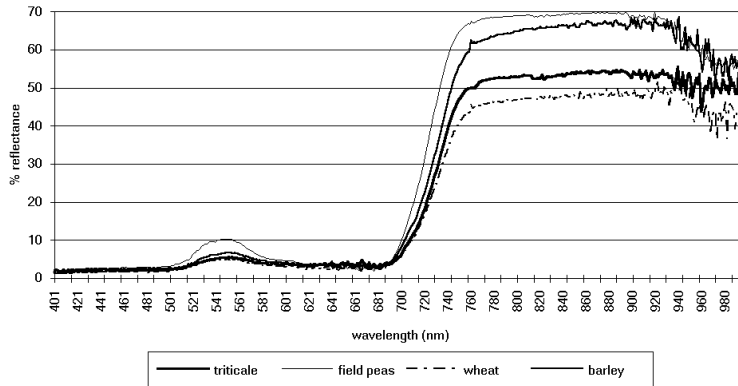


Figure 2. Spectral response of crop species, 19 September 1991

Figures 1 and 2 are examples of spectral response of different plant species showing the spectral response of four different crop species from the cultivar trial 1991. The main effect on the spectral responses is biomass for the cereal crops, although triticale does tend to have a slightly higher reflectance in the blue wavelengths. Field peas are generally a light green colour which is shown by the high reflectance in the green wavelengths, and also higher in the near infrared—possibly due to the broader leaf structure. The data consists of single measurements from a treatment plot.

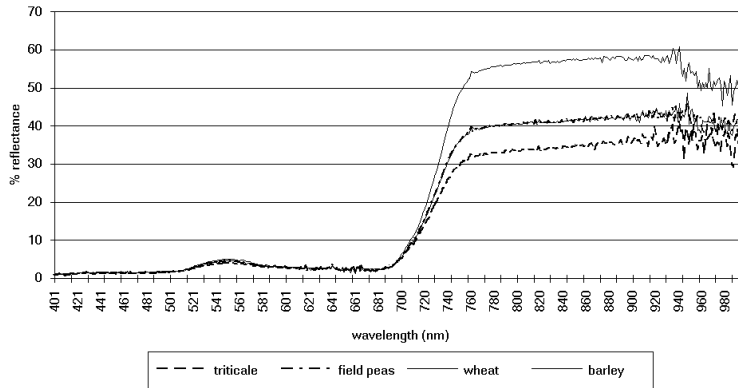


Figure 3. Change in clover canopy spectral response with plant biomass

Figure 3 is an example of spectral response change due to plant development showing data collected on the same day from areas of clover with different biomass (displayed as plant height). The spectral signature of clover/soil was from an area where the clover plants were still quite small and soil was clearly visible around the plants.

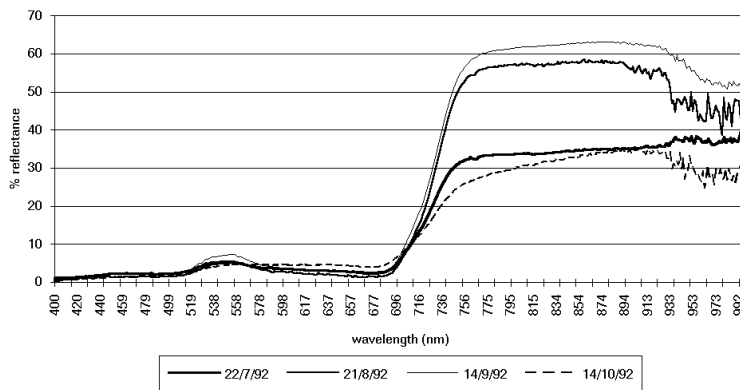


Figure 4. Change in wheat spectral response with stripe rust infection.

Figure 4 is an example of spectral response change due to plant stress showing the change in the spectral response for wheat which was infected with stripe rust (Source: van der Rijt, et al., 1992).

Ground truth

A commonly used term for observations made on the surface of the Earth with respect to remotely-sensed data is *ground truth* (Barrett and Curtis 1992). Other terms of a similar meaning are *in situ* data, or *collateral* data, but all refer to sampled data gathered in order to establish a relationship between the sensor response and particular surface conditions.

It is commonly used to determine the accuracy of categorized data obtained through classification.

Of utmost importance to the collection of ground truth is to obtain data within as short a time period of the acquisition of the sensor data as possible. If this is not the case, relationships established between the ground and sensor data can be unreliable due to changes which occur on the ground surface over time. This is especially true for crop studies, where the phenomena under investigation are continually changing: height and colour of crop, effects of stress or disease, percent cover, etc. Knowledge of the rate of change of these variables can help to identify a sufficient window of time to collect the ground truth with respect to the sensor overpass. For agricultural studies, normally the shorter the time period between these two aspects, the better.

Training Site Selection

As previously stated, supervised classification methods are based upon prior knowledge of the image, specifically the statistical nature of the spectral classes used to classify the image (Mather, 1986). It is important to collect training samples with the method of supervised classification to be performed in mind, as each method demands different statistical requirements. Lillesand and Kiefer (1994) emphasise that all spectral classes constituting each information class must be adequately represented in the training set statistics used to classify an image. Training estimates are commonly a function of the spatial resolution and geometrical accuracy of the remote sensing data (Barrett and Curtis, 1992).

When classifying an unknown pixel, the maximum likelihood algorithm evaluates the variance and covariance of the category spectral response patterns. It is assumed that the distribution of the training sample for each category is Gaussian. The maximum likelihood classifier delineates “equal probably contours”, with the shape of the contours expressing the sensitivity of the likelihood classifier to variance. Estimates of the mean vector and variance-covariance matrix of each class are required as inputs to the classifier. According to numerous authors (Mather, 1986; Jensen, 1986; Harrison and Jupp, 1990) the statistical validity of the result will largely depend upon two factors:

- the size, and
- representativeness
of the sample.

Sample size is usually related to the number of spectral bands from which the statistical samples are to be collected. For purposes of multivariate analysis, Mather (1987) recommends at least $30n$ pixels per class, where n is the number of spectral bands. According to Jensen (1986) ideally $> 10n$ pixels of training data are collected for each class.

There is a lack of standardisation of methods of data collection for training sites. While there are general guidelines to be given, the user should be aware that the tendency is to underestimate the number of samples needed for any particular study. Remember that the training site collection aims to determine the separable classes and subclasses in a given data set (Barrett and Curtis, 1992). The minimum sample sizes given here are valid only if the individual pixels within the training sample are independent (Mather, 1986). If a high spatial autocorrelation can be assumed, then a larger number of training samples should be obtained to yield unbiased results.

Statistics can be computed for each band and printed in the form of histograms, correlation matrices and spectral plots. One of these types of output can then be used to group areas with similar spectral responses.

In ER Mapper, regions were delineated and their spectral statistics calculated. A region can contain multiple polygons; for instance, several sub-regions can be delineated to represent the “barley” class.

For the sample project, regions for each of the classes were selected and spectral statistics were collected for each pixel found within the training region. Usually each region is composed of many pixels. In this project, at least 30 pixels for each region were collected. This allows for the inverse of the covariance matrix for each class to be calculated (Jensen, 1986) which is important for the maximum likelihood classification algorithm.

Drawing training regions is described in Chapter 19, “Supervised classification” in the *ER Mapper Tutorial* manual.

Histograms and statistics are then computed under the **Process** Menu and printed for each region. The mean and covariance of each crop type can be obtained from the selected regions. The major value of the histograms is to ensure that the training regions chosen approximate a Gaussian distribution.

Statistical summaries are also provided in the **View** Menu, where an area summary report, mean summary report, standard deviations, and distance between means can be obtained for either the image or regions of interest. Two windows are displayed, one to display the statistics, and the other to specify the classes to display.

An adequate statistical sample (>30) for each crop type is necessary at this stage as previously outlined. The samples of data from each region identified by the statistical process are used to train the pattern classifier; for example, the histograms for barley can be used as training sets for the automatic classification of barley.

It is important to realize that the processing stages within classification procedures are iterative: training classes are updated on the basis of classification results obtained from the previous training data, and the process continues until satisfactory results are achieved.

Classification methodology

Implementing the actual maximum likelihood classification in ER Mapper consists of two separate steps:

- 1 statistics extraction
- 2 the actual maximum likelihood calculations.

Twelve regions were trained upon using the classification schema given at the beginning of this chapter.

Spectral statistics for each region were submitted to the supervised classifier in the Process menu. The default maximum likelihood algorithm was used with equal prior probabilities.

At this stage regions can be added individually, or alternatively, as for this study, all regions can be added as input to the classifier.

The **Edit Class/Region Color and Name** option allows colours to be assigned. Upon completion and colour assignment to the classified image, the image was displayed for visual assessment. This is discussed later.

Training Class Refinement

Within the training signatures established there are often areas of confusion between the crops of interest and other land cover types such as forest or urban areas, and/or other crops under study (Barrett and Curtis). This is often the result of real spectral confusion. For this project, there was substantial spectral confusion between the large, mixed residential area, and another area of variable yet highly reflective “bare soil/transitional”. Confusion was present due to the large degree of variance inherent in the “residential” area, which actually contains semi-developed land, as well as developed land with a mixture of greenery, cement, roofs, etc., typical of “mixed-residential”. There are several ways to handle this situation, the most obvious being to retrain on one of the confused regions.

The general concept is to view a scatterplot of each region for comparison. It is convenient to plot the training regions versus the classified area (all bands) as an overlay onto the original image. If it is evident that there are different classes present, there ought to be a way to discriminate between them.

Thus, the first step taken to resolve this situation was to train on the other class (in this case, residential) in order to obtain a more discreet spectral signature for this region. Unfortunately, due to the large amount of variance in the “residential” region, retraining did not sufficiently resolve the problem.

Typicality Thresholds

The maximum likelihood classifier works upon forced allocation, where every pixel must be allocated to a class present. Thus, one way to limit the confusion is to place a typicality threshold on the class. If spectral plots show the “bare soil/stubble” to be closer to “residential” than any other class, one of the regions can be trained upon in order to put boundaries on its typicality.

The maximum likelihood classifier calculates the posterior (relative) probability of every pixel belonging to a class and forces it into the one with the maximum posterior probability. This could be a completely different class that happens to be spectrally similar. The classifier also provides an index of typicality for each class—for example, the probability of a pixel actually belonging to the class, generally scaled from 0 to 100.

Whether a pixel is likely to belong to any of the original training classes is also accounted for, where an index of typicality for each class suggests the probability of the pixel belonging to the corresponding training class. These values are also usually scaled from 0 to 100.

Thus, a typicality probability indicates whether a pixel is likely to belong to the corresponding training class. Each probability is interpreted as a “tail area” probability in the statistical sense, so the value of 1 is equivalent to a 1% significance level. The group membership probabilities are relative values of the pixel belonging to one or the other of the training classes. In other words, a value of 50 does not necessarily indicate that the pixel belongs in the corresponding class, only that it is the most likely among the training classes present. The typicality indicates if this is a reasonable result.

Once appropriate spectral statistics are collected, they can be resubmitted to the classifier. After it has been allocated, unless the pixel is within a specified degree of typicality for that class, it will not be classified.

Thus, if simply retraining upon one class still does not resolve the situation, one can use the concept of thresholding. If one specified a typicality of 1%, this means that anything allocated in the 1% tail (a long distance away from that class) will not get allocated. The user could specify the typicality as 5%, or could be really harsh and specify it as 10%. Thus, the 10% component will not be allocated. Essentially this means that the bulk (90%) of the pixels are typical of this particular class.

This idea of a threshold helps to identify what might be a separate class. In the case of “bare soil/transitional” versus “residential”, at the training stage the user may not know it should be a separate class, but when a typicality is later forced upon it, one class will be black from not being allocated.

Weighting the Classifier

In cases where discrimination between classes remains difficult, any available *a priori* information can be used to obtain a more accurate classification. The user can assign more weight to one class than another, with the weight applied according to the area of the class. Essentially the user is telling the classifier that the solution it comes up with must match

the fixed prior probabilities. It is quite common for users to have access to geographic information systems (GIS) from which areas of a known class can easily be obtained. It is fairly straightforward to estimate the proportion of the study area within the total image area to be classified. Areas for each class can therefore be used to weight the classifier, entered as prior probabilities.

A Note About Real-Time Classification

A particularly useful option in ER Mapper allows “real-time” classification using the “Classification Display” algorithm. Once training classes are determined, the classified pixels can be superimposed upon the raw satellite image to aid the analyst in the interpretation and relative accuracy assessment.

Displaying classification results

ER Mapper can display a Pseudocolor map of the resultant classes, with options to include masking with atypical pixels and a display of the posterior probability and typicality indexes for a specified class.

It is useful to assign individually selected colours to the classified image, as the colours assigned using the Auto-gen colors option are very similar to the colour of the class on the raw image. It can also be useful to display similar classes in the same colour to group them.

A note about unsupervised classification

There is often considerable difficulty because insufficient knowledge exists about the study area, spectral signatures show high variability, and supervised techniques generally demand that training sites lie within the survey area of interest. If one or more of these problems exist, a useful alternative is unsupervised classification. The unsupervised classification technique avoids these difficulties by not requiring training sites as the basis for classification. Unsupervised techniques group the multispectral data into a number of classes based on the same intrinsic similarity within each class. The basic premise is that values within a given cover type should be close together in spectral space, as opposed to data in different classes being comparatively well separated (Lillesand & Kiefer, 1994). The result of an unsupervised classification, therefore, is spectral classes. The meaning of each class in terms of land cover is obtained after data processing by checking a small area belonging to each class.

Classification accuracy assessment

The overall accuracy of the classified image can be computed by dividing the total number of correctly classified pixels by the total number of reference pixels. Likewise, the accuracies of individual categories can be calculated by dividing the number of correctly classified pixels in each category by the total number of pixels. Lillesand and Kiefer (1994) point out that error matrices should be used with caution; if the results are good, it means no more than that the training areas are homogeneous, the training classes were separable, and the classification strategy employed worked well in the training areas. In particular, they express concern with the sampling approach taken from which pixels will be used for accuracy assessment, and conclude that a concept of both random and systematic sampling should be employed. In other words, systematically sampled areas can be obtained early in the project, usually as part of the training site selection, and random sampling within the image after classification is complete.

Agricultural areas typically consist of homogeneous fields many hectares in area well suited for the 20-by-20m ground resolution pixel of SPOT XS. The digital numbers of the SPOT bands for that pixel are a composite of the spectral reflectance of the various materials (Sabins, 1987). Despite these problems, the resultant SPOT classification map clearly portrayed the major categories of land use and land cover as specified in the classification schema.

Recognition of homogenous features such as bare soil and water was fairly accurate as would be expected. However, as previously discussed, crop discrimination presents problems due to the similarity of the plant reflectance of different crops, the variability of the reflectance within fields, and the bare soil background of crops having less than 100% ground cover.

Reasonably good results were obtained for recognition of crops outlined in this study. There remained a light problem with respect to the residential region tending to be confused with the bare soil/transition region. However, this was satisfactorily resolved using the methodology outlined.

Summarizing the position of remote sensing in crop analysis

The crop calendar is an important guide to which data sets are likely to be most useful and should serve as a basis for ordering data.

If the area under study contains classes which are difficult to separate spectrally, are several procedures can be used to resolve the situation. If sufficient ground truth can be obtained, weightings can be assigned to the classifier prior to processing the image. In addition, multitemporal image analysis has been shown to improve classification accuracy, particularly in agricultural areas. Image ratios and transformations are also useful in removing redundancy.

Often, important areas of confusion exist between crops of interest and other land cover categories, such as forest or urban areas, and even with other crops under study. It is recognized that this is often the result of real spectral confusion. Two strategies often employed to improve the accuracy of classification are:

- grouping crops together to form a more homogeneous class for better spectral recognition, then splitting these group categories by ground information alone.
- masking of water, forest and urban areas by means of visual interpretation of images of previous years.

References

- Anderson, J.R., Hardy, E., Roach, J., and Witmer, R. (1976) *A land use and land cover classification system for use with remote sensor data*, US Geological Survey Professional Paper 964.
- Barrett, E.C. and Curtis, L.F. (1992) *Introduction to environmental remote sensing*, London: Chapman & Hall, 3rd edition.
- Harrison, B. and Jupp, D.L.B. (1990) *Introduction to image processing*, Melbourne: CSIRO Publications.
- Jensen, J.R. (1986) *Introductory digital image processing: a remote sensing perspective*, Englewood Cliffs: Prentice-Hall.
- Lillesand, T.M. and Kiefer, R.W. (1994) *Remote sensing and image interpretation*, New York: John Wiley & Sons, Inc, 3rd edition.
- Mather, P.M. (1987) *Computer processing of remotely-sensed images: an introduction*, Chichester: John Wiley & Sons.
- Sabins, F.F. (1987) *Remote sensing: principles and interpretation*, New York: W.H. Freeman and Company.
- van der Rijt, V. et al (1992) *Plant canopy spectral responses from field trials; a component of the airborne video imagery project*, Data Report 1992-1, Charles Sturt University, Wagga Wagga.

Vegetation in Remote Sensing FAQs

This FAQ has been used with permission. It is version 1.0 dated 13 October 1994.

The text has been formatted to be consistent with the manual but is otherwise unchanged.

Author

Terrill W. Ray, Division of Geological and Planetary Sciences, California Institute of Technology, Mail Code 170-25, Pasadena, CA 911255, USA.

Acknowledgements

Thanks to the following people for comments and suggestions (listed in no particular order):

A. Chehbouni - ORSTOM

Martin Hugh-Jones - Louisiana State University

Kjeld Rasmussen -

Mike Stevens - University of Nottingham

Revision history

Version 1.0

Major revision. Discussion of radiance vs. reflectance added. Addition of vegetation indices designed to minimize atmospheric noise (GEMI, ARVI, etc.). Addition of SPOT HRV bands. Numerous minor changes. Cautions regarding the use of SAVI, MSAVI, etc. added.

Version 0.7

Numerous minor non-substantive typographical errors fixed. Addition of question 14a. Some stylistic and grammatical problems dealt with.

Version 0.6

Major typographical error in TSAVI equation fixed and minor error in MSAVI2 fixed.

Version 0.5

Original version posted.

Conventions

In most cases, reflectance, apparent reflectance and radiance can be used interchangeably in this FAQ. (But see question #5 for some important considerations about this.)

Wavelengths are given in nanometers (nm).

The “origin” is the point of zero red reflectance and zero near-infrared reflectance.

The abbreviation SPOT refers to the Systeme Pour l’Observation de la Terre which has five bands of interest (the bandpasses may not be precisely correct since the document I am looking at lists the “proposed” bands):

- SPOT1 covers 430-470 nm
- SPOT2 covers 500-590 nm
- SPOT3 covers 610-680 nm

- SPOT4 covers 790-890 nm
- SPOT5 covers 1580-1750 nm

The abbreviation AVHRR refers to the Advanced Very High Resolution Radiometer which has two bands of interest:

- AVHRR1 covers 550-700 nm
- AVHRR2 covers 700-1000 nm

The abbreviation TM refers to the Landsat Thematic Mapper which has six bands of interest:

- TM1 covers 450-520 nm
- TM2 covers 520-600 nm
- TM3 covers 630-690 nm
- TM4 covers 760-900 nm
- TM5 covers 1550-1750 nm
- TM7 covers 2080-2350 nm

The abbreviation MSS refers to the Landsat MultiSpectral Scanner.

MSS bands are referred to by the old system:

- MSS4 covers 500-600 nm
- MSS5 covers 600-700 nm
- MSS6 covers 700-800 nm
- MSS7 covers 800-1100 nm

NIR is used to indicate a band covering all or part of the near-infrared portion of the spectrum (800- 1100 nm or a subset of these wavelengths). Examples: MSS7, TM4, AVHRR2.

R is used to indicate a band covering all or part of the portion of the visible spectrum perceived as red by the human eye (600-700 nm). Examples MSS5, TM3, AVHRR1.

List of questions

General

- 1) What are the important spectral characteristics of vegetation that I should know about?
- 2) I have some remote sensing data, what bands will show vegetation best?
 - 2a) TM data

2b) MSS data

3) I want to use band ratioing to eliminate albedo effects and shadows. What band ratios are best?

3a) TM data

3b) MSS data

4) Why is vegetation usually shown in red by remote sensing people?

5) What is the difference between radiance and reflectance?

Vegetation index

6) What is a vegetation index?

7) What are the basic assumptions made by the vegetation indices?

8) What is the soil line and how do I find it?

Basic indices

9) What is RVI?

10) What is NDVI?

11) What is IPVI?

12) What is DVI?

13) What is PVI?

14) What is WDV?

Indices to minimize soil noise

15) What is Soil Noise?

16) What is SAVI?

16a) Why is there a (1+L) term in SAVI?

17) What is TSAVI?

18) What is MSAVI?

19) What is MSAVI2?

Indices to minimize atmospheric noise

20) What is Atmospheric Noise?

21) What is GEMI?

22) What are the atmospherically resistant indices?

Other indices

23) What is GVI?

24) Are there vegetation indices using other algebraic functions of the bands?

25) Are there vegetation indices that use bands other than the red and NIR bands?

26) Plants are green, why isn't the green chlorophyll feature used directly?

Problems

27) How well do these vegetation indices work in areas with low vegetation cover?

28) What is "non-linear" mixing?

29) Is the variation in the soil the only problem?

30) What if I can't get a good soil line from my data?

31) How low a plant cover is too low for these indices?

Future directions

32) I hear about people using spectral unmixing to look at vegetation, how does this work?

33) Are there any indices which use high spectral resolution data?

Final question

34) What vegetation index should I use?

The questions and answers follow in full.

General

1) What are the important spectral characteristics of vegetation that I should know about?

A: The cells in plant leaves are very effective scatterers of light because of the high contrast in the index of refraction between the water-rich cell contents and the intercellular air spaces.

Vegetation is very dark in the visible (400-700 nm) because of the high absorption of pigments which occur in leaves (chlorophyll, protochlorophyll, xanthophyll, etc.). There is a slight increase in reflectivity around 550 nm (visible green) because the pigments are least absorptive there. In the spectral range 700-1300 nm plants are very bright because this is a spectral no-man's land between the electronic transitions which provide absorption in the visible and molecular vibrations which absorb in longer wavelengths. There is no strong absorption in this spectral range, but the plant scatters strongly as mentioned above.

From 1300 nm to about 2500 nm vegetation is relatively dark, primarily because of the absorption by leaf water. Cellulose, lignin, and other plant materials also absorb in this spectral range.

Summary:

- 400-700 nm = dark
- 700-1300 nm = bright
- 1300-2500 nm = dark (but brighter than 400-700 nm)

2) I have some remote sensing data, what bands will show vegetation best?

A: Basically a band covering part of the region from 700-1300 nm if you want the vegetation to be bright. (Using a band covering part of 400-700 nm would make vegetation dark, but this isn't the way we generally do things.)

2A) For TM data, either TM4 or TM5.

2B) For MSS data, either MSS6 or MSS7 (MSS7 is usually better since it avoids the transition near 700 nm).

3) I want to use band ratioing to eliminate albedo effects and shadows. What band ratios are best?

A: If you want the vegetation to turn out bright (which is usually the most sensible approach) ratio a band covering part of the range 700-1300 nm with a band covering either 400-700 nm or 1300-2500 nm. Ratioing a near-infrared band to a visible band is the traditional approach. Usually a visible band covering 650 nm is preferred since this is near the darkest part of the vegetation spectrum usually covered by remote sensing instruments. Basically you want a band where vegetation is bright on the top of the ratio, and a band where vegetation is dark on the bottom.

Although vegetation is more highly reflective in green than in red, early work showed that near-infrared-red combinations were preferable to green-red combinations (Tucker, 1979).

3A) TM: The traditional ratio is TM4/TM3. TM5/TM7 is also good, but many clays will also be fairly bright with this combination. I see no immediate reason why TM5/TM3 or TM4/TM7 wouldn't work, but they usually aren't used.

3B) MSS: The traditional ratio is MSS7/MSS5 MSS6/MSS5 is also used.

4) Why is vegetation usually shown in red by remote sensing people?

A: This is one of the apparently silly things done in remote sensing. There are three reasons for it:

The first (and rather pointless) reason is TRADITION. People in remote sensing have been doing this a long time and virtually everyone who has spent much time working with remote sensing will instinctively interpret red splotches as vegetation. Bob Crippen (not the astronaut) at JPL said that he spent some time trying to break this tradition by showing vegetation in green, but he was ultimately beaten into submission. (Consider it this way: you are a remote sensing professional, you usually give talks to remote sensing professionals. They expect vegetation in red so you don't have to add an explanation that "vegetation is shown as green." This simplifies your life.)

The second reason is the fact that the human eye perceives the longest visible wavelengths to be red and the shortest visible wavelengths to be blue. This is an incentive for remote sensing images to be set up so that the shortest wavelength is shown as blue and the longest one is shown as red. Usually a near-infrared band is the longest wavelength being displayed (this is especially true for MSS and aerial color infrared photography). Since vegetation is brightest in the near-infrared, vegetation turns out red. Using red for vegetation in digital data makes the digital data color scheme similar to that for color infrared film. This can make it easier for a person familiar with color infrared film pictures to adjust to the interpretation of digital remote sensing data.

The third (and only sensible) reason is to remind the audience that they are not seeing real colors. If vegetation is shown as green, the audience is more likely to subconsciously think that the image is true color, while if vegetation is red they will immediately realize that the image is false color.

5) What is the difference between radiance and reflectance?

A: Radiance is the variable directly measured by remote sensing instruments. Basically, you can think of radiance as how much light the instrument "sees" from the object being observed. When looking through an atmosphere, some light scattered by the atmosphere will be seen by the instrument and included in the observed radiance of the target. An atmosphere will also absorb light, which will decrease the observed radiance. Radiance has units of watt/steradian/square meter.

Reflectance is the ratio of the amount of light leaving a target to the amount of light striking the target. It has no units. If all of the light leaving the target is intercepted for the measurement of reflectance, the result is called "hemispherical reflectance."

Reflectance (or more specifically hemispherical reflectance) is a property of the material being observed. Radiance, on the other hand, depends on the illumination (both its intensity and direction), the orientation and position of the target and the path of the light

through the atmosphere. With effort, many of the atmospheric effects and the solar illumination can be compensated for in digital remote sensing data. This yields something which is called “apparent reflectance,” and it differs from true reflectance in that shadows and directional effects on reflectance have not been dealt with. Many people refer to this (rather inaccurately) as “reflectance.”

For most of the vegetation indices in this FAQ, radiance, reflectance, and apparent reflectance can be used interchangeably. However, since reflectance is a property of the target material itself, you will get the most reliable (and repeatable) vegetation index values using reflectance. Apparent reflectance is adequate in many cases.

Vegetation index

6) What is a vegetation index?

A: A vegetation index is a number that is generated by some combination of remote sensing bands and may have some relationship to the amount of vegetation in a given image pixel. If that sounds sarcastic or even insulting, it’s meant to. Jim Westphal at Caltech pointed out to me one day that vegetation indices seemed to be more numerology than science. This may be an overly harsh assessment, since there is some basis for vegetation indices in terms of the features of the vegetation spectrum discussed above; however, the literature indicates that these vegetation indices are generally based on empirical evidence and not basic biology, chemistry or physics. This should be kept in mind as you use these indices.

7) What are the basic assumptions made by the vegetation indices?

A: The most basic assumption made is assuming that some algebraic combination of remotely-sensed spectral bands can tell you something useful about vegetation. There is fairly good empirical evidence that they can.

A second assumption is the idea that all bare soil in an image will form a line in spectral space. This is related to the concept of the soil line discussed in question number 8. Nearly all of the commonly used vegetation indices are only concerned with red-near-infrared space, so a red-near-infrared line for bare soil is assumed. This line is considered to be the line of zero vegetation.

At this point, there are two divergent lines of thinking about the orientation of lines of equal vegetation (isovegetation lines):

1) All isovegetation lines converge at a single point. The indices that use this assumption are the “ratio-based” indices, which measure the slope of the line between the point of convergence and the red-NIR point of the pixel. Some examples are: NDVI, SAVI, and RVI.

2) All isovegetation lines remain parallel to soil line. These indices are typically called “perpendicular” indices and they measure the perpendicular distance from the soil line to the red-NIR point of the pixel. Examples are: PVI, WDV, and DVI.

8) What is the soil line and how do I find it?

A) The soil line is a hypothetical line in spectral space that describes the variation in the spectrum of bare soil in the image. The line can be found by locating two or more patches of bare soil in the image having different reflectivities and finding the best fit line in spectral space. Kauth and Thomas (1976) described the famous “triangular, cap shaped region with a tassel” in red-NIR space using MSS data. They found that the point of the cap (which lies at low red reflectance and high NIR reflectance) represented regions of high vegetation and that the flat side of the cap directly opposite the point represented bare soil.

THE SIMPLE WAY OF FINDING THE RED-NIR SOIL LINE: Make a scatterplot of the red and NIR values for the pixels in the image. I recommend putting red on the x-axis and NIR on the y-axis (the rest of the instructions assume this). There should be a fairly linear boundary along the lower right side of the scatterplot. The straight line that best matches this boundary is your soil line. You can either select the points that describe the boundary and do a least squares fit, or you can simply make a hardcopy and draw in the line that looks like the best fit. (You have to make a lot of judgment calls either way.)

Basic indices

9) What is RVI?

A) RVI is the ratio vegetation index which was first described by Jordan (1969). This is the most widely calculated vegetation index, although you rarely hear of it as a vegetation index. A common practice in remote sensing is the use of band ratios to eliminate various albedo effects. Many people use the ratio of NIR to red as the vegetation component of the scene, and this is in fact the RVI.

Summary:

- ratio-based index
- isovegetation lines converge at origin
- soil line has slope of 1 and passes through origin
- range 0 to infinity

Calculating RVI:

$$RVI = NIR / red$$

10) What is NDVI?

A) NDVI is the Normalized Difference Vegetation Index which is ascribed to Rouse et al. (1973), but the concept of a normalized difference index was first presented by Kriegler et al. (1969). When people say vegetation index, this is the one that they are usually referring to. This index has the advantage of varying between -1 and 1, while the RVI ranges from 0 to infinity. RVI and NDVI are functionally equivalent and related to each other by the following equation:

$$\text{NDVI} = (\text{RVI} - 1) / (\text{RVI} + 1)$$

Summary:

- ratio-based index
- isovegetation lines converge at origin
- soil line has slope of 1 and passes through origin
- range -1 to +1

Calculating the NDVI:

$$\text{NDVI} = (\text{NIR} - \text{red}) / (\text{NIR} + \text{red})$$

11) What is IPVI?

A) IPVI is the Infrared Percentage Vegetation Index which was first described by Crippen (1990). Crippen found that the subtraction of the red in the numerator was irrelevant, and proposed this index as a way of improving calculation speed. It also is restricted to values between 0 and 1, which eliminates the need for storing a sign for the vegetation index values, and it eliminates the conceptual strangeness of negative values for vegetation indices. IPVI and NDVI are functionally equivalent and related to each other by the following equation:

$$\text{IPVI} = (\text{NDVI}) / 2$$

Summary:

- ratio-based index
- isovegetation lines converge at origin
- soil line has a slope of 1 and passes through origin
- range 0 to +1

Calculating IPVI:

$$\text{IPVI} = \text{NIR} / (\text{NIR} + \text{red})$$

12) What is DVI?

A) DVI is the Difference Vegetation Index, which is ascribed in some recent papers to Richardson and Everitt (1992), but appears as VI (vegetation index) in Lillesand and Kiefer (1987). (Lillesand and Kiefer refer to its common use, so it was certainly introduced earlier, but they do not give a specific reference.)

Summary:

- perpendicular index
- isovegetation lines parallel to soil line
- soil line has arbitrary slope and passes through origin
- range infinite.

Calculating DVI:

$$\text{DVI} = \text{NIR} - \text{red}$$

13) What is PVI?

A) PVI is the Perpendicular Vegetation Index which was first described by Richardson and Wiegand (1977). This could be considered a generalization of the DVI which allows for soil lines of different slopes. PVI is quite sensitive to atmospheric variations, (Qi et al., 1994) so comparing PVI values for data taken at different dates is hazardous unless an atmospheric correction is performed on the data.

Summary:

- perpendicular index
- isovegetation lines are parallel to soil line
- soil line has arbitrary slope and passes through origin
- range -1 to +1

Calculating PVI:

$$\text{PVI} = \sin(a)\text{NIR} - \cos(a)\text{red}$$

where a is the angle between the soil line and the NIR axis.

14) What is WDV?

A) WDV is the Weighted Difference Vegetation Index which was introduced by Clevers (1988). This has a relationship to PVI similar to the relationship IPVI has to NDVI. WDV is a mathematically simpler version of PVI, but it has an unrestricted range. Like PVI, WDV is very sensitive to atmospheric variations (Qi et al., 1994).

Summary:

- perpendicular index
- isovegetation lines parallel to soil line
- soil line has arbitrary slope and passes through origin
- range infinite

Calculating WDVI:

$$\text{WDVI} = \text{NIR} - g \times \text{red}$$

where g is the slope of the soil line.

Indices to minimize soil noise

15) What is Soil Noise?

A) Not all soils are alike. Different soils have different reflectance spectra. As discussed above, all of the vegetation indices assume that there is a soil line, where there is a single slope in red-NIR space. However, it is often the case that there are soils with different red-NIR slopes in a single image. Also, if the assumption about the isovegetation lines (parallel or intercepting at the origin) is not exactly right, changes in soil moisture (which move along isovegetation lines) will give incorrect answers for the vegetation index. The problem of soil noise is most acute when vegetation cover is low.

The following group of indices attempt to reduce soil noise by altering the behaviour of the isovegetation lines. All of them are ratio-based, and the way that they attempt to reduce soil noise is by shifting the place where the isovegetation lines meet.

WARNING: These indices reduce soil noise at the cost of decreasing the dynamic range of the index. These indices are slightly less sensitive to changes in vegetation cover than NDVI (but more sensitive than PVI) at low levels of vegetation cover. These indices are also more sensitive to atmospheric variations than NDVI (but less so than PVI). (See Qi et al. (1994) for comparisons.)

16) What is SAVI?

A) SAVI is the Soil Adjusted Vegetation Index which was introduced by Huete (1988). This index attempts to be a hybrid between the ratio-based indices and the perpendicular indices. The reasoning behind this index acknowledges that the isovegetation lines are not parallel, and that they do not all converge at a single point. The initial construction of this index was based on measurements of cotton and range grass canopies with dark and light soil backgrounds, and the adjustment factor L was found by trial and error until a factor that gave equal vegetation index results for the dark and light soils was found. The result is

a ratio-based index where the point of convergence is not the origin. The convergence point ends up being in the quadrant of negative NIR and red values, which causes the isovegetation lines to be more parallel in the region of positive NIR and red values than is the case for RVI, NDVI, and IPVI.

Huete (1988) does present a theoretical basis for this index based on simple radiative transfer, so SAVI probably has one of the better theoretical backgrounds of the vegetation indices. However, the theoretical development gives a significantly different correction factor for a leaf area index of 1 (0.5) than resulted from the empirical development for the same leaf area index (0.75). The correction factor was found to vary between 0 for very high densities to 1 for very low densities. The standard value typically used in most applications is 0.5 which is for intermediate vegetation densities.

Summary:

- ratio-based index
- isovegetation lines converge in negative red, negative NIR quadrant
- soil line has slope of 1 and passes through origin.
- range -1 to +1

Calculating SAVI:

$$\text{SAVI} = \left\{ \frac{(\text{NIR} - \text{red})}{(\text{NIR} + \text{red} + L)} \right\} (1 + L)$$

where L is a correction factor which ranges from 0 for very high vegetation cover to 1 for very low vegetation cover. The most typically used value is 0.5 which is for intermediate vegetation cover.

16a) Why is there a (1+L) term in SAVI?

A) This multiplicative term is present in SAVI (and MSAVI) to cause the range of the vegetation index to be from -1 to +1.

This is done so that both vegetation indices reduce to NDVI when the adjustment factor L goes to zero.

17) What is TSAVI?

A) TSAVI is the Transformed Soil Adjusted Vegetation Index which was developed by Baret et al. (1989) and Baret and Guyot (1991).

This index assumes that the soil line has arbitrary slope and intercept, and it makes use of these values to adjust the vegetation index. This would be a nice way of escaping the arbitrariness of the L in SAVI if an additional adjustment parameter had not been included in the index. The parameter “X” was “adjusted so as to minimize the soil background effect,” but I have not yet been able to come up with an *a priori*, non-arbitrary way of

finding the parameter. The value reported in the papers is 0.08. The convergence point of the isovegetation lines lies between the origin and the usually-used SAVI convergence point (for $L = 0.5$)

Summary:

- ratio-based index
- isovegetation lines converge in negative red, negative NIR quadrant
- soil line has arbitrary slope and intercept
- range -1 to +1

Calculating TSAVI:

$$\text{TSAVI} = \{s(\text{NIR} - s \times \text{red} + a)\} / \{a \times \text{NIR} + \text{red} - a \times s + X \times (1 + s \times s)\}$$

where a is the soil line intercept, s is the soil line slope, and X is an adjustment factor which is set to minimize soil noise (0.08 in original papers).

18) What is MSAVI?

A) MSAVI is the Modified Soil Adjusted Vegetation Index which was developed by Qi et al. (1994). As noted previously, the adjustment factor L for SAVI depends on the level of vegetation cover being observed which leads to the circular problem of needing to know the vegetation cover before calculating the vegetation index which is what gives you the vegetation cover. The basic idea of MSAVI was to provide a variable correction factor L . The correction factor used is based on the product of NDVI and WDVI. This means that the isovegetation lines do not converge to a single point.

Summary:

- ratio-based index
- isovegetation lines cross the soil line at different points
- soil line has arbitrary slope and passes through origin
- range -1 to +1

Calculating MSAVI:

$$\text{MSAVI} = \{(\text{NIR} - \text{red}) / (\text{NIR} + \text{red} + L)\} (1 + L)$$

where $L = 1 - 2s(\text{NDVI})(\text{WDVI})$, and s is the slope of the soil line.

19) What is MSAVI2?

A) MSAVI2 is the second Modified Soil Adjusted Vegetation Index which was developed by Qi et al. (1994) as a recursion of MSAVI.

Basically, they use an iterative process and substitute $1 - \text{MSAVI}(n-1)$ as the L factor in $\text{MSAVI}(n)$. They then inductively solve the iteration where $\text{MSAVI}(n) = \text{MSAVI}(n-1)$. In the process, the need to precalculate WdVI and NDVI and the need to find the soil line are eliminated.

Summary:

- ratio-based
- isovegetation lines cross the soil line at varying points
- soil line has arbitrary slope and passes through origin
- range -1 to +1

Calculating MSAVI2:

$$\text{MSAVI2} = (1 / 2)(2(\text{NIR} + 1) - \text{sqr}\{(2 \times \text{NIR} + 1)^2 - 8(\text{NIR} - \text{red})\})$$

Indices to minimize atmospheric noise

20) What is Atmospheric Noise?

A) The atmosphere is changing all of the time and all remote sensing instruments have to look through it. The atmosphere both attenuates light passing through it and scatters light from suspended aerosols. The atmosphere can vary strongly across a single scene, especially in areas with high relief. This alters the light seen by the instrument and can cause variations in the calculated values of vegetation indices. This is particularly a problem for comparing vegetation index values for different dates. The following indices try to remedy this problem without the requirement of atmospherically corrected data.

WARNING: These indices achieve their reduced sensitivity to the atmosphere by decreasing the dynamic range. They are generally slightly less sensitive to changes in vegetation cover than NDVI. At low levels they are very sensitive to the soil background. (See Qi et al. (1994) for comparisons.)

NOTE: I seldom work with data without performing an atmospheric correction, so I have made no significant use of any of the indices in this section (T. Ray).

21) What is GEMI?

A) GEMI is the Global Environmental Monitoring Index which was developed by Pinty and Verstraete (1991). They attempt to eliminate the need for a detailed atmospheric correction by constructing a “stock” atmospheric correction for the vegetation index. Pinty and Verstraete (1991) provide no detailed reasoning for this index other than that it meets their requirements of insensitivity to the atmosphere empirically. A paper by Leprieur et al. (1994) claims to find that GEMI is superior to other indices for satellite measurements.

However, A. Chehbouni (who happens to be the fourth author of Leprieur et al. (1994) showed me some examples using real data (the analysis in the paper was based on a model) which strongly contradicted the Leprieur et al. (1994) conclusions. Qi et al. (1994) shows a violent breakdown of GEMI with respect to soil noise at low vegetation covers. I understand that there are several ongoing studies to evaluate GEMI, and I think that the jury is still out.

Summary:

- non-linear
- complex vegetation isolines
- range 0 to +1

Calculating GEMI:

$$\text{GEMI} = \text{eta}(1 - 0.25 \times \text{eta}) - \{(\text{red} - 0.125) / (1 - \text{red})\}$$

where $\text{eta} = \{2(\text{NIR}^2 - \text{red}^2) + 1.5 \times \text{NIR} + 0.5 \times \text{red}\} / (\text{NIR} - \text{red} + 0.5)$

22) What are the atmospherically resistant indices?

A) The atmospherically resistant indices are a family of indices with built-in atmospheric corrections. The first of these was ARVI (Atmospherically Resistant Vegetation Index) which was introduced by Kaufman and Tanre (1992). They replaced the red reflectance in NDVI with the term:

$$\text{rb} = \text{red} - \text{gamma}(\text{blue} - \text{red})$$

with a value of 1.0 for gamma. Kaufman and Tanre (1994) also suggested making the same substitution in SAVI which yields SARVI (Soil adjusted Atmospherically Resistant Vegetation Index). Qi et al. (1994) suggested the same substitution in MSAVI2 which yields ASVI (Atmosphere-Soil-Vegetation Index). Obviously the same substitution can also be made in MSAVI or TSAVI.

Qi et al. (1994) showed that this class of indices were very slightly more sensitive to changes in vegetation cover than GEMI and very slightly less sensitive to the atmosphere and the soil than GEMI for moderate to high vegetation cover. The atmospheric insensitivity and the insensitivity to soil break down violently for low vegetation cover.

Summary:

- ratio-based
- isovegetation lines cross as assumed by parent index
- soil line as assumed by parent index
- range -1 to +1

Calculating ARVI:

$$\text{ARVI} = (\text{NIR} - \text{rb}) / (\text{NIR} + \text{rb})$$

with rb defined as:

$$\text{rb} = \text{red} - \text{gamma} \times (\text{red} - \text{blue})$$

and gamma usually equal to 1.0

The parent index of ARVI is NDVI. The substitution of rb for red in any of the ratio-based indices gives the atmospherically resistant version of that index.

[NOTE: I view these indices for reducing atmospheric noise as late-evolving dinosaurs. The utility of a good atmospheric correction for remotely-sensed data is so high as to make the effort of performing a proper atmospheric correction worthwhile. These end runs around this problem may serve a useful purpose at present while better atmospheric corrections for data collected over land are being developed. However, the move towards atmospheric correction of remote sensing data is underway, and it is almost certainly the wave of the future. - Terrill Ray]

Other indices

23) What is GVI?

A) GVI stands for Green Vegetation Index. There are several GVIs. The basic way these are devised is by using two or more soil points to define a soil line. Then a Gram-Schmidt orthogonalization is performed to find the “greenness” line which passes through the point of 100% (or very high) vegetation cover and is perpendicular to the soil line. The distance of the pixel spectrum in band space from the soil line along the “greenness” axis is the value of the vegetation index. The PVI is the 2-band version of this, Kauth and Thomas (1976) developed a 4-band version for MSS, Crist and Cicone (1984) developed a 6-band version for TM, and Jackson (1983) described how to construct the n-band version.

Summary:

- perpendicular vegetation index using n bands
- isovegetation lines are parallel to soil line
- soil line has arbitrary orientation in n-space
- range -1 to +1

Calculating GVI:

Default version for MSS:

$$\text{GVI} = -0.29 \times \text{MSS4} - 0.56 \times \text{MSS5} + 0.60 \times \text{MSS6} + 0.49 \times \text{MSS7}$$

Default version for TM:

$$\text{GVI} = |-0.2848 \times \text{TM1} - 0.2435 \times \text{TM2} - 0.5436 \times \text{TM3} + 0.7243 \times \text{TM4} + 0.0840 \times \text{TM5} - 0.1800 \times \text{TM7}$$

24) Are there vegetation indices using other algebraic functions of the bands?

A) Yes. Rouse et al. (1973, 1974) proposed using the square root of NDVI+0.5, Goetz et al. (1975) proposed log ratios, Wecksung and Breedlove (1977) proposed arctangent ratios, and Tuck (1979) discussed the square root of the NIR/red ratio. These seem to have been generally abandoned. They make the same assumptions about the isovegetation lines and the soil lines as made by RVI and NDVI, and they have neither the value of common use or of ease of calculation. You will probably never see these, and there is really no good reason to bother with them.

25) Are there vegetation indices that use bands other than the red and NIR bands?

A) Yes. First, the various GVIs make use of more than just the NIR and red bands. In general, the GVI for a given multispectral sensor system uses all of the available bands. Secondly, there have been attempts to develop vegetation indices based on green and red bands as discussed in the next question.

Mike Steven at the University of Nottingham has recently informed me of some work on an index using NIR and mid-infrared bands. More on this will be included when I have received a paper from him.

26) Plants are green, why isn't the green chlorophyll feature used directly.

A) There are several reasons for this. First, the reason that plants look so green is not because they are reflecting lots of green light, but because they are absorbing so much of the rest of the visible light. Try looking at an area of bare dry soil and compare that to a grassy field. You will immediately notice that the grassy field is generally darker. It is generally easier to detect things when they are bright against a dark background.

Second, this was tried early in the history of satellite remote sensing by Kanemasu (1974) and basically abandoned after a study by Tucker (1979) which seemed to demonstrate that the combinations of NIR and red were far superior than combinations of green and red. The idea of using red and green with MSS data was resurrected in recent years by Pickup et al. (1993) who proposed a PVI-like index using MSS bands 4 and 5 which they called

PD54 (Perpendicular Distance MSS band 5 MSS band 4). They claimed a tassel cap like pattern in the scatterplot for these two bands, but most of the MSS data I have looked at doesn't show this pattern. A significant point for PD54 was that it detected non-green vegetation (dry grass).

Third, many soils have iron oxide absorption features in the visible wavelengths. As the soil gets obscured by vegetation cover, this feature becomes less apparent. It is likely that a great deal of the variance measured by the green-red indices is due to this instead of the plant chlorophyll feature (which is why PD54 might appear to be sensitive to non-green plant material). This is fine if you know that the iron oxide absorption in the soil is uniform across the image, but if the iron oxide absorption is highly variable, then this will confuse green-red indices.

Problems

27) How well do these vegetation indices work in areas with low vegetation cover?

A) Generally, very badly. When the vegetation cover is low, the spectrum observed by remote sensing is dominated by the soil. Not all soils have the same spectrum, even when fairly broad bands are being used. Both Huete et al. (1985) and Elvidge and Lyon (1985) showed that the soil background can have a profound impact and vegetation index values with bright backgrounds producing lower vegetation index values than dark backgrounds. Elvidge and Lyon (1985) showed that many background materials (soil, rock, plant litter) vary in their red-NIR slope, and these variations seriously impact measurements of vegetation indices. Then there is the problem of non-linear mixing.

28) What is "non-linear" mixing?

A) A lot of remote sensing analysis has been based on the concept of the Earth as spots covered by differently-colored paint. When the spots of paint get too small, they appear to blend together to form a new color which is a simple mixture of the old colors. Consider an area covered by 50% small red spots and 50% small green spots. When we look at the surface from far enough away that we can't see the individual dots, we see the surface as yellow. Different proportions of red and green dots will produce different colors, and if we know that the surface is covered by red and green dots we can calculate what the proportions are based on the color we see. The important thing to know is that any light reaching the observer has only hit one of the colored dots. That is linear mixing.

Non-linear mixing occurs when light hits more than one of the colored dots. Imagine a surface with a lot of small, colored bumps which stick out varying distances from the surface. We can now imagine that light could bounce from one colored bump to another and then to the observer. Now some of the light coming from the green bump bounced off of a red bump first, and this light will have characteristics of both the red and green bumps.

There is also light coming directly from the green bump that only bounced from the green bump. If we could see this individual green bump, it would not look as green as it should. Now, when the light from all of the bumps reaches the observer, the light looks different than when the bumps were simple spots even through the proportion of the area covered by each color is unchanged. (We are assuming that there are no shadows.)

A second way for non-linear mixing to happen is if light can pass through one material and then reflect off another. Imagine a piece of translucent plastic with half of the area covered by randomly placed translucent green spots placed on top of a red surface. Now light can pass through a green spot on the plastic and then reflect off of the red below before returning to the observer. Once again, the interaction of the light with multiple spots along its path changes the character of the light coming from each spot. Once again the color looks different than the linear case, which is just the case when light cannot pass through green spots.

The basic point is that non-linear mixing twists the spectra of the materials being observed into different spectra which do not resemble any of the targets. This can magnify the apparent abundance of a material. Consider the piece of translucent plastic with the translucent green dots. If we put it on top of a low-reflectivity surface, very little of the light that passes through the green dots will be reflected back, so all we see is the light directly reflected from the green dots. Now we put a highly reflective surface behind it, and we see a brighter green because we now see both the light directly reflected from the dots and most of the light which has passed through the green dots (which is green) is reflecting back from the highly-reflective background. If we didn't know better, we might think that we just had more green dots instead of a brighter background.

29) Is the variation in the soil the only problem?

A) No. Many of the commonly studied areas with low vegetation cover are arid and semi-arid areas. Many plants which grow in such areas have a variety of adaptations for dealing with the lack of water and high temperatures. (Even plants growing in areas with relatively cool air temperature have problems with heat regulation in dry climates since transpiration is the main way they keep cool.) These adaptations often decrease the amount of visible light absorbed by the plants and/or decrease the amount of sunlight striking the plants (hence the plants do not reflect as much light). These inherent qualities make arid and semi-arid vegetation hard to detect unless it is observed during periods of relatively abundant water when a whole new set of adaptations to maximize plant productivity takes effect.

30) What if I can't get a good soil line from my data?

A) If you're working in an area with high plant cover, this can be common. This makes it virtually impossible to use the perpendicular indices or things like TSAVI and MSAVI1. However, NDVI is at its best with high plant cover, so it is still available to you. The correction factor L for SAVI should be near 0 for this sort of situation, which makes SAVI

equivalent to NDVI. MSAVI2 also need no soil line. If you really want to use an index which requires a soil line, you will need to construct it with field and laboratory spectra, but this is not an easy task, and really not advisable.

31) How low a plant cover is too low for these indices?

A) These are rules of thumb, your mileage may vary:

- RVI, NDVI, IPVI = 30%
- SAVI, MSAVI1, MSAVI2 = 15%
- DVI = 30%
- PVI, WDVI, GVI = 15%

The more uniform your soil, the lower you can push this.

Future directions

32) I hear about people using spectral unmixing to look at vegetation, how does this work?

A) See question 22 for a thumbnail description of linear mixing. Basically, you assume that the given spectrum is a linear combination of the spectra of materials which appear in the image. You do a least squares fit to find weighting coefficients for each individual material's spectrum which gives the best fit to the original spectrum. The weighting coefficients are considered to be equal to the abundances of the respective materials. For detailed discussions of this see Adams et al. (1989), Smith et al. (1990), Roberts et al. (1994) and Smith et al. (1994). There is also the highly sophisticated convex geometry technique discussed in Boardman (1994).

33) Are there any indices which use high spectral resolution data?

A) Yes. Elvidge and Chen (1994) have developed indices of this kind. They depend on the fact that when you take a derivative of the red edge in the vegetation spectrum you get a bump at about 720 nm. It is known that the red edge can be seen in high spectral resolution data down to about 5% cover (Elvidge and Mouat, 1988; Elvidge et al., 1993). Three indices were developed. The first used the integral of the first derivative of the reflectance spectrum over the range 626-795 nm. The second took the first derivative of the reflectance spectrum, subtracted the value of the derivative at 625 nm and integrated the result over the range 626-795 nm. The third index used the integral of the absolute value of the second derivative of the reflectance spectrum integrated over the range from 626-795 nm. Of these three indices, the first one was found to have greater predictive power than RVI or NDVI, but less predictive power than SAVI or PVI. The index which used the second derivative

has greater predictive power than SAVI and PVI. The index which used the difference between the first derivative and the value of the first derivative at 625 nm had the greatest predictive power.

Final question

34) What vegetation index should I use?

A) NDVI.

Nearly everyone who does much with the remote sensing of vegetation knows NDVI, and its often best to stick to what people know and trust. NDVI is simple. It has the best dynamic range of any of the indices in this FAQ and it has the best sensitivity to changes in vegetation cover. It is moderately sensitive to the soil background and to the atmosphere except at low plant cover. To just take a quick qualitative look at the vegetation cover in an image, you just can't beat NDVI unless you are looking at an area with low plant cover.

PVI is somewhat less common in its use, but it is also widely accepted. It has poor dynamic range and poor sensitivity as well as being very sensitive to the atmosphere. It is relatively easy to use, and finding the soil line is important for using some of the other indices. It sometimes is better than NDVI at low vegetation cover.

You really should probably use SAVI if you are looking at low vegetation cover, and if you use a correction factor which is not 0.5 you had better be prepared to cite the Huete (1988) paper and the fact the correction factor is larger than 0.5 for very sparse vegetation. MSAVI is also good, but it has seen very little use. If you have high spectral resolution data, you should consider the Elvidge and Chen (1994) indices.

Remember that many of the indices which correct for the soil background can work poorly if no atmospheric correction has been performed. If you are planning to seriously use vegetation indices for a multitemporal study, you should take a close look at the variability of the soil, and you should do an atmospheric correction. There is some concern about vegetation indices giving different values as you look away from the nadir, but this may not be terribly serious in your application.

Summary:

In order of preference for each type of sensor:

- TM or MSS (or any broad-band sensor)
 1. NDVI (or IPVI)
 2. PVI
 3. SAVI (top of list for low vegetation)
 4. MSAVI2

- High Spectral Resolution Data (e.g. AVIRIS)
 1. First derivative index with baseline at 625 nm.

References

- Adams, J.B., Smith, M. O., and Gillespie, A. R. (1989) "Simple models for complex natural surfaces: a strategy for the hyperspectral era of remote sensing", in *Proc. IEEE Int. Geosci. and Remote Sensing Symp.* '89, IEEE, New York, 16-21.
- Boardman, J. W. (1994) "Geometric Mixture Analysis of Imaging Spectrometry Data", in *Proc. IEEE Int. Geosci. and Remote Sensing Symp.* '94, IEEE, New York, 2369-2371.
- Baret, F., Guyot, G., and Major, D. (1989) "TSAVI: A vegetation index which minimizes soil brightness effects on LAI or APAR estimation," in *12th Canadian Symposium on Remote Sensing and IGARSS 1990*, Vancouver, Canada, July 10-14.
- Baret, F. and Guyot, G. (1981) "Potentials and limits of vegetation indices for LAI and APAR assessment, *Remote Sensing of Environment*, vol. 35, pp. 161-173.
- Clevers, J. G. P. W. (1988) "The derivation of a simplified reflectance model for the estimation of leaf area index, *Remote Sensing of Environment*, vol 35., pp. 53-70.
- Crippen, R. E. (1990) "Calculating the Vegetation Index Faster," *Remote Sensing of Environment*, vol 34., pp. 71-73.
- Crist, E. P. and Cicone, R. C. (1984) "Application of the tasseled cap concept to simulated thematic mapper data," *Photogrammetric Engineering and Remote Sensing*, vol. 50, pp. 343-352.
- Elvidge, C. D. and Chen, Z. (1994) "Comparison of Broad-band and Narrow-band red versus near infrared vegetation indices," *Remote Sensing of Environment*, in review.
- Elvidge, C. D. and Lyon, R. J. P. (1985) "Influence of rock-soil spectral variation on the assessment of green biomass," *Remote Sensing of Environment*, vol. 17, pp. 265-269.
- Goetz, A. F. H. and 7 others (1975) "Application of ERTS images and image processing to regional geologic problems and geologic mapping in northern Arizona," in *JPL Technical Report 32-1597*, Jet Propulsion Laboratory, Pasadena, CA.
- Huete, A. R., Jackson, R. D., and Post, D. F. (1985) "Spectral response of a plant canopy with different soil backgrounds", *Remote Sensing of Environment*, vol. 17, pp.37-53.
- Huete, A. R. (1988) "A Soil-Adjusted Vegetation Index (SAVI)," *Remote Sensing of Environment*, vol. 25, pp. 295-309.
- Jackson, R. D. (1983) "Spectral indices in n-space," *Remote Sensing of Environment*, vol. 13, pp. 409-421.
- Jordan, C. F. (1969) "Derivation of leaf area index from quality of light on the forest floor," *Ecology*, vol. 50, pp. 663-666.

- Kanemasu, E. T. (1974) "Seasonal canopy reflectance patterns of wheat, sorghum, and soybean," *Remote Sensing of Environment*, vol. 3, 43-47.
- Kaufman, Y. J., Tanre, D. (1992) "Atmospherically resistant vegetation index (ARVI) for EOS-MODIS, in *Proc. IEEE Int. Geosci. and Remote Sensing Symp. '92*, IEEE, New York, 261-270.
- Kauth, R. J. and Thomas, G.S. (1976) "The tasseled cap--A graphic description of the spectral-temporal development of agricultural crops as seen by Landsat," *Proceedings of the Symposium on Machine Processing of Remotely Sensed Data*, Purdue University, West Lafayette, Indiana, pp. 41-51
- Kriegler, F. J., Malila, W. A., Nalepka, R. F., and Richardson, W. (1969) "Preprocessing transformations and their effects on multispectral recognition", in *Proceedings of the Sixth International Symposium on Remote Sensing of Environment*, University of Michigan, Ann Arbor, MI, pp.97-131.
- Leprieur, C., Verstraete, M.M., Pinty, B., Chehbouni, A. (1994) "NOAA/AVHRR Vegetation Indices: Suitability for Monitoring Fractional Vegetation Cover of the Terrestrial Biosphere," in *Proc. of Physical Measurements and Signatures in Remote Sensing*, ISPRS, 1103-1110.
- Lillesand, T. M. and Kiefer, R. W. (1987) *Remote Sensing and Image Interpretation*, 2nd edition, John Wiley and Sons, New York, Chichester, Brisbane, Toronto, Singapore, 721p.
- Pickup, G., Chewings, V. H. and Nelson, O. J. (1993) "Estimating changes in vegetation cover over time in arid rangelands using Landsat MSS data," *Remote Sensing of Environment*, vol. 43, pp. 243-263.
- Pinty, B. and Verstraete, M. M. (1991) "GEMI: A Non-Linear Index to Monitor Global Vegetation from Satellites," *Vegetation*, vol. 101, 15-20.
- Qi, J., Chehbouni, A., Huete, A. R., and Kerr, Y. H. (1994) "Modified Soil Adjusted Vegetation Index (MSAVI)," *Remote Sensing of Environment*, vol. 48, pp. 119-126.
- Qi, J., Kerr, Y., and Chehbouni, A. (1994) "External Factor Consideration in Vegetation Index Development," in *Proc. of Physical Measurements and Signatures in Remote Sensing*, ISPRS, 723-730.
- Richardson, A. J. and Everitt, J. H. (1992) "Using spectra vegetation indices to estimate rangeland productivity", *Geocarto International*, vol. 1, pp. 63-69.
- Richardson, A. J. and Wiegand, C. L. (1977) "Distinguishing vegetation from soil background information," *Photogrammetric Engineering and Remote Sensing*, vol. 43, pp. 1541-1552.
- Roberts, D. A., Smith, M. O. and Adams, J. B. (1993) "Green Vegetation, Nonphotosynthetic Vegetation, and Soils", in *AVIRIS Data, Remote Sensing of Environment*, 44: 117-126.

Rouse, J. W., Haas, R. H., Schell, J. A., and Deering, D. W. (1973) "Monitoring vegetation systems in the great plains with ERTS," *Third ERTS Symposium, NASA SP-351*, vol. 1, pp.309-317.

Rouse, J. W., Haas, R. H., Schell, J. A., Deering, D. W., and Harlan, J. C. (1974) "Monitoring the vernal advancement and retrogradation (greenwave effect) of natural vegetation," *NASA/GSFC Type III Final Report, Greenbelt, Md.* 371 p.

Smith, M., Roberts, D., Hill, J., Mehl, W., Hosgood, B., Verdebout, J., Schmuck, G., Koechler, C. and Adams, J. (1994) "A New Approach to Quantifying Abundance of Materials in Multispectral Images", in *Proc. IEEE Int. Geosci. and Remote Sensing Symp.* '94, IEEE, New York, 2372-2374.

Smith, M. O., Ustin, S. L., Adams, J. B. and Gillespie, A. R. (1990) "Vegetation in Deserts: I. A Regional Measure of Abundance from Multispectral Images", *Remote Sensing of Environment*, 31: 1-26.

Tucker, C. J. (1979) "Red and Photographic Infrared Linear Combinations for Monitoring Vegetation," *Remote Sensing of Environment*, vol. 8, 127-150.

Wecksung, G. W. and Breedlove, J. R., Jr. (1977) "Some techniques for digital processing, display, and interpretation of ratio images in multispectral remote sensing," in *Applications of Digital Image Processing, Proceedings of Society of Photo-Optical Instrumentation Engineers*, Bellingham, Washington, vol. 119, pp. 47-54.

Geophysical Data Imaging and Presentation

ER Mapper has the ability to process geophysical data, in combination with other software, and enhance geological interpretation through its unique image processing capabilities. The imaging can be an integral part of the interpretation process.

Author

Geoff Pettifer, Petroleum Unit, Department of Agriculture Energy and Minerals, PO Box 2145, MDC Fitzroy, Victoria, Australia.

Introduction

This chapter describes the principles underlying geophysical imaging, with some examples from the standard datasets supplied with ER Mapper. Fourier processing of geophysical data is covered in Chapter 11, “Fast Fourier Transforms”.

The approach taken is to consider first particular aspects peculiar to visualising geophysical data as opposed to systematically pre-rasterised satellite data, specifically the dynamic range and spatial distribution of geophysical data and the effects of gridding. The applications of standard ER Mapper functionality (e.g. kernels, equations etc.) are discussed in generalities including specific geophysical filters and then magnetics, radiometrics, gravity, seismic and electromagnetics are discussed in some detail.

Throughout, the over-riding theme is to use geophysical images, preferably using all available data in an integrated multiband dataset and with vector overlays showing the original data distribution (bias) from which the image was created by gridding. The latter is important to enable recognition of meaningful data and spatial frequencies (as opposed to gridding artefacts).

The use of an empirical and creative approach to combining and interpreting geophysical data is made possible by the power of ER Mapper. If the proper empirical approaches are used and due care is taken to relate to known geology, new relationships between, and interpretations of, the geophysics and geology, can be explored. The advantage of ER Mapper is that you can do 'what-if's' quickly and easily to see whether different processing options are useful or not.

A significant advantage of ER Mapper is that the dataset is stored only once and any processing to provide the different enhancements is defined in an algorithm and dynamically created on the screen as required. This means that no additional data storage is required if many different processing techniques are to be applied. The system is therefore ideal for geophysical imaging.

Geophysical data, unlike satellite data is in real world unquantized values. ER Mapper maintains data precision during all aspects of processing prior to quantizing them into 256 levels prior to display. Earlier image processing system were restricted in treating geophysical data as they only operated on byte data.

Geophysical methods

There are five main types of data that form the bulk of geophysical data collected and used by geophysicists, and which are amenable to geophysical data imaging and interpretation. They are gravity, seismic, airborne magnetics, airborne radiometrics and airborne EM.

In addition to these five are topography, the simplest geophysical property of the earth plus all ground based geophysical methods which can be gridded for imaging purposes.

Below is an explanation of some types of geophysical methods.

Magnetics measures the magnetic field over an area. Variations in magnetic composition of rocks produce variations in the magnetic field which can be interpreted in terms of geology to aid subsurface geological mapping to depths of several kilometres.

Radiometrics is a measure of total radioactivity and specific elements (potassium, thorium and uranium) in the top 1 or 2 metres of soil and rock over an area. Near surface geological and soil mapping can be aided using radiometrics.

Seismic methods are used in petroleum search to measure two-way seismic wave travel time from the seismic measurement datum to subsurface geological boundaries of significance. Variations in seismic velocity can be measured and reflect lithology porosity and hydrocarbon content variations. Two way time imagery is a recent application of imaging in seismic exploration.

Gravity measures the combined gravity effects of subsurface geological formations and structure. Variations in subsurface density produce variations in the gravity field which can help to interpret subsurface geology to depths of several kilometres.

Airborne EM (electromagnetics) is an emerging geological mapping tool which measures over many data channels the decay of an energizing electromagnetic field in the earth. EM responds to electrical conductivity of rocks in the first few hundreds of metres in the earth. Some airborne EM systems measure apparent conductivity of the earth at particular EM wave frequencies. Creative imaging of this data is in its embryonic stages in 1995.

Other datasets to aid geophysical interpretation

Geophysical imaging and interpretation is best carried out using and integrating, on ER Mapper, all available raster and vector data to aid the interpretation. How these ancillary datasets are generated (e.g. other mapping and gridding software packages) is an important consideration. Fortunately ER Mapper supports a wide range of raster grid (e.g. Landmark, ECS, Geosoft, Sierra, Charisma etc.) and vector import (e.g. DGN, DXF, ARC/INFO) and dynamic link (e.g. DXF and ARC/INFO) standards and in some cases (e.g. Intrepid) ER Mapper links very closely to geophysical processing/mapping packages.

These ancillary datasets to aid interpretation can include:

Raster datasets

- Gridded topography/bathymetry (DTM)
- Gridded borehole depths
- Seismic velocity and attribute (e.g. amplitude, phase) grids
- Landsat
- Radar
- Gridded geophysical properties
- Gridded borehole data attributes

- Gridded aircraft altimeter and or terrain clearance
- Gridded geochemistry

Vector datasets

- Culture (roads, rivers etc.)
- Flight line overlays
- Contours of the geophysical data
- Geophysical station and line locations
- Seismic fault polygons and lines
- Survey boundary polygons
- Geological boundaries
- Borehole locations
- Mapsheets
- Exploration licence areas
- Thematic map overlays from mapping software via DXF or DGN formats

Gridding and imaging

Gridding of geophysical data

Geophysical data unlike other remote sensing data is not usually collected on a standard grid (except for 3-D seismic and mining geophysics grid data). Geophysical data is usually gridded for contouring and imaging purposes. The gridding algorithms and criteria used can have a marked effect on the geophysical image aesthetics and the subsequent fourier operations and spatial filtering of an image grid.

There is considerable variation in the ability of gridding packages to adequately grid various data coverage biases without introducing gridding artefacts, which affect the integrity of images. Four main types of data distribution (and an infinite combination of these) are encountered with geophysical data and these are shown in Figure 1.

Figures

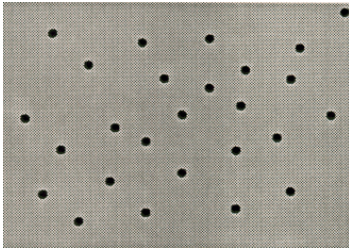


Fig 1a. Random point data (e.g. gravity)

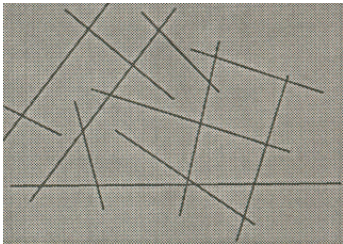


Fig 1b. Random line data (e.g. 2 D seismic)

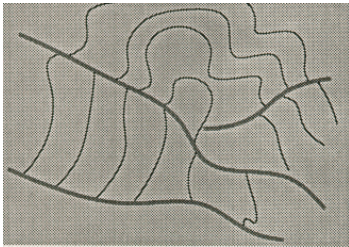


Fig 1c. Contour data, with faults (e.g. topography, seismic contours)

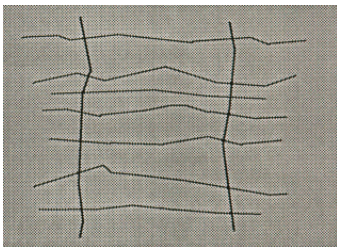


Fig 1d. Regular line data (e.g. airborne magnetics; 3-D seismic)

Gridding is a complex subject in itself, but users of geophysical images need to be aware of the possibility of gridding artefacts (e.g. one gridding algorithm may be optimized for random point data but perform poorly on contour data).

A simple way to recognise gridding artefacts is to apply a sun angle to an image (which has the “force_nosubs” kernel set) and then overlay a vector dataset showing the original geophysical data bias (points/lines/contours). Artefacts could include “pimples” at random point data; “terracing” with contour data and poorly levelled magnetics; trends following random line data; false (or conjugate) trends in directionally gridded data; “scalloping” along faults in seismic data and the “string of pearls” effect on linear anomalies in magnetic images.

Once recognised, there are three choices with gridding artefacts. The first is to minimize them by regridding the data with a different gridding algorithm and different gridding criteria. The second is to live with the artefacts and take account of them when interpreting further enhanced images (particularly spatial filtered images which tend to amplify artefacts). The third is to regrid the data with different gridding criteria and/or algorithms/software, compare the various grids and choose the one most suitable for the application.

Image grid spacing and geophysical data spacing

With most gridding algorithms the optimum grid spacing is about 20% (one-fifth) of the average data spacing (for aeromagnetic, seismic or contour data). This limit can be extended to 10% in some cases.

Line collected data such as airborne magnetics is a special case where grid spacing relative to line spacing and along line data intervals is important.

Unlike satellite or airborne scanner data, airborne magnetic data has high spatial sampling rates along flight lines (e.g. 8 to 50 metres) and lower spatial sampling across flight lines (e.g. flight-line spacings of 200m to 5 km).

Typically, data is gridded to a grid size of about 20% of the flight line spacing (or 10% at the limit). This means that in the gridding process the original magnetic data is often subsampled along flight lines and high frequencies in the data may be lost.

Furthermore, oversampling across flight lines may occur and false correlations and high frequencies between lines may be created. Some contouring algorithms attempt to cross correlate anomaly shapes between lines, and are generally only good at enhancing one trend direction. Others correlate anomalies poorly between lines and produce localized “bullseye” anomalies related to flight lines. Linear “bullseyes” or the “string of pearls” effect are common for linear magnetic features, with many gridding packages.

These effects are most pronounced on regional magnetic data (at 1.5km line spacing). Also improper choice of grid size close to the spatial frequency of near surface related magnetic anomalies can produce ‘aliasing’ of the data (erroneous low frequency, deep body anomalies) which cannot be simply corrected in the image.

Resampling of Image data in imaging

The relative pixel resolution between the geophysical grid to be displayed and the image window or hardcopy device is important. If the number of gridpoints (pixels) to be displayed in an image exceeds the available display device pixels the geophysical grid on disc will normally be resampled by ER Mapper before display and any equations or kernels will be applied to the resampled data grid.

This can be acceptable for many image applications but in some circumstances can lead to erroneous aliasing of the geophysical data. ER Mapper supplies a “force_nosubs” filter which ensures that no resampling of a geophysical grid from disk occurs before further filtering and ultimate display.

Regular use of this option is recommended with geophysical imaging, even though it does slow down redisplay speeds of large geophysical datasets.

A further useful facility in ER Mapper is the “smooth resampling” option which smooths the display to the display or hardcopy device resolution to eliminate spatial quantization or blockiness of the display image and enhance the aesthetics of the image.

General approach to geophysical imaging

The processing of geophysical data requires careful consideration of the characteristics of the data. The aim is to use colour to emphasize geologically important amplitude variations and spatial relationships in anomalies in the data. Processing the data without consideration of the data limits, range of amplitudes and spatial frequencies in the data may produce artefacts or false anomalies from which erroneous geological interpretation is made. Some of the considerations are described in the following subsections.

Visualizing Geophysical Data

Visualizing of geophysical data involves consideration of the data intensity, spatial frequency and processing aspects of the data. Human perception limitations also influence the care we must take in imaging geophysical data.

Variations in geophysical intensity are best expressed in geophysical images by assigning a continuous range of colours or ‘greytones’ to the range of intensity values. The dynamic range of geophysical data can be very large (e.g. 1000's of nanoTeslas in magnetics) compared to the available colours (256 for 8 bit screens).

Colour perception

The dynamic range of the data in geophysical applications is far greater than either the available colours or the final perceived colour differences. It is important to optimise the images to emphasize some aspect of the data. The key point is that a typical geophysical data set will need more than one image to display its full information content.

A number of algorithms are normally created which have different limits, transformations and look up table choices in order to interpret the dataset. Additional processing techniques such as kernels (filters) and formulae (equations) may be applied to the dataset to further enhance perception and to overcome possible dynamic range problems. This is discussed in more detail later.

The limitations of hardcopy devices imposes further restrictions on the dynamic range of the data. Colour variation and therefore perception varies considerably from one form of hardcopy to the other. Being aware of the limitations of hardcopy devices allows you to be critical of any hardcopy on which some interpretation is being performed.

Variations in geophysical anomaly spatial frequencies, relationships and continuity are best displayed in grey tone (or colordrape) sun angle images. Many spatial filters used in satellite image processing have limited use on geophysical data because of the generally smoothly varying nature of geophysical data. Several geophysical filters are available in ER Mapper to apply standard geophysical processing (e.g. upward and downward continuation and spatial derivatives) and directional filtering.

Fourier processing of geophysical data by internal software and dynamic linking of geophysical images to C user code are other facilities to enhance and aid geophysical data visualization in ER Mapper.

Data Familiarization

Before beginning any processing and interpretation of the data it is necessary to familiarize yourself with the data. Four common methods for examining the spatial/amplitude distribution of data, apart from use of the image statistics, are:

- non-cumulative histogram display
- display of the data using a “water-level” color look up table
- z-profiling
- traversing

Non-cumulative histogram display

The non-cumulative histogram display (default histogram) shows an image statistical distribution of data values. The cumulative histogram display shows the histogram equalized cumulative distribution of data. Zooming to different areas enables a quick assessment of values in different areas of the image. If regions in the dataset are of importance, use of the ‘inregion’ formulae to display particular region data only, can be useful to visualize the statistical variation within a geologically meaningful area (e.g. a geological unit polygon). Use of the ER Mapper vector dataset to region conversion facility is useful to designate regions and prior consideration needs to be given to maximizing the designation of meaningful areas as polygons in ancillary vector overlays.

Waterlevel Color Look Up Table

A useful technique for examining the spatial distribution and limits of the data in an image is the use of a “waterlevel” colour look up table which partitions the range of data into three distinct colour ranges. Data values from the minimum to a predetermined threshold are all blue. Values between this threshold and a higher threshold are greyscale, and values from the upper threshold to the maximum are yellow. In effect all of the data values below the lower threshold are below the water level and the yellow coloured values have been partitioned above the upper threshold. These values can be discounted and the greyscale values observed. So the look up table behaves as a bandpass in order to concentrate the mid range values.

One useful technique is to display your data with the ‘watercolor’ look up table, click to limits and slowly increase the lower limit of the transform linear graph along the bottom of the histogram display spreading the blue in the image. Similarly, the yellow in the image will spread as the top cut-off in the data's linear transform is reduced in a like fashion. Using the middle mouse to interrogate the top and bottom limits of the linear transform curve identifies the grey area bandpass values. Typing in limits produces a similar band pass image interrogation effect.

Z-profiling

Z-profiling (text or graph) indicates amplitude information for all bands in a dataset at once and is useful for detailed interrogation.

Traversing

More useful than Z-profiling is the traversing facility of ER Mapper which can be used to observe profiles across geophysical anomalies of interest. This can be applied to one dataset band at a time but it is easy to switch between bands, other coregistered datasets and to move the traverse around the image (e.g. along a linear anomaly strike to observe anomaly change along strike)

Using Transforms to improve displays

You can apply transforms to your data to improve the display.

Limits to actual (linear stretch)

As a default, data values from 0 to 255 are displayed using the 256 colours normally available on screen. While this may be fine for satellite data with, for example, 256 integer data values in the range 0 to 255, the data range for geophysical data is usually much greater than 256. Selecting Limits to Actual causes the data values to be split up into equal groups (a linear stretch) and assigned to the available colours.

Non-linear transforms

Other transformations (such as Gaussian, Histogram Equalize, 99% clip, 95% clip, real time) emphasize different aspects of the data. For example, Histogram Equalize provides maximum brightness.

For the non-linear transformations each quantization colour represents a different length of data interval. Changing limits for a fixed stretch affects the displayed image. These effects may include saturation or loss of detail in all or part of the image.

The effect of zooming on limits

When stretch limits are set to actual, the values used to define the stretch are those displayed in the window. This means that if the image has been zoomed only some of the data has been used to calculate the limits. If you pan to a different location in the dataset or perform a Zoom to All Datasets the transform may no longer be optimal.

Data viewing options

There are a number of ways to image and present geophysical datasets such as aeromagnetic data. They are described below.

Pseudocolor Single Band Display

Pseudocolor single band displays contribute useful information when comparisons are made with other pseudocolor displays.

Real Time Shading

While the use of pseudocolor shows the amplitude and illustrates some trends in the data, more subtle trends can be emphasized using sun angle shading. ER Mapper provides interactive shading so that you can change the elevation and azimuth with the mouse and see the results straight away. This is known as Real Time Shading.

Shading or sun angle simulates the illumination of the data as if it was a topographic surface. The position of the artificial sun which illuminates the data is specified by an elevation and azimuth angle.

Sun angle shading emphasizes trends perpendicular to and sometimes parallel to the sun azimuth. Watch out for gridding artefacts which may be emphasized using this method. Those trends which are perceptible at most azimuths, if not gridding artefacts, are the most likely to be real trends.

Use the 'force nosubs' filter with realtime shading to see maximum resolution of subtle trends.

Vertical shading (elevation 90 degrees) provides an unbiased display of the trends.

Note also that some data requires smoothing prior to sun angle imaging because of data noise and gridding artefacts.

Selecting different display stretches such as Histogram Equalize or Gaussian Equalize prior to shading produces a display with little or no difference in the shaded display. Clipping using 95% and 99% limits has a noticeable effect. Clipping may be usefully applied when mosaicing shaded images.

Shading with sun azimuth along flight line direction minimizes levelling problems.

Example:

examples\Data_Types\Magnetics_And_Radiometrics\Magnetics_Realttime_Sun_Shade

Color Draping

The use of the color drape display combines the advantages of directional information available from shading and amplitude information shown by the pseudocolour. Again use of the ‘force nosubs’ kernel particularly in the intensity layer is recommended to maximise enhancement of subtle gradients in the data.

There are a number of colour schemes that you can use. These are selected using the colour look up tables in the Algorithm window, for example, Rainbow1.

Colour draping over a vertical sun angle gives an unbiased colordrape effect.

Choice of display stretch for the intensity layer in a colour drape is important. Data should not be clipped. Histogram equalized stretch gives a very dark intensity background which may appear OK on the screen but can display too dark on certain lower colour resolution hardcopy devices. To solve this generally requires some experimentation with your own hardcopy devices. The logarithmic stretch (curved upwards on the transform graph) is very useful in reducing darkness in the intensity layer whilst retaining edge shadow. The skew of data (i.e. to higher or lower limits of the transform) can affect the relative enhancement of high or low spatial frequencies using a logarithmic stretch.

Often with high spatial frequency data (e.g. magnetics over surface volcanics) a colour drape display is very dark and ineffective.

If data has a wide distribution of amplitudes and spatial frequencies, use of the equations option to divide the geophysical intensity spectrum into discrete contiguous bandpasses enables multiple optimum sun angle stretches for each bandpass and maximum definition of subtle trends in widely variable data (e.g. topography data with steep mountains, gently undulating plateaus and plains). This technique produces a black line at the edge of each band pass in the intensity layer however.

Colordrape (plus use of kernels e.g. ‘force no subs’) trims the intensity layer of the image because a 3 x 3 kernel is used for the sun angle. Use of the dummy 3, 5, 7 etc. filters in the pseudocolor layer can trim the pseudocolor to the intensity image layer. Holes in an image are magnified by use of colordrapping. This can be a problem with some datasets (e.g. seismic faults containing null values).

The colordrape affords great flexibility in the colours used for draping. Colorbars used in map annotation utilize the colour limits and distribution of the output transform in the first active pseudocolor layer in an algorithm and do not display the intensity greyscales. For this reason the colour bars appear brighter in colour than their corresponding colours in the image.

Example: examples\Data_Types\Magnetics_And_Radiometrics\Magnetics_Colordrape

HSI

HSI provides an impressive metallic lustrous or dull continuous intensity background to a hue/saturation colour image. The HSI display overcomes the quantization and darkness problems of the intensity layer of a colordrape display.

Filters

Filtering of geophysical data can be done by fourier analysis methods or by use of spatial filter methods. Filtering can be done in the fourier domain in ER Mapper (v5.0+) or a geophysical package (e.g. AGP, GEOSOFT/GIPSI or Intrepid) or using the very limited spatial filters supplied by ER Mapper. Filter methods will be discussed here, and fourier analysis in Chapter 11, “Fast Fourier Transforms”.

Some filters, which are designed for cleaning up satellite images, are useful for crude sun angle and image smoothing of geophysical data. These include smoothing, frequency, edge enhancements and residual filters. Additional filters designed specifically for geophysical processing include the hanning filter and upward and downward continuation and second derivative filters.

All filtering applied to geophysical should be preceded by a force nosubs’ filter to ensure the data is sampled at the original dataset resolution not the display device/window resolution.

Below are examples of filters that can be applied to geophysical data:

Smoothing

Smoothing filters supplied with ER Mapper are:

- hanning3
- avg3
- avg31
- avg5
- avg7
- avg_diag
- avg_h_v
- avg_hor
- avg_ver.

These are used to smooth data noise and gridding artefacts, for example, for radiometric data and pre sun-angle. The hanning filter is probably best suited to geophysical data.

Frequency

Frequency filters may be highpass, lowpass or bandpass. Some ER Mapper supplied examples are:

- highpass_4
- lowpass_4

These are derived pass filters at spectral wavelengths of approximately a multiple of grid spacing. For example, highpass_4 passes high frequency (low wavelength) data with wavelength less than or equal to approximately four times grid spacing. There is a 3 db cutoff at 4 grid spacings.

Frequency filters may be useful in some cases, for example, to remove surface noise in magnetics. Note the highpass filter shows edges in data but ringing effects are noted. The low pass filter removes noise but retains a lot of high frequency.

Edge enhancement/directional

Some examples of ER Mapper's edge enhancement/directional filters are:

- East_West
- North_East
- North_South
- North_West
- NorthWest_5
- Sobel1
- Sobel2
- South_East
- South_North
- South_West
- West_East
- h_edge
- h_edge_5
- Laplacian
- Laplacian5
- sharpened
- sharpen
- v_edge
- v_edge_5

Edge enhancement or horizontal gradients can be carried out on raw located magnetic data or on the image grid. In most cases this can be done with a derivative technique. Edge enhancements are always useful to define structure and in some cases the edge enhancement filters highlight subtle structure better than real time shading. In other cases the edge filters severely amplify gridding artefacts.

With magnetics data, anomalies edges are shifted to the north in the Southern Hemisphere and to the south in the Northern Hemisphere. This is due to latitude effects on magnetics. Edge detection kernels are best applied to reduced to pole data --> import to fourier analysis package

Second derivative filters

There are also approximate spatial second derivative filters, for example from Henderson and Zeitz (Fuller, 1967):

- hz10_2nd_deriv
- hz13_2nd_deriv
- hz1960_2nd_deriv

Note that you can try appending smoothing filters to second derivative filters. But these filter responses are poor as they are approximate filters. The hz1960 filter is probably best.

Residual

These filters highlight local anomalous values and can be very sensitive to gridding artefacts in some cases:

- low_frequency
- residual_1
- residual_2
- thresh_3
- thresh5

Continuation

The following filters are the only true geophysical frequency filters for enhancing low or high frequency for deep or near surface sources.

- up_cont_half
- up_cont_1
- up_cont_2
- down_cont_half

- down_cont_1
- down_cont_2

Note that:

- On the Newcastle magnetics dataset downward continuation at 1/2 spacing (20m) enhances WNW dykes and fractures well.
- Downcontinuation 1 spacing becomes noisy, so apply/append avg3 and retry.
- Down_cont_2 spacing is next to useless unless flying height is a lot greater than grid spacing.

Try appending 2 dc_half filters and compare with dc_1. Differences could be due to the fact that filters are imperfect in response

- Upward continuation has little effect on the Newcastle magnetics data other than to filter out high frequencies in data. This is useful for defining gross effects of major magnetic bodies and filtering out magnetic noise, due to surface cover such as laterites and basalts.

Notes on the use of filters with geophysical data

For geophysical data, do not subsample because when processing and displaying images you can apply the kernel before or after subsampling. For geophysical applications you should normally apply the kernel to the complete dataset. To do this you must select **Process at dataset resolution** in the **Filter** dialog box.

Use of Equations in Geophysics

There are a number of ways to combine data from different bands in the same dataset, by using equations. They are:

- Mosaicing data with base level shifts. For example:

$\text{MagA} - \text{MagB} + \text{contrast}$

- Ratioing. For example:

K/Th ratio in radiometrics

or

$(\text{K} - \text{Kmin}) / (\text{Th} - \text{Thmin})$

This removes arbitrary level shifts in K and Th before ratioing. The latter formula is similar to Dark/Black pixel subtraction in satellite imaging.

- Show the Pseudo gravity effects of a layer using the Bouguer slab formulae. For example:

Bouguer slab effect of a layer = $2\pi\rho G \times \text{thickness}$

where ρ = density (T/m³) and G = Gravitational constant.

Any empirical equation can be experimented with to try to enhance some aspect of the geophysical data.

- Combining different data types. For example:
barometer - altimeter = DTM in airborne magnetics
- Classifying (see radiometrics).

Combining Filters and Equations

You can combine filters and equations in any way you like. For example:

Pseudo - Vertical Derivative

You can take the up_cont_half of a dataset and subtract the dataset from it. Display this as a pseudocolor image to see the pseudo-vertical derivative as a quick alternative to full fourier processing for vertical derivative.

To do this you would create a formula with “I1-I2”. In I1 you would have the original data with a up_cont_half filter applied to it, while in I2 you would have the original data with a vertical derivative filter applied to it.

Note that in this example the same band of the dataset is being used twice with different processing applied to it.

C User code links

Geophysicists like to apply their own processing to their data. ER Mapper affords a degree of flexibility to do this to a small grid of geophysical data adjacent to an image pixel, through the C User code links facility. This facility passes adjacent pixel values via an n x n kernel (where n is an odd number) to an external processing routine which takes the kernel values as inputs and returns a new central (to the kernel) pixel value. An example might be inner zone terrain corrections for gravity pixels using prism based modelling on the coregistered topography grid of pixels. The standard ER Mapper manuals describe how to construct your own C User code link.

Some standard kernels which employ external C code are supplied with ER Mapper and a useful one to try on your geophysical data is the “local_enhance” filter which allocates maximum pixel brightness based on a local histogram equalized stretch in a (31x31 sized) kernel centred on the current pixel. This is like a moving AGC on the data, normalising all data values to the range 0-255 and this maximizes subtle local effects. Use with care as the results can be quiet dramatic, especially where subtle anomalies are superimposed on large anomalies. Again an empirical approach is recommended.

Another filter is the “majority” filter which works on 8-bit integer datasets like a Classification layer from radiometrics data for example. The 3 x 3 filter chooses the majority value within the filter area and replaces the central pixel with the majority value. This can be used to “clean up” visually noisy classifications.

Other supplied filters can be found in the “usercode” kernel directory.

Interpretation using annotation

The on screen annotation capabilities of ER Mapper enable interpretation direct from images rather than from hardcopy. Intelligent use of the power of annotation can enable quicker interpretation of one dataset and checking against other datasets. For example it is possible to have two windows open in geolink mode, one showing magnetics the other gravity for the same area. The geolinking maintains the same zoom between the two windows. Annotating the magnetics interpretation vector and saving it regularly and then reloading it over the gravity image and redisplaying in the ‘gravity’ window enables regular checking of the magnetics interpretation with respect to the gravity as the magnetics interpretation progresses.

Other interpretations and ancillary vector data (e.g. hydrography, data distribution) can be overlaid in other colours to aid on-screen interpretation. To further aid interpretation and annotation the image mode can be changed between Pseudocolour, Colordrape and real-time sunangle. Zooming enables detailed interpretation and full resolution not afforded on hardcopy interpretation. Two windows (not geolinked) open on the same dataset, one at a regional zoom the other on a detailed zoom gives a regional perspective to a detailed interpretation of part of an image.

Topography, if available (with a hydrography overlay) is a useful other image window to have open and geolinked during interpretation, as it often has an influence on geophysical response, relevant to the interpretation.

Imaging magnetics

The magnetic data provided in the ER Mapper standard datasets is a detailed, high quality, airborne dataset from the Newcastle Range in north Queensland, Australia. Two datasets are included: total count and vertical derivative images.

The vertical derivative data is not normally available and is used in the algorithms below to illustrate the results obtainable from this processing. Additional algorithms provide a processing technique which approximates the results available from vertical derivative processing.

Magnetic data collection

An aeromagnetics dataset is commonly captured using a Caesium Vapour Magnetometer. Typical parameters of a modern detailed magnetic survey are:

- Flight-line spacing 200 m
- Along line sampling 8 m
- Tie-line spacing 2000 m

The data may have diurnal correction, levelling and IGRF correction applied. The final dataset will generally be gridded, for example to 40 m x 40 m cells.

Effect of Depth on Anomaly Shape

Magnetic signals are strongly influenced by the depth of the magnetic body. Magnetic anomalies from shallow bodies usually show high spatial frequency, whereas anomalies from deep bodies exhibit low spatial frequency. As a general rule, the “sharper” an anomaly the shallower the causative body.

Reliability of Gridded Magnetic Data

Many factors affect the reliability of magnetic image grid data, which needs to be considered when analysing magnetic images. The gridding process to produce the grid is crucial because magnetic data is often highly spatially variable and may exhibit several systematic directional trends.

Available contouring algorithms vary considerably in their ability to adequately grid magnetic data without producing artefacts. The gridding artefacts are noticeable particularly when applying kernels (or filters) to the grid that enhance the derivatives, edges or slope of the data surface. Real Time shading can amplify gridding artefacts. Often there is no simple way to overcome these artefacts other than to apply an averaging filter to the grid prior to Real Time Shade or other kernels.

Data Levelling Artefacts

Magnetic data along flight lines is “levelled” to eliminate altitude clearance differences effects and diurnal variations between adjacent flight lines. Levelling corrections are not always effective particularly on earlier regional data and can produce “striping” or “stepping” effects in the data. Sun angle images with sun illumination across line direction enhances the effect of levelling errors. Illumination along line direction is most effective in minimizing the visual impact of levelling errors.

Effect of Aircraft Altitude

In rugged terrain constant survey altitude can not be maintained and causing low aircraft ground clearance over ridges and high clearances in deep valleys. This is particularly severe with fixed wing surveys, less so with helicopter surveys. Magnetic response is related to distance from the aircraft and this means there is often a negative correlation between radar altimeter and magnetics. Therefore imaging of the aircraft radar altimeter gridded data may be useful in interpreting the magnetic image.

In favourable circumstances a DTM may be available or can be constructed from the aircraft barometer data, altimeter data and ground contours for calibration purposes.

Grid Manipulation of Magnetic Data

Grid filters for upward and downward continuation of magnetic data to enhance deep or shallow magnetic anomalies can be used on magnetic data. The bulk of geophysical filtering on magnetic data must be done in the fourier domain in ER Mapper or in an external magnetics mapping package (e.g. AGP, Geosoft / GIPSI or Intrepid).

ER Mapper can import and display raw and fourier domain processed grids from geophysical software. Once imported upward and downward continuation filters can be applied. ER Mapper provides the facility for this by filters for upward and downward continuation at one-half and one grid spacing, band pass and strike filters (Mufti, 1972; and Fuller, 1967).

Airborne radiometrics imaging

The radiometric data provided in the ER Mapper standard datasets is a detailed, high quality, airborne dataset from the Newcastle Range in north Queensland, Australia.

Radiometric data

Radiometrics is airborne ground geochemistry of the selected elements K, Th and U. A radiometrics dataset usually includes data for K, Th, U and Total Count. Typical datasets will have along-line sampling at 60 m intervals and a crystal volume of 33.5 litres. Listed below are factors that influence radiometric data collection and image reliability.

Survey accuracy and calibration

The accuracy of radiometric data depends on the size and counting statistics of the counting crystal used in an aircraft and the flight line spacing.

Earlier BMR regional surveys of Australia are at wide line spacing (1.5km) using very small crystals and generally only Total Count and possibly the potassium channel are statistically significant. Levelling of this early data is poor by modern standards also, however, because of the widespread availability of this early regional survey data it can be of some use in the absence of modern data.

Commonly, modern radiometrics exploration uses close line spacings of 200 - 400 metres (or less) and large crystals of 33.2 litres or 16.6 litres.

Radiometric surveys are typically calibrated to local standards for internal consistency and the unique response of the aircraft system used. Matching disparate radiometric surveys with different crystal volumes, aircraft and flying heights can be a problem. Only recently are attempts being made in Australia to standardise radiometric surveys between aircraft to units of equivalent ppm K, U and Th, based on the Canadian experiences.

Ground resolution

Survey altitudes affect survey resolution. Regional surveys are typically 75 to 150 metres ground clearance with a typical “field of view” or detector effective swath width of about 400 to 500 metres. With 1.5 km line spacing this leaves some 1 km of ground between lines uncovered by radiometrics and data has to be interpolated in the gridding process that generates the gridded data from the raw line data. Typically, pixel sizes for gridded regional data are 100 to 300 metres.

With detailed survey data of about 250 metre line spacing and 80 to 100 metre ground clearance (or less), the detector “swath” from adjacent flight lines overlap and provide more or less continuous coverage of the ground. Typical pixel sizes of detailed data are 50 to 100 metres.

As a result of large possible range of ratios of line spacings to swath widths and the statistical nature of the data, gridded radiometric data needs to be interpreted in conjunction with a flight-line overlay.

Image Striping

Radiometric corrections of airborne radon are not always effective and image “striping” can be a problem. The stripes are not simply related to grid lines on the image but flight lines on the original data. Generally, corrections need to be done on the original flight data and the data needs to be regridded to minimize or eliminate “striping”. This is in contrast to satellite data striping which is generally grid line related. Satellite image destriping methods may not be fully effective on radiometric data.

Aircraft Altitude

Altitude of the aircraft measured by the radar altimeter is important in determining the reliability of radiometric data, especially in mountainous terrain. As a general rule if aircraft ground clearance exceeds 250 to 300 metres, radiometrics data corrections for

deteriorating radiometric signals at certain heights are unreliable. Thus, in mountainous terrain, deep valleys show noisy, unreliable or erroneous radiometric signals, and mountain tops, where survey aircraft altitude is often lower than the average altitude, show strong radiometric signals.

Also, altitude, or more correctly terrain shape/curvature affects radiometric signals. Valleys tend to “focus” or increase radiometric signals artificially and ridges tend to “disperse” or decrease radiometric signals artificially.

Altitude can also affect radon “noise” in the data due to near ground radar inversion layers and this can be evident for radiometric data flown in early morning. Uranium channel responses may show a positive correlation with altitude.

Thus, given the importance of altitude for data quality, where available, a grid of altimeter (ground clearance) data is useful to help interpret the reliability of the airborne radiometric data images.

Geology, mineralization and soil mapping

Different types of geology have particular radiometric “signatures” associated with them, where a “signature” is a combination of high and low densities of different bands of data. To look for areas of likely mineral deposits, the signature of an area of known deposits is studied and then other regions are searched for similar patterns. Radiometrics is also particularly useful in environmental studies mapping the regolith and mapping soils for agricultural and soil salinity studies.

For example, BHP Pty. Ltd. initiated the airborne survey for epithermal gold exploration in the Newcastle Range Volcanics, Australia (see the Newcastle Range airborne dataset supplied with ER Mapper). The classic target signature is magnetic lows and radiometric potassium highs indicating possible hydrothermal alteration of the volcanics.

Example algorithm:

examples\Data_Types\Magnetics_And_Radiometrics\Radiometrics_Magnetics_RGBI.alg

Interpreting Radiometrics Data

In ER Mapper, radiometrics can be used in innovative ways for geological mapping.

Typical ways for showing radiometrics data are:

- As an RGB combination of Potassium, Thorium and Uranium (K, Th and U).

Note that the industry standard for radiometrics RGB display is K for Red, Th for Green and U for Blue. The least important data, which is Uranium, is sent to the blue gun as this is the colour that the eye is least sensitive to.

- As a pseudocolor image of a single band. For example, K, Th, U or Total Count)
- As a ratio of two bands by using formulae.

- In combination with other datasets such as magnetics. For example, with radiometrics as color and magnetics data as an intensity layer or vice versa.

NOTE: Interpretation of radiometric data (like satellite data) without ground truthing is not advised.

Ratios

Ratios can be displayed as single bands. Such as:

K/Th ($K - K_{min}/Th - Th_{min}$)

and

U/Th , K/U

In interpreting radiometric data, ratios are useful for the following reasons.

- 1 Ratios of channels in radiometrics have been used to diagnose or enhance various geological features, for example, for mineralization and clay types. These examples include:
 - K/Th
 - U/Th
 - U/K
 - $Th * K/U$
 - Th/K
 - Th/U
 - K/U
 - $U * U/Th$
 - $K/TC\%$
 - $Th/TC\%$
 - $U/TC\%$
 - $U * TC/Th$

Generally an empirical approach has been used. Actually any combination is empirically valid provided noise levels in the data do not dominate and proper empirical approaches are used.

Example algorithm:

examples\Data_Types\Magnetics_And_Radiometrics\Radiometrics_ratio_K_Th

- 2 They are useful to highlight a geological feature which may otherwise be almost indistinguishable from another feature on an K, U, Th and KUTH RGB image.

Note, ratios differentiate where simple bands do not. For example, carboniferous granite has a similar K, U, Th and TC response to ignimbrites of the similar age. However, granite shows a generally lower U/Th and higher Th/U than the ignimbrites. But K/Th and Th/U are similar. Also U/K is lower and K/U higher for many granites compared to ignimbrites.

3 Ratios can also be used as a classifier.

But, generally ratios are in the form of “(A-A min)/(B-B min)” because of negative minimum response. This is similar to dark pixel subtraction in Landsat atmospheric correction.

4 Ratios can be normalized.

Note that ratios also often sharpen geological boundaries for structural control of features. You can set up ratios by editing the formula for a layer, typing in the formula (for example, “I1/I2”), setting the inputs to the appropriate bands and rescaling the output.

5 Ratios can be combined. For example, RGB radiometrics over VD or DTM. Ratios can be used any other way you would like to combine the data.

Ratio Combinations (RGB)

Almost an infinite variety of RGB ratio combinations is possible and generally more than one is needed to define all geology.

Combining Radiometrics and Other Data

Radiometric data can be combined with Landsat TM, magnetic and other data. It is best to have a Digital Terrain Map to interpret radiometric data because soils can be transported downslope or throughout catchments, away from source rocks.

It can also be useful to overlay streams or river vectors to identify transported clays in valleys. For example, create a colour drape image with magnetics data as colour and radiometrics data as an intensity layer or vice versa. Alternatively, use the RGBI image with Potassium, Thorium, Uranium and Magnetics.

Radiometrics and Satellite Data

Combination of radiometric images with good satellite data (e.g. TM, SPOT) can enhance soil classification and enable swamps and water bodies to be identified (Wilford et al, 1992). With similar pixel sizes and different vegetation responses detailed radiometrics and TM data complement each other well as the information they can potentially provide. There is much scope for applied research and experimentation in combination of satellite and radiometric data.

Classification and Principal Components

Other processing that can be applied to radiometric data is classification and principal components.

Classification involves taking a large dataset with many variations in it, for example, many bands with many variable levels and dividing it into a small number of classes. You can either identify individual known types of mineralogy and then let ER Mapper compute the

probable mineralogy for the rest of the image, as in supervised classification, or have ER Mapper automatically identify separate classes to which you can then assign probable identities.

In radiometrics, different geology and soil have different K, Th, U concentrations which might reflect underlying *in situ* geology or transported soils.

Note that if people want to classify on other than single bands, for instance ratios, they must first save as a virtual dataset, define regions and statistics for new datasets, and then classify.

It is always important to try to classify radiometrics to see what it looks like. There are two techniques:

Supervised classification. Where you can use maximum likelihood or mahalanobis the interpreter can define training regions where you are confident of known uniform geology and a reasonably uniform response and use ER Mapper to classify the entire image into these training region classes.

Unsupervised classification. Where you can use an arbitrarily small number of classifications, for example, 10 or 20. If you use more, you will have trouble differentiating between the different classes.

Principal Components. Principle components are only useful where you have multiple bands of data. They are very difficult to interpret but may be of use in an empirical approach. You can be fairly sure that PC1 will show you the most common changes from the perspective of the radiometric data, even though it is not clear what those changes are. Therefore, PC1 can highlight prominent features in the area. The final PC, in radiometrics, which is generally PC4, normally has most noise. Because Uranium is most noisy, most of the Uranium noise will end up in PC4. You may want to look at the other principal components to see if they highlight strong features. Again an empirical approach using ground control (geological and / or soil mapping) is advised.

Principal components analysis on 3 band radiometrics (K, Th, U) and 4 band radiometrics (K, Th, U and Total Count) may be worth experimenting with to see which is more empirically useful.

Seismic reflection data imaging

Seismic data images supplied with ER Mapper are from a 3D seismic dataset

Introduction

Seismic imaging first started with 3D data (Tilbury and Bush, 1991) and has been used for 2D data. Care must be taken in preparation of the images to get a satisfactory result.

2D seismic data

Most available seismic horizon data is 2D data collected along a random series of lines. It is interpreted on a seismic workstation (e.g. Landmark, Charisma or GEOQUEST) where it can be exported as a grid or as interpreted horizons. Because of the large line spacings between 2D lines the grids produced by seismic workstation software are adequate for workstation interpretation guidance purposes, but they are mostly not suitable for imaging because the gridding algorithms may not be optimal for imaging. Export of the 2D seismic two-way time horizon data and fault polygon data to a seismic mapping package (e.g. Petroseis, Zycor or Radian CP3) is recommended for image quality gridding.

Also gridding of time thickness is problematical and probably needs to be done on the horizon time difference data rather than subtracting the two horizon grids. Care needs to be taken in both horizon and time isochron gridding with gridding with faults, across faults and in small fault blocks where little seismic control is available. The better the contour/fault editing capability of the seismic mapping package, the better its fault gridding capability (e.g. ability to assign two-way time values around fault polygons) and the better its ability to incorporate interpreter guidance in the attainment of a final grid / contour, then the better the final image result.

3D seismic data

3D seismic horizon data is growing in usage and volume and is readily exported as a grid from workstations to ER Mapper. With 3D data the grid resolution is so fine that pixelation at the 3D grid resolution using the gridding capabilities of the workstation produces image quality grids. With 3D data various seismic attributes can be exported to ER Mapper along with average and interval velocity grids.

Grids and fault polygon transfer to ER Mapper is necessary to successfully image the seismic data. ER Mapper's capability to import from the workstations directly is growing rapidly. Links to the seismic mapping packages is via ascii grid format transfer and DXF vector format or user shell scripts for polygons. Once in ER Mapper the individual horizon and isochron (time, velocity and attribute) grids need to be combined in a multiband dataset (with other data e.g. topography/bathymetry, gravity, magnetics) for analysis.

Imaging two-way time data

Pseudocolour or Colordrape images with solid fill fault polygons are a useful presentation. DXF (linked or imported) contour and seismic shotpoint map overlays can be instructive also. A reverse linear transform portrays shallow times as reds (structural highs) and deeper times as blues / violets (structural lows). For isochron data the normal linear transform shows thickest formations in reds and thinnest formations in blue / violet.

Creative operations on seismic image data

If velocity grids are bands of the seismic ER Mapper dataset, use of simple ER Mapper formulae can effect simple depth and formation thickness conversions.

Datuming of any horizon and aggregating of minor seismic units (e.g. between major unconformities) can also be easily effected. Ratioing of formation thickness can enhance relative thickness and aid in an understanding of geological activity (e.g. relative fault movement, deposition and erosion) throughout time.

Attribute data can be color draped over a two-way time structure (or formation isochron) intensity layer. If multiple attribute data related to physical properties of formations and sufficient well data is available, then the statistics and classification capabilities of ER Mapper affords possibilities for experimentation with new methods to determine hydrocarbon indicators.

Dip and Azimuth Displays in Seismic

ER Mapper enables dip and azimuth displays to be generated for 3D and 2D horizons (though beware gridding artefacts on 2D horizons). Several standard algorithms are provided under the “Application_seismic” directory and an azimuth lookup table gives the standard display look and feel (Dalley et al, 1989). The dip algorithm gives a display similar to a static sunangle.

Example algorithms:

- examples\Data_Types\Seismic\Horizon_Azimuth.alg
- examples\Data_Types\Seismic\Horizon_Dip

Data integration

Most importantly, previously disparate datasets (seismic, topography/bathymetry, magnetics, Landsat), all of which contribute to the structural understanding of an area are now easily integrated and available, to enhance the seismic interpretation by joint interpretation and comparison in ER Mapper. Figure 2 below shows an example of an integrated dataset from a study in the Otway Basin, Australia (Pettifer, 1992).

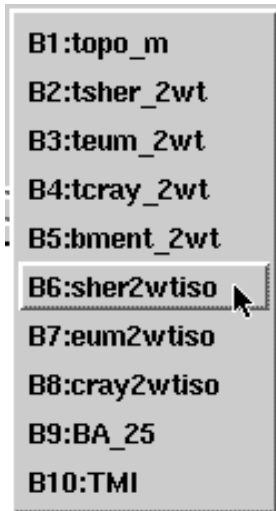


Figure 2.

Gravity imaging

Gravity data is available in Australia from AGSO National Gravity database and can be supplemented with new data. Old and new data, if properly tied to the IGSN71 gravity datum (gravity units used are in micrometers sec⁻²) and AHD height datums can be combined and regridded at any appropriate Bouguer reduction density for display as an image. Older gravity data may be referenced to the earlier Potsdam gravity datum and be in units of milligals and need conversion to the IGSN71 datum and then combination with IGSN71 data and total regridding before imaging.

Offshore gravity data can be displayed as Bouguer anomaly (with water replaced by the Bouguer density) or free air gravity. Bouguer anomaly onshore with free air anomaly offshore is a common convention.

Gravity image displays and spatial frequency

Gravity data (unlike magnetics, seismic, or any line collected data) is usually much sparser in data coverage, leading to lower spatial frequencies in the data.

Thus gravity data is particularly suited to colordrape imaging. Depending on gridding artefacts, structural trends in gravity data can be greatly enhanced with colordrapping. Minimum curvature gridding seems to give the best gridding with least station related “pimple” artefacts.

As the spatial frequencies in the gravity data only reflect the gravity data coverage, gravity images are best studied in conjunction with other higher spatially sampled data for an area (e.g. magnetics, topography etc.) to gain a better appreciation of near surface geological variation. Use of a gravity station vector overlay is highly recommended to understand the spatial frequency deficiencies and possible artefacts of your gravity image.

Vector Overlays

Gravity images can be displayed with geological boundary overlays, and station position overlays imported as DXF from geophysical mapping packages (e.g. AGP, Geosoft/GIPSI, Intrepid, Petroseis).

Gravity and Bouguer density choice in imaging

Gravity data can be affected by terrain and if topography images are available, ideally they ought to be combined with the gravity data. Apart from terrain corrections in gravity, incorrect and/or variable Bouguer (terrain) density can give terrain correlated spurious anomalies which mask the subsurface gravity effects. The Nettleton method of minimization of the correlation of Bouguer gravity with terrain can easily be effected over an entire image area or areas of uniform geology with ER Mapper in a gravity/topography multiband dataset. In the discussion that follows terrain corrections are ignored.

Bouguer Gravity combined with free air gravity, topography and/or bathymetry in a multiband dataset enables calculation of Bouguer anomaly at densities other than that used in the original Bouguer anomaly calculation on the point gravity data prior to imaging an gridding, using the equations capability of ER Mapper and the equations in gravity.

Bouguer gravity = Free air gravity - Bouguer plate correction

This reduces to:

$$BA_{\text{onshore}} = FA - 2\pi\rho G \times \text{elevation}$$

$$BA_{\text{offshore}} = FA + 2\pi\rho G(\rho_{\text{wb}} - \rho_{\text{water}}) \times \text{water depth}$$

where ρ_{wb} = water bottom density; ρ_{water} = water density; and G = Gravitational constant.

Using the “Save As Dataset” option a new multiband bouguer anomaly dataset can be created containing topography and bouguer anomaly calculated by the formulae above at a range of plausible densities for the area (say 1.9 to 3.3 T/m³ at 0.1 T/m³ intervals). If geological boundaries are available and shared in ER Mapper as attributed polygons within an ERVEC vector dataset, the polygons (preferably labelled by a geological name) can be imported as regions to the multiband bouguer anomaly dataset.

Calculation of statistics on the bouguer anomaly dataset will then enable analysis of the correlation of gravity and terrain for regions (ALL or individual geological regions). From this analysis a better bouguer anomaly image can be facilitated by a better choice of density. Use of the crossplotting facility will also enable a visual assessment of terrain/ bouguer anomaly correlation as well for various densities.

A word of caution: typically a topography image may be based on more data than the gravity image and therefore contain higher spatial frequencies than the gravity. In this case grid the terrain data from the gravity data alone using the same gridding algorithm and criteria and both topography and gravity should have the same spatial frequencies.

Gravity stripping

The above mentioned bouguer plate correction can also be used to enable a crude form of gravity stripping where subsurface depth horizons are available for an image area (for example, from seismic and tracehole data in sedimentary basin areas). Gravity stripping can be effected by calculating the approximate total effect of each layer at an appropriate density, and subtracting it from the free air gravity.

This technique can identify where gross gravity effects are coming from within a sedimentary basin but can introduce errors and artificial trends in the stripped gravity data at faulted edges of subsurface layers where the bouguer plate assumption breaks down.

A more rigorous approach to gravity stripping (or whole geology modelling) involves 3D modelling of terrain and is beyond the scope of this discussion and most gravity interpretations extant in the literature today. The NODDY software package enables forward modelling of gravity for complex structures and integrated seismic / gravity surveys / modelling is becoming more frequently used in the petroleum industry, so no doubt this area of gravity interpretation will evolve with a role for creative imaging in the interpretation process.

Gravity Profiling

Gravity profiles can be extracted from a gravity image using the profiling option. simple cross-sections can be digitized or existing vectors can be chosen for the profile (for example seismic traverses, flight paths or roads).

Dynamic links to user code

Dynamic links to user code enable further innovative use of ER Mapper with gravity and is an area worthy of further exploration. Crude nearzone terrain/water bottom connections of bouguer gravity is one example where the user code link could be useful.

Geophysical filters in gravity

Geophysical filters (previously discussed) can be applied to gravity data (for example, upward continuation). Downward continuation filters must be used with caution.

Airborne electromagnetics imaging

Resistivity

Earth resistivity is primarily a function of the interconnected porosity of the rock, the amount and quality of contained water, and degree of saturation. Electronically conductive minerals such as metallic sulphides which have very low resistivities generally contribute little to bulk resistivities of earth materials unless present in large quantities. Thus, earth resistivity is normally determined by ionic conduction through the pore spaces of rocks.

Intrusive rocks have low porosity and much higher resistivities than sediments. A sandstone aquifer, if saturated with fresh water, might have intermediate values. The presence of clay minerals also will lower resistivities significantly because of their surface electrical properties.

EM imaging

Airborne EM data varies from early time-domain (pulse decay) 6 channel INPUT data through to the modern SALTMAP and GEOTEM III multichannel systems. Apparent conductivity or raw channel voltage data is gridded as per conventional airborne magnetics. The sheer volume of data from a modern airborne EM system has seen a move toward 3D imaging as in seismic 3D, so it remains to be seen where the near future role for conventional image processing in fixed wing time-domain airborne EM. Certainly ER Mapper's multiband dataset capability and equations capability is ideal for imaging this data.

Helicopter bird EM systems (e.g. Dighem) use multifrequency EM to enable a range of effective depths of investigation and the data from these systems are readily amenable to gridding and ER Mapper imaging. These systems are popular in Canada. There are few case histories to establish an extant practice of imaging of EM data.

Ground based EM systems imaging

Mining grid geophysics often uses multichannel time-domain EM (e.g. SIROTEM, ZONGE, Geonics) and frequency domain EM (e.g. Geonics EM34) systems, all of which can be gridded and imaged with other geophysical data.

Topography

Surface topography is another geophysical anomaly method amenable to use with image processing in exploration. Curiously, apart from airphoto interpretation for geological structure and some geomorphological studies, there has traditionally, been little use of topography as another “geophysical” property to be used for interpretation purposes in geological mapping or exploration.

Topography and bathymetry: surface elevation, is the simplest of all physical Z values that can be attributed to an x,y position on the earth's geological surface. Surface elevation is therefore arguably the simplest measurable geophysical property of the earth. The earth's surface is the current day unconformity or disconformity and its shape is determined by current and previous geological processes. It can therefore be reasonably expected that knowledge of that shape combined with other surficial and interpreted subsurface geological and geophysical properties or attributes, may considerably enhance the understanding of local and regional geology.

Erosion is the principal agent of formation of the shape of either a subsurface or the surface topography unconformity, smoothing the topography, producing, low spatial frequency, long wavelength topographic anomalies. Steep structural relief on the present day surface or an older subsurface unconformity surface, may be related to structure, either directly by new faulting or by reactivation of existing older and deeper structure or by differential settlement (often manifest along pre-existing faults) and this produces high frequency, short wavelength topographic anomalies.

This wavelength separation of topographic anomalies makes topography, like other geophysical techniques, amenable to enhancement, detection and interpretation using standard imaging techniques. In the case of sedimentary basin exploration topography/bathymetry imaging is directly analogous to two-way time imaging.

Sources of topography data

Sources of digital elevation data for gridding, detailed mapping and imaging of topography and bathymetry, include topographic contour data, benchmarks, boreholes, cultural surveys, bathymetric surveys gravity stations and seismic traverses.

Fortunately, in parallel with the digital and computing revolution in geophysics, there has been an increase in the availability of digital terrain data from non-geophysical sources. In Australia spot height, contour and gridded terrain data is now readily available from national mapping authorities like the Australian Land Information Group (AUSLIG) or State mapping authorities from 1:100000 and 1:50000 scale mapping. In geophysically acquired topography the advent of GPS spot and continuous navigation in a readily useable digital form has lead to a revolution in topography geophysics (e.g. terrain models are a routine by-product of airborne geophysics).

Another potential source of data is unmigrated digital terrain derived from airborne geophysics, which has potentially a higher data density than AUSLIG data, but until recently, has not been given the quality control attention needed to make it of sufficient accuracy. SPOT satellite derived terrain models are another potential data source.

If all these data sources are utilised, then topography has the highest data density of any geophysical technique over the earth's surface. It is essentially "everyman's geophysics".

Topography in combination with other data

Topography is best used with other data. Draping of geophysical anomaly pseudocolour over terrain intensity is the most obvious application.

Use of terrain data with the shallowest seismic horizon and a weathering velocity enables a surface to the shallowest time horizon time to be calculated if necessary.

Combination of topography with geophysical anomalies is desirable to eliminate near surface effects on other geophysics.

References and further reading

Magnetics and gravity

Milligan, P.M., Morse, M. P., and Rajagopalan, S. 1992, 'Pixel map preparation using the HSV colour model', *Exploration Geophysics*, 23, 219-24

Reeves, C.R. 1992, 'New horizons for airborne geophysical mapping', *Exploration Geophysics*, 23, pp 273-80

Radiometrics

Dickson, B. L. and Scott, K. M., 1992, 'Interpretation of aerial gamma-ray surveys', *CSIRO Division of Exploration Geoscience Report 301* (144pp)

Geophysics and Geochemistry in the Search for Metallic Ores, Geological Survey of Canada Economic Geology Report 31, 1979... particularly:

Grasty, R.L. 'Gamma ray Spectrometric Methods in Uranium Exploration - Theory and Operational Procedures' (pp 147 - 162)

Killeen, P.G., 'Gamma Ray Spectrometric Methods in Uranium Exploration - Application and Interpretation' (pp 163-229)

Seismic

Dalley, R.M., Gevers, E.C.A., Stampfli, G. M., Davies, D.J., Gastaldo, C.N., Ruijtenberg, P.A., and Vermeer, G.J.O. 1989, 'Dip and azimuth displays for 3D seismic interpretation', *First Break*, 7, 86-96

Tilbury, L. A. and Bush, D. 1991, 'Image processing of interpreted 3D seismic data to enhance subtle structural features/lineations', *Exploration Geophysics*, 22, 391-6

Tilbury, L. and Barter, T. 1992, 'New technology - a major impact on a producing field: North Rankin Gas Field, North West Shelf', *APEA Journal*, 32, 20-32

Cockshell, C.D., Allender, J.F., and Vinall, D.R. 1993, 'Image Processing for seismic mapping saves papering the walls', *Exploration Geophysics*, 24, 407-14

Airborne EM

Anderson, A., Dodds, A.R., McMahon, S., and Street, G.J. 1993, 'A comparison of airborne and ground electromagnetic techniques for mapping shallow zone resistivity variations', *Exploration Geophysics*, 24, 323-32

Ground geophysics

Pettifer, G.R., Djordjevic, N., Heislors, D., Schaeffer, J., and Withers, J.A. 1989, 'Geophysical and image processing methods for detection of fireholes in brown coal, Latrobe Valley', *Exploration Geophysics*, 20(1/2), 153-8

Data integration

Conradson, K., and Nilsson, G. 1984, 'Application of integrated Landsat, geochemical and geophysical data in mineral exploration', *Proceedings of the Third Thematic Conference on Remote Sensing for Exploration Geology*, Colorado Springs, Colorado, pp499-511

Kowalik, W.S., and Glenn, W.E. 1987, 'Image processing of aeromagnetic data and integration with Landsat images for improved structural interpretation', *Geophysics*, 52, 875-84

Spencer, G.A., Pridmore, D.F., and Isles, D.L. 1990, 'Data integration of exploration data using colour space on an image processor', *Exploration Geophysics*, 20(1/2), 31-5

Pettifer, G., Tabassi, A. and Simons, B.A. 1991, 'A new look at the structural trends in the onshore Otway Basin, Victoria, using image processing of geophysical data', *APEA Journal* 31(1), pp213-28

Pettifer, G.R., and Paterson, R.G. 1992, 'An ideal image processing and interpretation system', *EMU Newsletter*, No3, Appendix 1 (Abstract and figure)

Wilford, J.T., Pain, C.F., and Dohrenwend, J.C. 1992, 'Enhancement and integration of airborne gamma-ray spectrometric and Landsat imagery for regolith mapping - Cape York Peninsula', *Exploration Geophysics*, v23, pp441-46

Pettifer, G.R., Simons, B.A., and Olshina, A. 1992, 'Advances in image processing for data integration in basin studies - Eastern Otway Basin - a case study', *Proceedings of the AAPG International Conference and Exhibition, Sydney - August 2-5, 1992*, p68 (Abstract)

Geophysical filters

Fuller, B.D. 1967, 'Two-dimensional frequency analysis and design of grid operators', *Mining Geophysics*, Volume 2, pp 658-708. SEG, Oklahoma

Mufti, T.R. 1972, 'Design of small operators for continuation of potential field data', *Geophysics*, v37, pp488-506

Image Processing in Mineral Exploration

Author

Peter Williams, Western Mining Corporation, Mineral Exploration Division, Perth, Western Australia.

Introduction

Since 1991 WMC Mineral Exploration Division has followed a strategy of decentralizing its Image Processing functionality into its Regional Exploration offices. To be able to do this effectively required Image Processing software which could be easily learnt and used, yet retain sufficient flexibility and functionality to be able to cater for the sophisticated user. Each regional office has between 2-5 gigabytes of geoscientific data, and the amount

of data is increasing at an alarming rate, as high resolution airborne geophysical datasets and other geoscientific datasets are acquired or become available from State and Federal Government Exploration initiatives.

The vast amount of data to be processed and analyzed biased the hardware choice towards Unix workstations. The image processing software package chosen was ER Mapper, developed by Earth Resource Mapping in Perth. The package met all the criteria at the time and has continued to develop in a direction which has enhanced its functionality in the mineral exploration industry.

Today ER Mapper is used by exploration geophysicists, geologists and geochemists in their own offices on a daily basis. Typically different geoscientific datasets in different forms are overlain at chosen scales, and relationships between the datasets are interpreted in terms of mineral prospectivity.

The data forms are raster or vector. Raster datasets are obtained by gridding of data gathered along lines onto an equidimensional grid (e.g. Airborne Geophysical mapping software or Geographical Information Systems).

Case studies of the use of ER Mapper in the exploration office follow.

Displaying geochemical data

Soil geochemical data gathered on lines 200m apart, employing sampling along the lines of 40m was gridded using carefully selected parameters that best honor the data. The equidimensional grid or mesh interval is 40m. The data was displayed using a pseudocolor look up table in which warm colors were higher values and cooler colors were lower values. The transformation from input gridded geochemical values to screen display values (normally ranging from 0 to 255 for an 8 bit display unit) was achieved via a linear function. This is typically referred to as a linear stretch. Many elements can be measured in a soil geochemical survey, and the grid of each element can be displayed as a band in a manner analogous to the bands in a Landsat image.

Combined geochemical data

Different gridded geochemical elements can be added together or ratioed, and referenced to other geoscientific datasets, given that the datasets use a common map projection. Generally use is made of the elements Nickel and Copper in Nickel exploration, and the range of values are referenced to airborne magnetic datasets. Magnetic high values can be caused by ultramafic rocks which host known nickel mineralizations. Coincident Nickel, Copper and magnetic highs are seen as encouraging.

For example you can show Nickel plus Copper grid values as pseudocolor overlain on a filtered version of gridded airborne magnetic data, displayed as intensity or tonal variations. In this case high values appear as white or lighter tones and low values appear as darker tones.

Geochemical fused with Landsat

The same gridded geochemical dataset can be referenced to Landsat data in a similar manner. For example, you can overlay geochemical data on band 1 of Landsat data, which records the reflected electromagnetic energy from the earth's surface in the 0.485 micron wavelength part of the spectrum. This part of the spectrum is sensitive to the presence of iron oxides at the surface, which is important when interpreting the significance of the variations of the geochemical data.

Conclusion

These are 3 simple illustrations of how ER Mapper is used to help process, visualize and analyze geoscientific datasets in the WMC exploration offices. Even though ER Mapper is increasing its computational functionality and visualization aids it is retaining its easy to learn and easy to use interface. The user now needs to be able to harness and direct this power in the direction of exploration effectiveness. Efficient software is useless unless it is used effectively, and this is the challenge to the user issued by such a product as ER Mapper.

Semi-Automatic Interpretation of Aeromagnetic Datasets

Authors

P.K. Williams and **Graham Staker**, Western Mining Corporation, 191 Great Eastern Highway, Belmont, Western Australia 6104

Introduction

For the at least the last 40 years, geophysicists involved in trying to extract information from aeromagnetic surveys have been designing of ways to speed up the process (Werner, 1953; McGrath and Hood, 1970; Gerard and Debergliia, 1975; Kilty, 1983; Shi, 1994). There are basically 2 main requirements for this to happen:

- A robust computationally efficient and fast mathematical algorithm, which will calculate solutions for each anomaly. As all interpreters know there are generally a number of possible solutions which can fit the aeromagnetic data for each anomaly. Hence for large surveys with a high density of anomalies there can be an enormous number of solutions for each survey.
- A way of displaying the results of the above process in a manner where the interpreter can then rapidly judge, based on his or her knowledge and experience, which solutions are the most appropriate for the anomalies in the specific Geological environment.

The Geophysical literature is abound with answers directed at the first requirement, but very few have effectively tackled the second requirement. Those that have, have typically not addressed the Three dimensional nature of the anomalies effectively. This note attempts to redress that limitation.

The semi-automatic interpretation algorithm

The algorithm used for the purpose of this paper is the improved Naudy Method, which is described in detail by Shi (1994). In essence the program tries to fit a number of two dimensional models to each anomaly encountered along a line of data. The models are those of a thin horizontal sheets, a vertical contact and a thin vertical dyke. For each selected anomaly along a line, several calculations are made for different windows of the line data, for each model. For each such calculation a degree of fit is calculated, termed a similarity coefficient, which is an indicator of the degree of mathematical fit between the calculated response and the measured line data. Each anomaly typically has several lines of data across it. Thus for any one anomaly there are often several models suggested by the program.

The program is applied in two stages. The first is one of *selecting* appropriate anomalies for more detailed analysis. The second involves doing the more detailed *analysis*.

Abbreviated time and motion study of the interpretation process

To attempt to put this interpretive process into a time and motion context, I have assumed that the average Mineral Aeromagnetic Survey has 3 independent magnetic anomalies per square kilometre (a conservative number for some geological environments). Each anomaly has on average 3 lines of data defining the anomaly (roughly assuming a line spacing of 200 meters) and that to analyse each anomaly, 3 different windows have been used and 3 different models (see above) used for each of the windows. These simple assumptions indicate, that for each square kilometre of surveyed ground (or for each 6 linear kilometres), there are 81 potential solutions suggested from such a semi automatic

interpretation process! It is not difficult to thus see how Professor David Boyd (Personal Communication) derived his estimates of interpreting aeromagnetic data at a rate of 16 kilometres per hour for surveys flown for Mineral Geophysics!

Traditional interfacing of algorithm output with data and interpreter

Traditionally the output from the program has been in profile form (Figure 1).

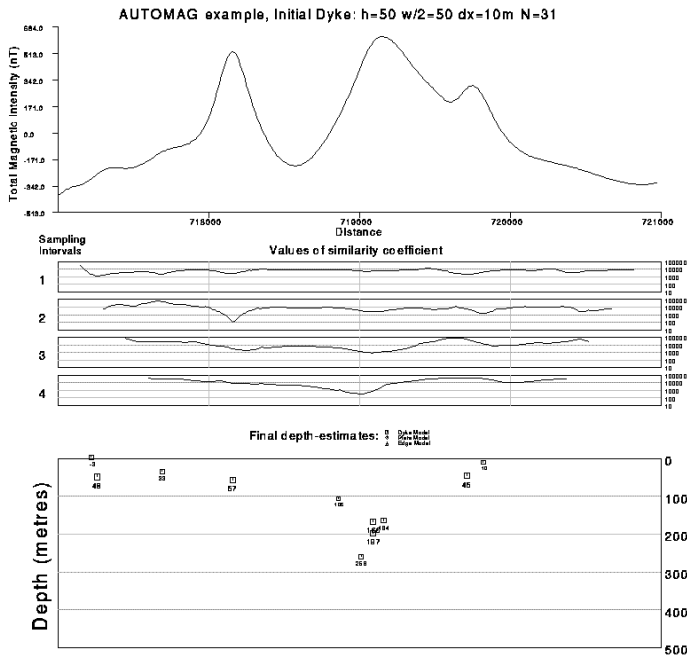


Figure 1 A typical output from the Naudy Aeromagnetic Semi Automatic Interpretation Algorithm.

This is difficult to work with as:

- It does not allow the interpreter to appreciate such critical information as strike direction or extent of the anomaly, the plan form of the anomaly, exactly where the line being analysed is with respect to the location of the anomaly peak, and other such information as the geological setting of the anomaly.
- It radically compresses the geometrical significance of the interpretation into a set of somewhat abstract symbols. (For instance a dyke is shown as a box whose dimensions are independent of the interpreted dimension of the model.)

In this traditional interface, the interpreter has to have access to a large number of paper maps and plans, which can make the job cumbersome and slow. Now this map and plan information is available digitally and can be displayed on the same computer as that which does uses the Semi Automatic Interpretation algorithm, very easily using such programs as ER Mapper.

Interfacing with ER Mapper

ER Mapper has the capacity to display both vector and raster information. Importantly in this context is its ability to store efficiently a number of bands of raster information. We also use ER Mapper's formula capability to help sift through the solutions output from the Semi Automatic Interpretation algorithm.

For the sake of brevity we consider only the output from the second part of the interpretive process. However it should be noted that a very similar style of interface can be easily applied to the first stage of the interpretive process, anomaly selection. The output consists of a similarity coefficient, sample window length, depth, halfwidth, susceptibility and dip estimates for each body type. This information is loaded into different bands in an ER Mapper BIL file. That is Band 1 will contain all and only similarity coefficients for a selected body type and sample window, Band 2 may contain the Depth estimates associated with the similarity coefficient (that is the similarity coefficient in band 1 is derived from a model which has a depth to source that is recorded in band 2), Band 3 the half width estimates, Band 4 the Susceptibility estimates, Band 5 the dip estimates (etc.).

This interpreted output from the analysis stage may then be quickly displayed and analysed by an interpreter, so that a final interpretive map can be constructed. The different modes of display of the selected out put are:

- The numerical output in each band can be displayed as a number in vector form (Figure 3, 4 and 5). The number is written to the immediate right of the point of calculation, with the point of calculation being shown as a single dot. This capability is via a dynamic link which can allow the user to make such decisions as, show all the interpreted vertical contacts which are interpreted with a degree of fit better than some chosen level within certain geographical bounds
- The output in each band can be displayed as strip raster information (Figures 2, 3, 4 and 5). The strip represents the least square best fit line, fit to the true flight path of the plane when gathering the data. When displayed in this manner it is possible to use selective stretching (that is using carefully chosen minimum and maximum values), as well as the formula functionality, for example, showing all depth estimates greater than 200 meter, and/or showing all bodies with interpreted susceptibility less than 5×10^{-3} SI units by assigning a value of 255 to Band 99 (say) in a position where those models fit this criteria, or a value of 0 to those positions where models do not fit that criteria

All of these displays can be superimposed onto various maps of the data, including raster images (Figures 2, 3, 4 and 5) or flight path or stacked vector plots of the aeromagnetic data or its derivatives (e.g. second horizontal derivatives, the analytical signal or reductions

to the pole) or in fact on maps of any pertinent Geoscientific information (e.g. topography, drilling isopach maps, geological outcrop maps, or regolith maps), so that the experience and knowledge of the interpreter/s can be quickly put to work, to derive a final interpretation. The interpreted widths can be plotted (Figure 2) in strip raster form over the pseudocolored Total Magnetic Intensity (TMI) without regard to the degree of fit or appropriateness of the model. The interpreted depths from all dyke models with exhibiting a good fit can be plotted (Figure 3) as numbers (below the sensor, in meters) and superimposed on a pseudocolored TMI image. The horizontal raster strips show the selectively stretched similarity coefficients for each of the model fits. White and red colours within this strip indicate a good fit, blue represents a poor fit. Similarly dip interpretations are shown in Figure 4 (dip in degrees measured clockwise from the horizontal), and magnetic susceptibility (value are in $\cdot 10^{-3}$ SI units) in figure 5. The final interpretation can then be drawn on the screen using ER Mapper annotation system and/or a digital map symbol library linked to ER Mapper.

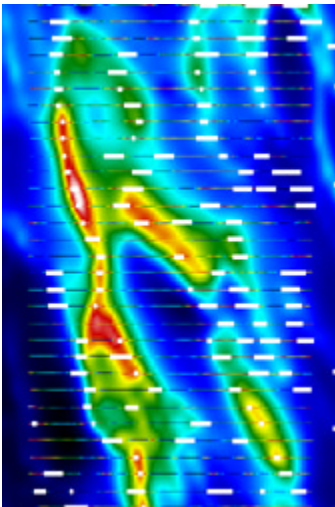


Figure 2 Interpreted widths output from the Improved Naudy Semi Automatic Interpretation Algorithm for the magnetic dyke model. The widths are displayed as white horizontal bars, and are superimposed on a pseudocolored raster image of the TMI.

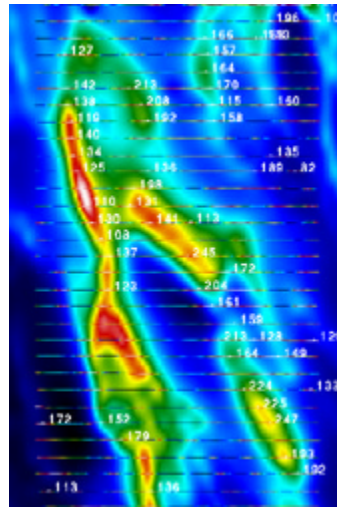


Figure 3 Interpreted depths output from the Improved Naudy Semi Automatic Interpretation Algorithm assuming a magnetic dyke model. The depths are displayed as meters below the sensor, and are superimposed on the pseudocolour raster image of the TMI.

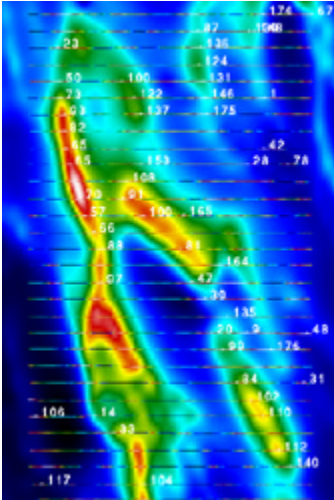


Figure 4 Interpreted magnetic susceptibility output from the Improved Naudy Semi Automatic Interpretation Algorithm assuming a magnetic dyke model. The susceptibility values are displayed as in SI units ($\ast 10^{-3}$), and are superimposed on a pseudocolor raster image of the TMI.

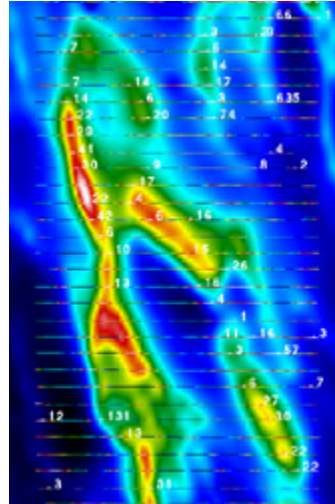


Figure 5 Interpreted dips output from the Improved Naudy Semi Automatic Interpretation Algorithm assuming a magnetic dyke model. The dips are displayed as the degrees of dip, when measured clockwise facing north and are superimposed on a pseudocolored raster image of the TMI.

The output from this interpretation, specifically geometrical and magnetic susceptibility information, can then be written to another file which can be input into quantitative magnetic modelling software such as ENCOM's MODELVISION. An exact mathematical calculation can then be performed and a more detailed and specific interpretation can be performed if needed.

Summary

The functionality in ER Mapper can be easily used to increase the efficiency and effectiveness of interpreting semi-regional to regional aeromagnetic data. These gains are achievable by interfacing a suitable semi-automatic interpretive algorithm, like the Improved Naudy method, with numerical and appropriate visualisation in a manner which allows the results of this analysis to be reconciled with the three dimensionality of the data as well as other datasets.

Acknowledgments

We would like to acknowledge permission from WMC to publish such information, and Digital Equipment Corporation for providing part of the money to fund this research. We would also like to acknowledge Dr. Shi for providing us with output from her Improved Naudy Method Computing Code.

References

Gerard, A. and Deberglia, N., 1975, 'Automatic three-dimensional modelling for the interpretation of gravity or magnetic anomalies', *Geophysics*, 40: 1014-1034

Kilty, K.T., 1983, 'Werner deconvolution of profile potential field data', *Geophysics*, 48: 234-237

McGrath, P.H., and Hood, P.J., 1970, 'The dipping dike case: A computer curve-matching method of magnetic interpretation', *Geophysics*, 35: 349-358

Shi, Z., 1993, *Automatic Interpretation of Potential Field Data Applied to the Study of Overburden Thickness and Deep Crustal Structures*, South Australia, PhD Thesis, The University of Adelaide, Department of Geology and Geophysics

Werner, S., 1953, *Interpretation of magnetic anomalies at sheet-like bodies*, Stockholm, Sveriges Geologiska undersok, Ser. C.C. Arsbok, 43

Custom-built Dynamic Links

Authors

Simon Crosato, an exploration geophysicist at the Central Norseman Gold Corporation, and **Bernie Plath** are employees of Western Mining Corporation.

Abstract

In this study ER Mapper has been used with the Ingres Geology Database to construct dynamic links to increase exploration effectiveness. Over thirty dynamic links from ER Mapper to different portions of the Central Norseman Gold Corporation (CNGC) Ingres geology database have been developed to date.

Introduction

The great need for an integrated, team approach to achieve successful exploration goals has been emphasised by many workers. This team consists of geologists, geophysicists and geochemists directly, and other key units such as data clerks and drafting staff indirectly. All provide a data processing service for the exploration effort depending on their field of expertise.

The team may be together, *but is the data* from each individual source *together*, and easily accessible by other team members? The answer in the past has been to spend large amounts of time preparing *and* updating numerous hardcopy plans to display the relevant data. Now, the increasing power of workstations is enabling large amounts of data to be processed in a short period of time. Thus, it is becoming increasingly viable to examine the data whilst in a digital form through image processing.

Western Mining Corporation (WMC) has chosen ER Mapper (Earth Resource Mapping) and Ingres (Ingres Corporation) as the corporate standard image processing and database package respectively. Over thirty links from ER Mapper to different portions of the CNGC Ingres geology database have been developed to date. These have proved popular and are commonly used every day, with requests for further data integration links accommodated when possible. This case history aims to outline the method of data integration utilising ER Mapper and Ingres at CNGC, with several examples.

Advantages of digital data integration

The advantages of dynamic links are many:

- **Only one copy of data exists in the database and this copy is accessible by anyone.** This is unlike the situation where many plans exist for the same dataset(s) with all of different vintage.
- **Updates from a single authorised input source are automatic to those who use the database.** This ensures that users always receive the most up-to-date copy of the data.
- **Scale independence.** Data is automatically registered to its correct position and scale on the screen, and is readily usable at regional or prospect scale.
- **Interpretation is made easier and more thorough** by simultaneously displaying *all* available data (or combinations thereof) for an area of interest.
- **Quality control of new data is on-going** via comparison with other known 'clean' datasets.
- **More efficient use of time.**

Conversely, there are not many disadvantages to digital data integration, except maybe the need to learn how to use the relevant computing packages.

Data Integration at CNGC

As the percentage of exploration under cover increases, geophysical methods become of great importance in targeting and lithological mapping. Modern, ultra-detailed geophysical surveys generate vast quantities of digital data that must be used efficiently and effectively. Software (including ER Mapper) has to be created to handle such processing using desktop workstations in real time. A major feature of ER Mapper is its ability to simultaneously display vector and raster data, thus enabling integration of data from multiple sources and types.

At CNGC, the Ingres database will eventually store all non-geophysical data (it currently stores drill hole, geochemical, leasing and target data). Data integration is achieved by extracting data from Ingres, and using ER Mapper as the display and manipulation tool (see Figure 1).

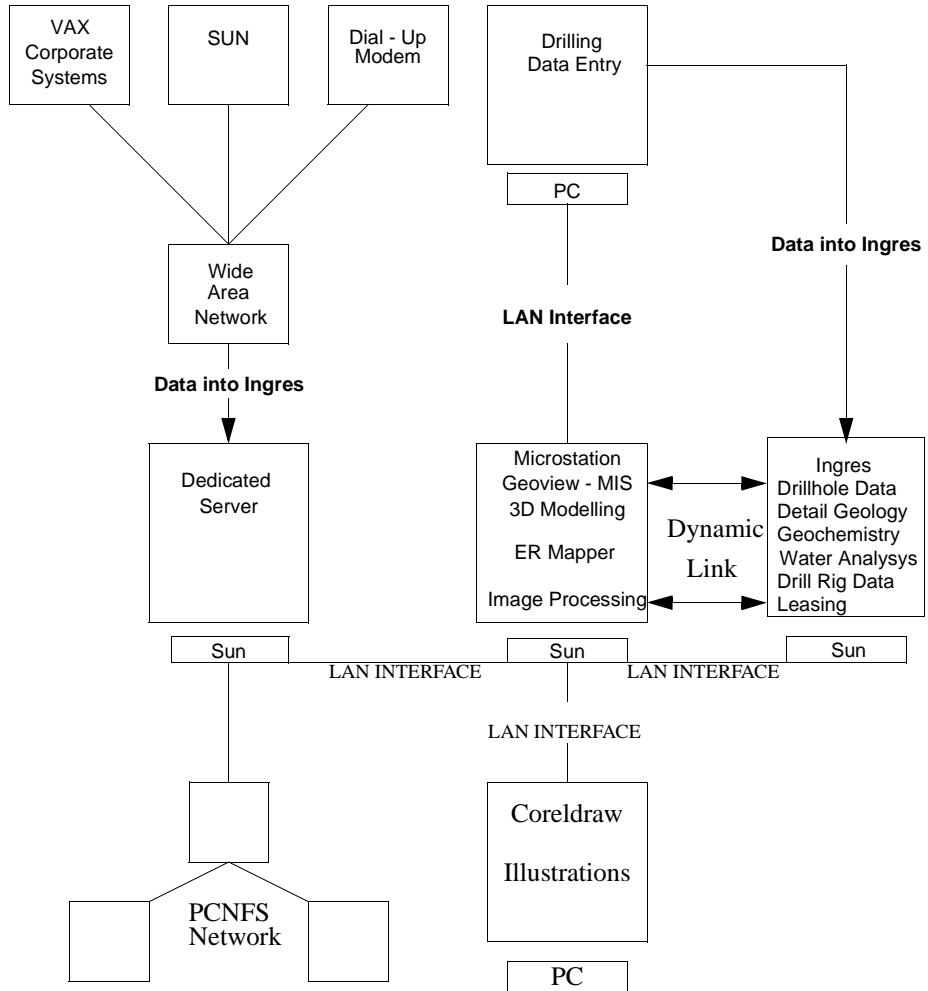


Figure 1 - Schematic diagram illustrating technical hardware and data flow.

What is SQL?

SQL (Structured Query Language) is the major high-level, non-procedural database language used in commercial data processing, and is the industry standard (ANSI) for relational databases such as Ingres. With SQL statements, the user tells the database what he/she wants; then the database determines how to obtain the information or how to compute it. Use of SQL does not require any previous programming knowledge.

The user translates a criteria structured information request into valid SQL commands. An example could be: *Extract all the aircore drill holes currently in the database that intersected ultramafic rocks and were drilled after the 1st of July, 1993, with nickel assays greater than 10000 ppm.*

Depending on how the database tables are linked together, the required SQL could be:

```
SELECT DISTINCT startdate, hole_type, key_type, ni_value% requested data fields
FROM drill_source dso2, drill_rock_code drc, drill_assay das %use listed tables as
search area
WHERE                                     % Following are the search criteria:
dso2.startdate > '01/07/93' AND          % holes drilled after 1/7/93
dso2.hole_type like 'AIRCORE%' AND      % hole type must be aircore
drc.key_type like 'U%' AND             % ultramafic criteria
das.ni_value >10000                    % nickel assay over 10000 ppm
```

There is no limit on the length or number of constraints placed in the SQL request. The above query may be entered interactively through the database server program or submitted in batch mode as a command file. The retrieved data is then written to the screen or an output file.

Data storage considerations

In order to have acceptable response times to reasonably complex database queries, significant thought must go into the way in which the data is stored. At CNGC, query time has been kept to a minimum predominantly by performing the body of the query overnight, and simply storing a pointer to the output value in another table. These dynamic link tables have been indexed on northing, and hence have short interrogation/extraction times via geographic area. This method of updating the dynamic link tables saves the database server searching through the entire database every time.

An example is the Maximum Gold Value in Hole link routinely used at CNGC. The database server stores the maximum gold assay found in each drill hole in a table with the hole's coordinates once every week. This entails searching through every drill assay for gold per hole and determining the maximum. If this search was to be performed every time an image was redrawn in ER Mapper, the time taken to compute/extract the relevant data

would be enormous and quite unacceptable. By utilising the dynamic link tables described above, the desired data search has already been completed, hence extraction and plotting is accomplished in minutes

Dynamic link construction

All database links developed at present work in the same general manner. The required data is primarily searched for by area, with further restrictions/criteria imposed in the actual database query (SQL). To facilitate easy extraction of data not necessarily to be utilised solely by ER Mapper, a C program containing embedded SQL statements has been written by B. Plath. This program takes minimum and maximum eastings and northings, a data type, and output filename arguments on the command line. Upon execution, the program constructs the SQL query and submits it to the database server. The data matching the SQL search criteria is then written to the output ASCII file, an example of which is reproduced in Appendix B. This data file may be utilised by other gridding, contouring and plotting packages.

Two broad classes of external link currently exist - these have been termed *hardwired* and *interactive* types. Although both classes extract data from the database according to the general rules listed above, each goes about this task in a different way.

Hardwired

In this link type, data extraction is performed by area (the active ER Mapper image window) and is displayed according to pre-set PostScript rules within the Bourne shell script. A good example of this is the End of Hole Geology link (see Appendix A). The primary geological rock code logged at the end of the hole is extracted for every drill hole within the image area (see Appendix B). The extracted data is then read by the link script record for record, and a plotting colour determined by the geological rock code according to the standard WMC legend.

Interactive

The most recent external link development has involved interactive entering of SQL script (file or keyboard input) into an ER Mapper overlay. The entered SQL may be altered between each display, allowing easy graphical comparisons between the requested datasets. This link type searches the database directly using a full query constructed by the C program. Query response time is acceptable because the more complex data restrictions/constraints (compared to a hardwired link) entered interactively 'sift' the data quite efficiently.

Overall, response time for each link type is in the order of a few minutes. It is quite common however, for the desired data to be extracted before large raster datasets have completed display within ER Mapper. In this case, no extra time is needed for the external link to be performed.

The current computing configuration at CNGC will soon be greatly improved with the addition of a faster workstation to solely run Ingres. The main image processing machine will then not have to perform the database extraction, increasing the efficiency of the data integration process enormously.

Dynamic operation within ER Mapper

In order to reduce confusion and the effort needed to extract data from the geological database, the dynamic linking function has been incorporated into ER Mapper utilising familiar X-Window buttons under the intuitive Add menu. Data integration is then as simple as ON/OFF, the internal intricacies quite invisible to users with limited computer literacy (save for operating ER Mapper).

Hardwired

For Hardwired links, the generated ER Mapper overlay is TRUECOLOUR, meaning that colour information is determined by the link, inside the PostScript plotting routines. This results in numerous pre-set choices depending on the data displayed and the standard colour scheme used.

Interactive

At present, the generated ER Mapper overlays for Interactive links are displayed in MONOCOLOUR, meaning that all data points satisfying the database search criteria are plotted on the screen in the colour selected using the colour button. This link type will change to TRUECOLOUR in the near future, when the PostScript has been modified to become intelligent enough to recognise the data type (e.g. geology or geochemical assay) it is plotting. Colour definitions will then be stored in the database, and become internally generated and invisible to the user.

After adding an Interactive link, the user must supply the 'where' clause of the SQL query (see *What is SQL?* above) before the data extraction can commence. The table linking and variable string definitions (these are standard for each table) are automatically performed by the SQL-building C program. Clicking on the chooser button activates the SQL query entry window.

For example, the SQL query:

```
drc.key_type like 'U%' and drc.key_field in ('RK', 'WR')
```

will extract all drill holes that have intersected either weathered (WR) or fresh (RK) ultramafic.

The user may also enter the name of a file containing the desired SQL 'where' clause (e.g. '@ultramafic.sql'). Alternatively, '@file' may be entered as the query, which in turn presents the user with an X-Window chooser listing all compatible SQL files.

The user may zoom and change the query as desired - the link script is intelligent enough to detect changes in the active image area or query, and extracts data only when necessary.

Example: Talbot Island

Talbot Island is an active nickel exploration project situated 18 km NNE of the Norseman town site. This site has been chosen to demonstrate external database dynamic linking because various different digital data types exist in this area. Among these are multi-element surface soil and drill core assays, detailed geological rock descriptions, and physical drill hole characteristics.

The nickel potential of Talbot Island was first recognised by McGoldrick (personal communication to S. Peters, 1990, 1991) and then later by CNGC personnel (Offe, 1992) after reconnaissance rock chip sampling returned highly anomalous nickel assays within a komatiite. Detailed soil sampling has been undertaken over amenable portions of the island, and has defined several strong anomalies (see Figure 2 below). The link to Ingres extracts all nickel soil geochemical assays in the active window, and displays them colour coded according to pre-defined threshold limits as outlined in the legend. The green vector overlay contains major topographic features, such as the island outline and the lake edge. The internal line on the island is the dune (west) and subcrop (east) boundary. Overlaid in a sand brown colour is the slightly out of date causeway/access track system on the island.

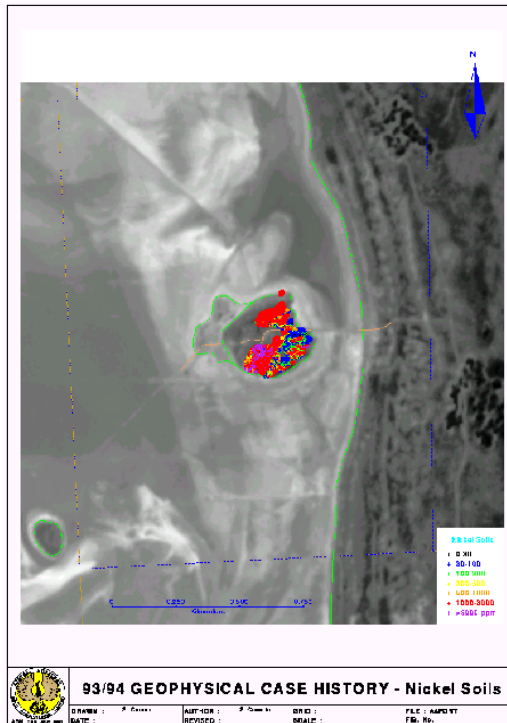


Figure 2- Map depicting Nickel Soil deposits

Also present in this image are dynamic lease boundaries. These boundaries have been stored within Ingres as separate straight line segments along with lease type (e.g. surveyed, reserve, Aboriginal site) and drawing attributes (e.g. line style, thickness, RGB colour). The tenement boundary link extracts all line segments falling wholly or partially within the active image window, creates the PostScript code to display them on the screen from the relevant attributes, and then reports all leases found to the user via an X-window interface, which may be dismissed or printed. As long as the surveyors keep the Ingres database updated with the current leasing information, the need for messy and time-consuming DXF file imports is eliminated.

Existing drilling information is an essential layer of data to be integrated with geophysical/geological interpretation and when further drilling is to be planned. Numerous hardwired links to the drilling database have been devised, one of which is demonstrated here. Collar and drill hole trace data is useful to analyse portions of ground already tested, and also to indicate areas of untested potential within the project area (see Figure 3). The surface projection of each drill hole is calculated from depth, dip and azimuth data extracted by the link, and then displayed as a straight line approximation. The hole type (e.g. aircore,

percussion, diamond) is tested by the link script, allowing hole types to be distinguished via different colours on the screen. A link that displays colour-coded collars and hole identifiers is also available.

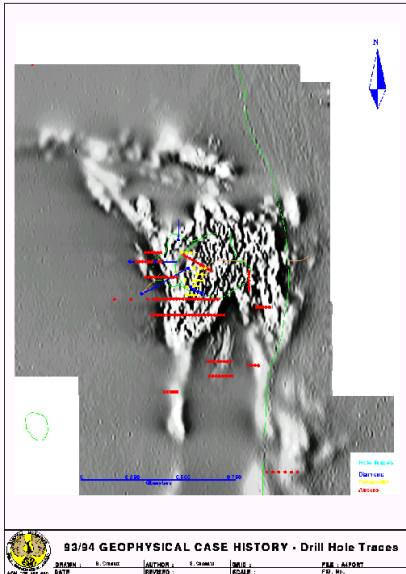


Figure 3 - Map of Drill Hole Traces

A broad scale geological interpretation can be generated and integrated with raster data by examining the geology logged at the end of the drill hole. A hardwired link to the rock code database extracts the key geological rock code for the end of hole (EOH) one metre sample from each drill hole within the active image area (see Appendix B). The link script tests the rock code (see Appendix A) to determine the standard WMC colour, and then displays a relevantly coloured cross at the collar position (see Figure 4). This display is obviously an incorrect projection if the hole is deep and shallowly-moderately dipping (e.g. a diamond hole). Correction to calculate the actual XY positional coordinate will take place in the near future. In the meantime, the EOH geology display should be viewed alongside the drill trace display for the same area, so the user is aware of when the dip factor is important, thus allowing the necessary mental correction to be made.

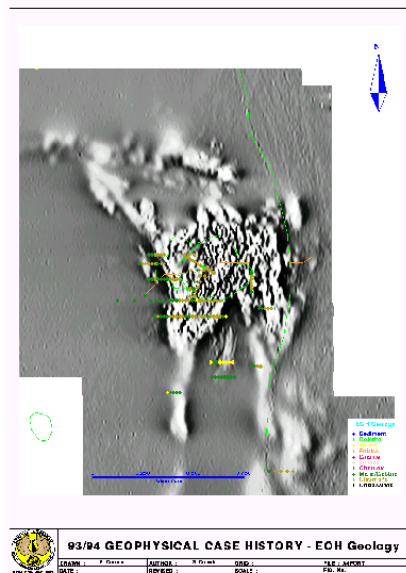


Figure 4 - Map depicting End Of Hole samples

When planning aircore/percussion drilling programs, it is desirable to be able to predict the expected hole depths in order to estimate the number of holes that can be completed per shift. To facilitate this, a hardwired link has been created to a database table that stores the depth to the Tertiary/Archaean boundary for all existing surface drill holes. This data may also aid geophysical data interpretation. For example, gravity data is influenced by the depth of semi-consolidated Tertiary sediment, so if the geometry of this veneer of low density rock is known, some effort may be afforded to correcting for its effect. Magnetic depth interpretation of Archaean sources can be strengthened by aircore holes indicating large depths of Tertiary over the anomaly with respect to surrounding areas.

As is expected at Talbot Island, the depth of Tertiary is small because the Archaean rocks crop out (or subcrop) in the immediate island vicinity (see Figure 5). The depth scale shown is probably too coarse to be relevant in the island vicinity, but the aircore holes in the SE of the image have penetrated Tertiary with depths between 40 and 60m (see yellow crosses in Figure 5).

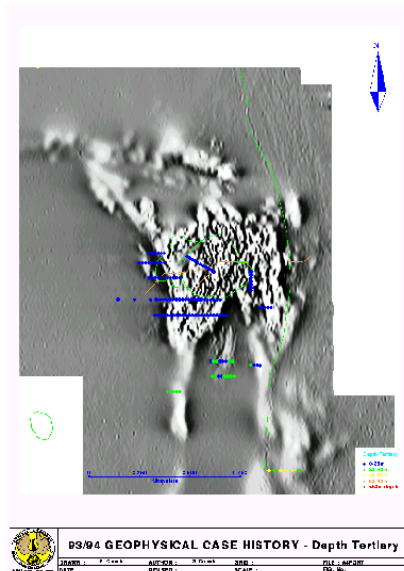


Figure 5 - Map depicting Depth of Tertiary Sediment

The interactive SQL links are the newest and most versatile yet developed at CNGC. As described above, they require the user to enter the SQL 'where' clause which restricts the data extracted to fall within certain criteria. At Talbot Island, it is important to know which holes have intersected fresh ultramafic. The appropriate 'where' clause to obtain this data would be:

```
drc.key_type like 'U%' and drc.key_field = 'RK'
```

where key_type matches all rock codes beginning with U (e.g. USOL, UACT, UTSM) and key_field must be equal to RK (corresponds to fresh rock; conversely, WR is the weathered rock code). This query will match a fresh ultramafic intersection anywhere in the hole because no constraints have been put on the depth at which the intersection may occur. The output is a display of the collars of all holes matching the where clause criteria (see Figure 68). It is evident that there are quite a few. Of interest is the discrete magnetic anomaly immediately to the west of the island shore. A fence of vertical aircore holes was drilled to intersect the anomaly source (see Figure 3). Of these nine holes, five encountered ultramafic in the last metre of the hole (see Figure 4). Only one intersected fresh ultramafic and is situated on the western-most end of the traverse (see Figure 6). This data suggests that the serpentinite source of the magnetic anomaly has not been thoroughly tested. Consequently, surface diamond hole ETS 5 (see western-most blue trace on traverse in Figure 3) has recently been completed to explain the magnetic anomaly source.

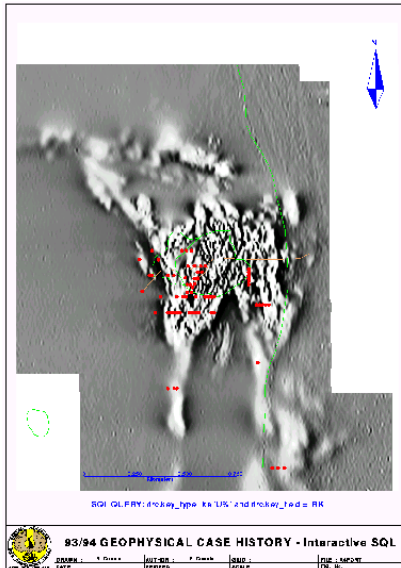


Figure 6- Interactive SQL-1

By incorporating drill assay information into the display, a subset of holes shown in Figure 8 define the nickel anomalous regions, allowing correlation with geophysical and other datasets. To demonstrate this, all drill holes having maximum nickel assays greater than 1% (10000 ppm) occurring in fresh ultramafic have been extracted from the database. The 'where' clause query used was:

```
drc.key_type like 'U%' and drc.key_field = 'RK'  
and da.element = 'NI_PPM' and max(value) >= 10000
```

Five drill holes satisfied the above criteria within the coordinate extents of the image window (Figure 7).

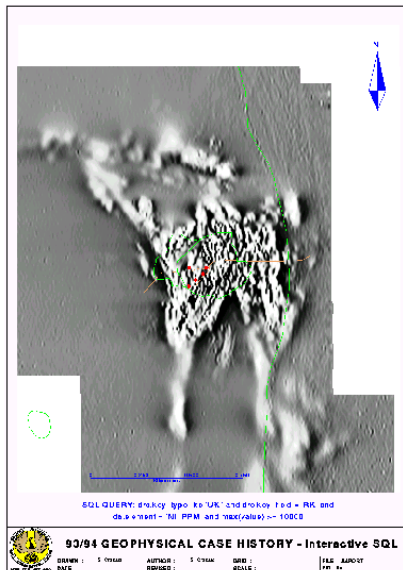


Figure 7 - Interactive SQL-2

When viewed in conjunction with Figures 2 and 3, it can be seen that the diamond hole has intersected a mineralised zone not seen in the rock chip/soil sampling, and the four percussion holes have tested the best part of the NE-trending soil anomaly at depth.

Future implications

There is no limit to the type of data that may be stored in modern relational databases. Already at CNGC, there is a move to enter all new exploration target information into the database, whilst also entering the backlog of historical targets when time permits. With this information readily on hand and easily graphically displayable, problems that have previously occurred such as targeting old, already targeted areas, will cease to exist. This facilitates a far more efficient use of time.

Time consuming tasks such as Form 5 reporting will require less effort in the future if the data can easily be obtained from Ingres and verified graphically with ER Mapper.

Other data types planned to be stored within Ingres at CNGC include:

- down hole geophysical data (e.g. DHEM, petrophysical logs)
- existing geophysical survey boundaries and survey parameters
- digitally scanned bitmaps (e.g. thin section photomicrographs of EOH rock units)

- existing and planned mine designs
- topographic elements (e.g. roads, creeks, clearings)
- accounting information (e.g. current and required lease expenditure)

Ways of increasing the efficiency of the database links within ER Mapper are constantly being investigated by ER Mapper technical support and CNGC computing/geophysical staff. If demand is great enough (the potential is certainly enormous), Earth Resource Mapping may even consider designing/writing a multi-functional direct link to Ingres (bypassing ASCII file step) similar to the one they have just written for ARC/INFO.

Conclusion

This document has aimed to outline the method of digital data integration developed at CNGC, which utilises links between an Ingres relational database and ER Mapper image processing software. The link process requires two steps:

- 1 Data extraction from Ingres facilitated by embedded SQL commands within C code.
- 2 Display within ER Mapper involving both Bourne Shell and PostScript programming.

Two classes of dynamic link (Hardwired and Interactive) have been devised to date, with the total currently available exceeding 30 different options. With Hardwired links, no user input is required. Activating an Interactive link allows the user to control the data extracted from Ingres by entering SQL commands.

The ability of data integration to help manage time more efficiently, and aid in more thorough and realistic interpretations is exciting, and obviously a major factor in the future direction of mineral exploration. A small demonstration of the power of this approach has been outlined with several different data types existing within the Talbot Island Nickel Project. The example used here is commonplace and used every day at CNGC.

Future development of dynamic database linking to image processing software will take place as the need grows. This will involve CNGC computing/geophysical staff, MIS, and possibly Earth Resource Mapping programming personnel.

References

Offe, L.A., (1992) - *Talbot Island Ultramafic, Norseman, Western Australia*; Internal CNGC Technical Report, CNG/T/004

Appendix A

EOH Geology HARDWIRED Dynamic Link for ER Mapper (Bourne Shell)

```
#!/bin/sh
#
#-----
# ermps_34_ingres COLOUR-CODED EOH GEOLOGY
#
# CREATED: S.Crosato (June '93)
# MODIFIED: S.Crosato (April '94) added legend
#
# EOH geology information is extracted from Ingres (key rock code only)
# and then displayed as colour-coded points at the collar location on the screen
# using standard WMC geological legend colours where possible.
#-----
#
# This script runs an Ingres query embedded in a C program
# (written by B. Plath) that enables image extents from ER Mapper
# to be passed for data extraction. Format is:
#
# ingres_2_xyz.exe 1 minEAST maxEAST minNORTH maxNORTH outputfilename
#
#     script code = 1 max gold in hole
#                 = 2 max gold in Tertiary
#                 = 3 max gold in Archaean
#                 = 4 depth to top Archaean
#
#                 . . .
#                 . . . etc.
#
# $TLX,$TLY,$BRX,$BRY are variables containing top left x, y
# and bottom right x,y coordinates of the active ER Mapper
# image.
#
# Output is the ASCII file erm_ingres_interface.txt which is renamed to
# something more meaningful before being imported into ERMMapper and
# displayed using PostScript.
#
# Any errors trying to run Ingres are redirected to STDOUT
#
#
# For the specified table, expects 3 columns in the format:
#
# EASTING NORTHING ROCK_CODE
#
# Arguments (see ER Mapper manuals for full details):
# 1 2 3 4 5 6 7 8 9 10 11 12 13 14 15
# cmd datum proj'n coord units rotation tlx tly brx bry canvasw canvash dpiX dpiY file
#
if [ $# -ne 15 ]
```

Chapter 10 Custom-built Dynamic Links ● Future implications

```
then
    echo "$0: Expected 15 Dynamic Link arguments." 1>&2
    exit 1
fi
cat <<EOF
%!PS-Adobe-1.0
% Table Circle dynamic link for table file $FILESPEC
% Args: $*
%
EOF
# Grab the arguments and set them up in meaningful variable names.

NAME=$0                # name of program, might change with the link COMMAND=$1
# should be "postscript"
DATUM=$2               # geodetic datum name
PROJECTION=$3         # projection name
COORDTYPE=$4          # type of coordinates (EN, LL, or RAW)
UNITS=$5              # Units (eg: METERS)
ROTATION=$6           # rotation
TLX=$7                # top left x coordinate
TLY=$8                # top left y coordinate
BRX=$9                # bottom right x coordinate
shift 9
BRY=$1                # bottom right y coordinate
CANVASWIDTH=$2        # window width (0 on init)
CANVASHEIGHT=$3       # window height (0 on init)
DPIX=$4               # x dots per inch (0 on init)
DPIY=$5               # y dots per inch (0 on init)
FILESPEC=$6           # file spec or choice string FILESPEC=/usr5/ermapper/
dataset/Data_Tables/EOH_geol_key.dat
FILESPEC=`echo $FILESPEC | tr -d \"` # bypass quotes

TLY=`echo $TLY | cut -c1-10` #take first 10 chars to make compatible
BRY=`echo $BRY | cut -c1-10` #with defined char strings in SQL query.
TLX=`echo $TLX | cut -c1-10`
BRX=`echo $BRX | cut -c1-10`

#.....Ingres link
cd /usr5/ermapper/dataset/Data_Tables
NEWFILE=0 #set newfile to true (default)

if [ -f bounds34.txt ] ; then
    read MAX_N1 MIN_N1 MAX_E1 MIN_E1 < bounds34.txt
    if [ "$TLY" -le "$MAX_N1" ] && [ "$BRY" -ge "$MIN_N1" ] && [ "$TLX" -ge
"$MIN_E1" ] && [ "$BRX" -le "$MAX_E1" ]
    then
        NEWFILE=1
        echo "ERM/INGRES link: Using existing data file EOH_geol_key.dat" > /dev/
console
        else
            echo "ERM/INGRES link: New bounds not contained in existing data file
EOH_geol_key.dat" > /dev/console
        fi
    fi
fi
```

```

if [ $NEWFILE -eq 0 ] ; then
    echo "ERM/INGRES link: Extracting data from Ingres ..... (EOH_geol_key.dat)" >
/dev/console
    echo "Using bounds: $TLY $BRY $TLX $BRX" > /dev/console
    $ING_EXES/ingres_2_xyz.exe 34 $TLX $BRX $BRY $TLY EOH_geol_key.dat > /dev/
console
    echo "EOH_geol_key.dat `wc -l EOH_geol_key.dat | cut -c1-8` data points found."
> /dev/console
fi

if [ "$TLY" -gt "$MAX_N1" ] || [ "$BRY" -lt "$MIN_N1" ] || [ "$TLX" -lt "$MIN_E1" ] ||
[ "$BRX" -gt "$MAX_E1" ]
    then echo "$TLY $BRY $BRX $TLX" > bounds34.txt #write bounds to file if needed
fi

#.....Truecolor PostScript plotting of data using awk

# [05] handle GEODETIC correction
if [ "$PROJECTION" = "GEODETIC" ]
then
cat <<EOF
/x_map {
    dup    ${BRX} gt                % is X > right hand side?
        { 360.0 sub }              % x was off the right hand side
        { dup ${TLX} lt            % is X < left hand side?
          { 360.0 add } if         % x was off the left hand side
        }
    ifelse
    ${TLX} sub
} def
EOF
else
cat <<EOF
/x_map { ${TLX} sub } def
EOF
fi

cat <<EOF
/x_scale { ${CANVASWIDTH} ${BRX} ${TLX} sub div } def
/y_scale { ${CANVASHEIGHT} ${TLY} ${BRY} sub div } def /size { x_scale 15 mul } def
/-size { x_scale -15 mul } def
/draw_cross { gsave                % get Northing (Y)
    ${BRY} sub
    y_scale mul
    exch                            % get Easting (X)
    x_map
    x_scale mul
    exch
    translate
    newpath
    2 from72pt setlinewidth
    -size 0 moveto
        % draw cross 30m diameter
    size 0 lineto
    0 -size moveto

```

Chapter 10 Custom-built Dynamic Links ● Future implications

```
    0 size lineto
    stroke
    grestore
} def
/Helvetica findfont ${CANVASWIDTH} 60 div scalefont setfont % define text size

/draw_legend_box {newpath
    0.999 0.999 0.999 setrgbcolor      % set background color to white
    0.86 ${CANVASWIDTH} mul 0 moveto    % draw background box
    0.86 ${CANVASWIDTH} mul 0.20 ${CANVASWIDTH} mul lineto
    ${CANVASWIDTH} 0.20 ${CANVASWIDTH} mul lineto
    ${CANVASWIDTH} 0 lineto closepath
}def

/draw_legend {
    0 1 1 setrgbcolor      % set color to cyan
    0.88 ${CANVASWIDTH} mul 0.18 ${CANVASWIDTH} mul moveto
    (EOH Geology) show

    0 0 1 setrgbcolor      % set color to blue
    0.87 ${CANVASWIDTH} mul 0.155 ${CANVASWIDTH} mul moveto
    (+ Sediment) show

    0 1 0 setrgbcolor      % set color to green
    0.87 ${CANVASWIDTH} mul 0.14 ${CANVASWIDTH} mul moveto
    (+ Dolerite) show

    1 1 0 setrgbcolor      % set color to yellow
    0.87 ${CANVASWIDTH} mul 0.125 ${CANVASWIDTH} mul moveto
    (+ Basalt) show

    1 0.647 0 setrgbcolor  % set color to orange
    0.87 ${CANVASWIDTH} mul 0.11 ${CANVASWIDTH} mul moveto
    (+ Felsics) show

    1 0 0 setrgbcolor      % set color to red
    0.87 ${CANVASWIDTH} mul 0.095 ${CANVASWIDTH} mul moveto
    (+ Granite) show

    1 0.745 0.890 setrgbcolor % set color to pink
    0.87 ${CANVASWIDTH} mul 0.08 ${CANVASWIDTH} mul moveto
    (+ Gneiss) show

    0.765 0.125 0.941 setrgbcolor % set color to purple
    0.87 ${CANVASWIDTH} mul 0.065 ${CANVASWIDTH} mul moveto
    (+ Chert etc) show

    0.133 0.545 0.133 setrgbcolor % set color to dark green
    0.87 ${CANVASWIDTH} mul 0.05 ${CANVASWIDTH} mul moveto
    (+ Mafic/Gabbro) show

    0.675 0.647 0.125 setrgbcolor % set color to brown
    0.87 ${CANVASWIDTH} mul 0.035 ${CANVASWIDTH} mul moveto
    (+ Ultramafic) show
```

```

    0 0 0 setrgbcolor          % set color to black
    0.87 ${CANVASWIDTH} mul 0.02 ${CANVASWIDTH} mul moveto
    (+ Unclassified) show

} def
/do_blue_cross {
    0 0 1 setrgbcolor          % blue
    draw_cross
} def
/do_green_cross {
    0 1 0 setrgbcolor          % green
    draw_cross
} def
/do_yellow_cross {
    1 1 0 setrgbcolor          % yellow
    draw_cross
} def
/do_orange_cross {
    1 0.647 0 setrgbcolor      % orange
    draw_cross
} def
/do_red_cross {
    1 0 0 setrgbcolor          % red
    draw_cross
} def
/do_brown_cross {
    0.675 0.647 0.125 setrgbcolor % brown
    draw_cross
} def
/do_pink_cross {
    1 0.745 0.890 setrgbcolor   % white
    draw_cross
} def
/do_black_cross {
    0 0 0 setrgbcolor          % black
    draw_cross
} def
/do_purple_cross {
    0.765 0.125 0.941 setrgbcolor % purple
    draw_cross
} def
/do_dgreen_cross {
    0.133 0.545 0.133 setrgbcolor % dark green
    draw_cross
} def

%
EOF

awk ` BEGIN{ FS="," }
      { if( $3~/U/ ) printf("%s %s do_brown_cross\n", $1, $2) } ` $FILESPEC
awk ` BEGIN{ FS="," }
      { if( $3~/GNI/ ) printf("%s %s do_pink_cross\n", $1, $2) } ` $FILESPEC

```

Chapter 10 Custom-built Dynamic Links ● Future implications

```
awk ` BEGIN{ FS="," }
      { if( $3~/FV/ ) printf("%s %s do_orange_cross\n",$1,$2) }' $FILESPEC
awk ` BEGIN{ FS="," }
      { if( $3~/MGB|MGN|M/ ) printf("%s %s do_dgreen_cross\n",$1,$2) }' $FILESPEC
awk ` BEGIN{ FS="," }
      { if( $3~/MB|MTB/ ) printf("%s %s do_yellow_cross\n",$1,$2) }' $FILESPEC
awk ` BEGIN{ FS="," }
      { if( $3~/FD|MD|DI/ ) printf("%s %s do_green_cross\n",$1,$2) }' $FILESPEC
awk ` BEGIN{ FS="," }
      { if( $3~/SV|SIF|SCT/ ) printf("%s %s do_purple_cross\n",$1,$2) }' $FILESPEC
awk ` BEGIN{ FS="," }
      { if( $3~/SS|VS|SND|MS/ ) printf("%s %s do_blue_cross\n",$1,$2) }' $FILESPEC
awk ` BEGIN{ FS="," }
      { if( $3~/GT|GO|GNGD|GR|GNGT|PG|SHQ|Q/ ) printf("%s %s do_red_cross\n",$1,$2) }'
$FILESPEC
      { if( $3!~/
GT|GO|GNGD|GR|GNGT|PG|SHQ|Q|SS|SV|VS|SIF|SCT|SND|FD|MGB|MGN|MB|MTB|MS|M|FV|U|MD|DI|G
NI/ ) printf("%s %s do_black_cross\n",$1,$2) }' $FILESPEC

if [ $? -ne 0 ]
then
    exit 1
fi

cat <<EOF

% Draw legend in bottom right corner of image window

draw_legend_box fill
draw_legend

% end of postscript EOF
```

Appendix B

EOH Geology Hardwired Link Database Query Output (Input to PostScript Plotting Script)

```

391200.000,6454000.000,MB           ,ET 4020R
391721.000,6452501.800,M           ,ET 1540R
391828.000,6452501.300,M           ,ET 1530R
391860.000,6452740.000,M           ,ET 3220R
391880.000,6452740.000,USOL        ,ET 3210R
391895.140,6452537.540,UTSM        ,ETS 3
391900.000,6452740.000,USOL        ,ET 3200R
391920.000,6452640.000,MGB         ,ET 4290R
391920.000,6452740.000,USOL        ,ET 3190R
391920.000,6452800.000,M           ,ET 3280R
391933.000,6452501.300,M           ,ET 1520R
391940.000,6452640.000,M           ,ET 4300R
391940.000,6452740.000,USOL        ,ET 4030R
391940.000,6452800.000,M,         ,ET 3270R
391960.000,6452400.000,M           ,ET 3540R
391960.000,6452640.000,UTCB        ,ET 4310R
391960.000,6452740.000,USOL        ,ET 4040R
391960.000,6452800.000,USOL        ,ET 3260R
391969.090,6452501.900,M           ,ET 1610R
391980.000,6452400.000,U           ,ET 3350R

```


Fast Fourier Transforms

Author

Maurice Craig is from CSIRO Division of Exploration and Mining, Leeuwin Centre for Earth Sensing Technologies, 65 Brockway Road, Floreat Park, Western Australia 6014.

Introduction

The original implementation of frequency-domain-processing capabilities was concerned with constructing a bridge to ER Mapper's existing 'formula processing' facility, thereby extending its usefulness to geophysicists needing to manipulate potential-field data in raster format. However, there is also provision for simple low-pass, high-pass and notch Fourier filtering of arbitrary images. The chapter is organised as follows:

- 1 Brief explanation of Fourier-transform images;
- 2 Illustration of notch-filter use to remove noise in aircraft scanner imagery;
- 3 Low-pass and high-pass Fourier filtering;
- 4 Account of capabilities for processing potential-field data (magnetics or gravity);
- 5 Illustration based on aeromagnetic data from Cape York Peninsula, Queensland;
- 6 Appendix - (A) Edge effects (B) Display of transforms.

No prior knowledge of Fourier methods is assumed, since even experienced ER Mapper users may be unfamiliar with this topic. But rapid progress is assured, and there are few techniques so well worth the effort expended in acquiring them. Those already expert in frequency-domain processing may find the first half of section 4 sufficient.

The Fourier transform of an image

Imagine a rectangular, backyard swimming-pool with a tiled, horizontal bottom. The form of the fluid surface, at a particular moment in time, can be described by specifying the water depth at each point. To obtain a digital image representation, we have only to assign a grey level to the mean instantaneous height of the water-column above each tile.

But this is not the only description possible. For example, if the water is sloshing from end to end, then it may be sufficient to indicate the wavelength, trough-to-crest height and phase (crest location). When the waveform is sinusoidal, these three numbers permit full reconstruction of all the grey levels in the previous description. Although not every configuration of the surface can so simply be encapsulated, by an appropriate superposition of waves travelling in different directions we can, in fact, match a 'wave' description to every 'height' description.

The theory of Fourier transformation (named for Joseph Fourier, a one-time associate of Napoleon) is concerned with making this equivalence precise and analytical. Thus, for every digital image one can compute its transform-image from which, by an almost identical inversion process, the original image is recoverable. The paired images are of the same dimensions and contain identical information. Although very different from one another, both forms are meaningful for those equipped to interpret them.

Notch filtering

Why bother with this complicated, alternative description by waves travelling in all directions? There are several answers. One of the most important of them may be illustrated by supposing that, as the water in our pool heaves back and forth, a light cross-wind creates surface ripples. This situation is closely analogous to the practical case of aircraft scanner imagery spoiled by detector vibration. We may wish to eliminate this 'noise' without corrupting the 'signal'.

The problem is an awkward one inasmuch as the ripples are 'everywhere in general, but nowhere in particular'. But such global effects in the 'space domain' (original image) can mirror merely local effects in the 'frequency domain' (Fourier image). In our case, the transform image will be zero everywhere except for two widely separated pairs of spikes - one pair to represent the gross waveform, the other one for the ripples. We can take advantage of their isolation to remove the latter spikes by setting the amplitudes at these locations to zero. The result of retransformation will be a ripple-free version of the original picture. By subtracting it from the true original, we get an image of the ripples alone.

The ‘notch-filtering’ process just described can not be recommended for noise removal generally. One reason is the overhead involved in forward and reverse transformation; another, deficiencies in localisation. For example, if the ripples are square waves rather than sinusoids (as in Landsat Thematic Mapper imagery with 16-line horizontal striping effects), then the representative spikes will be periodically repeated. Removing all their repetitions may then require more effort than alternative, space-domain processing strategies. However, with aircraft scanner data, where the noise may be virtually intractable by other methods, the technique is invaluable.

The ideas outlined above are illustrated in Figures 1-5. They relate to a 480x480-sample subscene (not included as a demonstration data-set) from roll-corrected, band-32 GERIS data collected over Coppin Gap, W.A. Space-domain processing to suppress aperiodic, horizontal line-striping (Figure 1) leaves an image free from obvious noise, except for the cross-track ‘shading’ visible as limb-darkening.

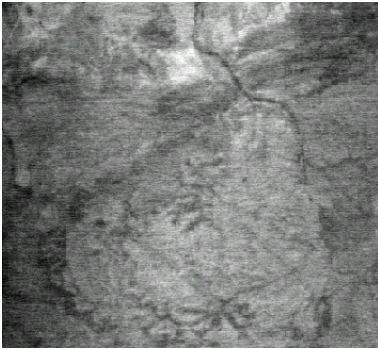


Figure 1

Figures 2 and 3 illustrate the corresponding Fourier transform. (More precisely, they are images of the ‘power spectrum’, showing amplitudes and directions but not phases of the waves; see Appendix (B).) Large values concentrate about the centre in Figure 2, producing an appearance reminiscent of globular star clusters. This is a typical pattern; spatial variation in most naturally produced images is gradual, so the long-wavelength (low-frequency) components predominate. The dark rectangles (notches) visible in Figure 2 mask wave components with amplitudes anomalously large for the high-frequency regions in which they occur. Fainter vertical streaks betray further noise artifacts that have not been masked.

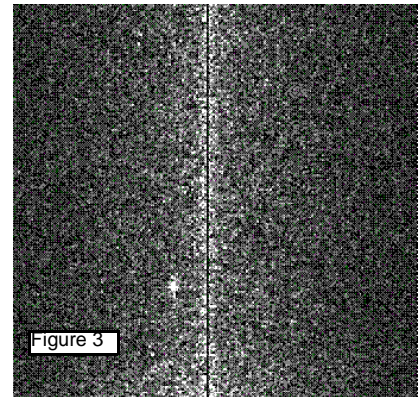
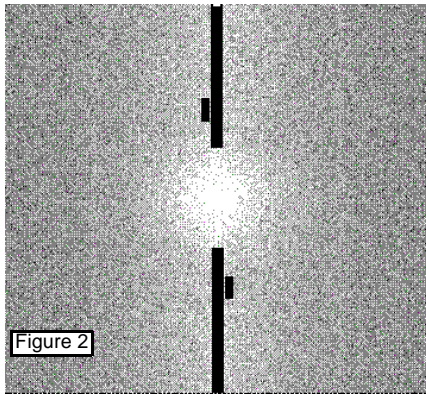


Figure 3, an enlargement of just the upper part of the image, shows its appearance before masking. The dark, central, vertical line attests to the success of the space-domain process for removing strictly horizontal stripes, but the lighter background betrays its inability to cope with sub-horizontal striping, even at very low angles. Figure 4 depicts the space-domain noise-pattern isolated by the larger paired rectangles in Figure 2.

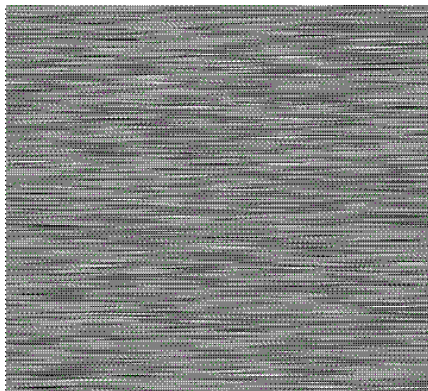


Figure 4

The two smaller notches cover paired, star-like noise-spikes, one of them clearly apparent just left of centre, about one-third from the bottom in Figure 3. It proved difficult to obtain a hardcopy illustration of the corresponding interference pattern, consisting of wave-fronts inclined at about 11.23° to horizontal, with approximately 110 crests intersecting the left margin of the image. Readers will be familiar with the curious effect, seen in wild-west movies, of wagon wheels that appear to rotate backwards. Its cause is the too-infrequent sampling of a periodic motion—the rotation of the spokes—by the camera shutter. A two-dimensional variant of this ‘aliasing’ phenomenon, wherein subsampling by the printing device produced a full 90° rotation of the wavefronts that we sought to illustrate, unexpectedly limited us to the mere verbal description given above. Figure 4 is probably likewise affected, but at least the textural appearance is similar to the unaliased original.

Low-pass and High-pass Fourier filtering

Granted the existence of the transform-image, and the recognition that each of its pixels corresponds to an undulating component of the input image, a wide range of possibilities lies open for effecting modifications to improve data-interpretation. For example, with an image much affected by random noise, picture quality may be improved by stripping out all the high-frequency components, which is to say resetting the Fourier image to zero in regions remote from the central, high-amplitude region.

Again, with better-quality data, we may wish to enhance edges (such as road boundaries in remote sensing data) by removing the more slowly varying components of the scenery. That end could be accomplished by annulling low-frequency terms within the Fourier image. Alternatively, the difference between input and low-pass images gives a high-pass-filtered image; one may also enhance edges without loss of geographic context by mixing the input data with a high-pass version of itself, in suitable proportions. There are still-more-creative possibilities, such as enhancing or suppressing trends with a particular range of orientations (strike filtering), but these capabilities have not been incorporated in the present version.

ER Mapper does, however, accommodate the low-pass and high-pass filtering operations needed for the noise suppression and edge enhancement just described. Low-pass filtering is done by multiplying the Fourier image by zero at high frequencies as just described. Conversely, high-pass filtering multiplies low frequencies by zero. But a further refinement is necessary: experience shows that if the demarcation between high and low frequencies is a sharp one, such as a circle or rectangle centred on the zero-frequency point in the Fourier image, then peculiar artifacts are observed following retransformation to the space-domain.

This phenomenon, usually called ‘ringing’, is further considered in Appendix (A). Here it is sufficient to note how it may be counteracted by allowing the multiplier to vary smoothly over a range of intermediate frequencies between the extreme values zero and unity. In Release 5.0, the user specifies two ellipses centred at the zero-frequency point, their principal axes proportional and aligned parallel to the sides of the image (Figure 12). The annular region between the two curves defines the set of intermediate frequencies. For low-pass filtering, the filter (i.e., the multiplier) is unity within the inner curve, zero outside the outer curve. Between the ellipses, its value drops in the same way as do the values of the function $(1 + \cos x)/2$, for x between zero and π . This type of filter is therefore known as a cosine roll-off filter. For high-pass filtering, the multiplier is obtained by subtracting the low-pass filter from unity (no actual subtraction of images is performed).

Finally, it seems desirable to reiterate the warning of the previous section about overuse of the Fourier transform. Suppression of ‘pepper-and-salt’ and ‘spike’ noise is generally better done in the space-domain, say with moving-average and median filters respectively. The existence of alternative means to the same end is never a sound reason for choosing the worse. A valid case for Fourier-domain low-pass filtering to remove noise would be a noisy or badly gridded aeromagnetic dataset that must for other reasons (see next section) be Fourier-transformed anyway. No particular advantage would be secured by noise-removal preprocessing in the space domain.

Fourier processing of potential-field data

Digital imagery is an excellent medium for storage, display and manipulation of spatially distributed readings such as many geoscientific datasets. The present section concerns measurements of the earth's magnetic or gravitational field. Here, the use made of the Fourier transform is quite different to the one outlined above, since in principle there is no need for visual inspection of the transformed image. In practice, one is well advised to check its appearance, thereby exploiting the unique opportunity to spot problems with the data that may have gone undetected.

A few remarks are first necessary regarding the assumed initial form of the data:

- The readings may result from ground measurements of the field made at regular spacings. At larger scales most datasets derive from sampling along the track of a survey aircraft or seagoing vessel. Thus, an interpolation step is needed to produce values on a regular grid. Here we assume that this preprocessing has already taken place. The data may therefore be supposed to reside in an ER Mapper image file but there is no assumption that they fill an entire rectangle. Locations at which data are unknown are assumed to be filled with a designated “blank” or “null” value, which the user must indicate to the program.
- The data are further assumed to be measured on one horizontal plane. The theory to be invoked does not directly apply to “draped surveys”, such as “aeromag” or “helimag” flown over precipitous terrain, where the pilot aimed at constant ground-clearance, rather than constant altitude. Further preprocessing to achieve “upward continuation from an uneven track” would then be indicated. Fortunately there are large regions of the world where surveys can be flown horizontally.
- By “measurements of the earth's field” are meant readings of some directional component of the vector field. But this case practically includes total-field magnetic anomaly data (almost the only kind readily available) since it can be shown that, except for very intense fields, the difference between the total field and its regional value (the IGRF) is approximately equal to the component of the residual field in the direction of the earth's field.

In summary, the data are assumed to be an ER Mapper image of some component of a magnetic or gravitational field measured on a horizontal plane, but possibly incomplete, incorporating a constant blank value at non-data points. The software allows processing of such pictures to images showing:

- A. Vertical continuation;
- B. First upward derivative;
- C. Second vertical derivative;
- D. Derivative in a specified direction in space;
- E. Field component in a specified direction in space;
- F. Reduction to the pole (meaningful in magnetic case only).

This list contains two surprises for the uninitiated. Firstly, why should one component of a vector field be sufficient information to compute the component in some other specified direction or, equivalently, the components in three mutually orthogonal directions (such as north, east, and down)? Secondly, why (to take the aeromagnetic case) should information gathered from one altitude be sufficient to deduce the corresponding information for another altitude, at which the aircraft did not fly? The answers, which depend on the physical significance of the readings, are not merely heuristic but form the basis for the algorithms employed.

Briefly, process E is possible because the force-field is conservative; it is the gradient (in the sense of vector calculus) of a scalar potential-function. Given one field-component, we can anti-differentiate it to get the potential, then re-differentiate in another direction to get a new component of the field. These operations are particularly simple in the Fourier-domain.

The scalar potential-function, hence also each of its directional derivatives (the field components), satisfies the three-variable Laplace differential equation, which serves to connect the values of its second partial derivatives in three mutually orthogonal directions. Knowing the function-value on the flight-plane (equivalent to knowing one field component), we can numerically evaluate two of the second derivatives - say those in the x and y directions, where (x, y) are Cartesian co-ordinates in the plane. Laplace's equation then determines the second derivative in the z direction, perpendicular to the plane.

The resulting knowledge about how the field varies vertically is sufficient to permit process A, movement to another stratum, either higher or lower. The correctness of this theory, and of the Fourier-domain processing capabilities can be verified by the use of simple models for which explicit analytical expressions of the field components are known. Examples include uniformly magnetised parallelepipeds, circular cylinders, and a few others. If images of the field at two levels are computed directly from these formulae, we can compare the values on the upper level with those obtained by continuation from the lower level, and vice versa. With suitable precautions the agreement is excellent. (Notwithstanding this concurrence of theory and experiment, a lingering sense of the miraculous may be found hard to dispel!)

In keeping with the warnings of previous sections, it is fair to add that process C is easier to effect by space-domain processing. With potential-field data, vanishing of the space Laplacian means that the plane Laplacian, for the horizontal plane, equals the negative of the second vertical derivative. It is well known that the plane Laplacian operator has a finite-difference approximation by a mask with (-4) at the central position, unity in the locations of its four nearest neighbours. Indeed, convolution with such a mask is often used for non-directional edge-detection in image processing generally. This remark also shows whence the second vertical derivative has the ability for which it is chiefly valued, that of outlining magnetic sources.

The other processes A-F can likewise be accomplished by suitable convolutions in the space-domain. But here the necessary masks are much less compact. The advantage of Fourier-domain processing is that point-operations (multiplications and divisions at each pixel, without regard to the values at neighbouring pixels) take the place of

computationally expensive convolutions. Computational overhead associated with the transform is offset by the consideration that, once it is to-hand, a host of different results can all be read off relatively cheaply.

Aeromagnetic data from Cape York Peninsula, Queensland

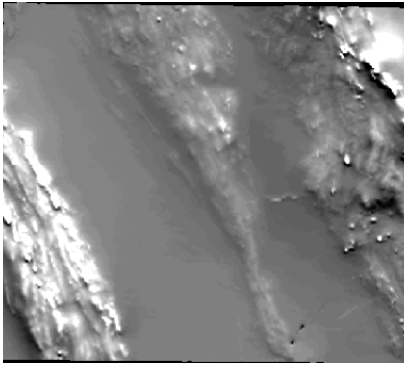


Figure 5

Figure 5. The examples/Shared_Data/Magnetics_Grid demonstration dataset, comprising total magnetic intensity data sampled at 80m elevation with a 200m line spacing, thence interpolated at 100m spacing in both horizontal dimensions. The image straddles the Great Dividing Range, rising just inland from Princess Charlotte Bay on the north-east coast of Australia. The region is bounded by longitudes $142^{\circ}57'19.3''$ and $143^{\circ}32'43.35''$, and between south latitudes $13^{\circ}59'20.32''$ and $14^{\circ}32'23.98''$, north being to the top of the image. For whole-scene processing purposes, the magnetic declination and inclination were taken as 6.4° and -42.1° , respectively.

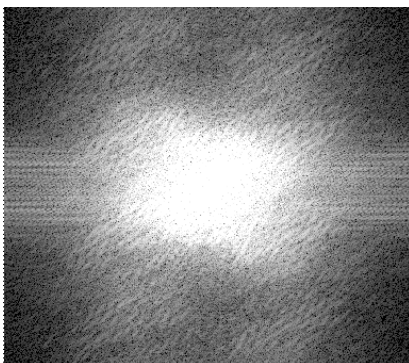


Figure 6

Figure 6. The power spectrum for this image. For uniformity, all power spectra illustrated are shown with input limits of 0 to 0.01, followed by a logarithmic stretch. The subsequent figures are as follows.

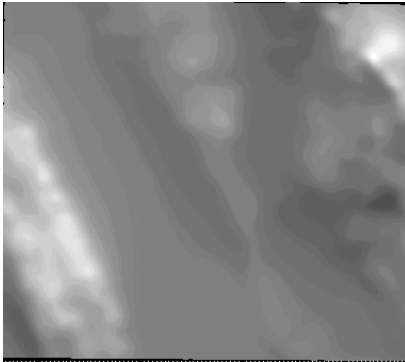


Figure 7

Figure 7. Upward continuation to 1200m. This operation is commonly used to isolate the contribution from magnetic sources deep below the surface.

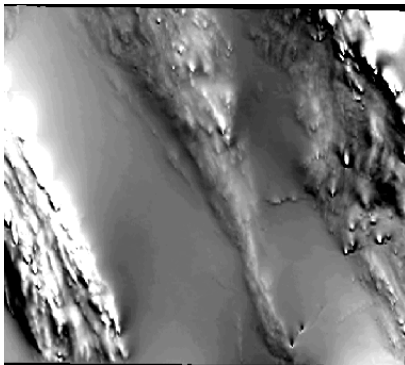


Figure 8

Figure 8. Field reduced to pole and downward continued to 40m. Downward continuation helps counteract attenuation imposed by the need to fly surveys at a safe ground-clearance.

Reduction-to-pole attempts improved spatial correlation, between magnetic anomalies and their sources, by giving the induced magnetisation a vertical direction. (It has been criticised for its distorting effect upon fields due to remanence not parallel to the induced component.)

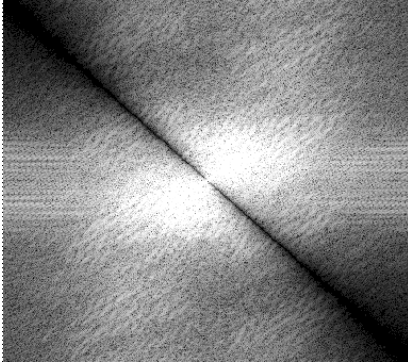


Figure 9

Figure 9. Power spectrum for horizontal derivative in the north-easterly direction.

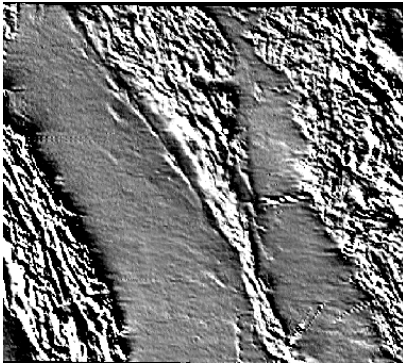


Figure 10

Figure 10. North-east derivative. Note the NW-SE trending “fringing reef” through the centre of the image, faintly visible in Figure 5, but strongly highlighted by its up-slope and down-slope gradients in Figure 10. Derivatives are available in arbitrary directions, not necessarily horizontal, e.g. parallel to the terrestrial field.

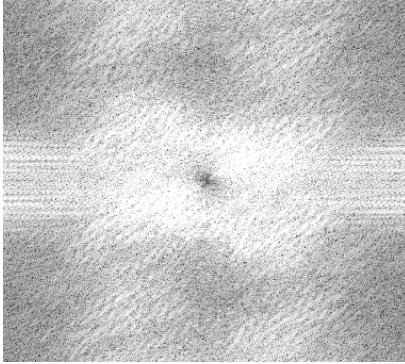


Figure 11

Figure 11. Power spectrum for second vertical derivative. The horizontal stripes through the centre are a noise artifact, but are not easy to separate from signal.

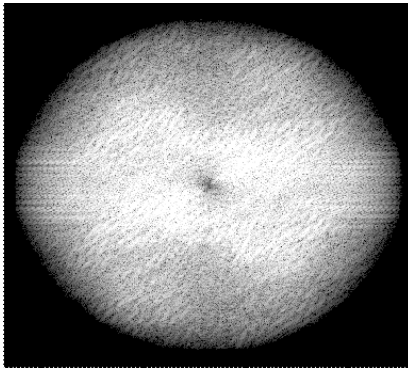


Figure 12

Figure 12. Appearance of Figure 11 following application of elliptical low-pass filter. (The transform being a poor candidate for such filtering, the improvement possible in Figure 13 is negligible.)

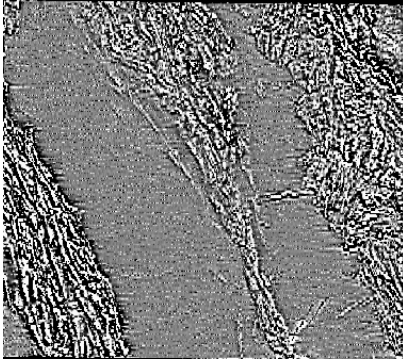


Figure 13

Figure 13. Second-vertical-derivative image. As noted above, this enhancement is commonly used for accentuating the edges of causative bodies. However, it can also emphasise faults of gridding and levelling, leading to 'edginess' (lack of spatial cohesion) and artifacts that may have dubious basis in reality.

These illustrations far from exhaust the capabilities, but should provide sufficient points of comparison for users to confirm the results of their own processing.

Appendix

(A) Edge effects

Sensible use of the Fourier transform requires a heightened awareness of sharp edges within images. The first purpose of this appendix is to alert users to one or two situations involving such discontinuities in the data.

The high-frequency content of imagery was attributed above to the fine detail within the picture, but there may be other causes. If a remotely sensed image is Fourier transformed after first being copied into a slightly larger file where the unfilled region is preset to some value such as zero, then the high-frequency region of the transform-image will relate to more than just the roads and rivers and shorelines. Fourier-image pixels of large magnitude (at low as well as high frequencies, but most noticeable at high frequencies, where they would not otherwise occur) will be needed to represent the discontinuous steps, where the original data drop abruptly to zero.

Of course, we do not usually thus embed space-domain imagery within a field of zeros. However, the low-pass filtering as first described in section 3, where parts of the transform-image are annulled, has precisely the effect of creating a sharp step to zero. Since the inverse transformation process is the same in its nature as the forward procedure (with only

the technical difference of a certain algebraic sign-change), we should expect trouble. This is the reason for implementing a cosine roll-off, instead of a simple ‘pill-box’ filter, in section 3 Low Pass and High Pass Fourier Filtering above.

The second instance of image discontinuity, though not its unpleasant effects, is well hidden. It was asserted earlier that the Fourier transform has the same dimensions as the image from which it derived. Users who inspect their transforms will find, on the contrary, that they are generally some 10% bigger in each dimension. This discrepancy results from a deliberate, pre-transformation enlargement of the data, which are copied to a bigger file as just envisaged. However, instead of a filling by zero values, the border region receives synthetic data extrapolated from the actual values. This extrapolation is done in such a way that, in a tiling of the plane by translated copies of the enlarged image, it would be difficult to locate the boundary between one tile and its neighbours.

Why is such a matching of data at the top and bottom, and at the left and right edges, considered necessary? Recall that the Fourier representation of an image explains the image in terms of waves. But waves naturally continue periodically forever. Consequently, the Fourier transform actually represents, not just the given image, but also the unbounded image obtained by its endless repetition as a tiling of the entire plane. Now, this unbounded image will contain discontinuities whenever the top and bottom, or left and right, fail to match one another smoothly in the original image. And in order to model these discontinuities, high-frequency terms of large amplitude will be needed.

Thus, even though an image may appear smooth, for purposes of Fourier transformation it counts as including jump-discontinuities if (as in nearly every practical case) data at opposite edges fail to match. This is of small concern with upward continuation and similar low-pass filtering operations. With high-pass filters like those for downward continuation or derivatives, ignoring the effects of ‘edge discontinuity’ is catastrophic. For, this amplification of high-frequency components is prescribed by a theory that assumes them to represent the physical structure of the field; there is no allowance for artifacts due to the approximation of the continuous Fourier transform of theory (Bracewell, 1965; Gunn, 1975) by the discrete transform used in the programs. When an image with edge-mismatch is high-pass filtered in the Fourier-domain then retransformed by inversion, the result is an image with severe ‘ringing’ - undulating patterns parallel to and strongest near the edges, but often propagating so far into the centre as to make the entire image useless for interpretation. Our backyard swimming-pool looks then as if an earthquake had just hit the suburb!

With data that include blank values, the enlargement and extrapolation process also interpolates. Particular circumstances can render image expansion undesirable. For example, a noise pattern whose wavelength is commensurate with the sampling interval could be isolated more precisely without it. Provision has therefore been made to enforce size-retention, if required. (With this option, edge-mismatch will produce a well marked St. George cross passing through the centre of the power spectrum.) But a null value must always be nominated and, if the program detects an input pixel with that value, it will ignore the override instruction. Expansion will also occur contrary to user wishes if the

original image-dimensions are not sufficiently highly composite numbers to suit the needs of fast transformation. More precise information on this point will be found in the Reference Manual.

(B) Display of transforms

The mathematics of Fourier transformation has some hard to ignore effects that may engender confusion. The following brief explanation will perhaps be helpful.

The Fourier transform of a real image (one whose grey-levels are of byte, integer or floating-point type) comprises complex numbers, equivalent to two real numbers for each pixel. This fact seems to imply a doubling of data. However, such Fourier transforms also have a type of symmetry, with respect to their centres (zero-frequency points), that implies redundancy. Thus, the real part of the pixel at (-x, -y) is the same as at (x, y), while the corresponding imaginary parts are equal in value but of opposite sign. Here, x, y are sample and line co-ordinates relative to the centre of the transform-image.

This symmetry must be kept in mind with notch-filtering, for example (Figure 2). Changes made to one part of the transform must be mirrored symmetrically with respect to the centre, or the product of alteration will not be the transform of any real image. In other words, the inverse transform would no longer be real.

The complex values complicate display of the Fourier transform. The usual solution is to produce an image of absolute values, or their squares (u^2+v^2 being the squared absolute value of the complex number $u+iv$), called the Fourier power spectrum. The 'Log-power spectrum', obtained by taking logarithms (preferably after adding a suitable positive constant, to avoid the singularity at zero), is also often useful, as a means of compressing the wide range of values. Power spectra show the orientation of wave-fronts (by pixel position) and the amplitudes of waves (by grey-level). They lack only the phase information, which depends on the relative magnitudes of real and imaginary parts.

As will be clear from these remarks, Fourier-transform images are in many respects inconvenient; whether to store, to display, or to manipulate. The so-called cosine transform, a close relative of the Fourier, has all-real values, no symmetry properties, and a high degree of natural immunity from ringing due to edge mismatch. Unfortunately it is less well suited to achieving the objective of processing of potential-field data.

References

- Bracewell R., 1965. *The Fourier transform and its applications*: New York, McGraw-Hill, 381 p.
- Gunn P. J., 1975. *Linear transformations of gravity and magnetic fields*. Geophysical Prospecting **23**, 300-312.
- Huang, T. S., Schreiber, W. F., Tretiak, O. J., 1971. *Image Processing*. Proc. IEEE, v. 29, p. 1586-1609.

Singleton, R. C., 1969. *An algorithm for computing the mixed radix fast Fourier transform.* IEEE Transactions on Audio and Electroacoustics **17**, 93-103.

Principal Component Analysis

Principle Component Analysis for Alteration Mapping Using Landsat TM Satellite Imagery

Author

Eric Augenstein, Americas Region Office, Earth Resource Mapping, 4370 La Jolla Village Drive, Suite 900, San diego, CA 92122-1253, USA.

Using Principal Component Analysis

The following image processing technique provides a simple, robust way to map alteration zones for mineral exploration using Landsat Thematic Mapper (TM) satellite imagery. It is based on the use of Principal Components Analysis (PCA) and is sometimes called the 'Crosta technique' after the researcher who carried out the initial studies (Crosta and McM.Moore, 1989).

The following steps describe how to build the PCA alteration mapping algorithm in ER Mapper. In order create the algorithm, you need to create and examine dataset statistics to account for variation in the spectral properties of different areas and TM images. After choosing the appropriate PCs for your image, you can display the result as an RGB algorithm for analysis. For complete details on the concepts and theory behind the PCA alteration mapping algorithm, please refer to the references listed at the end (this particular technique is described in the Loughlin paper).

- 1 Create two Virtual Datasets, one that contains TM bands 1, 3, 4 and 5 (this is dataset 1), and another that contains bands 1, 4, 5 and 7 (this is dataset 2).

Be sure to delete the transforms from each layer to avoid rescaling the data, and add a label to each layer indicating the band.

- 2 Calculate statistics for each of the Virtual Datasets.
- 3 Display the statistics for dataset 1 and examine the Covariance Eigenvectors.

Identify which PC has the greatest loadings (values) for TM bands 1 and 3 but that also has opposite signs (+ or -). Typically this is either PC3 or PC4. For example, in this dataset you would choose PC4 (you are looking at VDS bands 1 and 2 below as they refer to actual TM bands 1 and 3):

Cov. Eigen.	PC1	PC2	PC3	PC4
Band 1	0.568	0.115	-0.487	-0.654
Band 2	0.571	0.157	-0.300	0.747
Band 3	0.229	-0.973	-0.003	0.029
Band 4	0.547	0.123	0.820	-0.115

This PC represents the “iron oxide” (F) component.

Note: When examining the statistics, remember that the “Band” number above refers to the order of bands in the VDS, *not* to the actual TM band number. For example, TM band 3 may actually be Band 2 in your VDS. In this case, you must first determine which VDS band numbers correspond to TM bands 1 and 3, then examine the PC3 and PC4 statistics for those two bands.

- 4 Display the statistics for dataset 2 and examine the Covariance Eigenvectors. Identify which PC has the greatest loadings (values) for TM bands 5 and 7 but that also has opposite signs (+ or -).

Typically this is also either PC3 or PC4. This PC represents the “hydroxyl” (H) component.

- 5 Create a 2-band Virtual Dataset that calculates PC4 (or PC3 as appropriate) from bands 1,3,4,5 in one layer (the F image), and PC4 from bands 1,4,5,7 in a second layer (the H image).

Delete the transforms to avoid rescaling the data and add a label for each.

After saving the VDS, calculate statistics for it. You will use this VDS later to generate PC1 of the H and F images.

- 6 Create an RGB algorithm with the following contents (remember to use the appropriate PC for your scene; PC4 is shown below):

Red = PC4 of bands 1,4,5,7 (the “H” image)

Green = PC1 of the “H” and “F” images (using the Virtual Dataset created in step 5)

Blue = PC4 of bands 1,3,4,5 (the “F” image)

On each layer, apply a linear contrast stretch that clips the darkest portion of the histogram - you are interested in highlighting the frequently occurring values in the center of the histogram. You might start by applying a 99% clip and then moving the bottom node of the transform line in closer to the histogram center.

The resulting image is usually a dark bluish color composite image on which alteration zones are unusually bright. White pixels are both iron-stained and argillyzed, bright reds and oranges are more argillyzed than iron-stained, and bright cyan to bluish tones are more iron-stained than argillyzed.

Optional: To add the major structural features of the image back into your RGB algorithm, you can add an Intensity layer that generates PC 1 of the TM image and contrast stretch it. This may make it easier to interpret the image because the overall scene brightness or albedo information is restored to the scene. In some cases, however, it may detract from interpretation so you need to experiment.

In addition, you may wish to add low pass (averaging) filters to the RGB layers to smooth noise in the higher order PCs, and/or a high pass (sharpening) filter to enhance structural edge features in the PC 1 Intensity layer if you decide to use it.

References

- W.P. Loughlin, 1991. “Principal Component Analysis for Alteration Mapping.” *Photogrammetric Engineering and Remote Sensing*, Vol. 57, No. 9, September 1991, pp. 1163-1169.
- Crosta, A. P. and J. McM. Moore, 1989. “Enhancement of Landsat Thematic Mapper Imagery for Residual Soil Mapping in SW Minas Gerais State, Brazil: A Prospecting Case History in Greenstone Belt Terrain” *Proceedings of the 7th (ERIM) Thematic Conference: Remote Sensing for Exploration Geology*. Calgary, 2-6 Oct. pp. 1173-1187.

Part Two - *Case Studies*

13

Aerial Photography and Data Integration

**Aerial Photography and Data Integration in Environmental, Engineering and
Cartographic Applications**

Authors

James Cutler and **Justin Saunders**, Geographic Information Services Ltd. (GISL), PO
Box 85, Egham, Surrey TW20 8SE, UK.

Context: Data Gathering

It is frequently assumed that image processing is confined to the processing of remotely sensed data acquired from satellite borne sensors. In fact remote sensing has its origins in more prosaic circumstances, those of the humble balloon and it is in these more near-Earth surroundings that remotely sensed data offers a valuable tool to those concerned with the alteration, monitoring and evaluation and mapping of the Earth.

In Europe and North America in particular urbanisation and the spread of the automobile have resulted an increasing awareness of the fragility and temporal nature of much of what is taken for granted. In response increasingly stringent legislation requires that local/federal authorities and sectoral agencies are in a position not only to oversee their domain but also to provide documentary evidence on what exists or occurs and what should happen in the future. In some cases, for instance forest management in Canada, conventional satellite imagery has been used as an integral component of development strategies. However, in other areas, especially on the urban fringe, an area especially subject to developmental (and preservational) pressures, the demand is for near-real-time information; this information has to be cost-effective, accurate and easily integrated with existing data collation practices.

Aerial photography has played a major part in map composition since 1945. It has enabled cartographers to prepare accurate maps of previously inaccessible areas and, coupled to ground survey, has resulted in the production of large scale maps of the most densely populated areas. However, the drawbacks of cost, human and capital resources and time from flying to publishing now represent burdens that many local authorities cannot afford to bear. The search for an alternative methodology must be aware of the growth of information technology in surveying, database creation and information gathering; geographic information systems (GIS) have become a prominent tool in the armoury of such organisations as they seek to respond to public concerns and internal need in a cost-effective way.

The response has been to evaluate the way in which sporadic and specific aerial photography can be complemented by airborne video photography and how digital imaging techniques (either camera-originated or through scanning) can be used to minimise the cost of aerial photography. Image processing allows the user to extract the required information; it also provides a contextual medium to examine existing data, to document the landscape and to extract secondary information. Further, as a digital dataset, this approach allows integration with existing digital datasets and retains data integrity and unlimited recall.

Specific applications that require this kind of information include:

- village plans
- development applications/planning licences
- map updating
- environmental assessments

- transport corridors
- infrastructure development
- utilities mapping
- urban planning
- legislative obligations and infringements (e.g. Green Belt, SSSIs)

The attached images illustrate the way in which many of these applications can be addressed using ER Mapper.

Example: Transport Corridor Development

A local council, subject to local and national conflicts of interest with respect to the development of a new transport corridor, identifies a need to develop and maintain an up-to-date information management system for the area in question.

At the same time developers, be they government or commercial, consultants and pressure groups all have a need for information to guide, mitigate and ultimately justify the decisions made. While some may be concerned with issues of planning blight and confidentiality, others will be concerned about short and long-term impacts, access, compensation and the wider debate. The former may look to internal resources to meet objectives while the latter may depend on public information dissemination; all, however, would agree on one thing—that the key to successful development lies in the availability of up-to-date and accurate information.

Essential inputs to such a database would include:

all existing mapping

(both from the national authority and from local planning/survey offices)

- topography
- infrastructure
- political boundaries
- settlements
- drainage and watersheds

statutory designations

- landscape
- ecology
- archaeological/historical

- agriculture
- minerals
- health and safety

utilities

- water
- sewage
- electricity
- telephone
- gas
- pipelines

land ownership

- land registry
- four-figure field references/areas (MAFF)

demographics

- census data, etc.

archive material

- aerial photography, old maps, etc.

A quick assessment of the validity of this data would soon reveal that much of it was not adequately up-to-date and that some data collection would be required. Black and white aerial photography and colour infrared aerial photography are increasingly used to redress this balance where data gaps are identified; with the advent of digital aerial photography cameras, computer compatible images are readily available from these sources.

Alternatively, the hardcopy aerial photos may be scanned to produce the digital data. The spatial resolution of hardcopy aerial photography is proportional to flying height, film used and focal length of camera lens; with scanned or digital data the resolution of the digital device determines spatial resolution. The resulting resolutions are typically sub-meter and can be used to map features such as street lighting, man-hole covers and gardens.

Airborne video is an increasingly popular alternative; it is cheap and easy to obtain and, by generating digital data at source provides data in a format immediately ready for image processing. Spatial resolution is closely linked to flying height and has been used for pipeline surveys, catchment measurement and for adding detail to other lower resolution imagery such as SPOT Panchromatic data.

Georeferencing and Rectification

Neither process removes the need for rectification; however, the widespread availability of national mapping in digital form allows organisations concerned with spatial information management to obtain the required datasets easily. The ability simply to examine change, update existing maps, evaluate local, sectoral and regional policies and provide data in a format for use in the GIS as a result of the georeferencing of high resolution imagery with existing digital data represents a significant step forwards.

Using ER Mapper the client was able to import three scanned black and white and one colour infrared aerial photograph of the area under consideration. These were then georeferenced to digital national mapping data using the Geocoding Wizard in ER Mapper. For ease of interpretation the user defined regions on each aerial photograph to exclude fiducial marks (and other ancillary information) as well as the photo border and then uses a formula to mask out the region using the Formula button. The resulting strip of aerial photographs provided an excellent overview of the area of interest.

Integrating and updating vector data for planning

The national mapping data was then overlaid to illustrate the degree to which ER Mapper can provide workable rectification in near-real-time and to allow planners to identify areas where mapping has yet to be fully updated. In this example a recently developed site was clearly visible on the image but was evidently missing from the national mapping data; an area of forest had also clearly be seen to have been clear-felled. This form of raster–vector integration is a powerful presentation tool, especially when the outputs are linked to a GIS and other datasets.

While a developer would rapidly become aware of such a situation from on-the-ground investigations, initial corridor alignments depend on the information on the existing mapping; there is plenty of scope for embarrassment! The developer would commission an engineering consultant to design the transport corridor—horizontal and vertical alignments, curvature, drainage and construction requirements (in terms of cut and fill and sites) are among the first objectives to be identified. These materialise in the form of engineering drawings from systems such as MOSS and AutoCAD. ER Mapper imports files from these data sources very easily.

The developing authority will commission an environmental assessment either at its own discretion or in line with mandatory obligations and legislation. This will draw on a wealth of primary and secondary data sources to compile a picture of the state of the to-be-affected corridor and immediate environs. The preparation of digital datasets from these findings and the subsequent integration of these into spatial databases of both planners and

engineers is not yet a standard procedure. However, with ER Mapper any digital datasets can be brought in and overlaid on the imagery and existing mapping at an early stage. This can make significant contribution to engineering design both through realignment and the adoption of suitable mitigation measures and through recognition by planners of previously unidentified constraints to development.

Conclusion

Much is made of the volumes of data and the amount of information available today. Image processing technology coupled to GIS represents the foremost way in which this fact can be made to work for those affected by development. Data collection, compression and collation, brought to the desktop and the decision maker by the new technologies and the ever-evolving methodologies, enables users to evaluate decisions both in advance (and in hindsight), to assess impacts and to generate the outputs needed to explain and justify the final decision.

Monitoring Crop Production and Assessing Irrigation Requirements

**High Resolution Satellite Imagery for Monitoring Crop Production and Assessing
Irrigation Requirements**

Authors

James Cutler and Justin Saunders, Geographic Information Services Ltd. (GISL) PO
Box 85, Egham, Surrey, TW20 8SE, UK.

Introduction

One of the increasingly common sights in Africa and the Middle East are great patches of colour scattered across a seemingly barren landscape; an agricultural and environmental anomaly to many, others feel that these represent one of the few viable alternatives by which countries can both generate export revenues and feed their people. Crop circles or, more accurately, centre pivot irrigation, are one of the more visible ways in which the application of technology can alter the physical landscape. This chapter focuses on the role that a different technology can play in monitoring such developments at local and regional levels.

Context: Agricultural development

From Kansas to the Kalahari and from Saudi Arabia to Southern Spain, irrigation circles up to a kilometre in diameter are becoming a common agricultural characteristic. As visible from space as from the highway, they are the focus for mono-cropping and agricultural export in many developing countries and, in the more arid areas such as the Middle East, often symbolise the ability to stand alone. As such, considerable investments have been made in hydrogeological and hydrological investigations, borehole development, equipment, seed and fertiliser imports, and in training and recruitment.

As the global population doubles in the next 30-40 years, its main requirement will be adequate food and water. This means not only potable water (for drinking, cooking etc.) but water for agricultural use. To this end, focus is switching to agricultural and rural development programmes that take full account of the current and future water needs of the region.

Land inventory studies are among the first essential stages in any rural development project; making them is often difficult and increasingly constrained. The lands to be assessed are frequently unknown or undeveloped or may have undergone rapid changes. Planners increasingly require data that is detailed, complex and diverse, to devise programmes that are sociologically acceptable and economically and environmentally viable. Traditional techniques based on intensive ground surveys are cumbersome, unreliable and costly.

Hydrologists and others recognise the river-basin as the fundamental unit in effective water resource management and planning. Regional planners acknowledge that an up-to-date knowledge of current farming systems, land tenure systems, water resource dynamics (particularly the balance between abstraction and recharge in semi-arid catchments) and planning strategies are integral to the evolution of sustainable agricultural programmes. These needs place data gathering and effective information dissemination at the centre of all decision making.

Multispectral satellite imagery, available from the Landsat series of satellites since 1972 at resolutions of 80m and latterly 30m (with Landsat TM) were complemented and enhanced in 1986 with the launch of the first SPOT satellite. Carrying two sensors, one multispectral

with three bands in the visible and near-infrared and one wider panchromatic band, these sensors return imagery with a spatial resolution of 20m and 10m respectively. While SPOT has undoubted spectral resolution limitations, the increased spatial resolution has provided the resource planner with a new and valuable tool in data gathering.

Example: Irrigation development

A national agency maintains up-to-date projections on population growth and the associated demands in food and other goods and services. Such a forecasting system enables planners to identify impending shortfalls in production of any one of these goods and services. Many semi-arid countries are afflicted by rapidly growing populations, environmental fragility, weak economies and inadequate infrastructure. As new schemes come on stream to redress this imbalance the planners must monitor and evaluate their development not only to ensure that it is effective but also to devise new programmes.

Crop Production

There are a range of ER Mapper classification routines that allow the user to quickly differentiate between crops and to identify which areas are growing which crop. Irrigation circles were discriminated simply by applying a contrast stretch; in ER Mapper the Transformation dialog box and the histogram options allow the user to control exactly what is seen on the screen in real-time.

In very arid areas such discrimination may be all that is required to identify agricultural areas. However, in semi-arid areas the user must separate agricultural or cropped areas from natural vegetation and browse. Supervised maximum likelihood or unsupervised multi-spectral classification allows wheat, barley, lettuce and fallow circles to be identified. The ER Mapper annotation and map production system was used to create symbols identical in size to the irrigation circles. The resulting map product is a clear illustration of the power of ER Mapper to provide clear documentation to decision makers.

The area of the irrigated circles is easily calculated; with a 500m radius, the area is about 78 hectares. Considerable work has been done on crop yield estimation not only from satellite data but also from empirical evaluation of a large range of crops using different irrigation technologies under varying climatic conditions throughout the year. This allows vegetative biomass to be monitored throughout the growing season using satellite imagery and digital image processing techniques, and enables crop yield forecasts to be made and updated; this helps with marketing, exports, imports and pricing.

Vegetation indices have become a conventional means by which image processing can provide accurate estimates of biomass; the Normalised Difference Vegetation Index (NDVI) has been widely correlated with green biomass and final crop yields but has been criticised for its failure to accommodate densely vegetated areas or to make allowance for the influence of soil background on reflectance. The Perpendicular Vegetation Index (PVI) and the Soil Brightness Index (SBI) were derived to overcome these limitations but do

require ground data. ER Mapper contains a library of indices and band-ratios including NDVI, PVI and SBI; these are readily accessed and applied through the Formula dialog box.

NDVI can be used to derive grey scale images that can then be density sliced to produce an alternative but equally clear output.

Irrigation requirements

Various techniques use reference crop evapotranspiration rates based either on the Penman method or a class “A” pan to assess irrigation requirements. In semi-arid areas with sporadic rainfall, irrigation requirements are often assumed to be equivalent to crop evapotranspiration taking into account irrigation technique, soil type, leaching requirement, crop growth stage, crop yield demanded and frequency of irrigation application.

Intensive agricultural programmes in semi-arid areas, either extracting water from major rivers through dam construction and diversion/off-take structures or abstracting it from aquifers through tube-wells, makes tremendous demands on the water source. When to irrigate and how much to apply is very important for the proper growth of crops and water use efficiency. Irrigation enables the farmer to grow crops more-or-less continuously; climatic and other factors limit actual cultivation periods.

A satellite image based study of centre-pivot irrigated circles within a catchment over one or more years using ER Mapper will provide a very good indication of the number of crops being grown per circle per year, the type of crop, the yields generated and therefore the water demand of those farming systems. Water resource managers and those responsible for agricultural development can collude to ensure that abstraction rates for agriculture or other large scale activities such as mining, power stations and industry do not exceed aquifer recharge and do not adversely affect water quality in the catchment.

Conclusion

Satellite imagery offers a tool for our times, a cost-effective means of data gathering; ER Mapper is another tool, one that can exploit the widespread availability of remotely sensed data to provide information to decision makers in a coherent and systematic manner. As issues of environment and development become increasingly contentious and conflict-ridden, the ability to provide up-to-date and accurate information to help guide and resolve agricultural and rural development planning is essential.

Coastal Habitat Mapping

Author

Fiona Evans, Remote Sensing Applications Centre, Department of Land Administration (Leeuwin Centre For Earth Sensing Technology), 65 Brockway Road, Floreat, Western Australia, 6014.

Abstract

This application study involves two separate projects in two locations of Western Australia. One study area is Geographe Bay, in the south-west (33.3S, 115.3E), and the other is the Abrolhos and Montebello Islands, near Geraldton (28.5S, 114.4E).

In this study, ER Mapper has been applied to map coastal habitats because of its unique ability to process satellite data for nearshore habitat investigations. This information is useful for marine habitat protection and management, oil spill response and coastal management planning.

Introduction

Monitoring of our environment, is by necessity, presently being given a high profile. It has been realised that the use of leading-edge technology, where it can be shown to provide definitive information economically, will greatly increase the efficiency and effectiveness of projects. The length of the Western Australian (WA) coastline, is approximately 12,500km. The requirement for a conclusive study on marine habitats over a short period of time, necessitated the use of remotely sensed imagery in order to provide high quality information at the required scales.

Commonwealth Scientific Industry and Research Organisation (CSIRO), Division of Fisheries is undertaking a project to map the underwater features of the WA coastline at a scale of 1:250 000 with the support of the Western Australian Department of Transport. The study area of this project is located in Geographe Bay, in the south-west of Western Australia.

The final products from this project will be used by the Department of Environmental Protection (DEP), Department of Planning and Urban Development (DPUD), Local Government, Waterways Commission, Department of Transport, Conservation and Land Management (CALM), Western Australian Department of Agriculture (WADA), Department of Land Administration (DOLA) and the State Combat Committee.

The second project involves two study areas. They are located in the Abrolhos Islands, west of Geraldton, and Montebello Islands, north of Onslow, and are also in Western Australia.

The information obtained from the above projects will be used for marine habitat protection and management, oil spill response and coastal management planning.

Available imagery

A number of different sources of imagery were used to build up a picture of the area including aerial photography, scanned data and satellite imagery.

Aerial photography

There is, at present, a limited archive of aerial photography of the coastline of Western Australia with suitable specifications. Problems to date with the use of aerial photography for water coverage relate to having an appropriate sun angle, to reduce sunglint and thereby maximise water penetration, and to the prevailing weather conditions, as low wind currents are required. This is because low wind currents reduce surface scatter and produce low swell, thus reducing the concentration of suspended sediment. In addition to these problems, most of the photography is limited to land coverage, so often the inclusion of the sea at the end of flight lines is fortuitous.

Scanned data

Other imagery that is available for marine habitat mapping is provided by systems such as the Gascoyne MC Airborne Multispectral Scanner. The scanner allows the imagery to be flown under ideal weather conditions with high spatial resolution and multispectral capability in the visible, shortwave and thermal infrared. Scanner data are useful for mapping shallow waters and has been used in the Perth Metropolitan Coastal Waters Study. The Gascoyne scanner is limited in its coverage area by a field view of 900 metres and a flying height ranging from 1,000 to 10,000 metres, giving swath widths of 2-20 kms and a nominal spatial resolution of 2-20 metres.

Satellite imagery

Under ideal conditions, penetration of sea water by Landsat Thematic Mapper (TM), band 1, is superior to aerial photography. TM imagery was chosen, in part, for this project because of its cost advantage over aerial photography. Satellite data met all the specified base requirements of CSIRO for this project. TM data, which covers an area of 185km x 185km, have the advantage of being archived every 16 days since 1986, giving a vast choice of images from which to choose suitable cloud-free scenes.

After a search of the current archive of TM scenes, which are stored on microfiche at the Australian Centre for Remote Sensing (ACRES) and at the Remote Sensing Applications Centre, a scene containing bands 1, 2, 3 and 4 was selected for its clarity and penetration into water (wind, seas, tide). TM Bands 1, 2, 3 and 4 were used for the following reasons: Band 1 (blue band) can penetrate water to depths of 25 metres depending upon sun angle and water clarity; Band 2 (green band) is used to determine the turbidity component; Band 3 (red band) allows better delineation of the coastline; and Band 4 enhances both land and vegetation. The selected scene also showed features in water depths to 50 metres for the study area, a further requirement of the project.

Geographe Bay

Georectification and image enhancement

Georectification and image enhancement were required. The selected image was rectified to the Australian Map Grid (AMG) using a technique based on the selection of ground-control points which gave a root mean square (RMS) error of 1 pixel (25metres). The image was then enhanced using combination linear stretches to highlight bottom types such as reefs, seagrass, sand and rocks. Each enhancement was written to film on a Colorfire 240. Photographic prints were made at scales of 1:250 000 and 1:100 000.

Data integration

Field validation Trawl data has been used for this study. This data was collected during a Western Australian Fisheries Department survey in 1991 using a towed video system and Global Positioning System (GPS). The method is described in *Western Australian Fisheries- Bulletin No. 100*. The trawl data were gathered every 15 seconds and included latitude, longitude, time, date and substrate type. The latitudes and longitudes were converted to AMG co-ordinates, rasterized and merged with the TM data.

Bathymetry lines, supplied by the Western Australian Department of Transport, were digitised in ER Mapper file format, converted to DXF files then merged into the TM image. Files were converted to DXF files because they can be imported into a wide variety of image processing software.

Masking

The TM data were subsectioned using one of ER Mapper's *Regions* menu options. Both polygon and class type functions are available. Regions specified according to one or more polygons can be used to *mask* or block off part of an image.

In this case, the TM data were subsectioned to mask out the land using a level slice function. This function determines that digital numbers of less than a certain value represent water and that where greater than a certain value they represent land. This discriminating value will be different for each scene. This is used on band 4 because the water absorption properties of this band allows the interface between land and water to be separated. This permits the separate enhancement of the water using bands 3(R), 2(G) and 1(B).

The land was enhanced separately using bands 4(R), 3(G) and 2(B). The enhancement of this band combination suits delineation of the land-water interface, as well as showing terrestrial features.

Following the enhancement the two masked images were merged.

Image interpretation

The identification of the seagrass and other substrate types was done by a CSIRO marine biologist with local knowledge of the area. Polygons were hand drawn onto the image around features of similar tone, then labelled and digitised. These files were then archived for use in future projects such as the State Combat Committee's Oil Spill Response Group.

The Arolhos and Montebello islands

In another project centred on the Arolhos Islands, west of Geraldton, Western Australia (28.49S, 114.36E), and the Montebello Islands, north of Onslow, Western Australia (21.41S, 115.12E), thematic mapper imagery was used with SPOT panchromatic imagery.

How to merge images

The SPOT and Landsat TM data sets were merged to create an image that has the high resolution of the SPOT data, that is 10 metres, together with TM spectral qualities. The steps used to merge the two images were to:

- 1 Register SPOT to Transverse Mercator projection (Australian Map Grid).
- 2 Register the TM Band image to the SPOT panchromatic file.
- 3 Merge the data using a fusion algorithm from the 'Example_Data_Fusion' directory such as 'Sharpen_TM_with_Pan.alg'.

This algorithm merges three bands of the TM dataset displayed as Red, Green and Blue layers with the SPOT dataset displayed as an intensity layer. This is carried out instantly, without creating intermediate files.

Classification

Another method of identifying marine habitats includes the use of supervised and unsupervised classification techniques. However, the water column effect on the classification is apparent as the depth of water increases. This effect is caused by the absorption and scattering of light in the water which obscures the sea-floor reflectance variations.

In this situation low values are attributed to pixels defining features in deep water and higher values in shallow water for the same biological features. An algorithm to remove the water-column effects may need to be used to produce more accurate results.

An example of this problem was shown in an unsupervised classification routine of the Arolhos Island which identified approximately 20-25 classes. (Each group of islands in the Arolhos were classified separately due to changes in habitat). The depth of water around these islands is approximately 10 metres but there is still an effect from the water column. This was confirmed with field checking in an area where coral seen at 2 metres depth was of the same species as that at 8 metres. These groups were actually defined as different classes on the image using the classification routines.

Conclusion

The results achieved in the mapping of marine habitats around the Arolhos Islands, Montebello Islands and Geographe Bay, have verified that TM satellite imagery was the best source of data meeting the required specifications.

This application discusses a number of remotely sensed data that can be used for nearshore habitat mapping. It also suggests a number of routines such as supervised and unsupervised classifications that could be applied to the data to help determine the different marine habitats.

Thematic Mapper imagery was used in these projects because of the amount of coverage of a scene, the ability of band 1 to penetrate into the water to detect marine bottom types and the cost advantage over other systems for the large area of Geographe Bay. TM images also are archived every 16 days which allows for a larger selection of imagery.

ER Mapper allows the data to be manipulated in real time using steps that are easy to follow and understand. It has the ability to integrate vector and raster data with an easy to use graphical interface to produce enhanced products useful to all people.

Monitoring Environmental Change in Lake Turkana

The Use of Multi-temporal Satellite Imagery to Examine Environmental Change in Lake Turkana

Authors

James Cutler and **Justin Saunders**, Geographic Information Services Ltd. (GISL) PO Box 85, Egham, Surrey, TW20 8SE, UK.

Introduction

Environmentalists and hydrologists are chief among those who have accepted the river-basin as the fundamental unit in effective water resource management and planning. Regional planners acknowledge that an up-to-date knowledge of current farming systems, land tenure systems, water resource dynamics and planning strategies are integral to the evolution of sustainable agricultural programmes. That this point has been reached comes less from the political will than from the emergence of means by which change, especially degradation, in the whole environment can be recorded and reported. The improvement of data collection systems, the development of low-cost means of analysing and then disseminating the results could be deemed one of the early, if less public, benefits of the evolving information super-highway. That decision making can be at least in part determined by the presentation of previously remote and difficult to assimilate issues in terms of the stark reality that they represent is a triumph for the technology that makes it possible.

This technology revolves around remotely sensed data. Traditional aerial photography was supplemented, and may eventually be replaced in most forms, by the emergence into the public domain of satellite borne imaging systems in the early 1970s. Multi-spectral satellite imagery has been available from the Landsat series of satellites since 1972 at a spatial resolution of 80m and latterly from Landsat TM (since 1984) at a spatial resolution of 30m. One of the most important characteristics of these data sources is that the satellites cover exactly the same part of the Earth's surface at regular intervals (16-18 days in the case of Landsat).

Water resources, agricultural development and environmental change

From the Danube to the Mississippi and the Nile, trans-national water management bodies are being set up to try to ensure the fair and effective utilisation of water resources. In other basins (e.g. Tigris/Euphrates), negligence, political will and international stand-offs are combining to ensure uneven and destructive development. The Omo-Gibe catchment of south-west Ethiopia is a small but useful example illustrating the need for international cooperation and participation.

While no-one can argue that the major needs of the global population are food and water, there are many who forget, ignore or simply ride roughshod over the legitimate concerns of others to pitch short-term gain against long-term need, the powerful against the powerless and administrators and bureaucrats against the land users and guardians.

Water is perhaps the most important resource upon which future agricultural production depends. The hydrological cycle that charges the rivers, lakes and aquifers of any river basin feeds the soils, the trees and the crops. Sustainable agricultural production depends not only on the continuation of this cycle but on other characteristics that determine land

capability and land suitability. Micro-climatic factors, slope, soils, wildlife and farming systems can only be combined in a finite number of ways until their inter-relationships start to disintegrate. When this happens, the very sustainability of the system is called into question. There may be solutions but they are invariably short-term, consisting of chemicals and fertilisers and the dubious benefits of intensification. Soil erosion, water pollution, nutrient depletion and falling yields and incomes are all products of short-sighted development strategies.

However, until there is evidence it is frequently too late to pre-empt the development of agricultural systems that are, in the end, not sustainable. Thus, it is essential that case studies are produced and models evolved that enable the planner to cogently argue the case for more pragmatic development. Hard data on environmental change is notoriously difficult to obtain; proving the causal links is even harder. Hence the pressure on the monitoring and data collection systems to provide tangible evidence of change and to link it to changes in the use of the environmental and natural resources of the contributing regions.

Example: Erosion, Siltation and Lake Capacity

False colour image or Colordrape

The spectral resolution of Landsat satellite imagery allows the user to produce false colour composite images (FCCs) in ER Mapper using a Band 123 combination for MSS and Band 234 for TM. While the spatial resolutions do differ significantly, this is not a major disadvantage when evaluating trends and gross changes over time. The band combinations produce similarly coloured images for the same time of year.

Rectification

The next step is to ensure that both images are corrected to the national mapping series. This is easily done using the ER Mapper **Geocoding Wizard**; the user is prompted for map coordinates for ER Mapper to correct the imagery to the map sheets. In this case a nearest neighbour resampling algorithm was used to ensure DN value integrity.

Classification

A classification procedure was then adopted for each image. The objective of the analysis was to discriminate the water body from the surrounding land. Water has a very distinct spectral signature that enables easy discrimination; either of the infrared bands, which are completely reflected by water bodies, or the blue band, which allows for extended water penetration, can be used. In this case the infrared band in each FCC scene was used to

identify the extents of the water body. By combining a scattergram with the cursor values associated with **Cell Values Profile** Window (from the **View** menu) it was easy to identify the range of DN values associated with the water bodies.

With these values a simple classification algorithm was developed for the each image that created an effective “mask” or class for the lake. On the MSS scene this was coloured blue while on the TM scene this was coloured white. It was then a simple task to subtract the 1994 data from the 1973 data to gather a rough estimate of the change in the lake at the north end associated with the deposition of soil.

Image mosaicing and annotation

One of the unfortunate facts about the different generations of Landsat satellites is that their paths are very slightly different. This means that while the MSS scene covers the whole of the north end of the lake, the TM scene only covers about 90% of it, leaving out the Western edge. As an intermediate solution the MSS and the TM data were mosaiced and the two classifications overlain. ER Mapper’s annotation system was used to draw an approximation of the area to the west of the TM data that could be assumed (on the basis of all the other evidence) to have also become silted up. This was added to the 1994 data to give an improved statistic on environmental change.

Statistics

The approximate statistics extracted indicate that some 610 sq. km of lake have been lost as a result of soil deposited in the lake by the Omo-Gibe river system. It should be noted that this basin is about 77000 sq. km. Without some more precise bathymetric data it is not possible to estimate a total volume of silt but using simple figures (e.g. depth of new silt to an average depth of 5m), an erosion figure for the whole catchment of 20m³/ha/yr emerges!

Conclusion

When such data is coupled to parallel evidence in the dams and rivers of Northern Ethiopia and neighbouring Sudan, it is difficult to avoid the conclusion that there has been a dramatic change in the way in which land and water resources are being managed. Aware as we are of the recent history of drought, famine, warfare and widespread deforestation in this region it would be easy to describe the changes as self-inflicted. We are also aware that the soil rich and climatically rich Ethiopian highlands are both the heartland of much of modern international agriculture and their own mine of regeneration.

However, man-made environmental changes take many forms, from short-term expediency and necessity through political force (resettlement and trans-migration being significant factors in Ethiopian land and agricultural change) to long-term international transgressions of unrealised impact (atmospheric and oceanic in particular) and internationally imposed economic restructuring. It would be unwise for planners and decision makers in national

institutions and in donor agencies to plead political and economic expediency in the face of a wealth of data that, while not indicative of the proportionate role of causal factors, does provide solid evidence of the lasting and detrimental impact of poorly conceived and inadequately controlled agricultural development.

As more and more studies such as this preliminary investigation reveal the extent of environmental change and the associated decline in environmental (and human) condition so the role of satellite imagery, the function of ER Mapper and the role of the planner will be empowered by national and international organisations alike.

Monitoring the Gulf of Gdansk

Authors

Marek Graniczny, Director of the Department for Remote Sensing and Cartography, National Geological Institute (PIG), Warsaw, Poland.

Zbigniew Kowalski and **Michiel Zevenbergen**, Geodan Polska, GIS Consultants, Warsaw, Poland.

Background

The Baltic Sea is a unique water body characterised by extreme cold, slow circulation, extensive shallows and a narrow channel or channels to a more dynamic, conventional ocean regime. The countries that border the Baltic Sea have large coastal towns and, in some cases and more importantly, catastrophic industrial (and agricultural) legacies that have in themselves been the concern of environmentalists for some time.

Concern increased during the 1980s as the downstream impacts of smoke-stack industrial centres, large scale mono-cropping, intensive fertiliser use and acid rain deposition became increasingly self-evident (declining fish stocks, polluted beaches, red tides, deteriorating water quality) across the region culminating in the endorsement of the Helsinki Convention on sustainable use of the Baltic by Baltic Sea adjoining countries in 1990. With the collapse of the regimes of the former Eastern Europe and as concerns about the effects of

anthropogenic activities in changing nutrient runoff became more serious, a regional task force (HELCOMTF) was established. The members are all countries bordering the Baltic that have major rivers flowing into the sea and major multilateral financial institutions.

Poland, as one of the contracting parties, has pursued several programmes to monitor the flow of pollutants into the Baltic and to evolve adequate mitigation measures to reduce these outputs. This approach recognises that one cannot hope to manage impacts on a runoff-affected marine area without managing the man-induced exports to it from adjacent watersheds or to formulate land development programmes without considering potential impacts on ecologically and economically important downstream systems. It is in this context that the National Geological Institute in Poland (PIG) has carried out a pilot study to assess the use of satellite imagery to study the effects of pollution, sedimentation and algal growth in the Gulf of Gdansk caused mainly by the Vistula River.

Every year this river transports a heavy load of nutrients, nitrogen and phosphorus from a heavily urbanised and polluted hinterland that reaches as far as the coalfields of Silesia. This water (often carrying 4-5 times or more higher levels of nitrates and phosphates than in “undeveloped” outflow) mixes with the saline Baltic waters in the Gulf of Gdansk and eventually with the rest of the Southern Baltic Sea.

Bio-optical Algorithms

Traditionally, researchers and others collect marine-based measurements of sea-water variables at the same time as the satellite imagery is acquired. In this case there was no ground data coincident with the imagery, precluding supervised classification techniques from being used; therefore alternative techniques were evolved.

Bartolucci (1977) and Alföldi (1982) both suggest a non-linear relationship between reflectance and particles in suspension. The greatest discrimination in spectral response between clear and turbid waters occurs between 0.6-0.9 μm while the 0.51 μm to near-infrared bandwidth has several windows ideal for assessing phytoplankton related phenomena such as the near-surface concentration of chlorophyll-a pigments and ocean colour. Phytoplankton has a sunlight absorption peak in the blue band by virtue of its resident photosynthetic pigment, chlorophyll-a. The annual phytoplankton growth cycle (often peaking with algal bloom) depends on the effects of photosynthesis which are strongest in the summer months.

Image processing

Having acquired Landsat MSS and TM from the last 4 years, PIG have used ER Mapper for image processing. ER Mapper was considered particularly appropriate to the tasks in hand because of its algorithm module which allows the user to develop and edit in situ the complete description of the image processing tasks to be implemented. The study had to use formulae developed elsewhere; ER Mapper lets the user apply these very easily.

Principal Components Analysis (PCA)

ER Mapper simplifies this process in which data redundancy engendered by extensive interband correlation can be reduced. This transformation was performed on all Landsat MSS bands and the first 4 bands of the TM imagery. Subsequent multi-band enhancement and histogram equalisation created readily interpretable hardcopy.

Turbidity and Chlorophyll Concentration

The study used the formula developed by the REMONO project (REMOte sensing North Sea) in ER Mapper to assess turbidity in the Gulf of Gdansk:

$$Tu = -24.47 + (1.03 \times b1) - (1.65 \times b2) + (1.46 \times b3) + (0.30 \times b4)$$

Similarly, the following formula was used in ER Mapper to evaluate phytoplankton blooms:

$$Ch = -131.32 + (7.3 \times b1) - (13.91 \times b2) + (12.66 \times b3) - (3.63 \times b4)$$

where:

b1 = green (0.50-0.60mm)

b2 = blue (0.60-0.70mm)

b3 = reflective infrared (0.70-0.80mm)

b4 = reflective infrared (0.80-1.10mm)

These algorithms were applied to detect the sedimentation process and the intensity of algal growth. The thermal band from Landsat TM (10.40-12.50mm) was also incorporated at this stage because there is a strong correlation between sea surface temperature (SST) and phytoplankton blooms.

Comments

At the moment there is inadequate infrastructure and poor capacity to apply known methods to monitor the fast-deteriorating Baltic Sea marine environment. Remotely sensed data, marine based and laboratory measurements need to be integrated in a cost-effective way to provide a monitoring solution for the dynamic marine ecosystem of the Baltic. The potential role of satellite data could be seen in the images. In the MSS scene of 8 July, 1991 water masses from the Vistula were clearly visible as they moved east along the coast. The currents were clear because of the algal bloom synonymous at this time of year with the drift of warm water masses. In the same image the Russian port of Baltijsk could be identified as a possible major source of pollution. In the Landsat image, illustrating the utility of the Landsat TM thermal band for high temperature contrasts, significant temperature differentials were clearly visible in a 15km diameter from the mouth of the Vistula River.

The future

Several projects are about to start which will further enhance the knowledge and monitoring capabilities of the Gulf of Gdansk and for the whole Polish coastal zone. The focus of these programmes is an analysis of both currents and the sedimentation process, an applications sector that continues to evaluate the role of satellite imagery and for which intuitive image processing packages such as ER Mapper are very appropriate.

Boreal Forest Monitoring

Author

Kevin Corbley is a freelance writer and communications consultant in Aurora, Colorado, USA. He specializes in remote sensing and GIS technology.

Abstract

ER Mapper has been used to study lightning strikes and forest degradation in tundra-like regions with poor atmospheric conditions.

Locations

There are two study areas: one in the Yukon Flats, Alaska, where the lightning project is based; and the other in Anchorage at the Pacific Northwest Experiment Station, where boreal forest management is studied.

Introduction

Is lightning actually more likely to strike a second time in the same place? That's one of the theories USDA Forest Service researchers are investigating in Alaskan forests. The lightning strike project is part of a multiphase resource inventory program the Forest Service is conducting to develop improved methods of indentifying forest areas that are susceptible to, or have already undergone, catastrophic change.

Also, although Alaska and other northern regions are often characterized as barren tundra, many are actually covered with vast expanses of boreal or high-latitude forests. The conifers, aspens, birch and other species that comprise these forests survive in harsh yet delicately balanced ecosystems that are highly susceptible to forest fires, pollution and other more subtle environmental changes.

Lightning project

The lightning project is not nearly as far-fetched as it sounds. According to Ken Winterberger, a Forest Service remote sensing specialist and inventory forester, "Historical data indicates that previously burned forest areas receive more lightning strikes than non-burned areas. We are trying to determine if there is a cause-and-effect relationship."

The Alaska Fire Service maintains a network of 15 antennae sensors that record and locate lightning strikes across the state. When strikes are recorded in forested area during non-precipitation storm events, smoke spotting planes are dispatched to see if a blaze has been ignited and firefighters must be called in. That data is also being used in the study.

The foresters are testing the theory that burned areas promote the formation of clouds from which lightning bolts strike. The theory proposes that the charred areas left behind by forest fires appear dark and non-reflective. This dark surface is believed to heat the air above, creating the right conditions for cloud formation. Those built-up clouds could be the source of additional lightning bolts.

"What we are really concerned with in these projects is not the lightning itself, but the effects of the lightning," said Winterberger. "We are seeking new techniques to monitor catastrophic change that may assist in the management of northern forests."

Boreal forest project

The boreal forest research is being conducted by the Forestry Sciences Laboratory (FSL) in Anchorage, a field office of the Forest Service's Pacific Northwest Experiment Station. In recent years, the FSL has expanded its forest monitoring program to include applications of remote sensing and advanced spatial data analysis techniques.

In Alaska, the FSL often teams with forest land owners, environmental organizations and other groups with an interest in managing the forest's resources. The private sector groups usually assist in the projects as partners, offering funding or manpower. Because the ecosystem of high-latitude forests is so delicate and unique, the Forest Service often shares boreal forest information with other northern nations such as Canada, Norway, Sweden, Finland and Russia.

"We are trying to move our inventory program into the 21st century with image processing technology," said Winterberger. "Most of the organizations that use our inventory data would like it in digital form for analysis in geographic information systems."

Due to widespread application of digital data within the forest resource management community, and the Forest Service's plans to implement an agency-wide GIS, the FSL in Alaska has embarked on a pilot project to examine the capabilities of in-house image processing in their boreal forest projects.

"One of our goals is to create image analysis and processing algorithms tailored specifically to forest inventory applications," Winterberger said. "The algorithms developed here can be standardized, packaged and provided to researchers in other Forest Service labs or in other countries."

Customizing forestry applications

The Forest Service Laboratory in Alaska has equipped its facility with Sun Sparcstation workstations for all image processing and GIS projects. In choosing image processing software for the pilot study, the FSI determined that the ability to develop customized processing routines and to handle several types of digital data was a critical requirement.

"We selected ER Mapper software for image processing because its dynamic algorithm component allows the user to write custom programs in realtime and process several types of data as a virtual dataset," said Winterberger.

ER Mapper's algorithm-based design is a new image processing concept that enables the user to specify a sequence of formulas, filters or transformations for interactive application to raw datasets. Instead of being saved to an immediate data

file, the changes to the data are rendered directly on the display. The algorithm design reduces disk space and lets the user experiment with many processing functions in realtime on the workstation screen.

The FSL researchers are using the algorithm capability extensively in a joint project with the VN Sukachev Forest Institute in Moscow. Russian and U.S. foresters hope to develop new satellite image processing techniques capable of detecting catastrophic change in boreal forests and determining the degree of forest damage.

The project is taking place in the Norilsk area of north-central Siberia, the site of a major copper and iron smelting operation. Years of smelting have produced acid rain that has poured on the downwind forests for kilometers.

Russian scientists have collected extensive ground data, measuring the extent of tree damage in a 200-kilometer by 50 kilometer area downwind from the smelting operation. The pollution has spread downwind, causing varying degrees of tree damage. The most severe damage is located near the core with less destruction, or improved tree health, farther from the smelters.

The damage is well documented, and the degree of damage changes subtly away from the smelters," said Winterberger. "We are trying to see what image enhancement functions can detect the differences in spectral reflectance representing the variations in tree health."

The FSL has obtained several types of satellite data for the project including Landsat, AVHRR (Advanced Very High Resolution Radiometer) and Russian imagery. Researchers are experimenting with a variety of enhancement techniques to highlight the slight differences in spectral reflectance among various levels of forest damage. Promise has been shown using various edge enhancement filters.

"Using the algorithm component, we manipulate the image data right on the screen, applying filters, making adjustments and then running it again, all in realtime," said Winterberger. "It really speeds the development process."

To divide the Siberian trees into accurate classes based on their species and relative health, FSL uses a combination of unsupervised and supervised image classification techniques to improve the efficiency and accuracy of the classification process.

First, they choose subsets, or cluster blocks, of the larger image area that contain as much variation in cover types as they expect to find in the larger image. Usually the selected cluster blocks are areas where the cover types are well understood, such as areas previously imaged with aerial photography.

Next, they perform an ISODATA unsupervised classification on the cluster blocks which divides the smaller subset images into classes representing primary cover types or 'ecoregions'. Using the image data statistics for each ecoregion as training

classes, they then perform a supervised classification of the entire image area. This technique uses ISODATA to capture the primary cover type variation first, which is then used to refine the subsequent supervised classification of the satellite imagery.

Fusing, mosaicing, and virtual datasets

One of the problems the FSL faces in high-latitude projects is the lack of adequate data over many areas. The northern latitudes are frequently covered by clouds which thwart optical imaging sensors such as Landsat and SPOT. Data collection is further hindered by poor ground station coverage. Neither the Landsat nor SPOT station covers all of Alaska. Likewise, over Siberia where the joint U.S. Russian project is underway, downlink capability is poor because of a hole in coverage by TDRSS, the satellites that relay remote sensing data back to ground stations when the remote sensing satellite is not within range of the station.

“There are so many gaps in high-latitude imagery that we use whatever data we can lay our hands on... Landsat, SPOT, AVHRR, Russian and high-altitude photography,” Winterberger said. “Frequently, we have to use different datasets in the same classification project.”

To overcome this situation, FSL is making use of a new image processing technology called virtual datasets, which was introduced by Earth Resource Mapping in its 4.0 release of ER Mapper. Virtual dataset technology is an extension of the dynamic algorithm feature. It allows the user to access two or more separate datasets on disk as if they were a single dataset. The virtual dataset can be accessed for processing in realtime similar to the way algorithm functions are accessed without creating intermediate disk files.

The Forestry Sciences Laboratory has used the virtual datasets feature extensively for projects in Alaska and Russia where a combination of several types of image data was needed to create a complete image of cloudy or smoke covered areas so that visual analysis could be performed.

In those projects, the researchers combined all available imagery for a given area into one virtual dataset containing several different types of imagery, for example from Landsat and AVHRR, as well as multiple dates of the same type of imagery. By applying thresholding to the data or defining problem areas as polygon masks, cloud or smoke obscured pixels could be masked out and interactively filled with clear imagery of another type or different date for the same image area. By using virtual datasets, the researchers can work efficiently with the multiple datasets without having to merge them all into a single, very large disk file.

FSL is using a modification of the virtual dataset technique in the lightning study. The scientist are creating a virtual dataset of image data acquired by the Advanced Very High Resolution Radiometer (AVHRR) aboard a NOAA weather satellite, and the digitized lightning strike data recorded by the Alaska Fire Service antennae network.

In a pilot study in Yukon Flats in east-central Alaska, Winterberger's group has combined the two types of data to create a virtual data mosaic that is processed interactively. They are analyzing the virtual dataset to discover correlations between burned areas, revealed by the AVHRR thermal band, and lightning strike data recorded by the antennae network. The result is realtime composite display of the multiple datasets.

Implications

According to Winterberger, "The Forest Service doesn't make interpretations from information like the lightning project, but we supply the data to the forest land owners or environmental organizations so that they can develop appropriate management strategies."

The boreal lightning strike project and other forest management programs under way at the Forest Sciences Laboratory are also tied into a larger study - one of global proportion.

Some of the information being collected points to an increase in forest fires and a northern movement of the forests. Both could be related to the global warming scenario espoused by environmental scientists. Furthermore, according to Winterberger, Forest Service investigations into the delicate ecosystem balance of boreal forests may provide insight into this warming phenomenon.

The Forest Service has initiated a major program to equip each of its 150 forest offices in nine regions across the United States with advanced GIS and image processing capabilities. Many of the image processing techniques being developed for application in boreal forests by the FSL in Alaska will be standardized and used in forestry management programs throughout the National Forest system.

Conclusion

ER Mapper's flexible and realtime image data processing capabilities are well suited for integrating information that will help in boreal forest management. Its advanced technology not only makes the processing of more than one dataset possible as a single dataset, but its image enhancement capabilities are also useful when data is scarce owing to poor atmospheric conditions, helping interpretation. This was shown by the lightning strike and boreal forest applications.

SAR imagery in mineral and oil exploration

Authors

Frank Murphy and **Martin Critchley**, ERA-MAPTEC Ltd, 5, South Leinster Street, Dublin 2., Ireland.

Abstract

In this study ERS-1 Synthetic Aperture Radar (SAR) imagery was used in optically inaccessible areas such as those susceptible to cloud cover and thick vegetation.

Introduction

ERS-1 SAR (Synthetic Aperture Radar) provides a new and important remote sensing technique. It is particularly valuable for geological analysis in highly vegetated, cloud covered regions. The ability of SAR to penetrate clouds allows many of these regions to be studied on satellite imagery for the first time.

Many equatorial regions are the focus of current mineral and petroleum exploration interest. However, these areas are generally covered with rain forest and often have persistent cloud cover. For such areas cloud free optical satellite imagery, such as Landsat TM or SPOT is commonly unavailable. Consequently, the use of remote sensing techniques in these regions has been principally restricted to airborne radar. However, ERS-1 SAR now provides a highly cost effective means of undertaking regional analysis.

Characteristics of ERS-1 SAR imagery

The following features of ERS-1 SAR are important in mineral and petroleum exploration:

- ERS-1 SAR is very useful for geological analysis because its ability to penetrate clouds allows areas under persistent cloud cover to be studied on satellite imagery for the first time.
- Although SAR does not penetrate foliage to any great extent, the vegetation canopy frequently reflects variations of the surface topography, which may provide information on geological structure and stratigraphy.
- SAR also emphasizes subtle topographic variations which may be related to geological structures. Such features may not be obvious on vertical optical imagery.
- ERS-1 SAR has an advantage over airborne radar since it has a higher depression angle and consequently more information is obtained from the back slopes of mountains. On airborne radar the back slopes appear black and featureless.
- The depression angle of SAR highlights preferential erosion along faults, and consequently they appear more pronounced than on vertical optical imagery. The identification of faults and fault intersections is particularly important in mineral exploration.
- Intrusive bodies generally have a significantly different surface texture to the surrounding rock and thus tend to be emphasized on SAR imagery. These textural variations are also frequently reflected in the vegetation canopy. The identification of intrusives and their margins is of particular significance in mineral exploration.
- SAR images can also be used as base maps for logistical purposes in areas of persistent cloud cover which lack accurate topographic maps.
- ERS-1 SAR can also be used to obtain a base line landuse classification prior to exploration in remote regions. SAR image acquired during and after exploration can be used to determine if exploration has had any significant effect on the environment.
- Recent advances in SAR interferometry has enabled the generation of digital terrain models. This allows the construction of structure contour maps and calculation of fault displacement, for example, so has important implications for petroleum exploration.

We have recently undertaken two studies using ERS-1 SAR, one for oil exploration in Irian Jaya, the other for mineral exploration in Panama.

Panama case study

We were approached by a major mineral exploration company to undertake a regional structural analysis of western Panama. Much of the area is densely vegetated. Topographic maps are available; however, these show significant inaccuracies in the more remote areas, particularly in the shape and position of rivers and river junctions.

Satellite image availability and acquisition

The study area is covered by 3 Landsat TM scenes; however, no cloud free imagery was available. There was only one image in archive which did not have more than 30% cloud cover. This scene had 10% cloud cover in its northern quadrants, while its southern quadrants were cloud free. Cloud free SPOT imagery was unavailable.

It was decided that the best approach was to acquire the central TM scene which had the least cloud cover and three ERS-1 SAR scenes. These provided partial overlap with some of the cloudy areas on the Landsat TM, as well as coverage of the remainder of the study area.

ERS-1 SAR interpretation

The ERS-1 SAR provided a great deal of geological information which could be combined with the Landsat TM interpretation to produce a coherent structural synthesis for the area and enable the identification of exploration targets.

Correlation with Landsat TM

In the areas of overlap a useful correlation between the two forms of imagery could be made. In areas of sparse vegetation cover the geological structures identified were essentially similar, although there is a tendency for structures subperpendicular to the radar wave front to be less obvious on the SAR. However, a major advantage of the SAR over Landsat TM was found in the interpretation of the jungle covered areas. On the TM a number of widely spaced faults were identified, while considerable more structural detail could be distinguished in the same areas on the SAR.

Identification of fault zones

Fault zones could be identified on the SAR imagery. They are generally expressed as linear topographic lows, due to preferential erosion along the fault trace. Faults can also be identified by linear changes in surface texture, or by sudden linear elevation changes or breaks in slope. Some of the faults correspond to structures which had been previously mapped; however, a large number of previously unknown structures were also identified.

The depression angle of the SAR tends to emphasize the more subtle topographic features which often correspond to smaller scale faults. The identification of these enabled fault zones, composed of clusters of subparallel fault segment, to be mapped out.

It was possible to determine relative displacements on faults from their cross-cutting relationships and hence identify dilational zones along the fault trace. Such areas can be important for localizing mineralization. A large number of fault intersection zones could also be identified. Some of these may control mineralization and indeed many of the known mineral prospects in the region occur on, or close to, such intersections.

Identification of intrusive bodies

The main mineralizing event in Panama is associated with a phase of igneous activity. Consequently, many of the mineral deposits are closely associated with igneous intrusions. By using a combination of Landsat TM and SAR it was possible to identify a large number of intrusive bodies which in the right structural setting may be associated with mineralization.

In areas of good exposure the wide spectral range of Landsat TM is useful for discriminating intrusives from the surrounding rocks. However, since much of the study area is jungle covered the use of spectral properties was of limited value. By examining textural characteristics on the SAR it was possible to identify a large number of uniform texture. Intrusives can still be distinguished even where the area is densely vegetated by identifying subcircular areas with a more uniform vegetation canopy, a reflection of the surface topography.

Subcircular structures with topographically positive rims can also be distinguished and are interpreted to be extinct volcanic complexes.

Layover effect

A problem with all radar imagery is the layover effect which can become quite severe in rugged terrain. In Panama the terrain rises quite rapidly from the coastal lowlands to the Cordillera Central. In the mountainous west, the layover effect on the SAR is quite pronounced, but, because of the relatively high depression angle of the ERS-1 SAR compared to conventional airborne radar, it is possible to identify features on the backslopes.

Even where the layout is greatest on, or close to, the crest of the Cordillera Central, it is possible to trace fault zones across the mountain range.

Synthesis and exploration target generation

The large amount of data on fault zones and intrusives obtained from the interpretation of the ERS-1 SAR, together with data from the TM, allowed a coherent structural synthesis to be made. A chronology of deformation events was established on the basis of cross-cutting relationships between faults. The faults can be classified in terms of pre-mineralization and syn-mineralization structures. One of the most important results was the identification of a set of faults which were actively forming during igneous activity and which appear to localize many of the igneous intrusions. Fault zones in this orientation are also frequently associated with known mineralization.

The intersection zones between these faults and intrusive bodies represent areas of potential mineralization. The identification of such areas on the SAR allows a number of exploration targets to be generated.

On the basis of this interpretation the exploration company now has a geological framework on which to base their exploration program, as well as a number of targets to examine. In addition, the SAR images can be used as logistical base maps since they give a more realistic and accurate view of the terrain than existing topographic maps.

Irian Jaya case study

Irian Jaya has become the focus for petroleum exploration in recent years. The region is extremely remote, no detailed topographical maps are available and there is essentially no inland infrastructure. Much of the area is covered in dense rain forest. This poses a major logistic problem in petroleum exploration. The use of satellite imagery is an obvious technique to overcome this difficulty; however, the region is also associated with extensive and persistent cloud cover. Consequently, there is no cloud free optical satellite imagery available.

ERS-1 SAR provided the first opportunity for this area to be studied in detail using satellite imagery.

Satellite image availability and acquisition

We were requested by a petroleum exploration company to provide logistical base maps, geological and landuse interpretations from satellite imagery for an exploration concession in one of the more remote parts of Irian Jaya. ERS-1 SAR was the only form of imagery available which fulfilled the requirements. Six ERS-1 SAR scenes were required. A mosaic of these was produced. This gave the exploration company their first detailed overview of the terrain and provided them with an accurate base map which could be used for logistical purposes.

ERS-1 SAR interpretation

The study which is on going involves a number of phases:

Phase 1 involved the provision of an SAR mosaic with licence block boundaries, existing well locations and a UTM grid to act as a base map.

Phase 2 required a landuse/terrain classification using SAR within the licence block.

Phase 3 involves a geological interpretation of the SAR mosaic, and has yet to be completed.

Landuse/terrain classification

A landuse/terrain classification map was produced. This was partly to gauge agricultural activity and deforestation, as well as to provide an environmental base line before the onset of active exploration. By applying various filtering techniques the imagery was processed to highlight different landuse and terrain categories, principally in the basis of textural

features. It was not possible to directly define the nature of vegetation in each category, although plantations and areas of deforestation could be identified. Ground control is needed before the precise nature of each category can be established.

The terrain classification is important for logistical purposes, and provided an important aid in planning seismic surveys and drilling rig accessibility.

Geological interpretation

The SAR imagery enabled a geological analysis of this highly inaccessible region. By using textural characteristics it is possible to map out stratigraphic packages. In particular, areas of karstic limestone have a characteristic highly uneven, low lying surface. Interbedded sandstone /shale sequences can be distinguished by narrow resistant ridges alternating with more eroded bands. Using such criteria tentative stratigraphic correlations can be made, allowing a basic geological map to be produced which can be refined by the incorporation of ground data.

Major faults can be readily identified on the SAR. Some of these appear to be the bounding structures to downthrown blocks and their delineation is important in providing a preliminary assessment of the petroleum prospectivity of the area.

A fold and thrust belt was also identified. Gentle topographic domes seen on the SAR imagery are the surface expression of anticlines within the fold and thrust belt. The identification of these features is important since they are the most common form of petroleum trap. Even where the folds are very broad open structures, the side-looking nature of SAR emphasizes their topographic expression so they are more readily distinguished than would be possible from vertical optical imagery.

Planning of seismic surveys should take into account surface structures identified from image interpretation. Faults identified on the seismic profiles can be correlated with the fault surface traces identified on the imagery. This imposes constraints on the correlation of structures between adjacent seismic lines. Although this study is not yet complete the ERS-1 SAR has enabled analysis of landuse, nature of terrain, stratigraphy and structural geology. This could not have been possible using optical imagery. The exploration company will thus have a good logistical base map and a preliminary geological interpretation which can be refined by field verification.

Concluding points

- ERS-1 SAR has proved very useful for geological analysis in areas of persistent cloud cover. In many equatorial regions cloud free imagery is unavailable, and the ability of SAR to penetrate clouds allows these regions to be studied on satellite imagery for the first time.
- Regional geological studies can be undertaken using a mosaic of ERS-1 SAR images at a relatively low cost.
- The use of ERS-1 SAR imagery has been a valuable remote sensing technique for mineral exploration in Panama.

- It is particularly useful for geological analysis in densely vegetated areas.
- The Panama study has shown that fault zones tend to be emphasized by the SAR, even in areas of dense vegetation.
- Igneous intrusions can be recognized by textural contrasts on the SAR, which are often also reflected in the vegetation canopy. Such features in highly vegetated terrains tend to be less obvious on optical imagery.
- ERS-1 SAR is also of great benefit to petroleum exploration in equatorial regions, as seen in the Irian Jaya study.
- The imagery can provide a logistical base map in remote, poorly mapped areas which are characterized by persistent cloud cover. This can be used for planning seismic surveys or determining drilling rig accessibility.
- The identification of folds and fault blocks from the SAR can be used to provide a preliminary assessment of the petroleum prospectivity.
- The results of the Irian Jaya study indicate that there is great potential for the use of SAR for petroleum in areas of persistent cloud cover and dense vegetation.

Mapping Shelf Circulation

Mapping Shelf Circulation off Western Australia

Author

Alan Pearce, CSIRO Division of Oceanography, Marine Laboratories, PO Box 20, North Beach, Western Australia 6020 and **Heather Aquilina**, Earth Resource Mapping, Level 2, 87 Colin Street, West Perth, Western Australia 6005.

Synopsis

Thermal infrared satellite imagery is widely used to chart ocean currents by mapping sea-surface temperatures (SSTs) associated with different water bodies. The technique has been of particular value in monitoring the structure and behaviour of little-known ocean currents such as the Leeuwin Current off Western Australia.

Introduction

The Leeuwin Current is a stream of warm tropical water flowing southwards down the Western Australian coast (Cresswell and Golding 1980), completely different from the corresponding currents off the western coasts of southern Africa and South America, where cool currents flow northwards. Associated with the Benguela Current (South Africa) and the Humboldt Current (Peru/Chile) are seasonal ‘upwellings’ of nutrient-rich subsurface water onto the continental shelf, resulting in highly productive regions which support some of the world’s largest fisheries (Pearce 1991).

While its source is still unknown, it appears that the Leeuwin Current originates in equatorial regions north of Exmouth, but is also fed continually by surface waters of the south-eastern Indian Ocean flowing towards Australia (Godfrey and Ridgway 1985). On reaching Cape Leeuwin, it swings left and heads eastwards into (and sometimes across?) the Great Australian Bight. It flows most strongly during the autumn and winter months, and is responsible for transporting the larvae of many tropical marine organisms into southern waters (Maxwell and Cresswell 1981, Hutchins and Pearce 1994). It also seems to play an important role in recruitment to some Western Australian commercial fisheries such as the rock lobster, scallops and prawns in Shark Bay, and salmon and pilchards along the south coast (Lenanton et al. 1991, Pearce and Phillips 1994).

Satellite imagery has shown that the Leeuwin Current is a complex system of alongshore jets with periodic offshore meanders or waves which can carry the warm water over 200 km offshore (Legeckis and Cresswell 1981, Prata et al. 1986, Pearce and Griffiths 1991). Localised current speeds in these large meander-like features can exceed 1 m/s (2 knots), but average speeds are generally about half this. Surface temperature changes across the Leeuwin Current boundary off the west Australian coast are of order 1° to 2°C, but along the south coast (where the tropical waters meet Southern Ocean water) the SST differential can exceed 4°C.

Data

NOAA satellite imagery has been received and archived in Perth since late 1981 (Pearce 1989), giving us the longest time-series of NOAA images in Australia. Sea surface temperatures derived from the Advanced Very High Resolution Radiometer (AVHRR-2) on the NOAA satellites are used in this case study to map the circulation of the Leeuwin Current system, using a part scene of calibrated data supplied by Dr. I. Tapley (CSIRO Division of Exploration and Mining), prepared from source data courtesy of Curtin University. The orbit is NOAA7/17111 on 17 October 1984 covering an area off Western Australia from Shark Bay to Cape Leeuwin.

Each NOAA satellite passes over any particular part of the earth or ocean twice a day, and there are always two operational satellites, so any part of Western Australia is covered four times per day. However, thermal infrared radiation does not penetrate cloud, and so many passes cannot be used for ocean mapping—a severe limitation in southern waters during the winter months.

The AVHRR samples the earth's surface by scanning across the so-called swath of 2048 pixels of nominal (sub-satellite) size of 1.1 km. For each pixel, the radiance is sampled in 5 wavebands: one in the visible range, one on the near-infrared, one in mid-infrared, and two in the thermal infrared region of the electromagnetic spectrum. The visible and near-infrared bands are used for accurate land location and for cloud-screening, while the two thermal bands are used to derive the SST.

Algorithms

Sea-surface temperatures are derived from the raw radiance data sampled in the two thermal bands 4 and 5 by an essentially two-stage process:

- 1 The radiances for each pixel are converted to radiance (or brightness) temperatures by inverting the Planck function.

This step incorporates calibration data which is transmitted by the satellite and comprises the raw counts and temperature of an internal warm target within the satellite and the raw counts from space as a cold target. Because the radiant energy emitted by the earth's (or ocean) surface is partly absorbed by water vapour in the atmosphere, these brightness temperatures are generally lower than the true surface temperature and require a water vapour correction.

- 2 The correction is applied by using one of a number of algorithms.

These are generally of the form:

$$\text{SST} = a * T_4 + b * T_5 + c$$

where T_4 , T_5 are the brightness temperatures in AVHRR bands 4 and 5, and a , b and c are constants (which may include a zenith angle correction).

This may also be written:

$$\text{SST} = T_4 + A * (T_4 - T_5) + C,$$

showing that the brightness temperature T_4 is corrected by a difference factor proportional to $(T_4 - T_5)$ plus a constant.

A field study which compared satellite-derived SSTs (using a variety of algorithms) with in situ measurements from a boat off Perth indicated that an algorithm by McMillin and Crosby (1984) matched the surface data most satisfactorily; the bias was -0.14°C and the RMS difference about 0.55°C (Pearce et al. 1989). The McMillin and Crosby algorithm, which is now being routinely used for determining the SST in the Leeuwin Current region, has the form:

$$\text{SST} = 3.702 * T_4 - 2.702 * T_5 - 0.582$$

A second algorithm which gave similar results was that by Llewellyn-Jones et al. (1984):

$$\text{SST} = 3.908 * T_4 - 2.852 * T_5 - 2.058$$

(bias 0.19°C, RMS difference 0.62°C).

While dense clouds are generally quite obvious in satellite pictures, thin, scattered or sub-pixel cloud (i.e. clouds smaller than a pixel) can be very difficult to detect and yet can have a major effect on the SST. This is particularly important when digital data is extracted from a sequence of images to produce a time-series of SSTs for a specific area or when spatial or temporal averaging is carried out. A variety of cloud-screening techniques have been developed, all of which have some limitations; possibly the simplest involves flagging as cloudy all pixels whose radiance exceeds pre-set (or sometimes dynamically-derived) threshold limits in all five AVHRR radiometric bands or combinations of bands (Saunders and Kriebel 1988).

Data processing

The AVHRR_Leeuwin dataset used here was supplied calibrated. The calibration would have been accomplished by applying a non-linear correction to Band 4: 10.8 um and Band 5: 12.0 um (Prata 1985).

The data was viewed a number of ways to display and emphasise the Leeuwin current.

Gaussian transform

The Leeuwin_Current_Gaussian algorithm displays a Pseudocolor image of the calibrated data. In this algorithm the input values have been inverted using the ER Mapper Formula:

-INPUT1

to display high values as red and low values as blue/green.

A Gaussian Equalize post-formula transform was applied to enhance the ocean off the Western Australian coast, showing the warmer water of the Leeuwin Current.

Conversion of digital counts to brightness temperature

Although ER Mapper can easily display the oceanic currents off Western Australia, this is not sufficient for most climatological and biological/fishery applications where relative temperature gradients and absolute temperature are required.

Given two calibration points a linear calibration can be obtained which converts digital counts into radiance values. The conversion of the radiance values into brightness temperatures is done by inverting the Planck function.

The radiance corresponding to channel number i for a given brightness temperature is:

$$R_i = \int_{\nu_i} B[\nu_i, T] F(\nu_i) d\nu$$

where:

R_i is the radiance measured by channel i

B is the Planck function

V_i is the wavenumber for channel i

T is the brightness temperature

$F(v)_i$ is the spectral response function for channel i (discrete spectral response plot is available from NOAA)

Because the Planck function containing the brightness temperature is embedded within the integral, a transform and lookup table is normally created for a given wavenumber over a range of brightness temperatures. Brightness temperature values are derived by interpolating between points in the look-up tables.

The pre-formula transforms for Band 4:10.4 μm and Band 5:12.0 μm were derived from a 'counts-to-temperature' table for NOAA-7 provided by NOAA/NESS. The provided tables show a radiance and temperature value for Band 4 and Band 5 every second digital count.

A series of manual calculations were carried out to scale the digital counts and brightness temperature values between 0 and 1 for input into the ER Mapper algorithm file.

Digital Count	Scaled Digital Count	Channel 4		Channel 5	
		Temperature K	Temperature Scaled K	Temperature K	Temperature Scaled K
0		323.22		326.64	
2	0.002096	323.06	0.998916	326.46	0.998866
314	0.329140	296.03	0.815711	296.47	0.809905
328	0.343816	294.67	0.806493	294.96	0.800391
346	0.362683	292.89	0.794429	293.01	0.788104
362	0.379455	291.28	0.783516	291.24	0.776952
378	0.396226	289.65	0.772468	289.45	0.765673

This user-defined look-up table was then entered into the algorithm file using a text editor. Part of the algorithm file defining the transform is shown below.

```

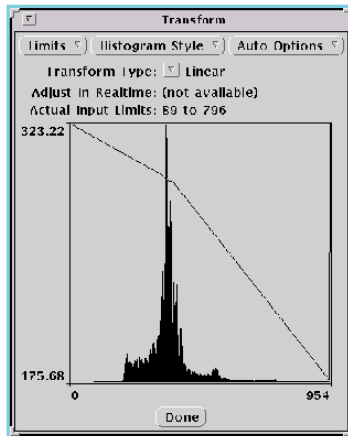
StreamInput Begin
  StreamInputID = 1
  Transform Begin
    Type = Linear
    MinimumInputValue = 0
    MaximumInputValue = 954
    MinimumOutputValue = 175.68000000000001
    MaximumOutputValue = 323.22000000000003
    LinearDef Begin
      NumberOfPoints = 8
      Points = {
        0.000000 0.000000
        0.002096 0.998916
        0.329140 0.815711
        0.343816 0.806493
        0.370748 0.782313
        0.396226 0.772468
        0.997904 0.010099
        1.000000 1.000000
      }
    LinearDef End
    DoInRealtime = No
  Transform End
StreamInput End
StreamInput Begin
  StreamInputID = 2
  Transform Begin
    Type = Linear
    MinimumInputValue = 0
    MaximumInputValue = 954
    MinimumOutputValue = 167.93000000000001
    MaximumOutputValue = 326.63999999999999
    LinearDef Begin
      NumberOfPoints = 9
      Points = {
        0.000000 0.000000
        0.002096 0.998866
        0.329140 0.809905
        0.343816 0.800391
        0.362683 0.788104
        0.379455 0.776952
        0.396226 0.765673
        0.997904 0.009892
        1.000000 1.000000
      }
    LinearDef End
    DoInRealtime = No
  Transform End
StreamInput End

```

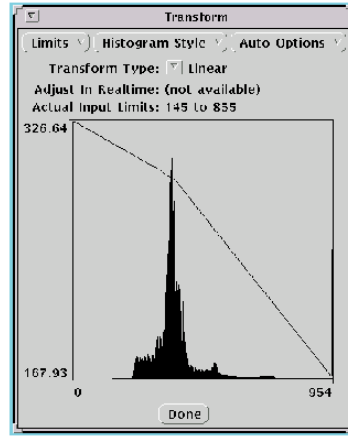
From these x and y values ER Mapper automatically derived a transform line, to convert the digital counts to brightness temperatures.

Once brightness temperatures for bands 3, 4, and 5 are derived, various algebraic combinations of these bands in fixed algorithms are used to derive SST.

Band 4



Band 5



Sea-surface temperatures using McMillan and Crosby (1984) formula

In this case the sea-surface temperature was derived using the algebraic expression proposed by McMillan and Crosby (1984):

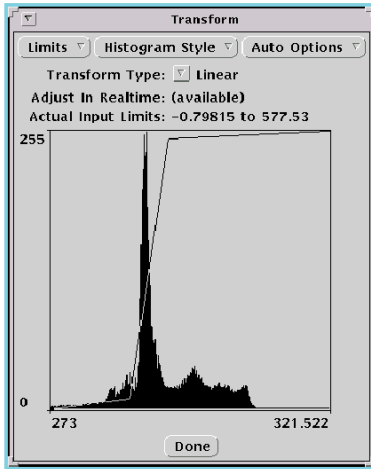
$$\text{SST} = -0.582 + (3.702 * B4) + (-2.702 * B5)$$

This is typed into the ER Mapper formula window as:

$$-0.582 + (3.702 * \text{INPUT1}) + (-2.702 * \text{INPUT2})$$

where INPUT1 is band 4 and INPUT2 is band 5.

The image was displayed using a 'rainbow' color look-up table and enhanced using a post-formula linear transform. The transformation was clipped by typing in a minimum input limit of 273K.



Sea-surface temperatures using the Llewellyn-Jones et al. (1984) formula

A second algorithm determined the Sea-surface temperatures using the algebraic expression proposed by Llewellyn-Jones et al. (1984):

$$SST = -2.058 + (3.908 * B4) + (-2.852 * B5)$$

This is typed into the ER Mapper formula window as:

$$-2.058 + (3.908 * INPUT1) + (-2.852 * INPUT2)$$

where INPUT1 is band 4 and INPUT2 is band 5.

The displayed image was again enhanced using a post-formula linear transform and 'rainbow' color look-up table.

3 x 3 pixel smoothing kernel to reduce the noise generated by the temperature-correction algorithm.

To reduce the noise generated by the temperature-correction algorithm a 3 x 3 smoothing filter was applied.

References

- Cresswell, G.R. and T.J. Golding (1980). 'Observations of a south-flowing current in the southeastern Indian Ocean,' *Deep-Sea Research* 27: 449-466.
- Godfrey, J.S. and K.R. Ridgway (1985). 'The large-scale environment of the poleward-flowing Leeuwin Current, Western Australia: longshore steric height gradients, wind stresses and geostrophic flow,' *Journal of Physical Oceanography* 15:481-495.
- Hutchins, J.B. and A.F. Pearce (1994). 'Influence of the Leeuwin Current on recruitment of tropical reef fishes at Rottnest Island, Western Australia,' *Bulletin of Marine Science* 54, 245-255.
- Legeckis, R. and G.R. Cresswell (1981). 'Satellite observations of sea-surface temperature fronts off the coast of western and southern Australia,' *Deep-Sea Research* 28: 297-306.
- Lenanton, R.C., L. Joll, J. Penn and K. Jones (1991). 'The influence of the Leeuwin Current on coastal fisheries of Western Australia,' Proceedings of the Leeuwin Current Symposium, Perth, 16 March 1991; *Journal of the Royal Society of Western Australia* 74, 101-114.
- Llewellyn-Jones, D.T., P.J. Minnett, R.W. Saunders and A.M. Zavody (1984). 'Satellite multichannel infrared measurements of sea-surface temperature of the N.E. Atlantic Ocean using AVHRR/2,' *Quarterly Journal of the Royal Meteorological Society* 110, 613-631.
- Maxwell, J.G.H. and G.R. Cresswell (1981). 'Dispersal of tropical marine fauna to the Great Australian Bight by the Leeuwin Current,' *Australian Journal of Marine and Freshwater Research* 32, 493-500.
- McMillin, L.M. and D.S. Crosby (1984). 'Theory and validation of the multiple window sea surface temperature technique,' *Journal of Geophysical Research* 89, 3655-3661.
- Pearce, A.F. (1989) 'A catalogue of NOAA/AVHRR satellite imagery received in Perth, Western Australia, 1981-87'. *CSIRO Marine Laboratories Report* 203, 36p.
- Pearce, A.F., A.J. Prata & C.R. Manning (1989). 'Comparison of NOAA/AVHRR-2 sea-surface temperatures with surface measurements in coastal waters.' *International Journal of Remote Sensing* 10(1), 37-52.
- Pearce, A.F. (1991). 'Eastern boundary currents of the southern hemisphere. Proceedings of the Leeuwin Current Symposium, Perth, 16 March 1991,' *Journal of the Royal Society of Western Australia* 74, 35-45.
- Pearce, A.F. and R.W. Griffiths (1991). 'The mesoscale structure of the Leeuwin Current: a comparison of laboratory model and satellite images,' *Journal of Geophysical Research* 96(C9), 16739-16757.
- Pearce, A.F. and B.F. Phillips (1994). 'Oceanic processes, puerulus settlement and recruitment of the western rock lobster *Panulirus cygnus*,' In Sammarco, P.W. & M.L. Heron (editors): *The bio-physics of marine larval dispersal. American Geophysical Union, Coastal and Estuarine Studies* 45, Washington DC., 279-303.

Prata, A.J., Pearce, A.F., Wells, J.B., and Carrier, J.M., 1986, 'Satellite sea surface temperature measurements of the Leeuwin Current,' *Proceedings of the First Australian AVHRR Conference held in Perth, Western Australia, on 22-24 October 1986*, Perth: CSIRO Division of Groundwater Research, pp 237-247.

Saunders, R.W. and K.T. Kriebel (1988). 'An improved method for detecting clear sky and cloudy radiances from AVHRR data,' *International Journal of Remote Sensing* 9, 123-150.

**Part Three -
*Oil and Gas***

Oil and gas

This section discusses the following issues related to using ER Mapper for Oil and Gas applications.

- General ER Mapper setup issues
- Getting seismic horizons into ER Mapper
- Getting geological and cultural vector data into ER Mapper
- Updating geological and cultural vector data within ER Mapper
- Moving updated vector data back to other products
- Generating hardcopy prints

The information in this section is not confined to ER Mapper but also covers issues with related software that is commonly used in conjunction with ER Mapper in the Oil and Gas industry.

ER Mapper for Unix required

In the oil and gas industry most users of ER Mapper use the Unix version rather than the PC version. This is because it is used with companion software products which are only available on the Unix platform. Thus most of the imports and dynamic links used for exchanging data are only available with the Unix version of ER Mapper. In particular, ER Mapper makes use of the Geoquest Geonet data exchange utility, a major tool for data sharing data with Schlumberger and Geoquest products. Since these products are strictly available on the Unix platform, the imports can not be included for the PC platform.

Note: All ER Mapper versions after 5.5A are only for PC platforms running Microsoft Windows.

Schlumberger Geoquest and Landmark imports

Here is a list of the various import utilities and their location on the Utilities menu for Schlumberger/Geoquest and Landmark products. For more information on these imports please see the relevant chapters in this section.

Schlumberger/Geoquest

Mapview	Import Schlumberger Formats/GeoQuest (IESX) MapView
GeoQuest (IESX) ASCII Grid Dump	Import Schlumberger Formats/GeoQuest (IESX) ASCII Grid Dump Geoshare half link

Landmark Raster

SeisWorks Horizons	Import Landmark Formats/ SeisWorks 3D Horizons
SeisWorks Seismic (3DVI)	Import Landmark Formats/SeisWorks 3D Seismic
Zycor Binary Grid from MFD	Import Landmark Formats/Zycor Grid from MFD
Zycor ASCII Grid	Import Landmark Formats/ Zycor ASCII Grid

Landmark Vector

OpenWorks 3.1 Wells	Import Landmark Formats/OpenWorks 3.1 Wells
Seisworks Fault Polygons	Import Landmark Formats/ SeisWorks Fault Polygons
Seisworks Manual Contours	Import Landmark Formats/SeisWorks Manual Contours
Zmap ZGF	Import Landmark Formats/Zycor Graphics File

Landmark Color Lookup Table

SeisWorks CLM to LUT	Import Landmark Formats/SeisWorks CLM to ER Mapper LUT
----------------------	--

Importing seismic data

ER Mapper is often used to enhance seismic data to highlight structure and to integrate seismic horizon data with other types of data, such as bathymetry, gravity and magnetics data. ER Mapper processes two-way-time horizons, as well as vertical slices through 3D seismic cubes. This chapter deals with ingesting seismic raster grid data into ER Mapper for enhancement and interpretation.

Seismic raster grid formats supported

Seismic data is generally stored in seismic workstation software formats such as SeisWorks or IESX, and loaded into ER Mapper as needed.

ER Mapper has a number of data exchange utilities designed to import seismic data from seismic workstation software. Many of these import routines retrieve data directly from the seismic product. However, for them to run successfully they need to have been set up first.

When importing data from Seismic workstations, there are a number of formats or exchange utilities that can be used. The main ones are listed below. Only raster horizon formats are listed here: vector formats are discussed in a following section.

Note: Many data exchange utilities and printing require some set up and configuration to be carried out first before they will run successfully.

The imports are available as options on the **Utilities** menu. Further, they can be run as stand alone programs in an ER Mapper terminal window. Thus, they can be included in a batch script. To open an ER Mapper terminal window select the **Utilities** menu **User Menu/Open Terminal Window** option. For information on available switches for a particular import type “*importname -h*”

Raster file import utilities

The following table lists ways to import seismic data using import programs from common file formats. Generally, these require less setup and configuration, but are not as powerful as the direct exchange utilities listed in the next section, which directly read seismic data from external software products. Only the specific formats commonly used for seismic data are listed here; ER Mapper also supports data imported from over 100 other formats.

Format options in ER Mapper	Description
SEG-Y NON IBM Disk File SEG-Y IBM Disk File	An ASCII exchange format, it is one of the simplest and most common data formats for exchanging seismic data. Most seismic products can create SEG-Y data files. However SEG-Y is not the preferred method for importing data because you must create an intermediate SEG-Y file to transfer from the seismic software to ER Mapper, and SEG-Y files tend to be very large. Also, because the format is so simple, some of the information may be lost.
Zycor ASCII Grid	A simple ASCII format that Zycor gridding software outputs.
GeoQuest IESX ASCII grid dump	An ASCII format that can be output by GeoQuest IESX.
GeoQuest (IESX) MapView ASCII grid	This is a native IESX MapView format. It can be directly imported into ER Mapper.

Format options in ER Mapper	Description
Charisma 2D XYZ Grid	A 2D ASCII grid format that Charisma can output.
Charisma 3D Inline Xline XYZ ASCII grid	A 3D ASCII grid format that Charisma can output.

SEG-Y

SEG-Y is a simple and common ASCII format used to exchange seismic data.

To import a SEG-Y tape

- 1 Select the **SEG-Y IBM Disk File** option from the **Utilities/Import Landmark formats** menu.
- 2 Specify the input device, for example:
/dev/nrst0
- 3 Specify the output ER Mapper dataset to create.

An IEEE 4 byte floating point ER Mapper Raster dataset will be created from the SEG-Y input tape.

Command line

```
importsegy inputpath/file outputpath/file.ers
```

Configuration and setup

There are no special configuration requirements; however, the following issues should be noted when importing SEG-Y data:

- The only data format tested has been type 1 (4 byte IBM floating point).
- Type 2 (4 byte fixed point) has been implemented but not tested.
- Type 3 (2 byte fixed point) and type 4 (4 byte fixed point with gain code) have not been implemented—you can not import SEG-Y data in these formats.
- As SEG-Y contains no map projection/datum details, the default of RAW/RAW projection/datum is set, unless you override this during the import, by manually specifying a map projection and datum. Note, however, that you will still need to modify the imported data file to specify an origin point and cell size, after importing, in order to fully define projection details.

- Because the headers don't contain any information on the number of traces on a tape, it is not possible to give a % complete status during this import.

Input data format

A SEG-Y tape contains a single file consisting of:

- a 3200 byte EBCDIC Job Identification header record
- a 400 byte binary File Identification record containing details of the file layout and data formats
- a number of trace records containing a trace header and trace data.

The EBCDIC header is converted to ASCII and copied to the ER Mapper dataset. The File Identification record is also copied to the head of the ER Mapper dataset. The trace headers are discarded.

Zycor ASCII grid

The Zycor ASCII file format is a raster format produced by the Zycor Z-Map Plus gridding package.

To import Zycor ASCII grids

- 1 Specify the source tape or input data file name, for example: `/usr/data/grid.dat`
- 2 Specify the output ER Mapper dataset to create.
An IEEE 4 byte floating point ER Mapper raster dataset will be created from the Zycor input file.

Command Line

```
importzmap_ascii_grid inputpath/file outputpath/  
file.ers
```

Configuration and setup

There are no special configuration requirements; however, the following issues should be noted when import Zycor ASCII grid data:

- The Zycor Grid Exchange Format does not have a specific field for the type of geophysical data contained in the file. The import program puts the text "Band 1" in for the band description. You may want to edit the .ers header file to put in a more meaningful description.

- The default of RAW/RAW projection/datum is set, unless you override this during the import, by manually specifying a map projection and datum.

Input data format

An example of the first few lines of the ASCII Zycor Grid Exchange format file is

```
! ZIMS FILE NAME: WESTEX SEISMIC GRID
! FORMATTED FILE CREATION DATE: FEB 24 92
! FORMATTED FILE CREATION TIME: 11:57
!
@WESTEX SEISMIC GRID HEADER , GRID, 5
15, 99999.00 , , 7, 1
23, 23, 0. , 55000.00 , 0. , 55000.00
38890.87 , 0. , 0.
@
+ RADIUS= 38891. INITGRIDMOD= 1 POSTGRIDMOD= 1 REGRIDMOD= 0 NUMPTS=
95
+ MINPTS/NODE= 1 OPT PTS/NODE= 4 MINSECT= 1 EXTEND= 38890.87
+ ISOCOM= 2.0 REFNS= 1 NO.PASSES= 10 CUTOFF= 0.2 SMOMOD= 0.2
-7135.546 -7185.889 -7236.498 -7287.622 -7338.023
-7385.425 -7426.534 -7457.695 -7477.753 -7490.585
...
```

GeoQuest (IESX) ASCII grid dump

This program reads ASCII data dumps from certain GeoQuest or IESX products.

Usage

Supply the data dump filename, and the name of the ER Mapper dataset in which you want the data to be stored.

You may also choose to subset the lines in the import.

Command Line

```
importgeoquest inputpath/file outputpath/file.ers
```

Configuration and setup

There are no specific setup requirements but the following must be considered:

- This import is designed to read space or newline separated ASCII digits, which may be dumped from Geoquest products.

- As GeoQuest ASCII grid dump contains no map projection/datum details, the default of RAW/RAW projection/datum is set, unless you override this during the import, by manually specifying a map projection and datum. Note, however, that you will still need to modify the imported data file to specify an origin point and cell size, after importing, in order to fully define projection details.

Input data format

The ASCII dump contains a header of the format

```
some_text number number number_of _cells number_of_lines
```

followed by floating point values.

Note: There are several GeoQuest products. This import is designed to read space or newline separated ASCII digits, which may be dumped from geoquest products.

Charisma 2D XYZ ASCII grid

This import reads an ASCII Charisma XYZ Grid File and constructs an ER Mapper raster file.

Usage

You must specify the input file name, for example: `/usr/data/grid.dat` and the output ER Mapper dataset to create.

An IEEE 4 byte floating point ER Mapper Raster dataset will be created from the Charisma XYZ input file.

Command Line

```
importcharisma inputpath/file outputpath/file.ers
```

Configuration and setup

There are no specific setup requirements but the following must be considered:

- The basic format for Charisma is X-position, Y-position, data value, so the cell size and origin point information are carried across during the import but the datum and projection will default to RAW/RAW unless a datum and projection are specified during import.

- The data must be on a REGULAR grid. That is, spacing between adjacent data points must be constant in the X-direction, and constant in the Y-direction.
- The Charisma XYZ Grid Format does not have a specific field for the type of geophysical data contained in the file. The import program inserts the text “Band 1” in for the band description. You may want to edit the .ers header file to put in a more meaningful description.

Import data format

The ASCII Charisma XYZ format contains lines with X-position (Easting), followed by Y-position (or Northing), followed by the data value at that point. After this are row and column indicators.

An example of the first few lines of such a file is:

```
361478.5 6245581.0 858 ROW 14 COL 88
361478.5 6245689.0 859 ROW 15 COL 88
361611.0 6245689.0 859 ROW 15 COL 89
```

Charisma 3D Inline Xline XYZ ASCII grid

This import reads a Charisma ASCII Inline Xline XYZ Format file produced from Charisma V3.7+ Gridload utility.

The import makes use of a configuration file to setup site specific default values, such as the rotation. The configuration file \$ERMAPPER/config/char3d.cfg can be edited using any text editor or you can update the file while running the import.

To run the Charisma 3D Inline Xline XYZ ASCII grid utility from the menu

- 1 From the **Utilities/Import Schlumberger formats** menu, select the **Charisma 3D Inline Xline XYZ ASCII grid** option
- 2 Specify the **Import File/Device Name**, for example:
`/usr/data/grid.dat`

The input file must be a disk file: the import cannot be run direct from a file on tape. This is because the program does a pass through the input file to ascertain extents and cell size information.

- 3 Click the **Output Dataset Name** file chooser button and specify the output ER Mapper dataset to create.
- 4 Click **OK** to start the import.
- 5 You will be prompted to enter the following:

- **The Easting/Northing units in the input file.**
This can be 'M' for 'Meters' or 'D' for 'Decimeters'. The origin values will be converted.
- **The Charisma Orientation code**
The Charisma specific code in the range 0 to 7 that specifies the origin and whether the input dataset inline is vertical or horizontal
- **The Rotation (Charisma V3.7)**
This is the rotation angle in seconds between the North-arrow and the vertical axis of the survey as specified in the Charisma project dump information.

Caution: Rotation is converted from Charisma to ER Mapper using:
ER Mapper rotation = (360 - Char_rotation/3600)
This is based on the rotation in seconds given in the Charisma project dump for *****charisma Version 3.7*****. Earlier versions of Charisma may calculate rotation from the first INLINE (row) to either the X or Y axis. This is untested and may be incorrect.

- **The INLINE or ROW and XLINE or COLUMN spacing**
These are found in the Charisma project dump information and should be entered as meters. The Import will convert the spacings to ER Mapper format depending on the orientation code, and row and line increments.
 - **The Row and Column increment**
The Inline/Xline increment can be found in the project dump.
- 6 If you enter any values to the above prompts you will be asked if you want to save the values you entered as the default values.
- An IEEE 4 byte floating point ER Mapper Raster dataset will be created from the XYZ input file.

Command Line

```
importcharisma3d -C $ERMAPPER/config/char3d.cfg  
inputpath/file outputpath/file.ers
```

The import program will prompt you for the information listed in the procedure above, and give a default choice.

Note: You must include the -C switch.

Configuration and setup

- The data file can include comments, either as comment lines or as trailing comments after data values. If a line does not have an inline as the first non-blank character, then that line is just ignored.
- The data must be on a regular grid. That is, spacing between adjacent data points must be constant in the X-direction, and constant in the Y-direction.

Note: This program **will not** grid irregularly spaced data. Use ER Mapper's Gridding Wizard if you want to do this.

- The data can be in fixed format or free format but it must contain the keywords and data specified above.
- The null cell value can be specified in the char3d.cfg config file and is used by the import, but the import will not prompt for this value.
- The XYZ format does not have a specific field for the type of geophysical data contained in the file. The import program puts the text "Band 1" in for the band description. You may want to edit the .ers header file to put in a more meaningful description.

Caution: The values specified in the configuration file are critical to the success of the import. The values vary depending on the project so it is important that you don't just accept the defaults. The values to use can be found in the Charisma Project Dump information. It is helpful to save the new values if you have a number of projects with the same parameters. If imported datasets fail to register correctly check the dataset header to make sure that the origin easting/northing values are specified in meters and the cell size is correctly specified in meters. Ensure that the rotation values are correct.

Input data format

An example of the first few lines of the ASCII input file is:

```

INLINE :20 XLINE :1 626458.70000 5756838.00000 156.92996
INLINE :20 XLINE :2 626482.65000 5756845.20000 156.88675
INLINE :20 XLINE :3 626506.60000 5756852.40000 156.87457
INLINE :20 XLINE :4 626530.55000 5756859.60000 156.82094
INLINE :20 XLINE :5 626554.50000 5756866.80000 156.73541

```

The basic format is:

INLINE : row_position XLINE : column_position X-position Y-position value

where,

- X-position is the easting in meters or decimeters
- Y-position is the northing in meters or decimeters
- value is the data value at that point

The Charisma configuration file

The format of the \$ERMAPPER/config/char3d.cfg file is:

```
#####  
# # This is the configuration file for the importcharisma3d  
# # default values.  
# #  
# # This file can be edited with any text editor. The only  
# # rules are that the names appear as below and have one  
# # space separating the name from the value. # # #  
#####  
INPUT_FILE /path/filename.xyz  
OUTPUT_FILE /path/filename.ers  
PROJECTION LOCAL  
DATUM WGS84  
UNITS decimeters  
ORIENTATION_CODE 6  
ROTATION 1182437.000000  
INLINE_INTERVAL 25.000000  
XLINE_INTERVAL 6.670000  
INLINE_INCREMENT 1  
XLINE_INCREMENT 1  
NULL_CELL_VALUE -999999.000000
```

GeoQuest (IESX) MapView ASCII Grid

This import reads a GeoQuest (IESX) MapView ASCII data file and constructs an ER Mapper raster file.

This import should be used in preference to the ASCII text dump import if possible as it will convert more information.

To import a GeoQuest (IESX) MapView file

- 1 Start the import by selecting the **GeoQuest (IESX) MapView** option from the **Utilities/Import Schlumberger formats** menu or by typing `Importmapview` in a terminal window.
- 2 Specify the input file name, for example:

```
/usr/data/grid.dat
```

- 3 Specify the output ER Mapper dataset to create.
- 4 Click **OK** to start the import.

An IEEE 4 byte floating point ER Mapper raster dataset will be created from the MapView input file.

Note: As GeoQuest (IESX) MapView Grid contains no map projection/datum details, the default of RAW/RAW projection/datum is set unless you override it during the import by manually specifying a map projection and datum.

Command line

```
importmapview inputpath/file outputpath/file.ers
```

Input data format

An example of the first few lines of such a file is:

```
B 1 0      8      8  0.1250000E+02  0.1250000E+02
0.4310028E+06  0.4310918E+06  0.6355005E+07  0.6355094E+07
431002.83386516355006.6749957 1.000
TOP CHALKAP1          - 3D pick
-0.3261754E+04 -0.3245083E+04 -0.3261081E+04 -0.3260774E+04 -
0.3260717E+04 -0.3260975E+04 -0.3246495E+04 -0.3246358E+04
-0.3261800E+04 -0.3244692E+04 -0.3261257E+04 -0.3260807E+04 -
0.3260537E+04 -0.3260868E+04 -0.3245658E+04 -0.3245172E+04
```

Generic issues related to importing raster grid data

Updating header files with projection/datum details

In several of the imports it is necessary to specify the projection and datum details manually. This requires that the header (.ers) file be edited. To do this:

- 1 Select the **Load Dataset** button from the **Algorithm** dialog or the Common Functions toolbar.
- 2 Select the .ers file that you wish to edit.
- 3 Select the **Info** button at the bottom of the dataset chooser dialog box. This will open the **Dataset Information** dialog.

- 4 From the **Dataset Information** dialog, click the **Edit** button. This will open the **Dataset Header Editor**.
- 5 Select the **Coord Space...** button. This will open the **Dataset Header Editor: Coordinates** dialog.
- 6 Change the datum and projection to the correct ones. Select **OK**.
- 7 Select **Save** from the **Dataset Header Editor**. Select **OK**.
- 8 Select **Cancel** from the **Dataset Information** dialog and select **OK** from the dataset chooser to load the dataset.

Editing registration information in header files

Again in some cases it is necessary to specify a registration coordinate, registration cell and cell size in order to properly register the file in coordinate space. To do this:

- 9 Click the **Load Dataset** button from the **Algorithm** dialog or the Common Functions toolbar.
- 10 Select the .ers file that you wish to edit.
- 11 Click the **Info** button at the bottom of the dataset chooser dialog box. This will open the **Dataset Information** dialog
- 12 From the **Dataset Information** dialog, click the **Edit** button. This will open the **Dataset Header Editor**.
- 13 Click the button labeled **Raster Info...** This will open the **Dataset Header Editor: Raster Information** dialog.
 - To change the registration information click **Registration Point...** This will open the **Dataset Header Editor: Registration** dialog. Edit the **Registration Coordinates** and the registration cell for the image. If the **Registration Cell** is the **Upper Left** then the **Registration Cell Values** are 0,0. Click **OK** to close the **Registration** dialog.
 - To change the cell size select **Cell Size** and change the x and y dimensions to reflect the actual cell size of the dataset. Click **OK** to close the **Cell Size Information** dialog.
- 14 Select **OK** to close the **Raster Information** dialog.
- 15 Click **Save** in the **Dataset Header Editor**. Select **OK**.
- 16 Click **Cancel** in the **Dataset Information** dialog and click **OK** in the dataset chooser to load the dataset.

Importing geological and cultural vector data

You can import the following data formats into ER Mapper:

Format

OpenWorks 3.1 Wells

Comments

Converts Landmark Well Data Export Format files to ER Mapper vector files. This format is the output file obtained by exporting the default Well Master Block format from OpenWorks, with no curves.

Format	Comments
Seisworks Fault Polygons	Converts Landmark Fault Polygons Export Format files to ER Mapper vector files. This format is the output file obtained by exporting the default format for fault polygons from SeisWorks
Seisworks Manual Contours	Converts Landmark Contours Export Format files. This format is the output file obtained by exporting the default format for manual contours from SeisWorks

OpenWorks 3.1 Wells—Import

This import reads Landmark Well Export files into ER Mapper vector format. All wells are imported. Most of the information in these files becomes the attribute of the well object. Files in Landmark Well Data Export format are obtained by exporting the default Well Master Block format from OpenWorks, with no curves. Use the “LGCRptFMT.wlx” format.

Input data format

```
Well
Master Block
Common Well Name : Well 1
Operator : DALLAS OIL
Lease Name : Stark
Lease Number : 0001 UWI : 00001
State : UNKNOWN
County : UNKNOWN
Country : UNKNOWN
Longitude : -57.38
Latitude : 20.70 X
Coordinate : 8189.00 Y
Coordinate : 35105.89
Total Depth : 7429.51
Plugged Back TD : 0.00
Completion Date :
Platform ID :
Field : PINTO
Current Class : OIL
```

To import OpenWorks 3.1 Wells

- 1 From the **Utilities/Import Vectors and GIS formats** menu select **OpenWorks 3.1 Wells**.

- 2 Enter the full pathname of the input file and the output dataset.

The output dataset will be registered in RAW co-ordinate space unless a Datum and Projection are specified from the interface. A rotation value for the grid can also be specified.

After clicking on the **OK** button, you will be prompted for the well symbol size to use and given examples of suggested sizes for various output map scales.

Note: A circle is drawn at the well location, and the well name appears to the bottom right of the symbol. The other information is stored as the attribute of the well symbol.

Command Line

```
importlandmark_well inputpath/file outputpath/file.erv
```

SeisWorks Fault Polygons

This import reads Landmark Fault Polygons Export format files into ER Mapper vector format. These files are obtained by exporting the default format for fault polygons from SeisWorks.

To import SeisWorks Fault Polygons

- 1 From the **Utilities/Import Vectors and GIS formats** menu select **Seisworks Fault Polygons** .
- 2 Enter the full pathname of the input file and the output dataset.

The output dataset will be registered in RAW co-ordinate space unless a Datum and Projection are specified from the interface. A rotation value for the grid can also be specified.

Command Line

```
importlandmark_fault inputpath/file outputpath/file.erv
```

Input data format

The format is:

```
Row Col Decimal Places  
X 1 12 3  
Y 13 24 3  
Z 25 36 3
```

```
PTYPE 37 40
SRCID 41 44
```

Where X is Eastings, Y is Northings, Z is Height, PTYPE is Point type (6 - Start, 7 - Intermediate, 8 - End). SRCID is not used in the import

Example

```
12345.688 567890.500 0.000 6 1
12346.531 567890.000 0.000 7 1
12346.625 567890.000 0.000 7 1
12346.469 567890.500 0.000 7 1
12346.469 567890.000 0.000 7 1
12346.969 567890.500 0.000 7 1
12346.344 567890.500 0.000 7 1
12346.469 567890.500 0.000 7 1
12346.719 567890.500 0.000 7 1
12346.688 567890.500 0.000 8 1
12346.500 567890.500 0.000 6 2
```

SeisWorks Manual Contours

This import reads Landmark Contours Export files into ER Mapper vector format. All contours are imported and the Z value is the attribute of the line.

To import SeisWorks Manual Contours

- 1 From the **Utilities/Import Vectors and GIS formats** menu select **Seisworks Manual Contours**.
- 2 Enter the full pathname of the input file and the output dataset.
The output dataset will be registered in RAW co-ordinate space unless a Datum and Projection are specified.
A rotation value for the grid can also be specified.

Command Line

```
importlandmark_cont inputpath/file outputpath/file.erv
```

Format

The Landmark Contour Export files are obtained by exporting the default format for manual contours from SeisWorks. The format is:

```
Row Col Decimal Places
X 1 12 3
Y 13 24 3
```

```
Z 25 36 3  
PTYPE 73 39
```

Where X is Eastings, Y is Northings, Z is Height, PTYPE is Point type (1 - Start, 2 - Intermediate, 3 - Open end, 4 - Closed end). For example,

```
597644.125 6184274.000 2135.637 1  
597658.000 6184236.000 2135.637 2  
597727.500 6184274.000 2135.637 2  
597658.000 6184298.000 2135.637 2  
597644.125 6184274.000 2135.637 4  
598110.562 6184274.000 2200.637 1  
598142.000 6184255.000 2200.637 2  
598263.000 6184230.500 2200.637 2  
598309.812 6184274.000 2200.637 2
```

Notes

- The contour height is stored as the attribute of the contour in the ER Mapper file (rather than as text). To view the height start the Annotation editor and select the line of interest. The height will be displayed as the Object Attribute.
- If PTYPE is not used in the file a new contour is recognized by a change in the Z value.
- Blank lines are ignored.

Updating geological and cultural vector data

Now that your vector data has been imported into ER Mapper you may want to make some changes to that data. You can do this using ER Mapper's annotation editor.

- 1 From the **Edit** menu, select **Annotate Vector Layer**. This will open the **New Map Composition** dialog.
- 2 Click the **File Chooser** button next to **Load from File**. The **Load Map Composition File** chooser dialog opens.
- 3 Locate your vector file and double click to select it.
- 4 Select **OK** on the **New Map Composition** dialog.

The Annotation **Tools** opens and the image should appear in the image window. If it does not, try selecting **Quick Zoom / Zoom to All Datasets** from the **View** menu. If your image changes, the extents must be incorrect for either the raster or the vector dataset. Setting image extents will be discussed later in this document.

You may also get a warning that your algorithm hasn't had its page defined. If so, you can select **Close** if you wish or **Page Setup...** to define the algorithm page. If you are intending to print your algorithm you must set up the page to control the size and placement of your output. See Chapter 16, "Printing" of the *ER Mapper User Guide* to see how to properly set up a page for printing.

- 5 In the annotation **Tools**, double-click on the **Poly Line** tool. This opens the **Line Style** dialog.
- 6 In the Annotation **Tools**, select the **Select/Edit Points Mode** tool.
- 7 Select the lines that you want to edit. (To select multiple lines you can use the shift-click or shift-click-drag methods.) When a line is selected a blue box appears at all nodes of the line.
- 8 Edit the settings in the **Line Style** dialog as desired.
- 9 When changes are complete, click the **Save** button on the Annotation toolbar. This saves the vector file not the entire algorithm.
- 10 Select **Close** from the Annotation **Tools**.

Moving updated vector data back to other products

Often, after editing and updating your vector data in ER Mapper, you'll want to take the data back to the original product. Although ER Mapper's list of exports is far less extensive than its imports, it is usually fairly easy to take the data back to the other products.

In ER Mapper there are basically three different formats that you will want to use to export your vector data back to other products:

- AutoCAD DXF
- SeisWorks Fault Polygons

AutoCAD DXF

This is probably the most common of the vector formats since most packages can read and write in DXF format.

Exportdxf identifies any layers in the vector file and ask you where to export them to. The layers are defined in the attribute field of the vectors.

SeisWorks Fault Polygons

This export creates a Landmark Fault Polygon Export Format file. This file can be imported into SeisWorks to be used in that package.

Generating hardcopy prints

ER Mapper has powerful map production and printing capabilities. However, you need to set up the printing devices correctly.

This section covers the following issues:

- Generating maps as a TIFF file
- How to create a map

Generating maps as a TIFF file

When creating a TIFF file, rather than saving the image as a TIFF file you could make a hardcopy plot in TIFF format. The hardcopy TIFF can be generated in either 8 bit or 24 bit format. The following section explains how to setup a TIFF export so that the TIFF file maintains the resolution of the ER Mapper dataset and an output file can be specified.

- 1 With the algorithm you want to print saved and displayed on the screen, select **Print** from the **File** menu.

The **Print** dialog appears. The **Algorithm** field automatically displays the current algorithm name so you will see your algorithm listed. If your algorithm was not open this field might be blank (if no algorithm is current) or show another algorithm. You can click the **File Chooser** button to select an algorithm.

- 2 Select the **Output Name** file chooser. The **Open Hardcopy Control** chooser opens.
- 3 Change directories to the 'hardcopy\Graphics' directory.
- 4 Double-click on one of the TIFF output formats to select it.
- 5 In the **Print** dialog, click **Setup**.
- 6 To maintain resolution, select the **Force 1 Dataset Cell = 1 Image Pixel** button. Once this is selected the **Force Single Page** button becomes active. Click this button.
- 7 Change the filter program line to specify the number of colors:
 - for 24 bit TIFF change the filter program line to:
`hetotiff -d24 /path/filename.tif.`
 - for 8 bit TIFF with compression change the filter program line to:
`sh -c 'hetoppm | ppmquant 256 | pnmtotiff - /path/ filename.tif'`
 - for 8 bit TIFF with no compression change the filter program line to:
`sh -c 'hetoppm | ppmquant 256 | pnmtotiff -none - /path/ filename.tif'.`

In each case /path is the path to the directory in which you want to write the tiff file and filename.tif is the name of the output file with a tiff extension added.
- 8 Select **OK** on the **Setup** dialog.
- 9 Select **Print** in the **Print** dialog.

How to create a map

When creating a map, there are three important things to consider:

- Page Setup
- Vector Data to Include
- Map Composition Items

Page Setup

For an algorithm, there are three different sizes that need to be set in order to make a map. They are page, contents and border sizes. These three sizes interact so that you must decide how they are determined. To do this the Page Setup dialog and

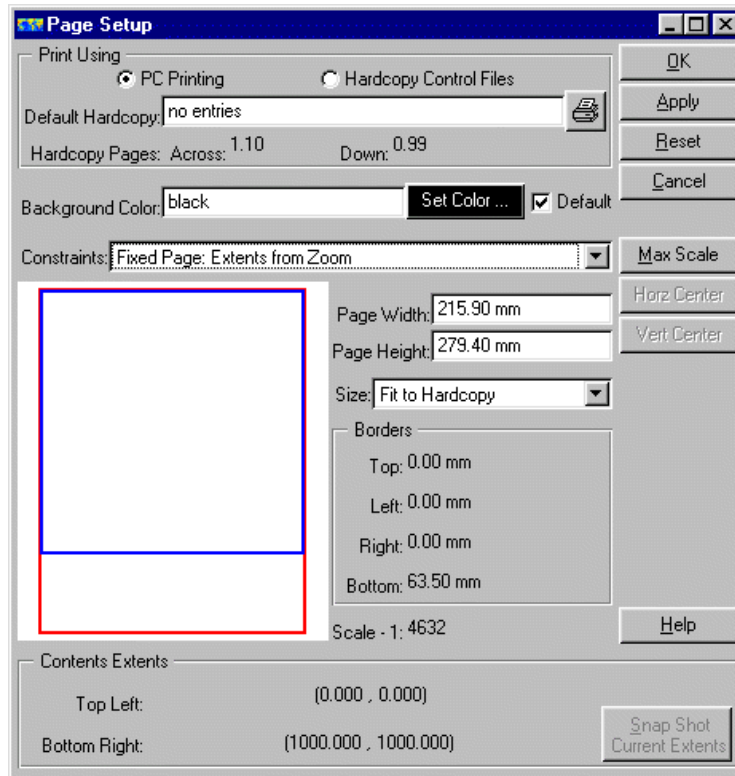
wizard offer you three constraints to choose from for defining an algorithm. The fourth constraint is the default constraint. It is not generally used for algorithms that will be printed and will not be discussed here. The constraints and their effects are:

Constraint	Explanation
Auto Vary: Page	ER Mapper automatically varies the page size based on the Borders and Scale that are selected. If the final page size is bigger than that of the hardcopy device, ER Mapper will attempt to strip print the image.
Auto Vary: Borders	ER Mapper automatically varies the borders based on the selected Page Size and Scale. This is typically the desired choice as most users have a specific output device in mind and want a particular scale.
Auto Vary: Scale	ER Mapper will automatically set the scale based on the page size and borders selected.
Fixed Page: Extents from Zoom	The page size can be selected and ER Mapper will automatically fit the image to that page size. Typically when creating a hardcopy map this selection is not used.

Once a constraint has been selected, you can vary the other two components. You can also set the background color. The following is an example of setting up a map:

- 1 Create an algorithm using a raster dataset.

- 2 From the **File** menu select **Page Setup**. The **Page Setup** dialog opens. In the window on the left of the dialog box the red box indicates the Page while the blue box indicates the Contents.



- 3 From the drop down list of **Constraints** select **Auto Vary: Borders**.
- 4 Change the **Background Color** to white.
- 5 From the **Size** pull down menu, select **US Letter**.
- 6 Change the **Scale** to an appropriate value such as 200000. This will depend on the scale of your data. Any scale that leaves some border space will do.
- 7 Select the **Horz Center** and **Vert Center** buttons. This will center the image on the page. Adjust the position as desired. (Often you'll want to place the image slightly higher than center to allow more room at the bottom to add map composition items. This can be done by changing the value for the **Top Border**; The bottom border will adjust automatically.)
- 8 Select **OK** or **Apply**.

Including Vector Data

Earlier in this chapter we discussed the mechanisms available for sharing data with companion software products. This section summarizes the steps for incorporating vector data into your image, assuming that you have decided which method to use and have configured your system to suit.

- 9 From the **View** menu select **Algorithm** to open the **Algorithm** dialog (if it is not already open).
- 10 In the **Algorithm** dialog click on the **Edit** menu.
 - to display data that has been imported into ER Mapper vector format, select **Add Vector Layer** and **Annotation/Map Composition**. This will add an Annotation layer to the algorithm.
 - to display data in the native format of external systems select the appropriate dynamic link (for example, **Dynamic Link to OpenWorks 3.1 Wells**).
- 11 In the **Algorithm** dialog, click the **Load a Dataset** or **Dynamic Link** button in the process diagram for the new layer.
- 12 Find the desired vector dataset and double-click to load it.
- 13 ER Mapper redisplay the raster image with the vector dataset displayed over the top.

Adding Map Composition Items

Map composition items are added using the Annotation tools. You can add Map items to an existing ER Mapper Annotation layer. However, it is a good idea to use a separate layer for the Map items so that you can easily turn them on or off independently.

- 14 On the main ER Mapper menu, click the **Edit** menu and select **Annotate Vector Layer...**
- 15 When the **New Map Composition** dialog opens, click **OK**.
- 16 If the Page Setup Warning opens, you can either select Close or follow the procedures outlined in the Page Setup section found earlier in this document.
- 17 From the annotation **Tools** select the **Map Rectangle** tool. The **Map Object Select** and **Map Object Attributes** windows open.
- 18 Select a category of map composition items from the **Category** drop down list, for example, Grid.
- 19 Select one of the map objects (for example, EN Grid), drag it over the area you want to place it and drop it.

- To resize these objects there are two choices. For objects like grids or clip masks, select the **Fit Grid** button in the **Map Objects Attributes** dialog. This will automatically resize the object to the size and location of the data. Or select the **Select and Move/Resize** tool. Click on the object to select it and resize it as you wish.
 - ER Mapper map objects are intelligent. For example, when you resize some of the objects, their values will change to maximize the allowed space. For example, if you resize a scale bar, the spacing of the scale bar will be adjusted as well. North Arrows are also intelligent in that if there is a rotation from true north in the dataset, the North Arrow will still point at true north regardless of direction.
- 20 Change the item parameters such as color or grid spacing in the **Map Object Attributes** dialog as desired. You can also add your own map composition objects to the available options. For information on adding map composition objects of your own, either consult the reference manual or contact your support provider.

Using the Page Setup Wizard

The **Page Setup Wizard** leads you sequentially through the page setup process. It does the same as **Page Setup**.

- 1 On the Standard toolbar, click on the **Page Setup Wizard** button.
- 2 In the **Introduction** dialog box, select **Algorithm displayed in current window**, and click on **Next>**.
- 3 In the **Use a template?** dialog box, select **Define new values with this wizard**, and click on **Next>**.
- 4 In the **Set background color** dialog box, set the background color to white and select your units of measurement,. Click on **Next>**.
- 5 In the **Set contents extents** dialog box, select **Use the current contents extents**, and click on **Next>**.
- 6 In the **Set pagesize** dialog box, select **Choose from standard portrait sizes**, and click on **Next>**
- 7 In the **Standard portrait** dialog box, select **US Letter**, and click on **Next>**
- 8 In the **Set borders** dialog box, select **Center Horizontally** and **Center Vertically**. Click on **Next>**
- 9 In the **Set scale** dialog box, select **Type in the scale**, and click on **Next>**.
- 10 In the **Set scale** dialog box, type in your required scale, and click on **Next>**.
- 11 In the **Finish** dialog box, select **Add a vector layer**, and open the file chooser to select a required vector layer. Save the algorithm under an appropriate name. Click on **Finish**.

Data viewing tips

The Intensity layer

ER Mapper provides a type of layer named Intensity. Used on its own it provides a monochrome image. Used with other layers the data in the Intensity layer controls the *brightness* (or intensity) of the image colors. Low data values in the Intensity layer produce dark colors in the image, and high data values produce bright colors. Intensity layers are used in the Oil and Gas industry to create shaded relief images that highlight structure.

To view your seismic dataset

Open an image window and the **Algorithm** dialog

- 1 On the Standard toolbar, click on the **Open Algorithm into Image Window** button.

If you are starting from scratch, your algorithm will have a single layer, which will be a Pseudocolor layer.

- 2 Change the Pseudocolor layer to an Intensity layer and load your seismic dataset. Select the two-way-time data band.

To use a formula to invert the dataset values

- 1 In the **Algorithm** window, click on the **Formula** button in the process diagram. 

The **Formula Editor** dialog box appears.

- 2 In the **Formula Editor** dialog, type a minus sign in front of the formula so that it looks like the following:

-INPUT1

This formula tells ER Mapper to negate (invert) all values in the dataset.

- 3 In the **Formula Editor** dialog click the **Apply changes** button and then the **Close** button.

The image appears as black initially because you need to adjust the transform to account for the new range of negative data values produced by the formula.

- 4 Click the **Transform** button. 

The **Transform** dialog box shows the negative data range produced by the formula in the **Actual Input Limits** fields.

- 5 From the **Limits** menu (on the **Transform** dialog), select **Limits to Actual**.

The X axis data range changes to match the Actual Input Limits.

ER Mapper draws the image again, this time using the full range of grey shades to display the image. Since you inverted the data values with a formula, structural lows (larger two-way time values) are shown as dark greys transitioning into structural highs shown as lighter shades.

To use sun shading

- 1 Turn on sun shading and display the shaded relief image using the **Open Sun Angle editor** button. 

- 2 Drag the small sun icon around to change the sun position.

This feature allows you to apply artificial illumination from any direction to highlight very subtle structural features.

Applications of sun angle shading

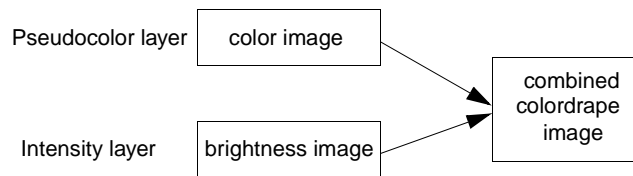
ER Mapper's sun angle shading feature is a very powerful tool for quickly identifying subtle features in time surfaces. It is commonly used for many applications, including to:

- identify small scale faulting, and relative through across faults
- identify subtle stratigraphic features (pinchouts, truncations, etc.)
- highlight data acquisition and/or processing artifacts
- highlight quality issues related to interpretation

Colordrapping

Colordrapping is the technique of draping one set of image data in color over another set of data that controls the color brightness or intensity. This allows you to effectively view two (or more) different types of data or methods of processing simultaneously in a *combined display*. Colordrapping is usually difficult and time consuming using traditional image processing products, but it is very fast and easy using ER Mapper's Intensity layer type.

The colordrapping technique has become a very popular and powerful tool for visualization of interpreted surfaces. For example, combining two-way time images shown as both color and as structure lets you create a shaded relief image that enhances subtle faults and color-codes their placement relative to depth. From these types of images, far more useful information can be derived than from conventional visualization techniques.



To create a colordrape image

- 1 In the **Algorithm** window, load your seismic dataset into an Intensity layer.
- 2 Duplicate the Intensity layer and change the layer type to Pseudocolor. (Duplicating the layer instead of adding a new one saves you from having to reload the dataset.)
- 3 Drape color over the shaded relief image by turning sun-shading on for the Intensity layer and off for the Pseudocolor layer.

Note: Sun angle shading is usually applied only to time surface datasets displayed in Intensity layers because two-way time describes structural features well. Sun shading is not normally applied to amplitude or attribute datasets which are generally displayed in color.

Note that by combining the two processing techniques into one image, you can simultaneously see structure as brightness relative to depth as color.

- 4 To use different color mapping transforms for the color layer click on the right-hand **Transform** button in the process diagram. 

The **Transform** dialog box opens showing the current lookup table and color mapping.

- 5 On the **Transform** dialog, click the **Histogram equalize**  button.

ER Mapper applies a histogram equalization transform to the data. Histogram equalization maximizes overall color contrast in the image at the expense of losing contrast in the structural highs and lows.

- 6 On the **Transform** dialog, click the **Gaussian equalize**  button.

ER Mapper applies a gaussian equalization contrast stretch to the data. This maximizes color contrast in the structural highs and lows, but tends to flatten out contrast in other parts of the image.

- 7 On the **Transform** dialog, click the **Create default linear transform**  button.

ER Mapper resets the color mapping back to a straight linear default.

- 8 You can display the shaded relief and color images separately by turning one of them off.

To drape amplitude data in color over time data

- 1 Highlight the Pseudocolor layer and change the band to select the amplitude data band.
- 2 Adjust the transform for the Amplitude color layer by selecting the layer and clicking on the right-hand **Transform** button in the process diagram. 
- 3 From the **Limits** menu, select **Limits to Actual** to display the image using the actual limits of the amplitude data.
- 4 On the **Transform** dialog, click the **Histogram equalize** button. 

Histogram equalization increases the overall color contrast in the amplitude data. Areas of high amplitudes are shown as reds, and low amplitude areas are shown in blues.

This colordrape image lets you easily associate variations in amplitude with structural features shown by the shaded two-way time surface in the Intensity layer. Using this technique, you can drape virtually any type of data in color over the shaded time surface to aid interpretation of subtle relationships.

Tips for Colordrape Algorithms

Generally the Intensity layer of a colordrape algorithm is used to show structural features derived from two-way time data, and the color layers are used to show amplitude, azimuth, isochrons, or any other derivative or attribute images you feel are useful. To use an existing algorithm as a “template” algorithm to apply the same processing to different datasets, simply load new datasets into the Intensity and Pseudocolor layers and adjust the transforms to account for the data ranges.

One colordrape variation some researchers use is to display a dip image in Intensity instead of shading from a specific compass direction. A dip image may delineate both sides of a fault more clearly, for example.

Training

If you would like training in using ER Mapper in oil and gas applications contact the ER Mapper office closest to you.

**Part Four -
*Supplied
Processing***

Supplied Algorithms

This chapter describes selected algorithms supplied with the ER Mapper distribution.

Typical use of the supplied algorithms is to load the algorithm and change the image to your own image, and then click on the **Refresh Image with 99% clip on limits**  button to run the algorithm with 99% transform clipping.

The processing carried out by algorithms depends on the type of data and the desired result. For example, the Landsat_TM/NDVI algorithm computes the Normalized Difference Vegetation Index (NDVI) from the Landsat TM imagery.

The supplied algorithms are designed as starting points for creating your own commonly used algorithms. They were created using the standard ER Mapper user-interface - they are not 'hard coded' into ER Mapper.

The algorithms and images supplied with ER Mapper are divided into sections, typically based on the type of data or the type of processing. The different sections are located in the following directories under **examples**.

Applications	Specific application examples; e.g. Mineral Exploration, Oil and Gas Exploration etc.
Data_Types	Examples which illustrate the the use of a specific type of data.

Functions_And_Features

Examples which illustrate a particular ER Mapper function or feature.

Shared_Data

Image datasets which are shared by one or more of the other examples directories.

Miscellaneous\Templates

Designed as templates to be used to create virtual datasets or images. Load the template algorithm, change to the new image(s), zoom to all datasets (if entire coverage is desired), and then save the resultant algorithm as a virtual dataset or as a real image. Most template algorithms do not have a final transform - this ensures that the data being processed is not modified by the template algorithm.

The example algorithms are designed to be used as-is. Simply load the algorithm, change the image, and click on the **Refresh image with 99% clip on limits**  button.

In addition to the example algorithms loaded with ER Mapper you can also choose to load other application example algorithms during installation. These are inserted into the appropriate examples directories.

The complete list of the examples directories are as follows. Each of these directories is organized as a section within this chapter, with more information about each algorithm.

Applications

Airphoto

Contains examples demonstrating orthorectification, mosaicing, and balancing of airphotos.

Fire_Risk

3D_Vegetation_over_DTM.alg

This algorithm defines a vegetation ratio called the Normalized Difference Vegetation Index or NDVI which has shown to be strongly correlated with the amount of vegetation (biomass). This is draped over an Intensity layer containing a Digital Terrain image band.

Vegetation.alg

This algorithm defines a vegetation ratio called the Normalized Difference Vegetation Index or NDVI which has shown to be strongly correlated with the amount of vegetation (biomass).

Land_Information

Contains algorithms related to Land Information applications.

Mineral_Exploration

3D_Mag_Colordraped_and_KTh_over_Mag.alg

This image has two surfaces. The bottom one is an aeromag colordrape using an elevation color lookup table. The upper image is a Potassium Thorium ratio draped over the aeromag data which is taking on the 3D appearance of elevation.

3D_Magnetics_and_Radiometrics.alg

A very powerful way to show magnetics data, known as colordrape. In this algorithm, magnetics data is used for both color and intensity (the two layers in the algorithm). For intensity, the sun-shading for the Intensity layer has been turned on to enable structure to be easily seen.

The transform can be modified in real time for both layers (for the Pseudocolor layer, changing coloring for the image; for the Intensity layer, changing the overall image brightness); sun-shading can also be modified in real time.

Note: If this algorithm is viewed using an ER Mapper 3-D viewer or printed using ER Mapper hardcopy stereo, the Intensity layer is used for height. This makes it easy to use this algorithm for 3-D output.

Magnetics_Colordraped_over_Real_Time_Shade.alg

This is an aeromagnetics scene viewed with color showing the total value of the magnetic signal and the shading (adjustable in real-time) showing the subsurface structure based on the magnetic anomalies.

Magnetics_Pseudocolor.alg

This is a gridded aeromagnetics scene viewed with color representing the total value of the magnetic signal. In this image red represents higher values and blue represents low values.

The color table can be changed in the Algorithm window to map the magnetic intensity values to another color range.

Newcastle_Map.alg

A very powerful way to show magnetics data, known as colordrape. In this algorithm, magnetics data is used for both color and intensity (the two layers in the algorithm). For intensity, the sun-shading for the Intensity layer has been turned on to enable structure to be easily seen.

The transform can be modified in real time for both layers (for the Pseudocolor layer, changing coloring for the image; for the Intensity layer, changing the overall image brightness); sun-shading can also be modified in real time.

Note: If this algorithm is viewed using the ER Mapper 3-D viewer or printed using ER Mapper hardcopy stereo, the Intensity layer is used for height. This makes it easy to use this algorithm for 3-D output.

Radiometrics_K_Th_Ratio.alg

This is a band ratio for Potassium and Thorium. Red indicates high K/Th values (high Potassium and low Thorium counts) and blue indicates low K/Th values (low Potassium and high Thorium counts).

Radiometrics_K_Th_U_RGB.alg

This is a radiometrics scene with Potassium values shown in red, Thorium shown in green and Uranium shown in blue. All data values are in counts-per-second.

Radiometrics_K_Th_U_RGB_over_Magnetics_RT.alg

Radiometrics_KThU_RGB.alg) draped over aeromagnetics highlighting structure using real time shading.

This is powerful as it is allowing us to correlate two different types of data in real time. The aeromagnetics data is integer numbers and the radiometrics data is real numbers. This is not possible with traditional software.

Radiometrics_KThU_RGB.alg

This is a radiometrics scene with Potassium values shown in red, Thorium shown in green and Uranium shown in blue. All data values are in counts-per-second.

Mt_St_Helens

Contains algorithms related to the Mt St Helens volcano.

Oil_and_Gas_Exploration

3D_Multi_Surface_TWT_and_Amplitude.alg

This algorithm combines Pseudocolor and Intensity layers of the time data. The illumination (shading) can be edited.

This image combines the illumination (greyscale) with a color layer of the time data. This type of display significantly enhances the structural contours by emphasising the main structural blocks.

3D_Seismic_TWT_Horizon.alg

This algorithm combines Pseudocolor and Intensity layers of the time data. The illumination (shading) can be edited.

This image combines the illumination (greyscale) with a color layer of the time data. This type of display significantly enhances the structural contours by emphasising the main structural blocks.

Telecommunications

Contains optionally loaded algorithms related to telecommunication networks.

World_Topography

Contains optionally loaded example algorithms that use the world DTM image dataset.

Data_Types

Airphoto

These algorithms give examples of airphotos integrated with other data. For more complete examples and algorithms that use airphoto data, see the applications_Land_Information optional examples.

Airphotos are usually scanned in as a RGB image using a desktop or drum scanner, which is then imported into ER Mapper format.

Unlike pure digital images, the resolution of airphotos is a function of both the scale that the airphoto was flown, and a function of the resolution of the scanned image.

Once a airphoto has been scanned in, it needs to be geocoded to the map projection using ER Mapper image rectification capabilities. Airphoto mosaics can easily be constructed using ER Mapper's interactive data fusion.

Airphoto_and_Landsat_TM_and_Vectors.alg

Demonstrates fusion of different resolution raster data (an airphoto and Landsat TM), and demonstrates the spatial information (roads, buildings and so forth) that can be resolved in airphotos.

As an airphoto of higher resolution than Landsat TM data, it is placed above the Landsat TM data in the algorithm.

A vector layer is also present in this algorithm.

RGB.alg

Shows airphoto data as an RGB image.

Vectors_from_Airphoto.alg

Shows an airphoto as an RGB image with vector data over the top. The vector data has been created using the ER Mapper annotation tool while editing over the airphoto.

To edit the vector data, click on the **Annotation** toolbar button.

Arc_info

ER Mapper can directly access ARC/INFO coverages for display and editing purposes. You can also convert between ER Mapper vector format and ARC/INFO format; for example you could create a classification polygon map using ER Mapper's Raster to Vector conversion, and save as an ARC/INFO coverage.

Note: ER Mapper can both import/export ARC/INFO coverages, and directly edited them.

You do *not* need to have ARC/INFO present on your system to be able to edit or access ARC/INFO coverages.

ER Mapper also supports an ARC/PLOT based dynamic link, which allows ARC/PLOT based information to be integrated into the ER Mapper imagery. This is the only link which actually requires ARC/INFO to be present, as it uses ARC/PLOT to generate the dynamic link data.

As with all information that can be displayed with ER Mapper, ARC/INFO data can be displayed over other information such as raster imagery, and can be included as map layers for final hardcopy maps.

After editing ARC/INFO coverages with ER Mapper, you should run ARC/INFO's clean or build utilities, as when changing coverages with ARC/EDIT.

Airphoto_with_roads.alg

This algorithm shows an ARC/INFO coverage over airphoto data. A typical use would be to update the ARC/INFO coverage based on the latest airphotos.

Fast_SPOT_Pan_with_roads.alg

This example shows San Diego and La Jolla roads on top of a SPOT Panchromatic image of San Diego.

SPOT_Pan_with_roads_and_drainage.alg

This example shows several ARC/INFO coverages - roads and drainage - shown over a SPOT panchromatic image. Each coverage is shown in a different color.

via_ARCPLOT_Airphoto_with_roads.alg

This example requires ARC/PLOT (UNIX only) to display a coverage over an airphoto. Although this dynamic link is slower than the other links (which directly access the coverage), it allows any ARC/PLOT based commands to be integrated into ER Mapper images or hardcopy.

via_ARCPLOT_Coast_with_boundaries.alg

Similar to `via_ARCPLOT_Airphoto_with_roads`, except it shows coastlines and boundaries using ARC/PLOT.

AutoCAD_DXF

DXF_Roads_over_Airphoto.alg

Shows an airphoto as an RGB image with vector data over the top. The vector data has been created using the ER Mapper annotation tool while editing over the airphoto.

To edit the vector data, click on the Annotation toolbar button.

Digital_Elevation

Digital Elevation image data processed with directional filters provides lineament detection. It can also be used to refine Landsat classification results.

Topographic or digital terrain data, once gridded, can be processed and displayed to highlight important physiographic features such as palaeo stream terraces in place gold and tin deposits.

You can also drape other images over topography. Topographic distribution of satellite band response and geophysical/geochemical anomalies are often used as a diagnostic tool.

DEM data can also be useful used in conjunction with stream or river vector images.

The algorithms supplied with ER Mapper for DEM data are listed below.

Slope_degrees.alg

This algorithm demonstrates the use of the *Slope* filter, which calculates the slope, or steepness, for a DTM. The numbers output from the *Slope_Degrees* filter range from 0 to 90. 0 indicates a flat area, with no slope; 90 indicates a vertical slope.

Although slope is useful by itself, a common use is to use formula to select only slopes with a maximum grade. For example, the following formula would only show slopes with less than 5 degrees of slope:

```
IF input1 <= 5 THEN input1 ELSE NULL
```

Note: For this formula to work, *input1* should be mapped to a DTM, and the input layer should have a *Slope_degrees* filter applied prior to the formula.

Slope_percent.alg

This algorithm demonstrates the use of the *Slope* filter, which calculates the slope, or steepness, for a DTM. The numbers output from the *Slope_percent* filter range from 0 to 200. 0 indicates a flat area, with no slope. 100 indicates a 45 degree slope, and 200 indicates a vertical slope.

Although slope is useful by itself, a common use is to use formula to select only slopes with a maximum grade. For example, the following formula would only show slopes with less than 5 percent of slope:

```
IF input1 <= 5 THEN input1 ELSE NULL
```

Note for this formula to work, *input1* should be mapped to a DTM, and the input layer should have a *Slope_percent* filter applied prior to the formula.

Aspect.alg

This algorithm demonstrates the use of the *Aspect* filter, which calculates the aspect or direction of slope for a DEM. The numbers output from the *Aspect* filter range from 0 to 361. Zero indicates a north facing slope, 90 indicates an east facing slope, and so on. The special number 361 is used to indicate areas that are perfectly flat (for example, water) with no aspect for the slope.

Although Aspect is useful by itself, a common use is to use formula to select only slopes facing a certain direction. For example, the following formula would only show slopes within 10 degrees of south:

```
IF input1 >=170 AND input1 <= 190 THEN 1 ELSE NULL
```

Note: For this formula to work, *input1* should be mapped to a DTM, and the input layer should have an Aspect filter applied prior to the formula.

Australia_Colordrape.alg

An example of colordrape, using a DTM for Australia. A colordrape algorithm uses the DTM in two ways: The image is color coded according to height (in this case, red is lower areas, blue are higher areas), and an intensity layer has sun shading turned on to highlight structure.

Note: If this algorithm is viewed using an ER Mapper 3-D viewers or printed using ER Mapper hardcopy stereo, the Intensity layer is used for height. This makes it easy to use this algorithm for 3-D output.

Colordrape.alg

This is the generic colordrape algorithm for DTMs. This algorithm has two layers: a Pseudocolor layer showing the DTM as color, and an Intensity layer showing the DTM structure by shading the Intensity layer.

This algorithm can be used for any DTM by loading the algorithm, loading your new DTM into the input image, and clicking on **Refresh Image with 99% clip on limits**  to re-clip the image.

Note: If this algorithm is viewed using an ER Mapper 3-D viewers or printed using ER Mapper hardcopy stereo, the Intensity layer is used for height. This makes it easy to use this algorithm for 3-D output.

Colordrape_shiny_look.alg

This algorithm demonstrates how ER Mapper's formula and algorithm processing can perform quite different results.

A DTM has been saved as a virtual dataset with two layers, Height (from the DTM) and Structure (from the DTM, but with sun shading applied). This virtual dataset is used as input into the Colordrape_shiny_look algorithm, which uses a HSI (Hue Saturation Intensity) model to highlight the image in such a way that it has a gloss or reflectance. This is achieved by modifying the saturation of the image based on the slope of the DTM.

Contours_from_Raster.alg

Demonstrates the use of formula to compute raster based contours from a DTM.

The general concept used for this algorithm is to:

- Scale the input DTM into a range of integer values, one value for each contour level desired. The following formula does this:

```
(CEIL(input1 / 100) * 100)
```

- Add a *Laplacian* filter after the above formula. The Laplacian filter will cause all edges to be shown as non-zero numbers, and all areas that are flat (areas between contour lines) to be zero.
- Add a *notch transform* to only show data above zero; otherwise show it as zero (which will be rejected from the classification layer).

All of the above is put into a classification layer, which then ‘classifies’ the image according to if a contour line should be present or not at each pixel.

For full vector based contouring, we recommend using one of the many products that do contouring with dynamic links to ER Mapper.

Dip.alg

This algorithm computes the DIP from a DTM. DIP is a measure of structure within the image. It is similar to having a sun-shaded image with the sun overhead. DIP shows structure in a DTM, regardless of angle.

Edge_Shaded.alg

This algorithm implements a 3 x 3 north-west shading filter on one band of image data.

Example Image: examples\Shared_Data\Australia_DTM

The result is as if the image was illuminated by a light in the north-west corner of the image. Because illumination is from the northwest, lineaments, faults and features running in a diagonal direction from north-east to south-west are highlighted.

The transform limits typed in were much narrower (-50 to 50) than the Actual Input Limits. Other transformations you can try are clipping the limits of the linear transform, or the Gaussian Equalize and Histogram Equalize from the Auto Options menu.

You can use different edge filters to highlight edges from different angles. Also consider using the Sun Angle shading option in layers instead of filters, which offers real time variation of sun angle and azimuth.

Greyscale.alg

A very simple display of a DTM as a pure greyscale image. This is the least useful way to display DTMs. A sun-shaded image, or better still a colordrape image, enables much more information to be extracted from the DTM.

Pseudocolor.alg

This algorithm displays a digital terrain model (DTM), using a Pseudocolor look-up table.

In this algorithm the red indicates areas of high elevation and blue indicates areas of low elevation.

Realtime_Sun_Shade.alg

This algorithm provides the means for using real time shading.

Description: This algorithm is simply a single layer, containing a DTM image, with real-time shading on the layer. Real time shading enables you to move the position of the sun relative to your image data. Illumination enhances lineaments, faults and features.

Ers1

Contains algorithms related to Radar.

Landsat_MSS

Landsat MSS is a second generation earth resources satellite with a wide synoptic view - a 185 km swath. It has a relatively large ground cell size (81.5 x 81.5 m) giving a poor spatial resolution, and from a geoscience point of view a very limited spectral resolution of four very broad bands in the green visible to near infrared region. Radiometric quantisation is 7 bits (0.5-0.8 um) and 6 bits (0.8 - 1.1um).

This wide synoptic view allows structural interpretation of large areas, contributing to the evaluation of the hydrocarbon and mineral potential of certain areas. The spectral data, although limited, has allowed the identification of iron oxide-rich lithologies and contributed significantly to lithological mapping.

See the *Customizing ER Mapper* manual for full characteristics of the Landsat MSS (Landsat 4).

The algorithms supplied with ER Mapper for Landsat MSS data contained in the examples\Data_Types\Landsat_MSS directory are listed below.

LandsatMSS_NDVI.alg

This algorithm defines a vegetation ratio called the Normalized Difference Vegetation Index or NDVI which has shown to be strongly correlated with the amount of vegetation (biomass).

$$(I1 - I2) / (I1 + I2)$$

$$(B4:0.95_um - B2:0.65_um) / (B4:0.95_um + B2:0.55_um)$$

Example Image: examples\Shared_Data\Landsat_MSS_27Aug91

LandsatMSS_PVI6.alg

Computes the Perpendicular Vegetation Index (PVI) for Landsat MSS 6, which is:

$$(((1.091 * I1) - I2) - 5.49) / \text{sqrt}((1.091 * 1.091) + 1)$$

Band 3: 0.75 um is mapped to Input1 (I1), and Band 2: 0.65 um mapped to Input2.

LandsatMSS_PVI7.alg

Computes the Perpendicular Vegetation Index (PVI) for Landsat MSS 7, which is:

$$(((2.4 * I1) - I2) - 0.01) / \text{sqrt}((2.4 * 2.4) + 1)$$

Band 4: 0.95 um is mapped to Input1 (I1), and Band 2: 0.65 um mapped to Input2.

LandsatMSS_Tasseled_Cap.alg

Three layers, each layer containing the formula for one of the tasseled cap vegetation calculations for Landsat MSS:

- Wetness
- Greenness
- Brightness

Turn on the layer for the appropriate tasseled cap to see the calculation.

Landsat_MSS_natural_color.alg

Generates a 'natural color' view from a MSS image. The formulae used are:

RED: Band 2: 0.65 um

GREEN: ((Band 2: 0.65 um * 3) + Band 4: 0.95 um) / 4

BLUE: Band 1: 0.55 um

This approximates a natural looking image from MSS imagery, with vegetation showing as green.

RGB_321.alg

Shows bands 3,2,1 as an RGB image. Vegetated areas show as red.

RGB_321_sharpened_with_SPOT_Pan.alg

Shows bands 3,2,1 of Landsat MSS as Red, Green, Blue. A SPOT Panchromatic image is included in the Intensity layer to sharpen the image. Landsat MSS has 80 meter cell resolution; SPOT Pan has a 10 meter cell resolution.

RGB_421.alg

This algorithm is a standard false color image obtained by assigning Band 4 (0.95 um) to the RED layer, Band2 (0.65 um) to the GREEN layer and Band 1 (0.55 um) to the BLUE layer.

Example Image: examples\Shared_Data\Landsat_MSS_27Aug91

This is a commonly used color combination for Landsat MSS composites because the image is similar to color infrared photography, particularly in the red rendition of vegetation.

TC_Greenness_over_Brightness.alg

A colordrape algorithm with the Greenness of vegetation shown in color (the Pseudocolor layer), and the brightness of vegetation shown as Intensity.

Landsat_TM

Landsat TM is a second generation earth resources satellite, and combines reasonable spatial resolution (cell size of 30 meters by 30 meters) with a reasonable range of spectral bands (7 bands in visible and near, short and mid infrared wavelengths). The first band covers the range from 450nm to 520nm, which roughly corresponds to blue light in the visible spectrum. Refer to the Open Standards manual for full characteristics of the Landsat TM (Landsat 5). Unlike airborne data, Landsat TM data is readily available for most of the world. The algorithms supplied with ER Mapper for Landsat TM data contained in the examples\Data_Types\Landsat_TM directory are listed below.

Abrams_Ratios.alg

This algorithm combines previously defined ratios into one RGB composite display. The ratio which highlights phyllosilicates (+clays, carbonates) is displayed in the red layer (Band 5/Band 7(1.6/2.2)). The ironoxide ratio (Band 3/Band 2(0.66/0.56)) is displayed in the green layer and vegetation (Band 4/3 (0.83/0.66)) is displayed in the blue layer.

```
( I1 - RMIN( ,R1 ,I1 ) ) / ( I2 - RMIN( ,R1 , I2 ) )
(B5:1.65_um - RMIN( , All, B5:1.65_um) ) / ( B7:2.215_um -
RMIN( , All, B7:2.215_um) )
```

Example Image: examples\Shared_Data\Landsat_TM_year_1985

In this algorithm pixels dominated by responses from phyllosilicates (clay mineral-carbonate)-rich outcrop, or soil, are red; those dominated by iron oxides are green and those by vegetation, blue. Pixels with responses due to mixtures of clay+iron oxide, will appear variously as red-orange-yellow. Areas of iron-rich soil with a grass cover will appear as cyan and areas of granite soil with a grass cover will be magenta.

Clay_ratio.alg

This algorithm implements the ratio that highlights clays, phyllosilicates and carbonates for Landsat TM. It does this by looking for high spectral responses in the 1.65um (band 5) wavelength and low responses in the 2.215_um (band 7) wavelength.

```
( I1 - RMIN( ,REGION1 ,I1 ) ) / ( I2 - RMIN( ,REGION1 , I2 ) )
(B5:1.65_um - RMIN( , All, B5:1.65_um) ) / ( B7:2.215_um -
RMIN( , All, B7:2.215_um) )
```

This ratio has difficulty in separating the response from clays et al. and vegetation. In the example Landsat TM image it is apparent that most of the response shown is due to vegetation. There are ways of combining the two algorithms (typically by using Red-Green-Blue false color) to highlight only oxides. These are discussed in more detail under the LandsatTM_abrams_ratios algorithm.

Colordrape_Greenness_over_Brightness.alg

A colordrape algorithm; the Greenness of vegetation is shown in color (Pseudocolor layer), and the brightness of vegetation is shown as Intensity.

Colordrape_NDVI_over_PC1.alg

A colordrape algorithm, with the NDVI vegetation index in color shown over PC1 as intensity.

As PC1 is often albedo from an image, this can be a good way to correlate vegetation with terrain.

Decorrelation_Stretch.alg

This algorithm carries out a decorrelation stretch by converting the image to principal component space, histogram equalizing PCs 1, 2 and 3, and then inverting back to normal space.

Edge_Shade_from_NE.alg

This algorithm implements a 3 x 3 north-east shading filter on one band of data; by default band 1.

Example Image: examples\Shared_Data\Landsat_TM_year_1985

The result is as if the image was illuminated by a light in the north-east side of the image.

Because illumination is from the north-east, lineaments, faults and features running in a diagonal direction from North-West to South-East are most strongly highlighted.

A filter is a spatial operation that is the result of moving a template over the source image, which generates output data based on spatial variations. Filters are used to detect and enhance edges, sharpen images, smooth images and remove noise.

Although this algorithm processes only a single band of data, filters are also useful to look at processed images (such as an image that highlights clays) to look for structural features such as lineaments.

In addition to the North-East shading filter used by this algorithm, there are other filters which may be used; for example, sharpening filters. User defined filters which carry out specialized processing may be added.

Greyscale.alg

This algorithm will show the first band of Landsat TM (blue visible light band) as a greyscale image. The result is a similar effect to an oblique photo of the area.

Example Image: examples\Shared_Data\Landsat_TM_year_1985

Iron_Oxide_ratio.alg

This algorithm implements the ratio that highlights iron oxides for Landsat TM, by looking for a higher spectral responses in the 0.66um (band 3) wavelength than in the 0.56um (band 2) wavelength. This is characteristic of the spectral response of iron oxides.

$\frac{(I1 - \text{RMIN}(, R1, I1))}{(I2 - \text{RMIN}(, R1, I2))}$

```
(B3:0.66_um - RMIN(, All, B3:0.66_um)) / (B2:).56_um -
RMIN(, All, B2:0.56_um))
```

Example Image: examples\Shared_Data\Landsat_TM_year_1985

This ratio has difficulty separating the response from iron oxides and dry vegetation.

Because these bands suffer from considerable atmospheric scatter, the resulting image is somewhat noisy. Smoothing the iron oxide ratio image with a 3 x 3 average filter will often make the image easier to examine.

Landsat_TM_area_specific_stretch.alg

This algorithm demonstrates stretching data within specific areas. This algorithm has Red, Green and Blue layers for land, and for water (a total of 6 layers).

The water layers have a formula to only show the data if it is over water. Band 5 is used to decide if a pixel is over water or not, by using the following formula:

```
IF INPUT1 < 20 THEN INPUT2 ELSE NULL
```

Where Input1 is mapped to Band 5, and Input2 is mapped to whatever band is to be displayed (depending on if it is a Red, Green or Blue layer).

The ELSE NULL means that over land, no pixels are shown for the water layer, so the land layers 'shine through' in these areas. This also means the transform for the water layers only show data for water.

The water transforms have then been stretched to highlight water.

Note: Water depth, kelp fields, and so on become visible with these enhancements.

Landsat_TM_Tasseled_Cap_in_RGB.alg

This shows the Brightness, Greenness and Wetness Tasseled Caps as Red, Green and Blue.

Lsfit.alg

This algorithm computes the Least Squares Fit for Landsat TM.

Pleasing_image.alg

Generates a ‘pleasing image’ for Landsat TM, based on a modified version of the Brovey Transform (using Landsat TM only).

It gives a very good looking image using only Landsat TM data.

Principal_Component_1.alg

Computes the Principal Component 1 (PC1) for Landsat TM. Only bands 1-5 and 7 are used in the formula. The generic formula is:

```
SIGMA(I1..I6 | I? * PC_COV(I1..I6 ), Region1, I?, 1))
```

Inputs I1 to I5 are mapped to bands 1 to 5. Input 6 is mapped to band 7. Region 1 can be whatever region is to be used to compute the PC, and is often the ‘All’ region. The final number **1** in the formula is the PC to compute; in this example, PC1. Changing this number generates a different PC.

RGB_321.alg

This algorithm is a ‘natural’ color scene comprising TM bands 3-2-1 (approximately equal to red-green-blue visible light) imaged in the red-green-blue computer monitor guns respectively.

Example Image: examples\Shared_Data\Landsat_TM_year_1985

The composite is not totally natural because the TM bands do not exactly match the red-green and blue spectral regions; bands 1 (blue visible) and 3 (red visible) have a lower spectral range than that which the eye recognizes as blue and red. This image looks partly realistic but there is an apparent absence of green vegetation (although the northeast corner and a southeast strip has blue-green coloration). The “greenness” response of plants is not a very strong one (compare the reflectance of vegetation in the green visible range, 0.56 μm , TM band 2), but the human eye is most sensitive to green (it has many more cones sensitive to green) and therefore magnifies the response relative to blue and red.

RGB_321_to_HSI_to_RGB.alg

Converts bands 3, 2 and 1 into Hue, Saturation, Color space from RGB space. Allows an image to be enhanced in HSI space instead of in RGB color space. ER Mapper can enhance HSI images in real-time.

RGB_341.alg

The ‘greenness’ of the ‘natural’ image can be improved by substituting TM band 4 for band 2. In band 4 (centred at 0.83 μm) in the near infrared, vegetation has very high reflectance.

Example Image: examples\Shared_Data\Landsat_TM_year_1985

LandsatTM_rgb_321 is basically the same as LandsatTM_rgb_341, except we have substituted band 4 for band 2.

By putting band 4 into the GREEN layer the high spectral response from vegetation (band 4) produces the greenness. This is now a false color image. This translates the response from a spectral band that is not from the visible range (has no ‘color’), into a visible wavelength so that we can ‘see’ a wavelength not normally used.

RGB_432.alg

This algorithm is similar to the LandsatTM_rgb_341 algorithm shown previously. LandsatTM_rgb_432 is another false color image, usually referred to as ‘standard’ false color. In this image TM band 4 is assigned to the RED layer, band 3 ($0.66\ \mu\text{m}$ = visible red) is in a green layer and band 2 ($0.56\ \mu\text{m}$ = visible green) in a blue layer.

Example Image: examples\Shared_Data\Landsat_TM_year_1985

The result of this RGB color composite is that the high reflectance of vegetation (0.83, TM band 4) makes vegetation appear red; red features, such as Fe-rich soils appear green, while green features appear blue.

This false color image is generally the one used to evaluate a particular image for a variety of resource-based applications. People interested in vegetation can see the location and density of vegetation; people interested in geology can make the same determination - and avoid the over-vegetated images.

The Gaussian Equalize transformation was applied to each band.

RGB_531.alg

This algorithm is a false color image which may be used to realize some lithological discrimination. TM band 5 (μm) is assigned to a red layer; band 3 (μm) to a green layer and band 1 ($0.48\ \mu\text{m}$) to a blue layer.

Example Image: examples\Shared_Data\Landsat_TM_year_1985

A GAUSSIAN EQUALIZE appears to give the desired results.

RGB_541.alg

Displays bands 5, 4, 1 as an RGB image.

RGB_541_to_HSI_to_RGB.alg

Converts bands 5, 4, 1 into Hue, Saturation, Color space from RGB space. Allows an image to be enhanced in HSI space instead of in RGB color space. ER Mapper can enhance HSI images in real-time.

Formula in the HSI layers are used to convert bands 5, 4, 1 from RGB color space to HSI color space.

RGB_542.alg

Landsat TM Composite, rgb = bands 5,4,2

RGB_741.alg

This is a false color image widely used for geological applications. TM band 7 (2.2 μm) is assigned to a red layer; band 4 (0.83 μm) to a green layer and band 1 (0.48 μm) to a blue layer.

Example Image:

examples\Shared_Data\EXAMPLES\SHARED_DATA\Landsat_TM_year_1985

The LandsatTM_rgb_321 algorithm above showed that while a near-natural image can be created, the image does not show a great deal of detail compared to other band selections. This is because generally the reflectances of terrestrial materials in adjacent spectral bands are similar.

The advantages of the LandsatTM_rgb_741 algorithm is that we achieve better color separation, improving detail and information.

A second advantage is that certain mineral groups of interest have distinctive spectral features in TM bands 7, 4 and 1.

In band 1, iron-bearing minerals have low reflectance whereas phyllosilicates, quartz, and other light coloured minerals have high reflectance. In band 7 phyllosilicates and carbonates have absorption features whereas hematite and, to a lesser extent goethite have higher responses. Therefore the 741 rgb composite allows a certain degree of lithological interpretation. Hematite-rich rock and soil is red, quartzites generally appear blue to blue-green because they are light coloured and have no iron, while limestones generally appear pale blue or lavender because of the absorption of carbonate in band 7 and their general pale colour (high in blue gun of the computer monitor).

Various cements and fracture fillings also add to the spectral responses. Fireburn scars, particularly recent ones, appear red and may be confused with hematite rich areas.

The GAUSSIAN EQUALIZE transformation was applied to each band.

RGB_Principal_Components_123.alg

Generates PC1, PC2 and PC3 and displays them as an RGB image.

RGB_Principal_Components_bands_741.alg

Generates a PC1, PC2, PC3 image using only bands 7, 4, 1 of the Landsat TM data. Because these bands show mineralogy, this can be a good image to highlight geology.

RGB_to_HSI_to_RGB.alg

A generic RGB to HSI to RGB colorspace algorithm. This algorithm has three layers (Hue, Saturation and Intensity), which are computed from the three bands selected to use as RGB. As the layers are in HSI color space, you can transform these in real time using the layer transforms. ER Mapper automatically converts HSI layers into RGB for final display.

Scan_line_noise_removal.alg

This algorithm demonstrates the removal of scan line noise removal.

Sensors_16.alg

Used by the Scan_line_noise_removal.alg to split an image into a view based on scan lines; there are 16 scan lines for Landsat TM.

Tasseled_Cap_Transforms.alg

An algorithm with three layers, each layer containing the formula for one of the tasseled cap vegetation calculations for Landsat TM:

- Wetness
- Greenness
- Brightness

Turn on the layer for the appropriate tasseled cap to see the calculation. Look at the formula for a given layer to see the exact formula used for Tasseled Cap Transformations.

Vegetation_NDVI.alg

Computes the NDVI (Normalized Difference Vegetation Index) for Landsat TM.

Vegetation_TNDVI.alg

Computes the TNDVI for Landsat TM.

These are various algorithms used to highlight vegetation. They all use the high near-infrared (NIR) reflectivity of green vegetation (band 4: 0.83um) compared to the high red chlorophyll absorption (band 3: 0.66um) to highlight vegetation.

$$\text{sqrt}(((I1 - I2) / (I1 + I2)) + 0.5)$$

$$\text{SQRT}((B4:0.83_um - B3:0.66_um) / (B4:0.83_um + B3:0.66_um)) + 0.5)$$

Example Image: examples\Shared_Data\Landsat_TM_year_1985

Note: Like most processing techniques for Landsat TM, this formula can enhance information other than vegetation, as there are materials other than vegetation that have a high spectral response in NIR and low spectral response in Red.

As dry vegetation has a different spectral response to green vegetation, this algorithm is not ideal for highlighting dry grass. The ratio of band 5 over band 7 (e.g. 1.65 um / 2.215 um) is better at highlighting dry vegetation. Unfortunately, the 5/7 ratio will also highlight hydroxides.

Magnetics_And_Radiometrics

The most common geophysical images manipulated and displayed by exploration companies are aeromagnetics, gravity and radiometrics. Such continuous tone images of gridded geophysical data interpolated from real samples preserve the information content of the raw data and are far more easily interpreted than contour maps.

These algorithms demonstrate processing airborne magnetics and radiometrics data. More examples can be found in the *applications_Mineral_Exploration* optionally installed images, which also demonstrate the processing of Landsat, DTM, SPOT, gravity, ARC/INFO and other types of data.

Aeromagnetics

Aeromagnetic measurements represent variations in the strength and direction of the Earth's magnetic field produced by rocks containing a significant amount of magnetic minerals, commonly magnetite. The shape and magnitude of an anomaly produced by one body of rock is complexly related to the body's shape, depth and magnetization.

Magnetization is determined by the amount and distribution of magnetic minerals and the magnetic properties of those minerals, which are influenced by a number of factors including the history of the rock. The location of the anomaly over the rock body is normally offset southward and is accompanied by a weak low on the northern side, called a polarity low. Anomalies on aeromagnetic maps when viewed as patterns generally express

structural, topographic, and lithologic variations. Anomalies due to crystalline rocks commonly dominate aeromagnetic maps because these rocks ordinarily are more magnetic than other rock types.

Radiometrics

Gamma-ray measurements detect the radiation emitted by radioisotopes in the near-surface rock and soil, which results from decay of the natural radioelements uranium-238, thorium-232, and potassium-40. The near-surface distribution of the natural radioelements is controlled by geologic processes, which enables the use of radioelement measurements in geologic mapping and mineral exploration.

Radiometric maps are often pseudo-geological outcrop maps or can be used for some mapping purposes.

Typically radiometrics is less affected by vegetation and agriculture than satellite data for determining soil/geology, providing a useful substitute for TM in vegetated areas or an adjunct to TM in arid areas.

Radiometric units can reflect in-situ or transported soils. Radiometric signals come from the first approximately 0.5m of soil.

The algorithms supplied with ER Mapper for geophysical data contained in the examples\Data_Types\Magnetics_And_Radiometrics directory are listed below.

Magnetics_1Q_Vertical_Derivative.alg

Shows the vertical derivative of magnetics.

Magnetics_2nd_Vertical_Derivative.alg

Shows the vertical derivative of magnetics.

Magnetics_3Q_Vertical_Derivative.alg

Shows the vertical derivative of magnetics.

Magnetics_and_Radiometrics_Colordrape.alg

Integrates surface information from Radiometrics with sub-surface information from magnetics as a colordrape algorithm.

The radiometrics Potassium count is shown in color (red is higher counts), draped over magnetics, which is shaded using real time sun-shading to show structure.

In this way, correlations between magnetics and radiometrics can be compared. On screen annotation could be carried out over this image if desired.

Magnetism_and_Vectors.alg

Shows magnetism as a simple greyscale image, with vector geology structure information in vector format over the magnetism. Vectors can be edited using the annotation tool.

Magnetism_Colordrap.e.alg

A very powerful way to show magnetism data, known as *colordrape*. In this algorithm, magnetism data is used for both color and intensity (the two layers in the algorithm). For intensity, the sun-shading for the Intensity layer has been turned on to enable structure to be easily seen.

The transform can be modified in real time for both layers (for the Pseudocolor layer, changing coloring for the image; for the Intensity layer, changing the overall image brightness); sun-shading can also be modified in real time.

Note: If this algorithm is viewed using an ER Mapper 3-D viewer or printed using ER Mapper hardcopy stereo, the Intensity layer is used for height. This makes it easy to use this algorithm for 3-D output.

Magnetism_Colordrap.e_map_legend.alg

This shows a cut-out of part of a magnetism image, as a colordrape. This algorithm is used as a legend in a map composition - the algorithm is embedded into the map. Any algorithm can be used as a legend item for a map.

Magnetism_Colordrap.e_shiny_look.alg

A demonstration of how ER Mapper's formula and algorithm processing can perform quite different results.

Magnetism data was saved as a virtual dataset, with two layers; value and structure (the same data, but with sun shading applied). This virtual dataset is used as input into the *Colordrape_shiny_look* algorithm, which uses an HSI (Hue Saturation Intensity) model to highlight the image in such a way that it has a gloss or reflectance. This is achieved by modifying the saturation of the image based on the slope of the magnetism data.

Magnetism_Colordrap.e_wet_look.alg

A demonstration of how ER Mapper's formula and algorithm processing can perform quite different results. Similar to the *Magnetism_Colordrap.e_shiny_look* algorithm, except that different transforms are used in saturation to achieve a wet look to the final image.

Magnetics data has been saved as a virtual dataset, with two layers; value and structure (the same data, but with sun shading applied). This virtual dataset is used as input into the `Colordrape_shiny_look` algorithm, which uses a HSI (Hue Saturation Intensity) model to highlight the image in such a way that it has a gloss or reflectance. This is achieved by modifying the saturation of the image based on the slope of the magnetics data.

Magnetics_Contours_from_Raster.alg

Demonstrates the use of formula to compute raster based contours from magnetics.

The general concept used for this algorithm is to:

- Scale the input magnetics into a range of integer values, one value for each contour level desired. The following formula does this:
$$(\text{CEIL}(\text{input1} / 100) * 100)$$
- Add a *Laplacian* filter after the above formula. The Laplacian filter will cause all edges to be shown as non-zero numbers, and all areas that are flat (areas between contour lines) to be zero.
- Add a *notch transform* to only show data above zero, otherwise show it as zero (which will be rejected from the classification layer).

All of the above is put into a classification layer which ‘classifies’ the image according to if a contour line should be present or not at each pixel.

For full vector based contouring, we recommend using one of the many products that do contouring with dynamic links to ER Mapper.

Magnetics_POB_Vertical_Derivative.alg

Shows POB vertical derivative from magnetics.

Magnetics_Pseudocolor.alg

This algorithm displays a magnetics image data as a single band Pseudocolor display.

The high-amplitude magnetics are shown as red and the low amplitude magnetics are shown as cooler blue-green colors.

Magnetics_Realttime_Sun_Shade.alg

This algorithm implements real time shading on a greyscale image.

Real time shade shades the aeromagnetic data as though it were topography obliquely illuminated by the sun, using a color scale (in this case greyscale) to show different values.

Magnetics_rgb_3angle.alg

An interesting algorithm that demonstrates the use of an RGB algorithm that has sun-shading turned on for each of the three layers. The sun is in a different position for each layer, with the result that structures in certain directions are shown in a certain color.

While difficult to interpret, it does have the advantage of showing all structure from a magnetics image for interpretation purposes.

Radiometrics_Magnetics_RGBI.alg

Shows radiometrics as RGB draped over a magnetics image. It enables detailed interpretation based on both the radiometrics and magnetics data.

Note: If this algorithm is viewed using an ER Mapper 3-D viewers or printed using ER Mapper hardcopy stereo, the Intensity layer is used for height. This makes it easy to use this algorithm for 3-D output.

Radiometrics_ratio_K_Th.alg

Shows Potassium over Thorium as a ratio, in color. It demonstrates the use of formula to compute data. The formula can be easily changed to show the ratio for any two bands of data.

RadarSat

Contains optionally loaded algorithms related to Radarsat

Seismic

The image dataset used in these algorithms was extracted from a Landmark seismic processing system. The image contains two channels (bands) of data: two-way time and amplitude of the reflected wave. The image is a 2-dimensional horizon, and this corresponds to a plan view of the gridded seismic data. All algorithms are in the algorithm directory 'Data_Types\Seismic'.

More complete examples using a 3D seismic survey can be found in the *application_Oil_and_Gas* optionally installed dataset directory.

Several horizon attributes can be calculated from the basic horizon time data. Two of these (dip and Azimuth) are powerful techniques for seismic interpretation. The dip is the amount of inclination of the horizon in the subsurface, and the azimuth is the direction of this inclination measured from a local reference direction, usually north. In their simplest form these attributes are given by:

$$\text{Dip} = ((dt/dx)^2 + (dt/dy)^2)^{1/2}$$

$$\text{Azimuth} = \arctan ((dt/dy) / (dt/dx))$$

Horizon_Azimuth.alg

This algorithm computes the azimuth attribute of an horizon. It is displayed using the azimuth lookup table: a 5-color Lookup Table representing the four primary directions. The additional color is required as the Lookup Table must wrap around; top and bottom colors must be the same.

The formula combines the easterly dip of the time data (dt/dx) with the northerly dip of the time data (dt/dy) to obtain the azimuth.

Example Image: examples\Shared_Data\Landmark_Seismic_Horizon

The major structural relationships are highlighted using the azimuth attribute. In particular the inter-relationship of faults and direction of throw can be determined. This is usually used in conjunction with the dip display to interpret the area.

Horizon_Colordraped.alg

This algorithm combines Pseudocolor and Intensity layers of the time data. The illumination (shading) can be edited.

Example Image: examples\Shared_Data\Landmark_Seismic_Horizon

This image combines the illumination (greyscale) with a color layer of the time data. This type of display significantly enhances the structural contours by emphasising the main structural blocks.

Horizon_Colordraped_Dip.alg

This algorithm combines a Pseudocolor time layer with either an intensity time layer with real time shading, or an intensity dip layer without real time shading. The result is similar, as the vertical illumination (intensity real time shade) is essentially the same as the dip attribute display.

The algorithm uses a step Lookup Table in Pseudocolor mode.

Example Image: examples\Shared_Data\Landmark_Seismic_Horizon

This image is similar to the seismic - colordrape result as it again is used to significantly enhance the structural contours by emphasising the main structural blocks. The step Lookup Table emphasises the structural contours.

Horizon_Colordraped_Step_LUT.alg

This algorithm combines Pseudocolor and Intensity layers of the time data with sun angle shading. It is identical to Horizon_Colordraped except that a step Lookup Table is used.

Example Image: examples\Shared_Data\Landmark_Seismic_Horizon

Horizon_Dip.alg

This algorithm computes the dip attribute of an horizon and displays it as a greyscale image. The formula combines the easterly dip of the time data (dt/dx) with the northerly dip of the time data (dt/dy) to give the true dip.

Example Image: examples\Shared_Data\Landmark_Seismic_Horizon

The major structural trends will be highlighted using the dip attribute. In particular the strike of faults can be determined. This display is usually used in conjunction with the azimuth display to interpret the area.

Horizon_IHS.alg

Horizon_Low_Amplitude.alg

Horizon_Pseudocolor.alg

This algorithm is a Pseudocolor image with the formula:

- INPUT1

Note the negative sign to invert seismic values.

Example Image: examples\Shared_Data\Landmark_Seismic_Horizon

This image is a color coded map of the basic interpreted horizon data. The data ranges from the structural highs (in red tones) to the surrounding troughs (in blue tones).

Horizon_Realtime_Sun_Shade.alg

This algorithm is a Pseudocolor image using real time shading.

Example Image: examples\Shared_Data\Landmark_Seismic_Horizon

Real time shade allows you to highlight structural lineations of interest. By varying the sun angle (both azimuth and illumination) particular features can be emphasised.

Note: The image from vertical illumination is essentially equivalent to the image using the Dip algorithm.

Once you are satisfied with the illumination direction using real time shade, the resolution of the image can be increased by changing the algorithm mode to Pseudocolor with a greyscale Lookup Table.

SPOT_Panchromatic

The HRV (High Resolution Visible) sensor is a pushbroom system designed primarily for agricultural studies, with four broad bands all in the visible region, concentrating on the spectral properties of vegetation between 0.6 and 0.8 μm .

A significant feature of the SPOT HRV sensor is that it can collect data either in the MSS mode over its image swath width (60 km) with a scene cell of 20 m, or by in-flight change convert two sensors to panchromatic sensing covering the same swath width with a scene cell of 10m resolution.

The following SPOT has been supplied by SPOT Imaging Services with the following acknowledgement:

**SPOT Imagery copyright CNES (1990)
Distribution SPOT Imaging Services, Sydney, Australia**

The algorithms supplied with ER Mapper for SPOT data in the examples\Data_Types\SPOT_Panchromatic directory are listed below.

Colorize_Regions_Over_Greyscale.alg

This algorithm ‘colors’ regions within the SPOT image, using the INREGION() formula to decide where the regions are. The colored regions are shown over the original imagery as greyscale.

Greyscale.alg

Displays SPOT Pan as a greyscale image. You can add a sharpening filter to this image to further sharpen the image.

Greyscale_Hospitals_and_Fire_Stations.alg

Table based dynamic links show hospitals and fire stations as circles over a SPOT Pan image. The tables contain the easting/northing location for each hospital and fire station.

In_Regions.alg

ER Mapper can attach vector based polygon regions to raster images. These regions can be used for statistics calculations, classification, or selecting raster data within regions.

This algorithm uses the “INREGION()” formula to show raster imagery only within certain regions.

Full conditional logic can be used, for example:

```
IF inregion(r1) AND NOT inregion(r2) THEN .....
```

Map region variables (r1, region2, etc.) into actual regions using the formula editor.

Vectors_over_Greyscale.alg

Shows vector based data over SPOT Pan imagery. The vector data can be edited.

Hybrid_contrast_stretch.alg

SPOT_xs

SPOT_XS_and_Pan_Brovey_merge.alg

Uses the Brovey transform to merge SPOT XS and SPOT Panchromatic imagery. The XS imagery is used for color and the Pan imagery for spatial sharpness.

SPOT_XS_natural_color.alg

A natural color image based on SPOT XS. This algorithm uses a weighted average of bands 2 and 3 for Green resulting in an image that shows vegetation in Green, not Red.

SPOT_XS_NDVI_colordraped_over_Pan.alg

Shows the NDVI in color calculated from SPOT XS, over SPOT Panchromatic as Intensity.

SPOT_XS_NDVI_veg_index_greyscale.alg

Computes the NDVI vegetation index from SPOT XS.

In this algorithm the vegetation indices are derived from the ratio of bands 3 and 2.

I1 / I2

B3:0.84_um / B2:0.645_um

Example Image: examples\Shared_Data\SPOT_XS

The bright areas will show the areas of vegetation (high ratio values).

SPOT_XS_rgb_321.alg

This algorithm is an RGB color composite of SPOT HRV Band 3 assigned to the Red layer, Band 2 to the Green layer and Band 1 to the Blue layer.

Example Images: examples\Shared_Data\SPOT_XS

examples\Shared_Data\SPOT_Pan

SPOT_XS_rgb_321_sharpened_with_SPOT_Pan.alg

This algorithm is an RGB color composite of SPOT HRV Band 3 assigned to the Red layer, Band 2 to the Green layer and Band 1 to the Blue layer.

It also contains an Intensity layer using SPOT Pan to sharpen the image. ER Mapper automatically converts from RGB to HSI, replaces Intensity (with the SPOT Pan data), and converts back to RGB color space.

Red, Green, Blue and Intensity can all be modified in real time with the layer transforms.

A sharper filter could be added to the intensity layer to further sharpen this image.

SPOT_XS_rotate_hue.alg

This algorithm rotates the hue.

Functions_And_Features

3D

The algorithms in this section are all related to the 3D visualization of imagery and vector data. Any data shown in 2D can also be shown in 3D, provided a suitable height component can be used - which does not have to be altitude from a DEM, although it often is.

The 3D examples can be viewed using the ER Mapper 3D viewers, and can also be printed as a stereoscopic pair by selecting the Stereo option within hardcopy.

In general, building a 3D algorithm is done with the following steps:

- 1 Define the algorithm, as a 2D view.

Include any raster imagery, vector data, dynamic links and so forth that are to be shown in the 3D view.

- 2 Add a Height layer (or several if mosaicing heights from several DEMs) to the algorithm.

Make sure height is scaled to 0-255 in the final transform - you can also use the transforms on Height layers to clip or exaggerate certain heights.

- 3 Save the algorithm.
- 4 Load the algorithm into one of the 3D ER Mapper views.

You can also print it as a stereoscopic hardcopy pair.

Note: The 3D views allow you to save your algorithm. This preserves the view position, background color, height exaggeration and other information related to your 3D view, ensuring that your next viewing of the data will be the same view.

Digital_Terrain_Map.alg

Demonstrates the use of DTM data in 3-D. This algorithm has two layers: a color layer and a height layer. The Pseudocolor color layer is the DEM, and the Height layer is also the DEM. Note that you can also use a conventional *colordrape* algorithm (with a Pseudocolor and a Intensity layer) for 3-D visualization. When a 3-D module of ER Mapper uses an algorithm without a Height layer, it will use Intensity for Height if there is an Intensity layer. Thus, any colordrape algorithm can be used for 3-D display.

The advantage of a color coded DEM in 3-D is that there are two visual clues to the DEM: the height, as shown by the 3-D module, and the color. Typically red is used to indicate high locations, and blue to indicate low locations, but any Lookup Table can be used to color code heights.

The final transform for the Pseudocolor layer could also be changed, for example to only highlight DEM values within a certain altitude range.

Landsat_over_DTM.alg

This example algorithm drapes Landsat TM satellite imagery over DEM data to provide a combined view with height from the DEM and color information from the Landsat TM data. Because Landsat TM has a 30 meter ground resolution per pixel, this type of view is only good for large regional overviews.

Note: The Landsat TM data and the DEM do not need the same resolution cell size.

Landsat_SPOT_fusion_over_DTM.alg

This example improves on the Landsat_over_DEM algorithm, by first combining the Landsat TM data with SPOT Panchromatic imagery to provide a crisper image which is then draped over the DEM.

As SPOT Pan is 10 meter resolution, and Landsat TM is 30 meter resolution, the spatial information from the SPOT imagery is combined with the spectral information from the Landsat TM imagery.

This algorithm uses the Brovey Transform to combine the Landsat and SPOT imagery, as the Brovey Transform generally provides a better result than the RGB/HSI transformation, which could also be used in this case.

Land_Use_Classification.alg

This example drapes a classified image (a Landsat TM image that has been classified into different types of land use) over a DEM image. This allows land use to be correlated with elevation, for example when looking for different types of forests, or when checking sensitive areas such as valleys for environmental impact problems.

A more sophisticated version of this algorithm could be created by defining an RGB satellite image then a Classification Display layer over the RGB image, showing the classification only in selected regions (using INREGION() in a formula). This combined image would be draped over a DEM in the Height layer, resulting in an image which shows classifications only in selected areas.

Magnetics.alg

By viewing airborne magnetics data in 3D, subtle structures within the magnetics may be more easily discerned. This algorithm is simply a colordrape algorithm - magnetics is both color and height in the algorithm.

Note: The height in this algorithm is in fact the magnetic intensity, not height of terrain. We use the magnetics field strength to indicate highs and lows. This can be done with any field based data, such as gravity maps.

Typically, vector based geology information would also be combined over this algorithm.

Note: Stereoscopic on screen viewing is particularly useful when viewing this type of data, as it shows subtle magnetic structures very well.

Radiometrics_over_Magnetics.alg

Similar to the Magnetics algorithm, except the Radiometrics channels of Potassium, Thorium and Uranium are shown in color and draped over the magnetics as height.

This is useful for correlating radiometrics information with magnetics.

Note: Instead of using raw magnetics as the height, one or more of the common geophysical filters such as upward continuations could be applied to the magnetics data before it is used as height.

Roads_and_SPOT_over_DTM.alg

Both a raster image (SPOT satellite imagery) and a vector image are draped over DEM data in this algorithm.

Any form of vector data, including dynamic links, can be draped over a 3D image.

Note: For best results the resulting 3D view should be displayed as a hardcopy stereoscopic pair rather than on-screen. This is because the vectors will be processed at hardcopy device resolution (typically very high compared to onscreen), resulting in clearly visible vectors. For on-screen viewing, the 3D image should be as high a resolution as possible.

Shaded_Digital_Terrain_Map.alg

Similar to the Digital_Terrain_Map algorithm, except the algorithm contains both a Height and an Intensity layer in addition to a Pseudocolor layer to provide color to the image.

The advantage in both a Intensity Layer (which is sun-shaded from a specified azimuth and elevation) and a Height layer is that the Intensity layer gives the feeling of a 'sun' from a certain position relative to the image, regardless of the orientation of the image in a 3D viewer. In other words, the Height layer contains a 3D sun shading source that is fixed relative to the viewer; the Intensity layer provides a form of sun shading that is fixed relative to the image.

This shaded 3D technique can be useful for creating realistic looking images, especially when combined with satellite or airphoto imagery for the color for the image. It is also handy when looking for structure - the Intensity layer would be shaded (using the sun shading window for the algorithm) to highlight structure in the desired direction.

Sin_curve.alg

This generates a test 3D image, which is a sine curve.

The actual sine image used is generated using a formula in a virtual dataset, and is an example of how to generate test data for research purposes.

SPOT_over_DTM.alg

This is a drape of SPOT Panchromatic (1 band) satellite imagery over a DEM. It gives good results for regional examination of an area.

The SPOT image could be combined with other imagery, for example Landsat imagery or a classified image, to draw attention to areas in color.

3D_multi_surface

DEM_SPOT_2_Surface.alg

Oil_and_Gas_Seismic_TWT.alg

This algorithm combines Pseudocolor and Intensity layers of the time data. The illumination (shading) can be edited.

Example Image: examples\Shared_Data\Landmark_Seismic_Horizon

This image combines the illumination (greyscale) with a color layer of the time data. This type of display significantly enhances the structural contours by emphasising the main structural blocks.

Radiometric_Magnetics_Correlation.alg

Airphoto_Tutorial

This directory contains the image data files required for the Airphoto Tutorial introduced in ER Mapper 6.2.

Class_Interactive_Compute

These algorithms demonstrate how the powerful ER Mapper formula capability can help you implement complete classification techniques using algorithms. Normally you would use Unsupervised and Supervised Classification within ER Mapper, which provide complete classification capabilities.

The following algorithms are useful for research into new classification techniques, and for conditional processing; for example, drawing on additional information as part of the classification process.

Classification Compute (using Classification layers) can be used to compute classifications. This should not be confused with displaying pre-computed classification files using Class Display.

Compute_MaxLike_Landsat_TM_1985.alg

This algorithm demonstrates how you can implement complete classification techniques using algorithms. Normally you would use Unsupervised and Supervised Classification within ER Mapper, which provide complete classification capabilities.

In this algorithm Maximum Likelihood has been implemented using formulae, with one layer in the algorithm for each class computed. Whenever ER Mapper processes an algorithm with Classification layers it assigns a pixel to the class layer with the highest number at that pixel.

This algorithm could be enhanced to carry out more sophisticated processing. For example, a Digital Elevation Model (DEM) could be added into the classification, or classification could be carried out only within certain regions.

Compute_Vegetation_over_RGB_541.alg

This algorithm demonstrates how you can implement complete classification techniques using algorithms. Normally you would use Unsupervised and Supervised Classification within ER Mapper, which provide complete classification capabilities.

In this example the algorithm contains a Landsat TM image, with bands 5,4,1 displayed as RGB. Over this is a Classification Layer which computes a vegetation index. In addition to computing the index, the Classification Layer has a conditional IF ... THEN ... ELSE statement:

```
IF NDVI > 0.25 THEN 1 ELSE NULL
```

The classification only returns true (1) if the vegetation index is greater than 0.25, indicating vigorous vegetation. Because the ELSE NULL statement causes any imagery under the classification layer to show through, where there is limited or no vegetation the backdrop Landsat TM image shows through.

This algorithm demonstrates how interactive formula processing allows complex formula to be developed and used for classification.

For example, if you had two Landsat TM images from different years and you wanted to show vegetation decrease, you could do the following to create an image to show vegetation decrease:

- Create an algorithm that computes the vegetation NDVI for the two years. There would be two layers in this algorithm, one for each year. Each layer would refer to a different image. Name the first layer NDVI_1993 and the second NDVI_1994 (or whatever the years are). Delete the final transform, to ensure that the data is not rescaled to 0..255.

- Load the `Compute_Vegetation_over_RGB_541.alg` algorithm, and change the algorithm so the RGB backdrop layers show whatever image you want as a backdrop; perhaps one of the Landsat images.
 - Load your previously saved NDVI algorithm into the Classification Layer of the algorithm (ER Mapper can load algorithms as well as images as input images for algorithms). Make sure you press **Apply - This Layer Only** to only load it into the Classification layer.
 - Change the generic formula in the Classification layer to something like the following:
- ```
IF i1 > 0.25 AND i2 < 0.25 THEN 1 ELSE NULL
```
- After mapping year one NDVI into I1, and year two NDVI into I2, the specific formula will look like:

```
IF NDVI_1993 > 0.25 AND NDVI_1994 < 0.25 THEN 1 ELSE NULL
```

In this example, we have decided to show a result if (a) the 1993 NDVI shows strong vegetation ( $NDVI_{1993} > 0.25$ ) and (b) the 1994 NDVI had a lower vegetation index than this ( $NDVI_{1994} < 0.25$ ). This modification shows vegetation only where it had decreased between 1993 and 1994.

## Classification

### `ISOCLASS_Landsat_TM_year_1985.alg`

This shows the display of classified data (using Supervised or Unsupervised Classification) as a layer of an algorithm.

---

**Note:** Before displaying classified images, you should make sure that the class colors are correct.

---

This algorithm is the most simple form of display, showing just the classified image.

More sophisticated algorithms can be built, for example:

#### **Put raster imagery behind the classified data as a backdrop**

Class Display layers are shown on top of raster layers, but under vector and dynamic link layers. If you only wish to show some classes, or show classes for some regions, you can put a raster image under the image as a backdrop.

#### **Selective display of classes**

Use the formula in a Class Display layer to only show some layers, for example:

```
IF input1 != 5 and input1 != 7 THEN input1 ELSE NULL
```

In this case, the classes would be displayed only if they are not classes 5 or 7.

#### **Clean up the classified data**

---

**Note:** You can insert a *ranking* filter, such as adaptive median, to remove small areas of classes. You must use a formula that does not reprocess the data into non-integer results, so smoothing filters (for example Average) should not be used.

---

Ranking filters replace the value with one of the other values in the neighbourhood, so can be used for cleanup.

---

**Note:** Although a “cleaner” classified image might look better, it is technically inaccurate compared to the original data. However, it is sometimes useful to clean up a classified image before running raster to vector conversion, as otherwise a lot of small polygons can be generated. Also consider enhanced classifiers.

---

### Show classes only in regions

Use the INREGION() function in formulae to only show classes within regions. For example:

```
IF inregion(r1) and not inregion(r2) THEN input1 ELSE NULL
```

## Classification\_Display

### ISOCLASS\_classification.alg

This algorithm uses the INREGION() function in formulae to only show classes within regions. For example:

```
IF inregion(r1) and not inregion(r2) THEN input1 ELSE NULL
```

## Contours

This directory has the following algorithms that demonstrate the use of contours in images:

- contours\_auto\_range.alg
- contours\_fancy.alg
- contours\_labels.alg
- contours\_line\_styles.alg
- contours\_multi\_color.alg
- contours\_thick\_lines.alg

## Data\_Fusion

Data fusion is the combination of multiple types of data into a single view. For example, sharpening a Landsat TM image with a SPOT Panchromatic image is data fusion. The following algorithms give examples of different types of data fusion.

### Brovey\_Transform.alg

The Brovey transform is a method to fuse different data together using one image; for example Landsat TM for spectral or color information, and the other image for spatial or sharpness. The technique gives very good results for Landsat TM / SPOT Panchromatic merges, resulting in a better image than a conventional HSI transformation.

The Brovey transform can be applied to any type of data.

When applied to Landsat TM / SPOT Panchromatic, the formula used is as follows:

RED:  $B5 / (B2 + B4 + B5) * SPOT$

GREEN:  $B4 / (B2 + B4 + B5) * SPOT$

BLUE:  $B2 / (B2 + B4 + B5) * SPOT$

As this formula requires input from multiple images, a *virtual dataset* containing the seven Landsat TM bands and the 1 SPOT Panchromatic band is used as input.

The normal steps to create a Brovey Transform image are:

- 1 Create a algorithm, or a virtual dataset, containing the bands from the Landsat TM and the SPOT Pan image

There is a Template algorithm that can be used. Save this algorithm (or virtual dataset).

- 2 Load the Brovey\_Transform algorithm
- 3 Change the input image to your new image

The Brovey Transform does a particularly good job of highlighting water in a natural fashion, and showing land in a natural looking image.

You can further sharpen this image by applying sharpening filters to the SPOT Pan.

---

**Note:** You do *not* have to grid the Landsat TM and SPOT into similar cell sizes - ER Mapper merges images of different cell resolutions. The virtual dataset that gives a combined view into the Landsat TM and SPOT Pan is an abstracted view of the images - it does not store an intermediate image.

---

## Brovoy\_Transform\_SPOT\_XS\_and\_Pan.alg

The Brovov transform is a method to fuse different data together using one image. For example SPOT XS for the spectral or color information, and the other image for spatial or sharpness. The technique gives very good results for SPOT XS / SPOT Panchromatic merges, resulting in a better image than a conventional HSI transformation.

The Brovov transform can be applied to any types of data.

When applied to SPOT XS / SPOT Panchromatic, the formula is as follows:

RED:  $B3 / (B1 + B2 + B3) * \text{SPOT Pan}$

GREEN:  $B2 / (B1 + B2 + B3) * \text{SPOT Pan}$

BLUE:  $B1 / (B1 + B2 + B3) * \text{SPOT Pan}$

As this formula requires input from multiple images, a *virtual dataset* containing the 3 SPOT XS bands and the 1 SPOT Panchromatic band is used as input.

The normal steps to create a Brovov Transform image are to:

- 1 Create an algorithm, or a virtual dataset, containing the bands from the SPOT XS and the SPOT Pan image.

There is a Template algorithm that can be used. Save this algorithm (or virtual dataset).

- 2 Load this Brovov\_Transform algorithm
- 3 Change the input image to your new image

The Brovov Transform does a particularly good job of highlighting water in a natural fashion and showing land in a natural looking image.

You can further sharpen this image by applying sharpening filters to the SPOT Pan input.

---

**Note:** You do *not* have to grid the SPOT XS and SPOT Pan into similar cell sizes - ER Mapper handles merging images of different cell resolutions. The virtual dataset that gives a combined view into the SPOT XS and SPOT Pan is an abstracted view into the images - it does not store an intermediate image.

---

## Landsat\_TM\_and\_SPOT\_Pan\_IHS\_merge.alg

This algorithm carries out a conventional IHS (HSI) merge of Landsat TM and SPOT Panchromatic. There are three layers in this algorithm: Hue, Saturation and Intensity. The Hue and Saturation layers have formulae in the layers to compute Hue and Saturation using three selected bands from a Landsat TM image. The Intensity layer is simply the SPOT Panchromatic.

The RGB based Landsat TM bands are converted into Hue and Saturation; Intensity uses the SPOT Pan image. ER Mapper automatically converts Hue, Saturation, Intensity layers back into RGB color space when displaying them, so you do not need to manually carry out this step.

The result is an image containing the color information from Landsat TM and sharpness from SPOT Panchromatic.

This general concept can be applied to any algorithm where one image has color information and the other has spatial information.

---

**Note:** Hue, Saturation and Intensity can be modified in real time using the Transformation dialog box.

---

To use this algorithm with your own data:

- 1 Load the algorithm
- 2 Change the input images (Landsat TM and SPOT Pan) to reflect your own data.

### Landsat\_TM\_and\_SPOT\_Pan\_RGBI.alg

This algorithm does an RGB -> HSI -> RGB merge of Landsat TM and SPOT Pan. Similar to the Landsat\_TM\_and\_SPOT\_Pan\_IHS\_merge algorithm, except ER Mapper automatically converts to and from HSI color space.

The RGB data from Landsat TM is converted into HSI space, the Intensity is replaced with the SPOT Panchromatic image, and the result is converted back to RGB space.

As SPOT Panchromatic has a higher spatial resolution than Landsat TM (10 meters versus 30 meters), the result is an image that is sharper and contains more spatial detail such as roads.

Where the Landsat\_TM\_and\_SPOT\_Pan\_IHS\_merge algorithm enables you to change Hue, Saturation and Intensity in real time, this algorithm enables you to change Red, Green, Blue and Intensity in real time. Use whichever algorithm is more appropriate.

---

**Note:** If this algorithm is viewed using an ER Mapper 3-D viewers or printed using ER Mapper hardcopy stereo, the Intensity layer is used for height.

---

## Radiometrics\_and\_Magnetics\_RGBI.alg

This algorithm does an RGB -> HSI -> RGB merge of Radiometrics (Potassium, Uranium, Thorium) and airborne Magnetics. Similar to the Landsat\_TM\_and\_SPOT\_Pan\_IHS\_merge algorithm, except ER Mapper automatically converts to and from HSI color space.

The RGB data from the Radiometrics image is converted into HSI space, the Intensity is replaced with the Magnetics image, and the result is converted back to RGB space. As the Magnetics image is field strength data, it is sun-shaded to highlight structure.

This demonstrates how to integrate two very different types of data into a single image that is still easy to understand. The color information comes from the Radiometrics, and the intensity comes from the shaded Magnetics.

Where the Landsat\_TM\_and\_SPOT\_Pan\_IHS\_merge algorithm enables you to change Hue, Saturation and Intensity in real time, this algorithm enables you to change Red, Green, Blue and Intensity in real time. Use whichever algorithm is more appropriate.

You can also change the Sun Shading position in real time in this algorithm.

---

**Note:** If this algorithm is viewed using an ER Mapper 3-D viewers or printed using ER Mapper hardcopy stereo, the Intensity layer is used for height. This makes it easy to use this algorithm for 3-D output.

---

## Sharpen\_TM\_with\_Pan.alg

This is the Brovey transform under a different name. Refer to the **Brovey\_Transform** algorithm for full details.

## SPOT\_XS\_and\_SPOT\_Pan\_RGBI.alg

This algorithm does a RGB -> HSI -> RGB merge of SPOT XS and SPOT Pan. Similar to the Landsat\_TM\_and\_SPOT\_Pan\_IHS\_merge algorithm, except ER Mapper automatically converts to and from HSI color space.

The RGB data from SPOT XS is converted into HSI space, the Intensity is replaced with the SPOT Panchromatic image, and the result is converted back to RGB space.

As SPOT Panchromatic has a higher spatial resolution than SPOT XS (10 meters versus 20 meters), the result is an image that is sharper and contains more spatial detail such as roads.

Where the Landsat\_TM\_and\_SPOT\_Pan\_IHS\_merge algorithm enables you to change Hue, Saturation and Intensity in real time, this algorithm enables you to change Red, Green, Blue and Intensity in real time. Use whichever algorithm is more appropriate.

---

**Note:** If this algorithm is viewed using an ER Mapper 3-D viewers or printed using ER Mapper hardcopy stereo, the Intensity layer is used for height. This makes it easy to use this algorithm for 3-D output.

---

### Transparent\_Airphoto\_and\_Landsat\_TM\_321.alg

This algorithm shows an airphoto overlaid onto a Landsat satellite color composite image. The airphoto has been made partially transparent.

There are two surfaces in this algorithm. The top surface is a Red Green Blue color composite airphoto. The bottom surface is a Landsat TM satellite image, with satellite bands 3, 2 and 1 in the Red, Green and Blue channels respectively. Smoothing has been set on the Landsat image.

To achieve the transparency of the airphoto, the transparency value of the airphoto surface has been set to 65%. The transparency of the airphoto can be varied at will from 0% (opaque) to 100% (totally transparent) using the Transparency slider on the Surface tab for the airphoto surface, in the Algorithm window.

## Data\_Mosaic

### Interactive\_mosaic\_of\_4\_datasets.alg

This shows the interactive mosaic capability of ER Mapper. When there is more than one layer of the same type (for example Red or Pseudocolor layers) in an algorithm, those layers are automatically mosaiced together. The images do not have to cover the same area, and do not have to have the same cell resolution.

This algorithm merges 4 different images - Landsat TM, SPOT XS, SPOT Pan and an airphoto - together into a single image.

---

**Note:** Each image has a different resolution.

---

### Virtual\_Dataset\_mosaic.alg

This algorithm demonstrates how to treat multiple images as a single image for the purposes of mosaicing. The Interactive\_mosaic\_of\_4\_datasets algorithm has been saved as a virtual dataset. No data is stored - only the algorithm describing how to recreate the data.

The virtual dataset has been used as input into this algorithm.

---

**Note:** It appears that the virtual dataset only has one band of data, which in fact is built up from four separate input images.

---

For example, this enables a transformation to be applied that affects all the input data, rather than just one of the images.

## Dynamic\_Links

ER Mapper has the powerful ability to *dynamically link* with external systems. For example, an Oracle dynamic link might run an SQL query through an Oracle based DBMS, extract the results, then display the results in a graphical format.

Dynamic links are fully documented user extendable open standards. A wide range of dynamic links are included as part of ER Mapper; more are continually being added.

### Symbols.alg

This algorithm demonstrates the use of the Tabular Data -> Symbols dynamic link.

### Tabular\_Data\_as\_Circles.alg

A simple dynamic link demonstrating taking a table of data, in this case geochemical assay values, and displaying it over imagery with the table of data shown as circles - the larger the circle, the greater the assay value.

### Truecolor\_Color\_Spiral.alg

A dynamic link demonstrating generating truecolor (24 bit color) PostScript as a layer over imagery. Any PostScript based output can be used as a dynamic link.

### User\_Example\_Dynamic\_Link.alg

An example dynamic link documented in the Customizing ER Mapper manual.

## Fft

### FFT\_Highpass\_Power\_Spectrum.alg

This algorithm applies a high-pass power spectrum to an FFT image. This algorithm can be run through the FFT inverse to highpass filter an image in the frequency domain.

### **FFT\_Lowpass\_Power\_Spectrum.alg**

This algorithm applies a low-pass power spectrum to an FFT image. This algorithm can be run through the FFT inverse to lowpass filter an image in the frequency domain.

### **FFT\_Notch\_Power\_Spectrum.alg**

This algorithm applies a notch filter power spectrum to an FFT image. This algorithm can be run through the FFT inverse to notch filter an image in the frequency domain.

### **FFT\_Power\_Spectrum.alg**

This algorithm applies a power spectrum to an FFT image. It can be used to view an FFT image.

### **Input\_Image.alg**

This algorithm shows the input image used in these FFT examples, prior to FFT processing.

### **Output\_Image\_Highpass.alg**

Shows the sample image after a highpass filter has been applied using FFTs.

### **Output\_Image\_Lowpass.alg**

Shows the sample image after a lowpass filter has been applied using FFTs.

### **Output\_Image\_Notch.alg**

Shows the sample image after a notch filter has been applied using FFTs.

## **Geocoding**

This directory contains algorithms with geocoded and non-geocoded images:

- ARC\_INFO\_vectors\_warped.alg
- Landsat\_MSS\_not\_warped.alg
- Landsat\_MSS\_over\_SPOT\_Pan\_warped.alg
- Landsat\_MSS\_warped.alg
- SPOT\_Pan\_warped.alg

## Gridding

Contains example input sources and output gridded images to demonstrate the ER Mapper Gridding Wizard

## HSI\_Transforms

### Landsat\_TM\_and\_SPOT\_Pan\_IHS\_merge.alg

This algorithm carries out a conventional IHS (HSI) merge of Landsat TM and SPOT Panchromatic. There are three layers in this algorithm: Hue, Saturation and Intensity. The Hue and Saturation layers have formulae in the layers to compute Hue and Saturation using three selected bands from a Landsat TM image. The Intensity layer is simply the SPOT Panchromatic.

The RGB based Landsat TM bands are converted into Hue and Saturation; Intensity uses the SPOT Pan image. ER Mapper automatically converts Hue, Saturation, Intensity layers back into RGB color space when displaying them, so you do not need to manually carry out this step.

The result is an image containing the color information from Landsat TM and sharpness from SPOT Panchromatic.

This general concept can be applied to any algorithm where one image has color information and the other has spatial information.

---

**Note:** Hue, Saturation and Intensity can be modified in real time using the Transformation dialog box.

---

To use this algorithm with your own data:

- 1 Load the algorithm
- 2 Change the input images (Landsat TM and SPOT Pan) to reflect your own data.

### RGB\_to\_HSI\_to\_RGB.alg

A generic RGB to HSI to RGB colorspace algorithm. This algorithm has three layers (Hue, Saturation and Intensity), which are computed from the three bands selected to use as RGB. As the layers are in HSI color space, you can transform these in real time using the layer transforms. ER Mapper automatically converts HSI layers into RGB for final display.

## Language\_Specific\_Links

- [Korean\\_Australia.alg](#)

- Korean\_Australia.kor
- Korean\_San\_Diego.alg
- Korean\_San\_Diego.kor
- Korean\_Text.alg
- Korean\_Text.kor

## Map\_Objects

### Example\_3D\_Map\_Items.alg

### Example\_Fonts.alg

Shows some of the fonts available in map composition.

### Example\_Grids.alg

Shows some of the ways that map grids (Easting Northing and Latitude Longitude) can be generated.

### Example\_Map\_Items.alg

Some of the map composition items available.

### Example\_Map\_Symbols\_\*.alg

Displays the map symbols defined by the numbers.

### Example\_North\_Arrows.alg

Some of the North Arrows supplied as standard map objects.

### Example\_Scale\_Bars.alg

Some of the Scale Bars supplied as standard map objects.

### **Example\_Symbols.alg**

### **Example\_Text.alg**

Some of the fonts - including multiple language support - available in map composition.

### **Example\_Titles.alg**

Shows different styles of text that can be used for map titles.

### **Example\_Z\_Scales.alg**

Shows some of the Z-scales (image values) available such as triangles, color strips, greyscale strips, HSI triangles, and so on.

### **Fonts.alg**

Displays a list of the fonts supported.

## **Map\_Production**

These demonstrate the use of map composition within ER Mapper.

### **Complex\_San\_Diego\_Map.alg**

A complete map which includes items such as multiple fonts, rotated text, embedded algorithms for legends, auto generated scale bars, Z-values and grids, clipped regions, and dynamic links to external vector formats.

### **Landsat\_TM\_With\_simple\_grid.alg**

A simple example of Landsat TM imagery with an EN grid.

### **Map\_Symbols\_In\_Use.alg**

This algorithm is a 'natural' color scene comprising TM bands 3-2-1 (approximately equal to red-green-blue visible light) imaged in the red-green-blue computer monitor guns respectively. An Annotation layer containing a number of map symbols is super-imposed on it.

## Newcastle\_Magnetics\_Map.alg

Simple example of a map of airborne magnetics data (colordraped), with vector data, dynamic links to external tabular data, and map composition objects on the map.

## Simple\_San\_Diego\_Map.alg

A very simple map showing two types of raster data (Landsat TM and an Airphoto), with a simple map composition created over the imagery.

## Map\_Legends

These algorithms are used as part of maps (see Map\_Production). In other words, they are included as legends within maps.

---

**Note:** Any algorithm can be used as a map legend item.

---

- Legend\_San\_Diego\_Balboa\_Park.alg
- Legend\_San\_Diego\_Brovey\_Thumb.alg
- Legend\_San\_Diego\_Downtown.alg
- Legend\_San\_Diego\_Drainage.alg
- Legend\_San\_Diego\_ISOCLASS.alg
- Legend\_San\_Diego\_Roads.alg
- Legend\_San\_Diego\_Vectors.alg

## Radar

Contains algorithms highlighting ER Mapper's radar functionality.

## Regions

### SPOT\_Pan\_in\_Regions.alg

ER Mapper can attach vector based polygon regions to raster images. These regions can be used for statistics calculations, classification, or selecting raster data within regions.

This algorithm uses the "INREGION()" formula function to show raster imagery only within certain regions.

Full conditional logic can be used, for example:

```
IF inregion(r1) AND NOT inregion(r2) THEN
```

Map region variables (r1, region2, etc.) into actual regions using the formula editor.

### **SPOT\_Pan\_in\_Regions\_over\_Landsat\_TM.alg**

ER Mapper can attach vector based polygon regions to raster images. These regions can be used for statistics calculations, classification, and selecting raster data within regions.

The “INREGION()” function in formulae can be used to show raster imagery only within certain regions.

This algorithm uses this function to show SPOT Panchromatic imagery (10 meter cell size) within certain parts of the image, and show this over the top of Landsat TM imagery (30 meter resolution).

Because both layers are Pseudocolor, ER Mapper automatically mosaics these two layers. Change the layers to Red and Green to see the example with the Landsat TM and SPOT Panchromatic imagery in different colors to highlight the interactive INREGION() processing carried out.

## **Spatial\_Filters**

### **Adaptive\_Median\_noise\_removal.alg**

The Adaptive Median filter is a high speed median filter that preserves edges.

Three median filters are generated:

#1:

```
x - x
- x -
x - x
```

#2:

```
- x -
x x x
- x -
```

#3:

```
- - -
- x -
- - -
```

And then the median is taken from these three medians.

## Aspect.alg

This algorithm demonstrates the use of the *Aspect* filter, which calculates the aspect or direction of slope for a DEM. The numbers output from the Aspect filter range from 0 to 361. Zero indicates a north facing slope, 90 indicates an east facing slope, and so on. The special number 361 is used to indicate areas that are perfectly flat (for example, water) with no aspect for the slope.

Although Aspect is useful by itself, a common use is to use formula to select only slopes facing a certain direction. For example, the following formula would only show slopes within 10 degrees of south:

```
IF input1 >=170 AND input1 <= 190 THEN 1 ELSE NULL
```

---

**Note:** For this formula to work, *input1* should be mapped to a DTM, and the input layer should have an Aspect filter applied prior to the formula.

---

## Average.alg

This filter takes an average of the cells in the filter box. The result is a blurring, or averaging, of the image.

## Brightest\_Pixel.alg

## Deviation.alg

This filter computes the mean for the box filter area, and then returns the deviation of the center pixel from this mean. In other words, it reports how different the pixel is from the neighboring pixels.

This filter can be used to highlight structure, to remove noise, and to enhance edges in an image.

## Edge\_highlight.alg

This filter is an edge enhancement filter. This particular example highlights edges from the North East. Increasing the size of the filter (this example is 3x3) will highlight only major structures and edges.

## Edge\_sharpen.alg

This 3x3 Edge sharpening filter enhances edges in the image. It can often be used to highlight roads. If this filter is added back into the original image (using a formula of  $INPUT1+INPUT2$ ) where  $INPUT1$  is the original image,  $INPUT2$  is the image with the edge sharpen filter added, it has the effect of enhancing edges in the image.

The edge sharpening filter is often known as a Laplacian filter

## Ford.alg

This filter enhanced high frequency data, such as road networks. An ideal filter for highlighting urban infrastructure

## Gaussian\_avg\_std\_dev\_1.0.alg

This filter applies a Gaussian average to the image, in this case with a standard deviation of 1.0 (other standard deviations may also be used).

This will blur an image. Unlike a standard box average filter,

this filter has a circular rolloff, and so provides a more natural averaging. Subtracting this average from the original image will result in showing high frequency changes - typically structure.

### Gaussian\_removed.alg

Demonstrates the use of a gaussian filter to show high frequency structure (for example roads or coastlines) in an image by subtracting the gaussian average filter from the original data. The formula in this algorithm is:

```
INPUT1 - INPUT2
```

Input1 is the original data, and Input2 is the original data with a gaussian filter inserted before the formula.

### Highlight\_structure.alg

Highlights structure by running two Brightest Cell ranking filters in sequence then a gaussian filter, and subtracting all of this from the original data.

### Median\_noise\_removal.alg

Applies a median filter to remove noise from an image. This filter has been implemented as a C function, which is dynamically linked into ER Mapper during algorithm execution.

Laplacian.alg

Majority.alg

Sharpen\_11x11.alg

Sharpen\_3x3.alg

### Slope\_degrees.alg

This algorithm demonstrates the use of the *Slope* filter, which calculates the slope, or steepness, for a DTM. The numbers output from the *Slope\_Degrees* filter range from 0 to 90. 0 indicates a flat area, with no slope; 90 indicates a vertical slope.

Although slope is useful by itself, a common use is to use formula to select only slopes with a maximum grade. For example, the following formula would only show slopes with less than 5 degrees of slope:

```
IF input1 <= 5 THEN input1 ELSE NULL
```

---

**Note:** For this formula to work, *input1* should be mapped to a DTM, and the input layer should have a *Slope\_degrees* filter applied prior to the formula.

---

## Sobel.alg

# Vectors\_and\_Imagery

## Vectors\_from\_Airphoto.alg

Shows an airphoto as an RGB image with vectors digitized on-screen from the airphoto as a vector layer. These vectors can be edited by clicking on the annotation toolbar icon.

## Vectors\_over\_SPOT\_Pan.alg

Shows vectors imported from USGS DLG-3 format over SPOT Panchromatic imagery. The vectors were the original data used to geocode the raster imagery in these examples. Zooming in to the vector data reveals inaccurate and incomplete data for many new areas. This vector data can be updated by clicking on the annotation toolbar icon.

## Virtual Datasets

The following algorithms demonstrate the use of virtual dataset.

## Landsat\_TM\_Cloud\_and\_Water.alg

This algorithm uses a virtual dataset which has 'cloud' and 'water' layers - true/false layers which return true if a pixel is water or cloud.

The algorithm uses this virtual dataset to classify an image to show water and cloud. Where there is no water and no cloud, the original imagery is shown as an RGB image.

## Landsat\_TM\_Cloud\_removal.alg

Demonstrates the use of virtual datasets to remove cloud. The algorithm uses two Landsat images, one with cloud, and one with no cloud. The image with cloud has the following formula for each layer:

```
IF IS_CLOUD THEN NULL ELSE INPUT1
```

This formula will result in 'null' data where there is cloud. The other Landsat image is shown under the cloudy image, so it shines through where there is cloud in the first image.

This algorithm is intended as an example to show how to remove cloud from images, and fuse multiple images together to end up with a cloud free view of an area.

---

**Note:** The formula used to decide if cloud is present considered ‘see through’ cloud to be acceptable. This formula can be changed to be more stringent in rejecting cells that are partially cloudy.

---

## Miscellaneous/Templates

### Common

These are common processing or display algorithms. A typical use is to load the algorithm and change the image to your own data.

#### **Classified\_data.alg**

Displays a classified image. This is the same as starting with a new algorithm and image window, adding a Class Display layer, and loading your classified image into the layer.

#### **Color\_coded\_intervals.alg**

An algorithm to take data (such as DTM or Magnetics), and color code the data based on intervals. For example, show all data in the range of 0 to 20 as Blue, data from 21 to 40 as Green, 41 to 60 as Yellow, and so on.

Uses Classification layers with a formula in the layer to generate the intervals.

#### **HSI\_to\_RGB.alg**

Takes data in HSI color space and converts it to RGB space. You would not normally need to do this - a simpler way is to just have Hue, Saturation and Intensity layers in your algorithm. ER Mapper will automatically convert these to RGB when displaying the results.

This algorithm is only really useful if you have data in HSI space, but want to modify the transforms in RGB space (using HSI layers would mean that you would modify the data in HSI space, which is what you normally want to do).

#### **HSI\_to\_RGB\_usercode.alg**

Uses usercode formulas to convert data from HSI components to RGB components. This is not normally necessary in ER Mapper, but can be useful for example for saving an HSI-enhanced image as red-green-blue image bands for transfer to another system.

### RGB.alg

Displays data as RGB.

### RGB\_autoscale.alg

Autoscales data as an RGB image using statistics from the image to compute an autoscale factor.

It is simpler to use a normal RGB image, and click on **Refresh Image with 99% clip on limits**  to scale the data.

### RGB\_BCET\_autoscale.alg

Autoscales data as an RGB image, using the BCET function.

It is simpler to use a normal RGB image, and click on **Refresh Image with 99% clip on limits**  to scale the data.

### RGB\_to\_HSI\_to\_RGB.alg

Takes RGB data and computes HSI. The data is shown in the algorithm as Hue, Saturation and Intensity layers.

This is useful if you have RGB based data but want to enhance it in HSI color space.

### Single\_Band\_Greyscale.alg

A one layer algorithm that displays the image as Greyscale.

## Dataset\_Output

These algorithms will replicate input data. They are used when creating output images that have been processed in some way. These algorithms do not have final transforms to ensure the data is not modified.

### Landsat\_MSS.alg

An algorithm set up with as many layers as exist in Landsat MSS data. Each layer has been named in accordance with the normal naming for this data. There are no final transforms on the layers.

### **Landsat\_TM.alg**

An algorithm set up with as many layers as exist in Landsat TM data. Each layer has been named in accordance with the normal naming for this data. There are no final transforms on the layers.

### **Landsat\_TM\_scan\_line\_noise\_removal.alg**

An algorithm set up to generate scan line noise removed TM imagery.

### **SPOT\_Pan.alg**

An algorithm set up with as many layers as exist in SPOT Pan data (one layer). The layer has been named in accordance with the normal naming for this data. There is no final transforms on the layer.

### **SPOT\_XS.alg**

An algorithm set up with as many layers as exist in SPOT XS data (3 bands). Each layer has been named in accordance with the normal naming for this data. There are no final transforms on the layers.

## **FFT**

### **First\_Vertical\_Deriv.alg**

### **First\_Vertical\_Deriv\_Power\_Spectrum.alg**

### **Highpass\_Filter.alg**

A template algorithm used to generate highpass filtered FFT imagery.

### **Lowpass\_Filter.alg**

A template algorithm used to generate lowpass filtered FFT imagery.

### **Notch\_Filter.alg**

A template algorithm used to generate notch filtered FFT imagery.

Reduce\_to\_Pole.alg

Reduce\_to\_Pole\_Power\_Spectrum.alg

Second\_Vertical\_Deriv.alg

Second\_Vertical\_Deriv\_Power\_Spectrum.alg

Vector\_Deriv.alg

Vector\_Deriv\_Power\_Spectrum.alg

Vector\_Field.alg

Vector\_Field\_Power\_Spectrum.alg

Vertical\_Continuation.alg

## Vertical\_Continuation\_Power\_Spectrum.alg

### Virtual\_Datasets

These algorithms are used to generate virtual datasets; these are processed versions of data. For example, a virtual dataset might be used to create an 8 band virtual dataset containing the 7 Landsat TM bands and the 1 SPOT Pan band, giving in effect a virtual 8 band 10 meter resolution image.

Typical use for these algorithms is to load the algorithm, change the layers to reflect your own data, then save the resultant algorithm as a virtual dataset or as another algorithm.

### DEM\_Height\_Slope\_Aspect.alg

For a DEM (DTM) elevation image, this algorithm generates a three layer view into the data:

- Height - the original height data in the DTM
- Aspect - direction of slope in the DTM
- Slope - the steepness of slope in the DTM

A virtual dataset (or algorithm) created using this template can be used in conditional formula; for example to only show areas with a certain slope and aspect.

### Landsat\_TM\_and\_SPOT\_Pan.alg

An eight band algorithm that contains 7 layers used to input Landsat TM data, and one band used to input SPOT Pan data.

This algorithm is used as input into other algorithms that require access to both Landsat and SPOT data within a single formula - the Brovey transform is an example.

### Landsat\_TM\_PC1-6\_HistEq.alg

Gives a histogram equalized view into PCs 1 to 6 for Landsat TM.

### Landsat\_TM\_transformations.alg

### Landsat\_TM\_two\_years.alg

A 14 band (layer) algorithm used when formula requiring input from two Landsat TM images (such as for change detection) is required.

### **LandVD\_TM\_transformations.alg**

### **Magnetics\_uc1\_and\_full.alg**

Generates 1/2 and full upward continuations for Magnetics data.

### **Magnetics\_uch\_and\_dch.alg**

### **Magnetics\_uch\_and\_full.alg**

### **Magnetics\_uch\_full\_and\_dch.alg**

### **RGB\_to\_HSI.alg**

Takes RGB data and generates a view into the data that is HSI based.

### **Test\_Patterns.alg**

Generates various test patterns. Each test pattern is a layer (band) of the algorithm.

## **Miscellaneous/Test\_Patterns**

### **3D\_Cube.alg**

### **HSI\_wheel.alg**

Generates an HSI color wheel. Useful for balancing hardcopy output with screen colors.

### **3D\_Julia\_Fractals.alg**

Demonstrates the use of a C based formula to compute the Julia fractal.

### **rgbcmyk\_bands.alg**

Generates an RGBCMYK color strip. Useful for balancing hardcopy output with screen colors.

## Test\_Patterns.alg

An algorithm demonstrating the use of a virtual dataset that generates test patterns. Most of these test patterns are created using formula within each layer of the virtual dataset. This is useful for research purposes to test algorithms against specific test patterns.

The virtual dataset contains the following test pattern bands:

- Sine wave
- Linear Scale
- Checker board
- Cross hatch
- Diagonal triangles
- Random

The algorithm displays an addition of the Sine wave with Random, to result in a sine pattern with random variations.

## Shared\_Data

This directory, and those below it, contain common image datasets used by the example algorithms.

# Supplied Filters

A filter (or kernel) is defined in ER Mapper to be an operation that processes a cell based on the cells which are surrounding it in the spatial domain. Filters supported are convolutions (e.g. average filters) and threshold filters (convolution with threshold).

Filters are applied by choosing the **Filter** button from the process diagram in the **Algorithm** dialog box for the current layer.

Filters are text files and are located in the kernel directory. Please refer to kernel directory for details about a particular filter.

As well as the filters provided with ER Mapper, it is important to note that it is possible to use other types of filters. See Chapter 12, “Filter files (.ker)” in the *Customizing ER Mapper* manual for more information on filter formats.

Some of the filters provided with ER Mapper are described below.

## DEM filters

### **aspect**

Calculates aspect in degrees from North.

### **slope**

Calculates the slope from 0 to 200%

### **slope\_degrees**

Calculates the slope from 0 to 90 degrees.

## Edge filters

### **Different**

This filter uses graphical convolution to highlight differences in contour algorithms. The filter used is:

```
-1 -1 0
-1 3 0
 0 0 0
```

Scale factor = 1

### **Gradient\_X**

This filter uses graphical convolution to highlight the gradient in the X direction. The filter used is:

```
0 -1 1
```

Scale factor = 1

### **Gradient\_Y**

This filter uses graphical convolution to highlight the gradient in the Y direction. The filter used is:

```
0
-1
 1
```

Scale factor = 1

## Gaussian filters

### **std\_dev\_0.391**

Standard deviation = 0.391

**std\_dev\_0.625**

Standard deviation = 0.625

**std\_dev\_1.0**

Standard deviation = 1.0

**std\_dev\_1.6**

Standard deviation = 1.6

## Geophysics filters

### Frequency filters

These are derived pass filters at spectral wavelengths of approximately a multiple of grid spacing. They are useful in some cases for removing surface noise from aeromagnetic data.

**high\_pass\_4.** This filter passes high frequency (low wavelength data with wavelength less than or equal to approximately four times the grid spacing). Removes low frequency data with wavelengths greater than 4 times the grid cell size.

Used to remove deeper/broader (regional) features allowing analysis of shallow/narrower features.

**low\_pass\_4.** Removes high frequency data with wavelengths smaller than 4 times the grid cell size. Used to remove shallow/narrower features allowing analysis of deeper/broader (regional) features. High frequency data may be mostly noise depending on wavelength so can be used to remove noise in some cases.

**bandpass\_3\_5.** Band pass filters remove wavelengths below a minimum wavelength and above a maximum wavelength. In this case wavelengths longer than 5 grid cells and wavelengths shorter than 3 grid cells will be removed. Another way of stating the result is that wavelengths between 3 and 5 grid cells will remain for analysis.

Used to enhance features of a particular wavelength ie. features from/with a particular depth/width Used most commonly in the seismic business.

## Continuation filters

**down\_cont\_1, down\_cont\_2, down\_cont\_half, downhalf.** These are the only true geophysical frequency filters for enhancing low or high frequency, deep or near surface sources respectively.

Downward Continuation of potential field data such as gravity or magnetics. These filters transform the data by shifting the point of observation down vertically. They calculate what the field measured at one flight height (say 300m) would be if it had been measured at a lower flight height (say 100m).

The filter values `_1`, `_2`, `half` refer to the vertical continuation distance in numbers of grid cells.

Downward Continuation is used to enhance near surface or high frequency features in the data. Continuation should not be done below ground level as the algorithm becomes unstable.

**up\_cont\_1, up\_cont\_2, up\_cont\_half.** Upward Continuation of potential field data such as gravity or magnetics. These filters transform the data by shifting the point of observation up vertically. They calculate what the field measured at one height (say 2m i.e. ground survey) would be if it had been measured at a higher flight height (say 100m).

The filter values `_1`, `_2`, `half` refer to the vertical continuation distance in numbers of grid cells.

Upward Continuation is used to suppress near surface or high frequency features in the data. It can be useful for suppressing noise caused by magnetite/maghemite in soils in ground magnetic surveys. Median filters are also effective for removing noise spikes in these kinds of surveys.

## Derivative filters

Horizontal and vertical first and second derivative filters are also in common use for calculating gradients of magnetic and gravity fields.

**Horizontal.** The horizontal derivative is the rate of change of values in the horizontal plane i.e. from 1 pixel to the next. The simple filter `[-1,0,1]` calculates an EW horizontal derivative at the centre pixel by subtracting the two outside pixels from each other. To calculate the true horizontal gradient it is necessary to divide the result by the horizontal distance between the two outside pixels (nt/metre).

This filter is also referred to as a NS edge detection filter.

Application of this filter to the result of the above will produce the EW 2nd horizontal derivative i.e. the gradient of the gradient.

**Vertical.** The first vertical derivative or vertical gradient is the rate of change of values in the vertical plane ie.height. Therefore a vertical derivative can be roughly simulated in ER Mapper using the difference between two continuation filters. For instance a value upward continued to 100m minus a value upward continued to 200m will give the change in field per 100m vertically. Dividing by 100 will give the vertical gradient (nt/metre).

These filters have been written up in the EMU USERS GROUP EMU Forum Volume 2 issue 2. They are implemented as algorithms and use the virtual dataset feature and are named `Magnetics_vds.ers` and `Magnetics_quarter_deriv.alg`.

**Second Derivative.** The derivative filters supplied are from Henderson and Zeitz (Fuller,1967). These filters are used for edge enhancement and crude sunangle effects.

## Residual

Residual filters highlight local anomalous values.

## Edge

Edge enhancement filters.

# High pass averaging filters

## Ford

This is a convolution filter designed to enhance high-frequency detail of images. It is very useful for urban areas. For more information on the design of this filter, reference the author's article in:

Ford, G. E., V.R. Algazi, and D. I. Meyer, 1983. "A Noninteractive Procedure for Land Use Determination," *Remote Sensing of Environment*, Vol. 13, pp. 1-16.

## Sharpedge

3x3 edge sharpen filter using the following array.

```
-1 -1 -1
-1 8 -1
-1 -1 -1
```

Scale factor = 1

### highpass\_1x33

High pass (central minus filter window mean).

### Sharpen11

11x11 high pass filter using the following array:

```
-1 -1 -1 -1 -1 -1 -1 -1 -1 -1 -1
-1 -1 -1 -1 -1 -1 -1 -1 -1 -1 -1
-1 -1 -1 -1 -1 -1 -1 -1 -1 -1 -1
-1 -1 -1 -1 -1 -1 -1 -1 -1 -1 -1
-1 -1 -1 -1 -1 -1 -1 -1 -1 -1 -1
-1 -1 -1 -1 -1 241 -1 -1 -1 -1 -1
-1 -1 -1 -1 -1 -1 -1 -1 -1 -1 -1
-1 -1 -1 -1 -1 -1 -1 -1 -1 -1 -1
-1 -1 -1 -1 -1 -1 -1 -1 -1 -1 -1
-1 -1 -1 -1 -1 -1 -1 -1 -1 -1 -1
-1 -1 -1 -1 -1 -1 -1 -1 -1 -1 -1
```

Scale factor =121

### Sharpen2

General edge sharpening filter using the following array:

```
-1 -1 -1
-1 14 -1
-1 -1 -1
```

Scale factor = 6

## Low pass averaging filters

The low-pass averaging filters are used to smooth data noise and gridding artifacts. For example, radiometric data may need an averaging filter before applying a sun angle filter.

### avgx

These averaging filters average each pixel based upon surrounding pixels. The 'x' in the filter name is the dimension of the square filter. For example, 'avg3.ker' filter is a 3 x 3 matrix. The larger the dimension of the filter the greater the smoothing effect will be.

```

1 1 1
1 1 1
1 1 1

```

Scale factor = 9

Non-square filters have both dimensions in their name, for example 'avg\_33x1.ker'.

### avg\_diag

The diagonal average filter includes the four corner neighbor pixels in the average:

```

1 0 1
0 1 0
1 0 1

```

Scale factor = 5

### avg\_hor

The horizontal average includes right and left neighbor pixels in the average:

```

0 0 0
1 1 1
0 0 0

```

Scale factor = 3

### avg\_ver

The vertical average filter includes the pixels above and below:

```

0 1 0
0 1 0
0 1 0

```

Scale factor = 3

### avg\_h\_v

The avg\_h\_v average filter includes the horizontal and vertical neighbors of the pixel in the average.

```

0 1 0
1 1 1
0 1 0

```

Scale factor = 5

## **eps**

The description of the "Edge Preserving Smoothing" filter can be found in:

Nagao, M. and T. Matsuyama. 1979. Edge Preserving Smoothing. Computer Graphics and Image Processing, vol. 9, pp. 394-407.

This filter uses a 5 x 5 moving window. Within the window, it looks at a series of "subwindows" (north, south, east, west, northeast, southeast, northwest, and southwest). It then replaces the central pixel of the window with the mean of the most homogeneous subwindow (that is, the subwindow with the lowest variance).

# Ranking filters

## **adaptive\_median\_5x5**

This is a high-speed adaptive median filter; being three medians, then the median of the three results.

## **brightest\_pixel\_5x5**

This filter returns the brightest pixel in the kernel

## **darkest\_pixel\_5x5**

This filter returns the darkest pixel in the kernel

## **deviation\_3x3**

Deviation filter

## **deviation\_5x5**

Deviation filter

## **majority.ker**

This filter is used for smoothing classified images. It replaces the one central pixel with the majority class.

## **median\_11x11**

This filter calculates median values

**median\_3x3**

Median filter

**median\_5x5**

Median filter

## SAR filters

**adaptive\_median\_5x5**

This is a high-speed adaptive median filter; being three medians, then the median of the three results. This filter differs from the `adaptive_median_5x5` Ranking filter in that it is applied before the dataset is subsampled.

**average\_5x5**

This is a 5x5 averaging filter which uses the following array:

```

1 1 1 1 1
1 1 1 1 1
1 1 1 1 1
1 1 1 1 1
1 1 1 1 1
1 1 1 1 1

```

Scale factor = 25

**median\_5x5**

This median filter is applied before any data subsampling takes place.

**std\_dev\_0.625**

This is a Gaussian: Standard Deviation=0.625 filter which is applied before any data subsampling takes place.

**std\_dev\_1.6**

This is a Gaussian: Standard Deviation=0.625 filter which is applied before any data subsampling takes place.

frost

glcm\_contrast\_u

glcm\_dissimilar

glcm\_entropy\_u

glcm\_homo\_u

glcm\_inv\_moments\_1\_u

glcm\_inv\_moments\_2\_u

glcm\_inv\_moments\_3\_u

glcm\_max\_prob\_u

glcm\_mean

glcm\_moments\_1\_u

glcm\_moments\_2\_u

glcm\_moments\_3\_u

glcm\_std\_dev\_u

glcm\_uniform\_u

lee

leek

lees

mtf

mtfk

mtfs

sarsim\_u

sigma\_u

## Seismic

### Easterly\_dip

This filter uses graphical convolution to highlight easterly dips.. The filter used is:

|    |   |   |
|----|---|---|
| 0  | 0 | 0 |
| -1 | 0 | 1 |
| 0  | 0 | 0 |

Scale factor = 1

### Hanning\_3

The Hanning 3x3 filter used is:

```
.06 0.10 0.06
0.10 0.36 0.10
.06 0.10 0.06
```

Scale factor = 1

### Northerly\_dip

This filter uses graphical convolution to highlight northerly dips.. The filter used is:

```
0 1 0
0 0 0
0 -1 0
```

Scale factor = 1

## Standard Filters

### Sobel1

The Sobell 3x3 kernel filter used is:

```
1 2 1
0 0 0
-1 -2 -1
```

Scale factor = 1

### Sobel2

The Sobell 3x3 kernel filter used is:

```
-1 0 1
-2 0 2
-1 0 1
```

Scale factor = 1

**darn**

This filter uses graphical convolution to highlight darn holes. The filter used is:

```
-1 0 -1 0 -1
0 2 2 2 0
-1 2 -8 2 -1
0 2 2 2 0
-1 0 -1 0 -1
```

Scale factor = 8

**default**

This as the default filter having a single cell with a value of 1.

**force\_nosubs**

This default filter forces no subsampling.

**h\_edge**

Horizontal edge operation uses graphical convolution to highlight horizontal edges (but not vertical ones). The filter used is:

```
-1 -1 -1
0 0 0
1 1 1
```

Scale factor = 1

**h\_edge\_5.ker**

Horizontal edge operation uses graphical convolution to highlight horizontal edges (but not vertical ones). The filter used is:

```
-1 -1 -1 -1 -1
0 0 0 0 0
0 0 0 0 0
0 0 0 0 0
1 1 1 1 1
```

Scale factor = 1

### lap\_clean.ker

The laplacian operation uses graphical convolution to highlight clean edges. The filter used is:

```
-1 -1 -1
-1 17 -1
-1 -1 -1
```

Scale factor = 9

### laplacian.ker

The laplacian operation uses graphical convolution to highlight outline edges. The filter used is:

```
-1 -1 -1
-1 8 -1
-1 -1 -1
```

Scale factor = 1

### laplacian5.ker

A 5x5 laplacian filter. The filter used is:

```
-1 -1 -1 -1 -1
-1 -1 -1 -1 -1
-1 -1 25 -1 -1
-1 -1 -1 -1 -1
-1 -1 -1 -1 -1
```

Scale factor = 1

### low\_freq

Low frequency filter highlights unchanging areas. The filter used is:

```
-1 -1 -1
-1 1 -1
-1 -1 -1
```

**sharpen**

This operation uses graphical convolution to accentuate the differences between the centre pixel and the surrounding ones.

```
-1 -1 -1
-1 9 -1
-1 -1 -1
```

Scale factor = 1

**thresh3.ker**

A 3x3 averaging filter with a threshold = 5. The filter used is:

```
1 1 1
1 1 1
1 1 1
```

Scale factor = 1

Threshold = 5

**thresh5.ker**

A 5x5 averaging filter with a threshold = 5. The filter used is:

```
1 1 1 1 1
1 1 1 1 1
1 1 1 1 1
```

Scale factor = 1

Threshold = 5

**v\_edge**

Uses graphical convolution to highlight vertical edges (but not the horizontal ones). The filter used is:

```
-1 0 1
-1 0 1
-1 -0 1
```

Scale factor = 1

### **v\_edge\_5**

Uses graphical convolution to highlight vertical edges (but not the horizontal ones).  
The filter used is:

```
-1 0 0 0 1
-1 0 0 0 1
-1 0 0 0 1
-1 0 0 0 1
-1 0 0 0 1
```

Scale factor = 1

## **Sunangle Filters**

### **East\_West**

3x3 East West sun filter using the following array:

```
-1 0 1
-1 0 1
-1 0 1
```

### **North\_East**

3x3 North East sun filter using the following array:

```
0 -1 -1
1 0 -1
1 1 0
```

### **North\_South**

3x3 North South sun filter using the following array:

```
-1 -1 -1
0 0 0
1 1 1
```

### **North\_West**

3x3 North West sun filter using the following array:

```
-1 -1 0
-1 0 1
0 1 1
```

## North\_West\_5

5x5 North West sun filter using the following array:

|    |    |    |    |   |
|----|----|----|----|---|
| 0  | 0  | -1 | -1 | 0 |
| 0  | -1 | -1 | 0  | 1 |
| -1 | -1 | 0  | 1  | 1 |
| -1 | 0  | 1  | 1  | 0 |
| 0  | 1  | 1  | 0  | 0 |
| -1 | -1 | -1 | -1 | 0 |
| -1 | -1 | -1 | 0  | 1 |
| -1 | -1 | 0  | 1  | 1 |
| -1 | 0  | 1  | 1  | 1 |
| 0  | 1  | 1  | 1  | 1 |

## South\_East

3x3 South East sun filter using the following array:

|   |    |    |
|---|----|----|
| 1 | 1  | 0  |
| 1 | 0  | -1 |
| 0 | -1 | -1 |

## South\_North

3x3 South North sun filter using the following array:

|    |    |    |
|----|----|----|
| 1  | 1  | 1  |
| 1  | 0  | 0  |
| -1 | -1 | -1 |

## South\_West

3x3 South West sun filter using the following array:

|    |    |   |
|----|----|---|
| 0  | 1  | 1 |
| -1 | 0  | 1 |
| -1 | -1 | 0 |

## West\_East

3x3 West East sun filter using the following array:

|   |   |    |
|---|---|----|
| 1 | 0 | -1 |
| 1 | 0 | -1 |
| 1 | 0 | -1 |

# Usercode

## **average**

Averaging filter written in C.

## **kernel.template**

A template file for crating user defined C filters

## **local\_enhance**

Does a local histogram equalise on the data, accepting any range of input data and outputting values between 0 and 255.

## **majority**

This kernel can be used for smoothing classified images. It calculates the majority class within the kernel window. If the class of the central cell is different from the majority, it is changed to the majority. If there is no majority class the central cell is left unchanged. This filter is typically used for smoothing classified images. An average filter is inappropriate because the values are just labels and have no numerical relationship (the average of classes 2 and 4 is not class 3!)

## **median**

Median filter written in C

## **modefilt**

The mode filter replaces a pixel value by the majority value in the kernel.

It is a suitable filter to smooth a classification image as there is no numerical calculation involved in the filtering.

## **rm2badli**

Removes two bad lines using a conditional filter

## **rmbadlin**

Removes bad lines using a conditional filter

### **w\_loc\_me**

This filter adjusts the local mean values to a given DN value (110) without changing the local contrast. A user specified kernel (31\*31 by default) is used to calculate and adjust the local mean values. Square root distance to the central pixel is used as the weight of the contribution of each neighbour pixel in order to reduce the edge effects.

This technique can enhance the texture information of very bright and very dark image areas. It is useful for analysing the textures of high contrast images.





# Index

## Numerics

- 2-D seismic data 145
- 3-D example algorithms 332
- 3-D perspective viewing 49
- 3-D seismic data 145
- 3-D seismic two-way-time horizons, displaying 26
- 3-D viewing 343
  - 3-D flythrough 49
  - algorithm 325, 327
  - draping vectors 49
  - fallback modes 49
  - height layers 49
  - stereo 50, 334
  - sun shading 335
  - texture mapping 49
  - view position 49
- 3-D visualization 332

## A

- Abrams\_Ratios.alg 316
- abstracted views into DEMs 54
- abstracting data 52
- accuracy and calibration of radiometric data 139
- accuracy assessment of classifications 82, 93
- acid rain 233, 240

## Index

- adaptive\_median\_5x5 filter 370, 371
- Advanced Very High Resolution Radiometer 252
- aerial photography 211, 212, 222, 228
- aeromagnetic surveys 159
- aeromagnetism 323, 343
  - algorithms 323
  - merging with radiometrics data 26
  - semi-automatic interpretation 159
- AGC 136
- agricultural development, application of remote sensing 218, 228
- agriculture, application of classification 79
- airborne electromagnetics data 123, 150
- airborne radar 244
- aircraft altitude 140
- aircraft altitude effects 139
- airphoto example algorithms 307
- Airphoto\_and\_Landsat\_TM\_and\_Vectors.alg 308
- Airphoto\_with\_roads.alg 309
- Alaska, remote sensing applications in 238
- albedo 317
- albedo effects, eliminating with band ratios 100
- algorithm examples
  - 3-D 332
  - airphotos 307
  - ARC/INFO 308
  - classification 336
  - data fusion or merging 340
  - digital elevation 309
  - dynamic links 345
  - FFT 345
  - geophysics 323, 324
  - gridding 347
  - Landsat MSS 313
  - Landsat TM 315
  - map composition 348
  - map legends 350
  - processing kernels 351
  - raster and vector integration 355
  - regions 350
  - seismic 327
  - SPOT Pan 330
  - SPOT XS 331
  - test patterns 355
  - virtual datasets 355
- algorithm templates
  - common 356

- dataset output 357
  - FFT 358
  - virtual datasets 360
- algorithms supplied with ER Mapper 303
- alteration mapping 205
- alteration zones 207
- AML scripts, used to integrate data with ER Mapper 35
- annotating images 137, 230, 308
- annotation
  - editing cultural vector data 285
- anomaly shape 138
- ARC/INFO data importing and dynamic links 123
- ARC/INFO example algorithms 308
- ARC/INFO viewing 308
- ARC/PLOT based dynamic link 308
- ARC/PLOT scripts, used to integrate data in ER Mapper 35
- Archaean 176
- area inventory using classification 79
- area specific stretch 318
- argillyzed 207
- arid areas, problems with vegetation indices 114
- artifacts, errors in DEMs 41
- artifacts, from data levelling 138
- ARVI vegetation index 110
- aspect 310, 360
- ASPECT filter 55
- aspect filter 363
- aspect from DEMs 52, 53
- aspect, in fire risk 57
- Aspect.alg 310, 352
- atmospheric effects, eliminating 73
- atmospheric noise 109
- atmospherically resistant indices 110
- Atmospherically Resistant Vegetation Index 110
- attribute data
  - colordrapping over two-way time structure 146
  - highlighting within a region 33
- attribute highlighting 24, 31
- Australia\_Colordrape.alg 311
- AutoCAD 215
- AutoCAD DXF, exporting to 286
- automatic data fusion 22
- average filter 380
- average\_5x5 filter 371
- averaging filters 47, 368
- avg\_diag filter 369

## Index

avg\_h\_v filter 369  
avg\_hor filter 369  
avg\_ver filter 369  
AVHRR data 97, 240, 252  
Azimuth 328  
azimuth displays in seismic 146

## B

backdrop images 24  
Baltic Sea, remote sensing applications in 233  
band ratios for detecting change 74  
band ratios to eliminate albedo effects and shadows 100  
bandpass\_3\_5 filter 365  
bands for showing vegetation 100  
barley, classification of 219  
bathymetry data 151  
    displaying 26  
    integration into ER Mapper 224  
BCET 357  
BIL (Binary Interleaved by Line) image file format 66  
bio-optical algorithms 234  
blaze 238  
Boreal forest project 239  
borehole depths 123  
borehole locations 124  
Bouguer density 148  
brightest\_pixel\_5x5 filter 370  
brightness 318, 322  
Brightness layer 314  
brightness of vegetation 315, 316  
Brightness temperature values 255  
Brovey transform 28, 331, 341  
    algorithm 31  
    RGBI data fusion 29  
Brovey transform algorithm 340  
Brovey\_Transform.alg 340  
Brovey\_Transform\_SPOT\_XS\_and\_Pan.alg 341  
byte order 66

## C

C program for dynamic links 171  
C/Fortran user code 136  
Canada, remote sensing applications in 212

- carbonates 321
- cartographic applications 211
- Cell Values Profile 230
- centre pivot irrigation 218
- centreline network updating 67
- change detection 67
  - using band ratios 74
- change image, creating 74
- Charisma 2D XYZ ASCII grid import 268, 272
- Charisma 3D Inline Xline XYZ ASCII grid import 268, 273
- Checker board test pattern 362
- chlorophyll 112, 323
- chlorophyll concentration 235
- classification
  - accuracy assessment 93
  - displaying results 92, 338
  - for crop yield estimation 219
  - for erosion, siltation and lake capacity monitoring 229
  - for irrigation requirements analysis 219
  - in forestry 240
  - maximum likelihood classifier 88
  - methodology 90
  - multispectral 81
  - of crop type 79
  - of fire risk 58
  - of geophysical data 143
  - of marine habitats 225
  - real-time 92
  - schema 83
  - typicality thresholds 91
  - unsupervised 92
  - using DEM data 59
  - weighting classes 91
- classification example algorithms 336
- classification highlighting 34
- Classification layers
  - used to highlight 32
- classification techniques using algorithms 336
- classification-height images 51
- classified images
  - algorithm 356
  - comparing 33
  - merging with airphotos and satellite imagery 26
  - viewing in 3-D over a DEM 334
- Classified\_data.alg 356
- clay 316

## Index

- clay mineral-carbonate 316
- clay types 142
- Clay\_ratio.alg 316
- cloud 355
- cloud removal 241, 355
- clouds, penetrating with radar 243
- coastal habitat mapping 221
- color and intensity, using to merge datasets 23
- color highlighting 34
- color perception 127
- color strips 349
- Color\_coded\_intervals.alg 356
- colordrape images 51
  - algorithms 311, 325
  - for displaying DEMs 44
  - for displaying geophysical data 131
  - in 3-D viewing 334
- Colordrape.alg 311
- Colordrape\_Greeness\_over\_Brightness.alg 316
- Colordrape\_NDVI\_over\_PC1.alg 316
- Colordrape\_shiny\_look.alg 311
- colordraping
  - tips 299
- Colordraping, using to view oil and gas data 297
- Colorize\_Regions\_Over\_Greyscale.alg 330
- combined geochemical data 156
- combining data for what-if processing 52
- combining data, see merging data
- combining images 297
- common algorithm templates 356
- comparing results using normalised difference image 72
- comparing two classified images 33
- complex numbers in Fourier processing 202
- Complex\_San\_Diego\_Map.alg 349
- Compute\_MaxLike\_Landsat\_TM\_1985.alg 337
- Compute\_Vegetation\_over\_RGB\_541.alg 337
- continuation filters 134
- contours 125
  - generating a DEM from 40
  - of geophysical data 124
  - raster line generation 48, 312, 326
- Contours\_from\_Raster.alg 312
- convolution filter 377
- copper 156
- correcting SAR data with DEMs 59
- correlations between magnetics and radiometrics 324

- creating a change image 74
- crop
  - canopy 85
  - condition 79
  - production 219
  - production monitoring 217
  - type classification 79
- crop calendar considerations for classification 93
- crop circles 218
- crop discrimination 84
- crop signatures 84
- crop yield estimation 219
- Cross hatch test pattern 362
- Crosta technique 205
- cubic convolution resampling 71
- cultural vector data, updating in ER Mapper 285
- Custom-built Dynamic Links 167
- customizing forestry applications 239

## D

- darkest\_pixel\_5x5 filter 370
- darn filter 375
- data
  - enhancement 69
  - ERS-1 SAR imagery 243, 244
  - geophysical 124
  - satellite imagery 223, 252
  - scanned 223
  - smoothing 127
  - sources 68
  - storage considerations 170
  - two-way time 145
- data currency 67
- data fusion
  - formulas for 36
  - using color and intensity 24
  - using region highlighting 33
- data gathering 212
- data integration 211
  - bathymetry 224
  - geophysical 168
  - raster and vector 51
  - raster and vector algorithms 355
- data inversion formulas 296

## Index

- data levelling artefacts 138
- data merging
  - example algorithms 340
- data mosaicing 22
  - formulas for 36
- data. See also particular data types
- dataset output algorithms 357
- dataset resolution 22
- datasets
  - creating different views for the same data 24
  - displaying with color and intensity 23
  - merging or fusing 21
- decorrelation stretch 317
- Decorrelation\_Stretch.alg 317
- DEM\_HEIGHT filter 55
- DEM\_Height\_Slope\_Aspect.alg 360
- demographics 214
- DEMs 39
  - applications 42
  - aspect from 52
  - bounding with polygon regions 47, 54
  - combining with other data for classification 52
  - combining with other data for what-if processing 52
  - correcting SAR data with 59
  - creating 40
  - displaying and processing 41, 43
  - in 3-D viewing 334
  - integrating with other data 50
  - mosaicing 46
  - processing 51
  - range of height from 52, 53
  - selecting values within certain regions 52
  - slope 52
  - smoothing 47
  - sources and quality 40
  - steepness 52
  - using for classification 59
- depression angle, of radar data (SAR) 244
- depth estimates 162
- derivative filters 366
- detecting change 67
- development applications 212
- deviation filters 370
- DGN data import 123
- diagonal average filter 369
- Diagonal triangles test pattern 362

- Difference Vegetation Index 105
- different filter 364
- different views from the same data 24
- digital elevation example algorithms 309
- Digital Elevation Models 39
- Digital Terrain 309
  - viewing in 3-D 333
- Digital\_Terrain\_Map.alg 333
- Dip 328
- dip and azimuth displays in seismic 146
- dip computation from a DTM 312
- Dip.alg 312
- directional filters 133, 309
- discrete transform in Fourier processing 201
- disk space
  - minimizing with virtual datasets 54
- display of transforms in Fourier processing 202
- displaying and processing DEMs 41, 43
- displaying classification results 92, 338
- displaying images 82
- down\_cont filters 366
- downward continuation filter 132, 366
- drainage, remote sensing application 213
- drill hole traces 175
- drilling isopach maps 163
- drilling programs 176
- DTM data in 3-D 333
- DVI vegetation index 105
- DXF data 64, 145
- DXF data import and dynamic link 123
- dye sublimation printer 80
- dyke 161
- dyke models 163
- dynamic link construction 171
- dynamic links example algorithms 345
- dynamic links from multiple sources 62
- dynamic links to user code 149
- dynamic links to vector data and GIS 123
- dynamic links, custom built to geology databases 167
- dynamic operation within ER Mapper 172

## E

- East\_West filter 378
- easterly\_dip filter 373

## Index

- Eastern Europe 233
- Easting Northing map grids 348
- edge effects in Fourier processing 200
- edge enhancement filters 47, 133, 193
- edge shading filter 312
- Edge\_Shade\_from\_NE.alg 317
- Edge\_Shaded.alg 312
- Edit Class/Region Color and Name 90
- effect of aircraft altitude 139
- effect of depth on anomaly shape 138
- electromagnetic data 123, 150
  - imaging 150
- elevation data
  - combining with other data 26
  - Digital Elevation Models (DEMs) 39
  - displaying 26
- EM imaging 150
- embedded algorithms 349
- End of Hole Geology 171
- engineering applications 211
- enhancing data 69
- enhancing edges 193
- enhancing images 82
- environmental assessments, remote sensing applications 212
- environmental fragility in semi-arid countries 219
- environmental monitoring applications 211, 222, 227, 242
- environmentalists, applications for 228
- eps filter 370
- equal probability contours 88
- equations in geophysics 135
- erosion monitoring 229
- ERS-1 imagery 243
  - characteristics 244
- Europe, remote sensing applications in 212
- example algorithms 304
- example algorithms, see algorithm examples
- example dynamic link 345
- Example\_Map\_Composition\_Grids.alg 348
- Example\_Map\_Composition\_Items.alg 348
- Example\_Map\_Composition\_Scale\_Bars.alg 348
- Example\_Map\_Composition\_Text.alg 349
- Example\_Map\_Composition\_Titles.alg 349
- Example\_Map\_Composition\_ZScale.alg 349
- exploration effectiveness 167
- exploration geophysicists, applications for 156
- exploration licence areas 124

- exploration target generation 246
- exporting vector data 286
- extrapolation for filling in Fourier processing 201

## F

- fallback modes in 3-D perspective viewing 49
- fallow circles, classification of 219
- false color 315, 320
- false color images
  - for displaying DEMs 44
- Fast Fourier processing 189
- fault zones
  - identifying 245
- faults 312, 313
  - identifying with SAR 248
- feathering mosaiced images 46
- fertiliser use 233
- FFT algorithms 358
- FFT filtering 41
- FFT processing, see Fourier processing
- FFT\_Highpass\_Power\_Spectrum.alg 345
- FFT\_Lowpass\_Power\_Spectrum.alg 346
- FFT\_Notch\_Power\_Spectrum.alg 346
- FFT\_Power\_Spectrum.alg 346
- filter
  - adaptive\_median\_5x5 370, 371
  - ASPECT 55
  - aspect 363
  - average 380
  - average\_5x5 371
  - avg\_diag 369
  - avg\_h\_v 369
  - avg\_hor 369
  - avg\_ver 369
  - bandpass\_3\_5 365
  - brightest\_pixel\_5x5 370
  - darkest\_pixel\_5x5 370
  - darn 375
  - deviation 370
  - different 364
  - down\_cont 366
  - downward continuation 132
  - East\_West 378
  - easterly\_dip 373

## Index

eps 370  
force\_nosubs 375  
gaussian 354  
GOOD\_HEIGHTS 55  
GOOD\_REGIONS 55  
gradient\_X 364  
gradient\_Y 364  
h\_edge 375  
hanning 132  
Hanning\_3 374  
high\_pass\_4 365  
highpass\_4 133  
horizontal derivative 366  
kernel.template 380  
lap\_clean 376  
laplacian 376  
local\_enhance 380  
low\_freq 376  
low\_pass\_4 365  
lowpass\_4 133  
majority 370, 380  
median 370, 380  
modfilt 380  
North\_East 378  
North\_South 378  
North\_West 378  
North\_West\_5 379  
northerly\_dip 374  
nosubs 130  
rm2badli 380  
rmbadlin 380  
sharpedge 367  
sharpen 377  
sharpen11 368  
sharpen2 368  
slope 363  
SLOPE\_DEGREES 55, 310, 354  
slope\_degrees 364  
SLOPE\_PERCENT 310  
sobel 374  
South\_East 379  
South\_North 379  
South\_West 379  
std\_dev 364, 371  
thresh 377  
TM\_NDVI 55

- v\_edge 377
- vertical derivative 367
- w\_loc\_me 381
- West\_East 379
- filters
  - averaging 47
  - continuation 134
  - DEM\_HEIGHT 55
  - derivative in a specified direction 194
  - directional 133
  - edge enhancement 47, 133
  - example algorithms 351
  - field component in a specified direction 194
  - frequency 133
  - geophysical 132
  - geophysical filters 128
  - geophysical gravity filters 150
  - geophysics 365
  - high-pass Fourier 189, 193
  - low-pass Fourier 189, 193
  - majority 48
  - notch Fourier 189, 190
  - ranking 48, 370
  - reduction to the pole 194
  - reduction-to-pole 197
  - residual 134
  - second derivative 134
  - SLOPE 55
  - smoothing 132
  - sun angle 47
  - supplied 363
  - vertical continuation 194
  - vertical derivative 194
- fire risk
  - creating maps 24
  - displaying 23
  - identifying 42, 56
- fire-break road design, application for DEMs 42
- Fireburn 321
- firefighting 238
- first upward derivative filter 194
- First\_Vertical\_Deriv.alg 358, 359
- First\_Vertical\_Deriv\_Power\_Spectrum.alg 358
- fish stocks 233
- flight line overlays 124
- floating point operations 30

## Index

- floods, applications for DEMs 43
- foliage height distribution 85
- fonts 349
  - list of 349
- force\_nosubs filter 375
- forest degradation 237
- forest management maps 25
- forest management, remote sensing application 212
- forest monitoring 237
- foresters, applications for 238
- forestry, customizing applications 239
- formula, using to view oil and gas data 295
- formulas 336
  - INREGION vunction 54
  - inverting data values 296
- formulas for data fusion and mosaicing 36
- Fourier processing 189
  - discrete transform 201
  - display of transforms 202
  - edge effects 200
  - example algorithms 345
  - low and high pass filters 193
  - of potential-field data 194
  - power spectra 202
  - real image 202
- frequency filters 133
- Frequency-domain-processing 189
- fusing data
  - common ways 25
- fusing data using color and intensity 24
- fusing data, see also merging 21

## G

- Gamma-ray 324
- Gaussian equalisation 72, 312, 320
- gaussian filter 354
- Gaussian\_removed.alg 354
- GCPs (Ground Control Points) 69
- GEMI vegetation index 109
- geochemical data display 156
- geochemical data merged with Landsat 157
- geochemists, applications for 156, 167
- geolinking windows 137
- geological applications 321

- geological interpretation using SAR imagery 248
- geological interpretations, applications for DEMs 42
- geological outcrop maps 163
- geologists, applications for 156, 167
- geology 141
- geology databases, links to 167
- geometric coincidence 83
- geometrical significance 161
- geophysical 323
- geophysical anomaly spatial frequencies 128
- geophysical data imaging 121, 122, 127
- geophysical data spacing 126
- geophysical filters 128
  - in gravity 150
- geophysical station and line location data 124
- geophysical survey boundaries 179
- geophysicists, applications for 167
- geophysics example algorithms 323, 324
- geophysics filters 365
- GeoQuest (IESX) ASCII grid dump import 271
- GeoQuest (IESX) MapView import 276
- GeoQuest IESX ASCII grid dump import 268
- Geoquest imports 264
- geoscientific data 155
- GIS 212
- GIS and forestry 239
- GIS data, overlaying on airphotos 64
- GIS, displaying in ER Mapper 35
- GIS, links to 123
- Global Environmental Monitoring Index 109
- gloss 326
- goethite 321
- GOOD\_HEIGHTS filter 55
- GOOD\_REGIONS filter 55
- gradient\_X filter 364
- Gradient\_Y filter 364
- graphics formats, printing to 50
- gravity 123, 147, 323
  - combined with vectors 148
  - Fourier processing 194
  - profiling 149
  - stripping 149
- gravity and Bouguer density choice in imaging 148
- Green Vegetation Index 111
- greenness 318, 322
- greenness of vegetation 315, 316

## Index

- Greenness layer 314
- greyscale images 317
  - algorithm 313
  - for displaying DEMs 44
- greyscale strips 349
- Greyscale.alg 313, 317, 330
- Greyscale\_Hospitals\_and\_Fire\_Stations.alg 330
- gridded borehole depths 123
- gridded data
  - reliability 138
- gridding data 40, 126
  - geophysical 124
- grids 349
- ground based EM systems imaging 150
- ground resolution 140
- ground truthing 82, 88
- Gulf of Gdansk, monitoring using remote sensing 233
- GVI vegetation index 111

## H

- h\_edge filters 375
- hanning filter 132
- Hanning\_3 filter 374
- hardcopy. See printing
- header file 66
- height 360
- height layers for 3-D viewing 49, 333
- helicopter surveys 139
- hematite 321
- high frequency information, displaying 25
- high performance of virtual datasets 54
- high precision of virtual datasets 54
- high spatial frequency data 131
- high spectral resolution vegetation indices 115
- high\_pass\_4 filter 365
- high-frequency content of imagery 200
- Highlight\_structure.alg 354
- highlighting
  - classifications 34
  - data of interest 24
  - images only within a certain area 34
  - regions 24
  - regions combined with backdrop images 33
  - vegetation 24

- water 31, 32
  - with color on a greyscale image 34
- highlighting structure 354
- highpass filtered FFT 358
- high-pass Fourier filters 189, 193, 345, 346
- highpass\_4 filter 133
- Highpass\_Filter.alg 358
- Histogram equalisation 312
- histogram equalization 47, 72, 298
- histograms
  - non-cumulative 128
  - using with classification 84
- hole depths 176
- homogenous features recognition with classification 93
- Horizon 328
- Horizon\_Azimuth.alg 328
- Horizon\_Colordraped.alg 328
- Horizon\_Colordraped\_Dip.alg 328
- Horizon\_Colordraped\_Step\_LUT.alg 329
- Horizon\_Dip.alg 329
- Horizon\_IHS.alg 329
- Horizon\_Low\_Amplitude.alg 329
- Horizon\_Pseudocolor.alg 329
- Horizon\_Realttime\_Sun\_Shade.alg 329
- horizontal average filter 369
- horizontal derivative filters 366
- hot wind in fire risk 56
- HRV 330
- HSI 319, 325, 349
- HSI color wheel 361
- HSI imaging 132, 312, 342, 347
- HSI\_to\_RGB.alg 356
- HSI\_to\_RGB\_usercode.alg 356
- HSI\_wheel.alg 361
- HSV imaging 28
- Hue Saturation Intensity, see HSI
- hydrography data 137
- hydrologists, applications for 218, 228

## I

- Identifying fault zones 245
- identifying intrusive bodies 246
- IESX seismic software 267
- IHS merge 341, 347

## Index

- image
  - display 82
  - enhancement 82
  - interpretation 224, 242
    - using annotation 137
  - lower resolution overview 64
  - processing 234
- image, see also data
- image differencing 75
- image discontinuity 201
- image mosaicing 230
- image processing in mineral exploration 155
- image rectification 41
- image striping 140
- image values 349
- import
  - Charisma 2D XYZ ASCII grid 268, 272
  - Charisma 3D Inline Xline XYZ ASCII grid 268, 273
  - GeoQuest (IESX) ASCII grid dump 271
  - GeoQuest (IESX) MapView 276
  - GeoQuest IESX ASCII grid dump 268
  - oil and gas software 264
  - OpenWorks 3.1 Wells 280
  - SEG-Y 268, 269
  - SeisWorks Fault Polygons 281
  - SeisWorks Manual Contours 282
  - Zycor ASCII grid 268, 270
- importing and exporting 65
- importing vector data 123
- In\_Regions.alg 331
- incorrect registration, errors in DEMs 41
- Infrared Percentage Vegetation Index 104
- infrared response for vegetation 84
- infrared satellite imagery 251
- infrastructure development, remote sensing applications 213
- Ingres 167
- Input\_Image.alg 346
- INREGION function 33, 36, 54
- INREGION() function 350
- integrating data 211
  - DEM and other data 50
- intensity layer, using in the oil and gas industry 295
- Interactive\_mosaic\_of\_4\_datasets.alg 344
- intercellular air spaces and vegetation indices 99
- interfacing with ER Mapper 162
- Interferometric SAR processing for generating DEMs 40

- interpretation using annotation 137
- interpreted dips 164
- interpreting radar (SAR) data 245
- Intrepid dynamic links 123
- intrusive bodies 244
  - identifying 246
- IPVI vegetation index 104
- iron 320
- iron oxide 206, 316, 318
- iron oxide absorption 113
- Iron\_Oxide\_ratio.alg 318
- iron-bearing minerals 321
- iron-stained 207
- irrigation requirements assessment, remote sensing application 217, 219
- ISOCLASS\_Landsat\_TM\_year\_1985.alg 338
- ISODATA unsupervised classification 240
- isovegetation lines 106
- iterative training classes 89

## J

- Julia fractal 361
- Julia\_Fractals.alg 361

## K

- K/Th ratio for radiometrics data 135
- kernel
  - north-east shade 317
  - north-west shading 312
- kernel.template filter 380
- kernels, see filters

## L

- lake capacity monitoring 229
- land ownership 214
- Land\_Use\_Classification.alg 334
- Landmark imports 264
- Landsat MSS 234, 313, 314
  - example algorithms 313
- Landsat TM 234
  - algorithms 315
  - data

## Index

- example algorithms 315
- merging with airborne magnetics surveys 25
- merging with SPOT Pan 25, 29, 30
- merging with SPOT Pan over DEMS 334
- viewing in 3-D 333
- Landsat TM data 100, 205, 240
- Landsat\_MSS.alg 357
- Landsat\_MSS\_natural\_color.alg 314
- Landsat\_over\_DTM.alg 333
- Landsat\_SPOT\_fusion\_over\_DTM.alg 334
- Landsat\_TM.alg 358
- Landsat\_TM\_and\_SPOT\_Pan.alg 360
- Landsat\_TM\_and\_SPOT\_Pan\_IHS\_merge.alg 341, 347
- Landsat\_TM\_and\_SPOT\_Pan\_RGBI.alg 342
- Landsat\_TM\_area\_specific\_stretch.alg 318
- Landsat\_TM\_Cloud\_and\_Water.alg 355
- Landsat\_TM\_Cloud\_removal.alg 355
- Landsat\_TM\_PC1-6\_HistEq.alg 360
- Landsat\_TM\_scan\_line\_noise\_removal.alg 358
- Landsat\_TM\_Tasseled\_Cap\_in\_RGB.alg 318
- Landsat\_TM\_transformations.alg 360, 361
- Landsat\_TM\_two\_years.alg 360
- Landsat\_TM\_With\_simple\_grid.alg 349
- LandsatMSS\_NDVI.alg 314
- LandsatMSS\_PVI6.alg 314
- LandsatMSS\_PVI7.alg 314
- LandsatMSS\_Tasseled\_Cap.alg 314
- landuse/terrain classification map using SAR 247
- lap\_clean filter 376
- Laplacian filter 326
- laplacian filters 376
- larvae 252
- Latitude Longitude map grids 348
- layers
  - Intensity 295
  - order in mosaicing algorithms 46
- layover effect in radar processing 246
- leaf area indices 85
- least squares fit 318
- Leeuwin Current 252
- legends 349
- legislative obligations and infringements, remote sensing application 213
- lettuce, classification of 219
- levelling artefacts 138
- levelling problems in DEMs 46
- lightning strikes 237, 238

- lineament detection 309
- lineaments 312, 313
- linear leveling 47
- Linear Scale test pattern 362
- links to vector data and GIS 123
- local anomalous 134
- local\_enhance filter 380
- low frequency filter 376
- low vegetation cover and vegetation indices 113
- low\_pass\_4 filter 365
- lower resolution overview image files 64
- lowpass filtered FFT 358
- low-pass Fourier filters 189, 193, 346
- lowpass\_4 filter 133
- Lowpass\_Filter.alg 358
- Lsfit.alg 318

## M

- MAFF 214
- magnetics data
  - collection 138
  - displaying 26, 122
  - displaying over a satellite image 27
  - imaging 137
  - viewing in 3-D 334
- Magnetics.alg 334
- Magnetics\_1Q\_Vertical\_Derivative.alg 324
- Magnetics\_2nd\_Vertical\_Derivative.alg 324
- Magnetics\_3Q\_Vertical\_Derivative.alg 324
- Magnetics\_and\_Radiometrics\_Colordrape.alg 324
- Magnetics\_and\_Vectors.alg 325
- Magnetics\_Colordrape.alg 325
- Magnetics\_Colordrape\_map\_legend.alg 325
- Magnetics\_Colordrape\_shiny\_look.alg 325
- Magnetics\_Colordrape\_wet\_look.alg 325
- Magnetics\_Contours\_from\_Raster.alg 326
- Magnetics\_POB\_Vertical\_Derivative.alg 326
- Magnetics\_Pseudocolor.alg 326
- Magnetics\_Realttime\_Sun\_Shade.alg 326
- Magnetics\_rgb\_3angle.alg 327
- Magnetics\_uc1\_and\_full.alg 361
- Magnetics\_uch\_and\_dch.alg 361
- Magnetics\_uch\_and\_full.alg 361
- majority filter 370, 380

## Index

- majority filters 48
- map
  - creating a 61, 290
- map composition 349
  - example algorithms 348
  - multiple language support 349
- map composition items 36
- map grids 348
- map legends
  - example algorithms 350
- map titles 349
- Map\_Symbols\_In\_Use.alg 349
- mapping shelf circulation 251
- maps
  - fire risk 24
  - forest management 25
  - landuse/terrain classification 247
  - mineral exploration 25
  - precipitation 25
  - updating with remote sensing 212
- maps, showing integrated data 24
- marine environment 235
- marine habitat protection 221
- marine organisms 252
- masking 224
- masking of water, forest and urban areas 94
- Maximum Gold Value 170
- maximum likelihood classifier 88, 219, 337
- measurements of the earth's gravity field 194
- median filter 354, 380
  - for removing errors in DEMs 41
  - in change detection 76
- median filters 370
- Median\_noise\_removal.alg 354
- merging data 241
  - Brovey transform and RGBI 29
  - classified and airphoto or satellite imagery 26
  - ERS-1 and Landsat TM 246
  - geochemical and Landsat 157
  - gravity and vectors 148
  - Landsat TM and aeromagnetic surveys 25
  - Landsat TM and SPOT Pan 25
  - Landsat TM and SPOT Pan over DEMs 334
  - radiometrics and aeromagnetic surveys 26
  - radiometrics and satellite imagery 143
  - using color and intensity 24

- merging data, see also fusing 21
- mineral exploration industry 156
- mineral exploration maps 25
- mineral exploration with radar data 243
- mineralization 141, 142, 246
- mixed-residential class in classification 90
- modfilt filter 380
- MODELVISION 164
- Modified Soil Adjusted Vegetation Index 108
- monitoring crop production 217
- monitoring environmental change. See environmental monitoring
- MONOCOLOR layers 35
- MONOCOLOUR layers 172
- mono-cropping 233
- mosaicing data 22, 230, 241
  - algorithm 46
  - DEMs 46
  - formulas for 36
  - strip of aerial photographs 215
- mosaicing data algorithm 344
- MOSS 215
- MSAV vegetation index 108
- MSAVI2 vegetation index 108
- MSS data 97, 100
- multiple language support 349
- multispectral
  - classification 81, 219
  - satellite imagery 218
  - sensing of crops 84

## N

- native GIS format 64
- natural color 314, 319, 331
- NDVI 314, 322, 331
- NDVI vegetation index 51, 104, 116, 219, 316
- near surface sources 134
- nearest neighbour resampling 71
- new road development, identifying with satellite imagery 67
- Newcastle\_Magnetics\_Map.alg 350
- nickel anomalous regions 178
- nickel mineralizations 156
- nickel potential 173
- NIR 323
- NIR data 97, 112

## Index

- NOAA satellite imagery 252
- noise removal 33, 322, 354
- non-cumulative histogram display 128
- non-linear mixing 113
- non-NULL data, transforming 28
- normalized difference image for comparing results 72
- Normalized Difference Vegetation Index 104
- normalized difference vegetation index 314
- North America, remote sensing applications in 212
- North Arrows 348
- North\_East filter 378
- North\_South filter 378
- North\_West filter 378
- North\_West\_5 filter 379
- northerly\_dip filter 374
- nosubs filter 130
- notch filtered FFT 358
- notch Fourier filtering 189, 190, 346
- notch transform 326
- Notch\_Filter.alg 358

## O

- ocean current charting 251
- oil and gas industry, using ER Mapper in 263
- oil spill response 221
- OpenWorks 3.1 Wells import 280
- order of layers in mosaicing algorithms 46
- Output\_Image\_Highpass.alg 346
- Output\_Image\_Lowpass.alg 346
- Output\_Image\_Notch.alg 346
- overlying GIS or CAD data 64
- oversampling 126

## P

- panchromatic data 68
- pattern recognition phase in classification 84
- PC1 36, 316, 319, 322
- PCA. See Principal Components Analysis
- Penman method 220
- pepper-and-salt noise 193
- performance and virtual datasets 54
- Perpendicular Vegetation Index 105
- Perpendicular Vegetation Index, see also PVI vegetation index 314

- petroleum exploration, applications of radar data 244
- Petroseis 145
- photogrammetric generation of DEMs 40
- phyllosilicates 316, 321
- pipeline design, application for DEMs 42, 58
- pixel to pixel registration 71
- pixel transform 28
- Planck function 254
- planning, remote sensing applications 212
- plant development and stress 85
- plant leaves and vegetation indices 99
- Pleasing\_image.alg 319
- POB vertical derivative 326
- political boundaries, remote sensing application 213
- polygon regions 35
- polygons
  - using to define areas of interest 24
- polynomial rectification 69
  - polynomial order 71
- potassium 327
- potassium-40 324
- power spectra in Fourier processing 202
- power spectrum image in Fourier processing 197, 345
- precipitation maps 25
- principal components analysis 36, 75, 143, 205, 235
- Principal\_Component\_1.alg 319
- printing 289
  - stereo pair images 50, 335
  - stereo pairs with vectors 50
  - test patterns 355
  - TIFF format 289
  - to graphics formats 50
- priority of vector layers 35
- processing DEMs 51
- profiles 161
- pseudocolor colordrape, using for displaying data 26, 27
- pseudocolor images 130, 313
- Pseudocolor.alg 313
- PVI vegetation index 105, 116, 220, 314

## Q

- quality control 168
- quantizing data 122
- quartz 321

## R

- radar data
  - characteristics 244
  - correcting with DEMs 59
  - geological interpretation 248
  - in mineral and oil exploration 243
  - interpretation 245
  - layover effect 246
- Radian CP3 145
- radiance and reflectance 101
- Radiometric 324
- radiometric correction 83
- radiometrics 123, 323, 343
  - algorithms 324
  - imaging 139
  - interpreting 141
  - K/Th ratio 135
  - merging with aeromagnetics surveys 26
  - merging with satellite data 143
  - over magnetics in 3-D 335
- Radiometrics\_and\_Magnetics\_RGBI.alg 343
- Radiometrics\_Magnetics\_RGBI.alg 327
- Radiometrics\_over\_Magnetics algorithm 335
- Radiometrics\_ratio\_K\_Th.alg 327
- random line data 125
- random point data 125
- Random test pattern 362
- range of heights from a DEM 52, 53
- ranking filters 48, 370
- raster and vector data integration 51
- raster and vector integration example algorithms 355
- raster contour line generation 48
- raster data
  - rectifying to vector data 70
- raster dataset resolution 22
- raster to vector conversion 35
- ratio combinations (RGB) 143
- ratio vegetation index 103
- ratios in geophysics 135, 142
- real image in Fourier processing 202
- real time “Sun” shaded images 326
- realtime “Sun” shaded images
  - for viewing geophysical data 130
- realtime “Sun” shaded images 329
  - for displaying DEMs 44

- realtime “sun” shaded images
  - algorithm 313
- real-time classification 92
- Realtime\_Sun\_Shade.alg 313
- rectifying images 41, 69, 215, 223, 229
  - pixel to pixel registration 71
  - rectifying raster data to vector data 70
  - RMS errors 70
  - selecting control points 69
- Red Green difference image 74
- Reduce\_to\_Pole.alg 359
- Reduce\_to\_Pole\_Power\_Spectrum.alg 359
- reduction to the pole filters 194
- reduction-to-pole Fourier processing 197
- reflectance 101
- reflectance spectra 106
- regions
  - displaying attribute data within 33
  - example algorithms 350
  - highlighting 24
  - highlighting combined with backdrop images 33
  - highlighting data example algorithms 330
  - showing DEM values within 54
- registering data to ground control points 69
- registering datasets
  - pixel to pixel registration 71
- regolith maps 163
- regular line data 125
- reliability of gridded magnetic data 138
- removing noise from images 33
- resampling 71, 127
- residual filters 134
- resistivity 150
- resolution of scanned images 307
- resolution requirements for merging datasets 22, 344
- RGB -> HSI -> RGB 342
- RGB to HSI to RGB 322, 347
- RGB.alg 308, 357
- RGB->HSI->RGB 28
- RGB\_321.alg 315, 319
- RGB\_321\_sharpened\_with\_SPOT\_Pan.alg 315
- RGB\_321\_to\_HSI\_to\_RGB.alg 319
- RGB\_341.alg 319
- RGB\_421.alg 315
- RGB\_432.alg 320
- RGB\_531.alg 320

## Index

RGB\_541.alg 320  
RGB\_541\_to\_HSI\_to\_RGB.alg 321  
RGB\_542.alg 321  
RGB\_741.alg 321  
RGB\_autoscale.alg 357  
RGB\_BCET\_autoscale.alg 357  
RGB\_Principal\_Components\_123.alg 322  
RGB\_Principal\_Components\_bands\_741.alg 322  
RGB\_to\_HSI.alg 361  
RGB\_to\_HSI\_to\_RGB.alg 322, 347, 357  
RGBCMYK color strip 361  
rgbcmk\_bands.alg 361  
RGB-Height images 51  
RGBI algorithm 28  
RGBI images 28  
ringing 193  
RIP (Raster Image Processing) engine 63  
river transports 234  
rm2badli filter 380  
rmbadlin filter 380  
RMS errors in rectification 70  
road boundaries, enhancing 193  
road centreline network 69  
roads draped over DEM in 3-D 335  
Roads\_and\_SPOT\_over\_DTM.alg 335  
rotated text 349  
RVI vegetation index 103

## S

SAR filters 371  
SAR interferometry 244  
SAR. See radar data  
satellite imagery 223  
    availability and acquisition 247  
SAVI vegetation index 106, 107  
SBI (Soil Brightness Index) 219  
scale bars 348, 349  
scale independence 168  
scan line noise removal 322  
scan line noise removed 358  
scan lines 322  
Scan\_line\_noise\_removal.alg 322  
scanned data 223, 307  
scattergrams 90

- scene brightness, in change detection 75
- Schlumberger imports 264
- scripting language 64
- seasonal effects, eliminating 73
- sea-surface temperatures 253
- sea-surface temperatures (SSTs) 251
- second derivative filters 134
- second vertical derivative 194
- Second\_Vertical\_Deriv\_Power\_Spectrum.alg 359
- sedimentation and erosion, applications for DEMs 43
- SEG-Y import 268, 269
- seismic data 123, 144, 327
  - example algorithms 327
- seismic data, importing into ER Mapper 267
- seismic datasets, viewing 295
- SeisWorks Fault Polygons import 281
- SeisWorks Manual Contours import 282
- SeisWorks seismic software 267
- selecting control points for rectification 69
- semi-arid areas, problems with vegetation indices 114
- semi-arid countries, remote sensing in 219
- Semi-Automatic Interpretation of Aeromagnetic Datasets 159
- Sensors\_16.alg 322
- shaded relief images. See sun angle shading
- Shaded\_Digital\_Terrain\_Map.alg 335
- shadow strips, errors in DEMs 41
- shadows, eliminating with band ratios 100
- sharpedge filter 367
- sharpen filter 377
- Sharpen\_TM\_with\_Pan.alg 343
- sharpen11 filter 368
- sharpen2 filter 368
- sharpening Landsat TM imagery 22, 31
- shelf circulation 251
- shiny colordrape images
  - for displaying DEMs 45
- siltation monitoring 229
- Simple\_San\_Diego\_Map.alg 350
- Sin\_curve.alg 335
- Sine wave test pattern 362
- Single\_Band\_Greyscale.alg 357
- slope 360
- SLOPE filter 55
- slope filter 363
- slope, generating from DEMs 52, 53
- slope, in fire risk 57

## Index

- slope\_degrees 52
- SLOPE\_DEGREES filter 55, 310, 354
- slope\_degrees filter 364
- Slope\_degrees.alg 310, 354
- SLOPE\_PERCENT filter 310
- Slope\_percent.alg 310
- smelting 240
- smoke spotting 238
- smoke-stack industrial centres 233
- smooth resampling 127
- smoothing 127
- smoothing filters 132
- Sobel filters 374
- soil 85
- Soil Adjusted Vegetation Index 106
- soil line 103, 114
- soil mapping 141
- soil noise 106
- sources and quality of DEM data 40
- sources of topography data 151
- South\_East filter 379
- South\_North filter 379
- South\_West filter 379
- spatial sampling 126
- spectral characteristics of vegetation 97, 99
- spectral pattern recognition 81
- spectral reflectance characteristics 84
- spectral response of crop species 86
- spectral unmixing 115
- SPOT data 96
  - viewing in 3-D 334
- SPOT HRV 330
- SPOT Pan 358
- SPOT Panchromatic 341
- SPOT Panchromatic data 68, 80, 330, 336
  - example algorithms 330
- SPOT Panchromatic images 331
- SPOT XS 93, 331, 341, 358
- SPOT XS data
  - example algorithms 331
- SPOT\_over\_DTM.alg 336
- SPOT\_Pan.alg 358
- SPOT\_Pan\_in\_Regions.alg 350
- SPOT\_Pan\_in\_Regions\_over\_Landsat\_TM.alg 351
- SPOT\_Pan\_with\_roads\_and\_drainage.alg 309
- SPOT\_XS.alg 358

- SPOT\_XS\_and\_Pan\_Brovey\_merge.alg 331
- SPOT\_XS\_and\_SPOT\_Pan\_RGBI.alg 343
- SPOT\_XS\_natural\_color.alg 331
- SPOT\_XS\_NDVI\_colordraped\_over\_Pan.alg 331
- SPOT\_XS\_NDVI\_veg\_index\_greyscale.alg 331
- SPOT\_XS\_rgb\_321.alg 332
- SPOT\_XS\_rgb\_321\_sharpened\_with\_SPOT\_Pan.alg 332
- SQL 170
- SSTs (sea-surface temperatures) 251
- statistic used for erosion and siltation estimates 230
- statistical sample in classification 89
- statistics calculations 350
- statistics, in classification 84
- statutory designations, remote sensing application 213
- std\_dev filters 364, 371
- steepness, from DEMs 52
- stereo pair images 50
- stereo pairs 335
  - with vectors 50
- stereo viewing 50, 334
- strike filtering 193
- strip of aerial photographs 215
- striping 140
- structural features 207
- structure, displaying 26
- subsampling and geophysical data 135
- sub-sectioning data 63
- subsectioning data 224
- sun angle 130
- sun angle filters 47
- sun shading viewing 335
- sun shading, using to view oil and gas data 296
- supervised classification 82, 219
- supplied algorithms 303
- surface information from Radiometrics 324
- survey boundary polygons 124
- susceptibility values 164
- suspended aerosols 109

## T

- table based dynamic links 330
- table of data dynamic link 345
- Tabular\_Data\_as\_Circles.alg 345
- tasseled cap vegetation 314

## Index

tasseled cap vegetation calculations 322  
tasseled caps 318  
Tasseled\_Cap\_Transforms.alg 322  
TC\_Greenness\_over\_Brightness.alg 315  
template algorithms 304  
template algorithms, see algorithm templates  
terraces, errors in DEMs 41  
terrain, displaying with principle components 36  
Tertiary 176  
test 3-D image 335  
test patterns example algorithms 355  
Test\_Fonts.alg 349  
Test\_Patterns.alg 361, 362  
text 349  
texture mapping in 3-D perspective viewing 49  
thermal infrared satellite imagery 251  
thorium 327  
thorium-232 324  
thresh filters 377  
thresholding in change detection 76  
TIFF format, printing to 289  
tiff, printing to graphics files 50  
TM data. See Landsat TM  
TM\_NDVI filter 55  
TNDVI 322  
topographic variations, emphasizing with radar data 244  
topography 122, 151, 310  
    sources of data 151  
training region refinement 90  
training site selection 82, 88  
Transformed Soil Adjusted Vegetation Index 107  
transforms 129  
    in Fourier processing 202  
transmittance of canopy components 85  
transport corridors, remote sensing applications 213  
Transverse Mercator projection 225  
traversing 129  
tree damage 240  
triangles 349  
TRUECOLOR layers 35  
Truecolor\_Color\_Spiral.alg 345  
TRUECOLOUR layers 172  
TSAVI vegetation index 107  
tundra-like regions 237  
turbidity 235  
two-way time data 145

typicality thresholds 91

## U

unsupervised classification 92, 240  
 unsupervised multi-spectral classification 219  
 updates from a single authorised source 168  
 updating vectors 215  
 Upward Continuation filter 366  
 uranium-238 324  
 urban planning, remote sensing application 213  
 User\_Example\_Dynamic\_Link.alg 345  
 usercode filters 380  
 USGS DLG-3 355  
 utilities mapping, remote sensing application 213

## V

v\_edge filters 377  
 vector based geology information 334  
 vector based polygon regions to raster datasets 331  
 vector based polygons 350  
 vector data 69, 308  
 vector data, overlaying on raster backdrops 64  
 vector polygons of high fire risk 58  
 Vector\_Deriv\_Power\_Spectrum.alg 359  
 Vector\_Field\_Power\_Spectrum.alg 359  
 vectors  
   displaying over raster data 24  
   draped over DEM 335  
   draping over perspective views 49  
   importing and viewing with dynamic links 123  
   updating 215  
   viewing over stereo pairs 50  
 Vectors\_from\_Airphoto.alg 308, 355  
 Vectors\_over\_Greyscale.alg 331  
 Vectors\_over\_SPOT\_Pan.alg 355  
 vegetation 320, 323, 331  
   highlighting 24  
   in fire risk 57  
   shown in red 101  
   spectral characteristics of 97, 99  
 vegetation canopy, penetrating with radar 244  
 vegetation in remote sensing 95  
 vegetation indices 98, 337

## Index

- ARVI 110
  - atmospherically resistant indices 110
  - basic assumptions 102
- DVI 105
- GEMI 109
- GVI 111
- IPVI 104
- MSAV 108
- MSAVI2 108
- NDVI 51, 104, 116, 219
- problems in arid and semi-arid areas 114
- PVI 105, 116, 220
- questions and answers 102
- RVI 103
- SAVI 106, 107
- SBI 219
- TSAVI 107
- WDVI 105
  - with low vegetation cover 113
- vegetation, dry 323
- vegetation, green 323
- Vegetation\_NDVI.alg 322
- Vegetation\_TNDVI.alg 322
- vegetative biomass monitoring using classification 219
- vertical average filter 369
- vertical continuation filter 194
- vertical derivative filters 367
- vertical derivative in geophysical data processing 136
- vertical derivative of magnetics 324
- vertical edges filter 377, 378
- vertical illumination 330
- Vertical\_Continuation.alg 359
- Vertical\_Continuation\_Power\_Spectrum.alg 360
- via\_ARCPLOT\_Airphoto\_with\_roads.alg 309
- via\_ARCPLOT\_Coast\_with\_boundaries.alg 309
- view position in 3-D perspective viewing 49
- village plans, use in development applications 212
- virtual datasets 241
  - and principal components analysis 206
  - example algorithms 355
  - for difference imaging 75
  - template algorithms 360
  - with DEMs 55
- Virtual\_Dataset\_mosaic.alg 344
- visibility impact design, applications of DEMs 42
- visualizing geophysical data 122, 127

## W

- w\_loc\_me filter 381
- warping. See rectifying images
- water 355
- water quality 233
- water resources management 230
- water resources monitoring 228
- water, highlighting 32
- water, mapping shelf circulation 251
- Waterlevel Color Look Up Table 129
- watersheds, remote sensing application 213
- wave frequencies electromagnetic data 123
- WDVI vegetation index 105
- Weighted Difference Vegetation Index 105
- weighting the classifier 91
- West\_East filter 379
- Western Australia, remote sensing applications in 221
- wet look 325
- wetness 318, 322
- Wetness layer 314
- what-if processing 52, 56, 122
- wheat, classification of 219

## Z

- Z-profiling 129
- Z-scales 349
- Z-values 349
- Zycor 145
- Zycor ASCII Grid import 268
- Zycor ASCII grid import 270